HUMAN T-CELL LEUKEMIA VIRUS TYPE I BASIC LEUCINE ZIPPER FACTOR (HBZ) MODULATES CELLULAR DNA DAMAGE REPAIR AND ANTIOXIDANT RESPONSES TO PROMOTE HOST CELL SURVIVAL AND LEUKEMOGENESIS

by

Amanda Williams Rushing

April, 2018

Director of Dissertation: Isabelle M. Lemasson, Ph.D.

Department of Microbiology and Immunology

Brody School of Medicine, East Carolina University

Abstract

Approximately twenty million people worldwide are infected with Human T-cell Leukemia Virus type 1 (HTLV-1). HTLV-1 establishes a life-long, chronic infection which can result in the development of severe HTLV-1 associated diseases: Adult T-cell Leukemia (ATL) or HTLV-1-associated myelopathy/ tropical spastic paraparesis (HAM/TSP). ATL is a fatally-aggressive lymphoproliferative disorder of HTLV-1-infected $CD4^+$ T-cells. HAM/TSP is a debilitating neurodegenerative disorder that greatly reduces quality of life. There exists a distinct lack of effective vaccine and therapeutic options for both ATL and HAM/TSP patients. Though the mechanisms that drive HTLV-1 pathogenesis remain poorly understood, extensive study of the virus has revealed the

importance of two viral regulatory proteins in disease progression: Tax and HBZ. Tax is a transcriptional regulator which is important for establishing initial infection; however, Tax is highly immunogenic and stimulates a robust antiviral immune response. To evade immune detection, HTLV-1 host cells often silence Tax expression through the transcriptionally repressive activity of the basic leucine zipper factor HBZ. HBZ is expressed throughout all phases of infection and plays important roles in maintaining host cell survival and clonal expansion. HBZ expression is sufficient to induce ATL-like disease progression in *in vivo* models, supporting its contribution to leukemogenesis in patients. Here, we report novel functions of HBZ that may promote the long-term survival of infected lymphocytes, including the direct upregulation of antioxidant response gene expression, the detoxification of reactive oxygen species, and the prevention of oxidative stress-induced cell death. We also evaluated the contribution of HBZ to the accumulation of genetic abnormalities which may promote leukemogenesis. Here, we report that HBZ contributes to genetic instability by affecting the double-stranded DNA damage repair system non-homologous end joining (NHEJ), possibly through specific interactions with DNA repair proteins. These findings support the role of HBZ in promoting leukemogenesis through the accumulation of chromosomal abnormalities which arise from double-stranded DNA breaks. Together, the data presented here indicate that HBZ is an important driving force in the prolonged survival and transformation of HTLV-1-infected lymphocytes.

HUMAN T-CELL LEUKEMIA VIRUS TYPE I BASIC LEUCINE ZIPPER FACTOR (HBZ) MODULATES CELLULAR DNA DAMAGE REPAIR AND ANTIOXIDANT RESPONSES TO PROMOTE HOST CELL SURVIVAL AND LEUKEMOGENESIS

A Dissertation Presented to:

The Department of Microbiology and Immunology

Brody School of Medicine, East Carolina University

Submitted in Partial Fulfillment of the Requirements for the Degree of

Doctor of Philosophy

in

Microbiology and Immunology

By

Amanda Williams Rushing

April 2018

HUMAN T-CELL LEUKEMIA VIRUS TYPE I BASIC LEUCINE ZIPPER FACTOR (HBZ) MODULATES CELLULAR DNA DAMAGE REPAIR AND ANTIOXIDANT RESPONSES TO PROMOTE HOST CELL SURVIVAL AND LEUKEMOGENESIS

by

Amanda Williams Rushing

Approved by:

Director of Dissertation: _____

Isabelle M. Lemasson, Ph.D.

Committee Member: _____

Everett C. Pesci, Ph.D.

Committee Member: _____

Rachel L. Roper, Ph.D.

Committee Member: _____

Richard A. Franklin, Ph.D.

Committee Member: _____

Li Yang, Ph.D.

Department Chair,

Microbiology and Immunology: _____

Everett C. Pesci, Ph.D.

Dean of the Graduate School: _____

Paul J. Gemperline, Ph.D.

Acknowledgements

First and foremost, I would like to extend my sincerest thanks to my advisor Dr. Isabelle Lemasson for her years of dedicated mentorship and support. To my committee members Dr. Everett Pesci, Dr. Rachel Roper, Dr. Richard Franklin, and Dr. Li Yang: I would like to thank you all for your continued guidance. To my fellow members of the Lemasson Laboratory, both past and present: I would like to thank you all for helping to make the lab environment a fantastic place to work. I would like to especially thank Dr. Nicholas Polakowski and Kimson Hoang for their invaluable contributions to my training and to my work. I would also like to thank the rest of the faculty and staff of the Department of Microbiology and Immunology at the Brody School of Medicine for their assistance and support.

Finally, I would like to thank my parents, Terry and Teresa Williams, for encouraging me and loving me through every single step of my journey. And most importantly, I want to thank my husband, Blake Rushing, for his unending love, his unwavering support, and his willingness to walk this path by my side.

Table of Contents

List of Tables

List of Figures

List of Abbreviations

AA	Amino acids
AD	Activation domain
allo-HSCT	Allogeneic hematopoietic stem cell transplantation
Alt-NHEJ	Alternative non-homologous end joining
ARE	Antioxidant response element
ATL	Adult T-cell Leukemia
AZT	Zidovudine
BER	Base excision repair
BR	Basic region
bZIP	Basic leucine zipper
CA	Capsid
CBP	CREB-binding protein
CD	Central domain
CDK	Cyclin-dependent kinases
CNC	Cap'n'Collar
C-NHEJ	Classical non-homologous end joining
CNS	Central nervous system
CREB	cAMP response element binding protein
CTL	Cytotoxic T-cell
DBD	DNA-binding domain
DMEM	Dulbecco's Modified Eagle's Medium
DNA	Deoxyribonucleic acid
DNA-PK	DNA protein kinase
DNA-PKcs	DNA protein kinase catalytic subunit
DSB	Double-stranded DNA break
Env	Envelope
GFP	Green fluorescent protein

GLUT1	Glucose transporter 1
HAM/TSP	HTLV-associated myelopathy/tropical spastic paraparesis
HBZ	HTLV-1 basic leucine zipper factor
HDACi	Histone deacetylase inhibitors
HMOX-1	Heme oxygenase I
HPSG	Heparin sulfate proteoglycans
HR	Homologous recombination
HTLV-1	Human T-cell Leukemia virus type 1
HTLV-2	Human T-cell Leukemia virus type 2
ICAM-1	Intercellular adhesion molecule 1
IF	Interferon
IN	Integrase
iNOS	Inducible nitric oxide synthase
IR	Irradiation
IV	Intravenous
LC-MS	Liquid chromatography mass spectrometry
LC-MS/MS	Liquid chromatography tandem mass spectrometry
LFA1	Lymphocyte function-associated antigen 1
LTR	Long terminal repeat
MA	Matrix
minP	Minimal promoter
MMR	Mismatch repair
MTOC	Microtubule-organizing center
NC	Nucleocapsid
NER	Nucleotide excision repair
NHEJ	Non-homologous end joining
NHEJ-C	Non-homologous end joining, compatible ends
NHEJ-I	Non-homologous end joining, incompatible ends

NO	Nitric oxide
NPC	Nuclear pore complex
Nrf2	NF-E2 related factor 2
Nrf2-DN	Nrf2 dominant negative
NRP-1	Neuropilin 1
ORF	Open reading frame
PBMC	Peripheral blood mononuclear cell
PIC	Pre-integration complex
PIKK	Phosphatidylinositol-3-kinase-like kinase
Pol	Polymerase
Pro	Protease
RNOS	Reactive nitrogen and oxygen species
RNS	Reactive nitrogen species
ROS	Reactive oxygen species
RPMI	Roswell Park Memorial Institute
RT	Reverse transcriptase
RxRE	Rex responsive elements
SEM	Standard error of the mean
sMaf	Small Maf
SU	Surface glycoprotein
Tax	Transactivator X
TM	Transmembrane glycoprotein
TOF	Time-of-flight
TxRE	Tax-responsive element
U3	Unique/ Untranslated 3'
U5	Unique/ Untranslated 5'
VDAC	Voltage-dependent-anion-selective channel protein
VS	Virological synapse

WT	Wild type
ZIP	Leucine zipper

Chapter 1

Human T-cell Leukemia Virus: An Introduction

The Discovery of Human T-cell Leukemia Virus: Retroviruses possess a positive sense, single-stranded RNA genome and infect a wide variety of species. A defining feature of retroviruses is the necessity of the retroviral genome to be reverse transcribed into a double-stranded DNA intermediate, which is then permanently integrated into the genome of the host cell. The transcription of integrated viral DNA, known as the provirus, is regulated by host and viral transcriptional machinery.

The study of retroviruses began in 1911, with the discovery of the avian retrovirus Rous Sarcoma Virus[1]. In the years that followed, retroviruses infecting a wide variety of host species were described as the causative agents of an array of malignancies, anemias, and neurological disorders. It wasn't until 1980 that the first human retrovirus was isolated from the lymphocytes of a patient diagnosed with a cutaneous T-cell lymphoma[2]. Shortly thereafter, another group isolated a retrovirus from cell lines established from patients with Adult T-cell Leukemia (ATL), as well as from freshly isolated lymphocytes[3]. Genome sequencing of both viruses confirmed them to be a single virus, which was subsequently named Human T-cell Leukemia Virus type I (HTLV-1) and determined to be the causative agent of ATL[4]. Additional work also characterized HTLV-1 as the etiologic agent of a debilitating neurological disorder known as HTLV-1-associated myelopathy/ tropical spastic paraparesis (HAM/TSP)[5,6]. Importantly, though HTLV-1 establishes a lifelong, chronic infection, not all individuals experience symptoms or develop disease. Unknowing viral transmission from asymptomatic carriers is known as silent transmission[7].

Following these reports, a structurally similar virus, HTLV-2, was isolated from a patient diagnosed with a hairy T-cell leukemia[8]. Though this virus was also isolated from a leukemia patient, it is unclear whether HTLV-2 was the causative agent of the disease. HTLV-2 has been shown to be less pathogenic than HTLV-1 and has not been clearly linked to leukemogenesis. However, in rare cases, HTLV-2 infection is associated with the development of neurological disorders showing some similarity to HAM/TSP [9]. More recently, two additional HTLV strains were identified, HTLV-3 and HTLV-4, however neither of these two strains has yet been linked to disease [10,11]. Due to its definitive link to human disease, HTLV-1 will be the focus of this literature review, and the subject of the research presented here.

Epidemiology: HTLV infection is not distributed evenly across the world, but rather there are distinct areas in which the virus is considered endemic. High rates of HTLV-1 transmission occur in Japan, in which some areas have a seroprevalence as high as 37%[7]. Other HTLV-1 endemic regions include the Caribbean islands, sub-Saharan Africa, and regions of South America. HTLV-1 is also a significant concern outside of these major endemic regions, with foci of infected populations reported in Iran, Romania, and in central Australian aboriginal populations[12]. Unlike many other retroviruses, HTLV-1 possesses a high degree of genetic stability. This likely related to the limited dependence upon *de novo* viral replication during chronic infection. As a result, only a few subtypes of the virus exist (types A-G), each of which vary only by a few nucleotides. Each subtype is typically constrained to a specific geological region and pathogenicity is not reported to be impacted by these small genomic variations[13]. Additionally, there are no significant differences between viral genotypes infecting

asymptomatic carriers and genotypes which cause disease, suggesting that pathogenesis relies on other, non-viral factors[14]. HTLV-2 infection is less common, with endemic areas constrained to West Africa and Native Amerindian populations in the Americas[15]. Additionally, HTLV-2 is more commonly reported in intravenous (IV) drug-using populations throughout the world[16].

Interpersonal Transmission: One of the major routes of HTLV-1 infection is from an infected mother to her child through breastfeeding, which occurs at a rate of about 20%. The risk of transmission increased with prolonged length of breastfeeding, and with high maternal proviral load[17,18]. Proviral load in HTLV-1 carriers is quantified by quantitative PCR, and because the majority of infected cells are shown to contain a single copy of the provirus, proviral load therefore corresponds to the number of HTLV-1-infected cells within the host[19,20]. Because cell-free virions are reported to be unstable and poorly infectious, maternal transmission is likely facilitated by the transmission of infected lymphocytes that are actively producing viral particles, which are transmitted to target host cells *via* cell-to-cell transmission[21–23]. Another major route of transmission is through unprotected sexual contact, in which it is presumed that the virus is passed in infected leukocytes found in semen and cervical secretions[23]. For both modes of transmission, the mechanism through which viral particles or virally-infected cells cross the mucosal epithelium and establish infection remains unclear.

HTLV-1 is highly infectious when transmitted through infected whole blood. Blood transfusion was reported to be an important risk factor for HTLV and seroconversion rates have been reported to be as high as 44% after one exposure to HTLV-1-positive whole blood[24–26]. Though the rates of transfusion-associated HTLV-1 infection were

once much higher, screening methods that detect anti-HTLV antibodies have significantly reduced transfusion-acquired infection[7]. Notably, transplant-acquired infections have also been reported, typically in cases in which organ donors are from HTLV-endemic areas[27]. Intravenous drug use also remains an important mode of transmission.

Viral Structure: The HTLV-1 virion is an enveloped deltaretrovirus with a moderately-sized diameter of 100nm (**Figure 1.1**). The viral core is composed of virally-encoded capsid (CA) proteins which form a poorly-defined polyhedral structure. Enclosed within the capsid are two identical strands of its positive-sense RNA genome stabilized by nucleocapsid (NC) proteins, as well as the viral protease (Pro), integrase (IN) and reverse transcriptase (RT)[28,29]. The core is surrounded by a layer of matrix (MA) proteins and an outer membrane, or envelope, which is derived from the host cell membrane. The envelope is studded with envelope glycoproteins (Env) that facilitate the adhesion of the viral particle to receptors on the target cell membrane prior to viral entry[28].

Cellular Transmission and *De Novo* Infection: After HTLV-1-infected leukocytes are passed to a new host, they are thought to come into contact with host dendritic cells. Some hypotheses suggest that virions produced from the infected cell collect on the surface of the dendritic cell and are transmitted to $CD4^+$ T-cells when dendritic cells make contact, as evidence supports that the majority of proviral load is attributable to $CD4^+$ T-cells[30]. However, some evidence supports that dendritic cells themselves may become infected, as dendritic cells are shown to be more receptive than $CD4^+$ T-cells to HTLV-1 infection *in vitro* and virally-infected dendritic cells were observed in peripheral

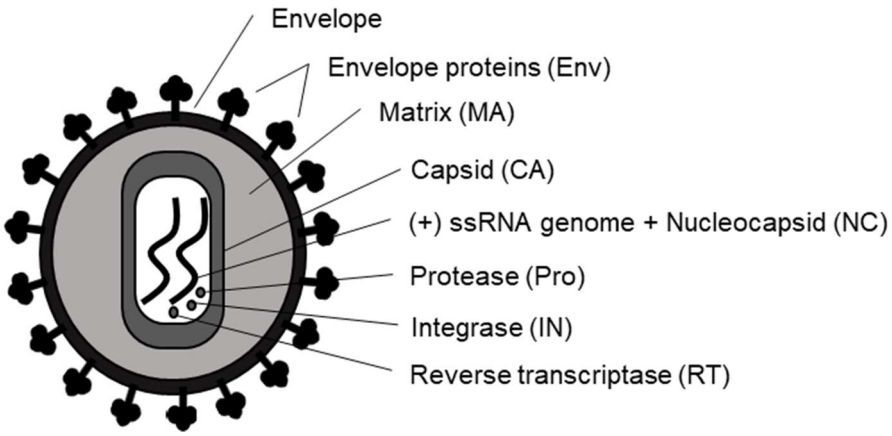

Figure 1.1: The structure of Human T-cell Leukemia Virus. The viral particle is composed of an outer envelope membrane, studded with viral envelope proteins (Env), which include surface glycoprotein (SU) and transmembrane glycoprotein (TM) subunits (not shown). The envelope surrounds a layer of matrix protein (MA). The viral core consists of capsid proteins (CA), which surround two copies of the positive-sense, single-stranded RNA genome stabilized by nucleocapsid proteins (NC). The viral enzymes protease (Pro), integrase (IN), and reverse transcriptase (RT) are also packaged into the capsid.

blood *in vivo*[31,32]. More investigation will be required to determine the role of dendritic cells in establishing HTLV infection.

HTLV-1 productively infects $CD4^+$ T-cells, but the cellular receptors that are exploited to facilitate viral entry are not completely understood. Glucose transporter 1 (GLUT1) is upregulated in activated $CD4^+$ T-cells and has been demonstrated to be an important receptor for HTLV-1 virions[33–35]. Additional work supports that heparin sulfate proteoglycans (HSPG), which are also upregulated upon T-cell activation, promote infection by HTLV-1, but not HTLV-2, indicating a degree of transmission variability between HTLV types[35–38]. Recent work has also implicated the neuropilin 1 receptor (NRP-1) as a receptor for HTLV-1 entry[35,39,40]. The tri-receptor complex model of HTLV-1 infection proposes that HSPG make initial contact with viral envelope glycoproteins to tether the virus to the host cell membrane. Close proximity increases the likelihood that an interaction will form between NRP-1 and the envelope proteins, triggering a conformational change which exposes the GLUT1 binding site on the envelope protein, which initiates fusion of the viral envelope with the host cell membrane[35].

HTLV-1 virions are most efficiently transmitted through cell-to-cell contact, as cell-free virions are reported to be unstable, possibly due to instability of membrane-bound Env proteins and some intrinsic instability of the viral core structure[41]. One major route of cell-to-cell transmission is through the formation of a virological synapse (VS), which is composed of interacting cellular adhesion proteins lymphocyte function-associate antigen 1 (LFA1) and intercellular adhesion molecule 1 (ICAM-1). Synapse formation anchors the two cells together and results in polarization of the microtubule-

organizing center (MTOC) in the infected cell toward the cell junction, which appears to be important for viral transmission (**Figure 1.2.A**)[41,42].

Interestingly, biofilm-like extracellular viral assemblies have also been reported in conjunction with the VS. These assemblies are reported to contain viral particles and are composed of the carbohydrates collagen and galectin-3, as well as the proteoglycan agrin (**Figure 1.2.B**)[43]. It is postulated that these structures serve multiple functions, including enhancing viral transmission, serving as protective structures to counteract immune recognition and prevent damage to virion structures during cellular migration through blood and lymph circulation[44]. Finally, HTLV-1 viral particles may also be transmitted to target cells through contact of filopodia-like cellular conduits, though some evidence supports that a smaller version of the VS located at conduit termini may still facilitate transmission[41,45,46].

As with all retroviruses, HTLV-1 viral DNA is permanently integrated into the host cell genome. Therefore, the proliferation of infected cells also represents a clinically important mechanism through which proviral load is increased (**Figure 1.2.C**)[14]. During mitosis, the proviral DNA is efficiently replicated and packaged into daughter cells. This process, known as clonal expansion, contributes significantly to viral pathogenesis and will be discussed in more detail later in this chapter.

Retroviral Replication: Once the virus enters a $CD4^+$ T-cell, the retroviral genome must be reverse transcribed into a dsDNA intermediate and trafficked to the nucleus for integration. Reverse transcription of the retroviral genome remains poorly understood, yet it is hypothesized that the viral capsid structure is degraded as it traffics through the cytoplasm, and that the initiation of reverse transcription may be linked to capsid

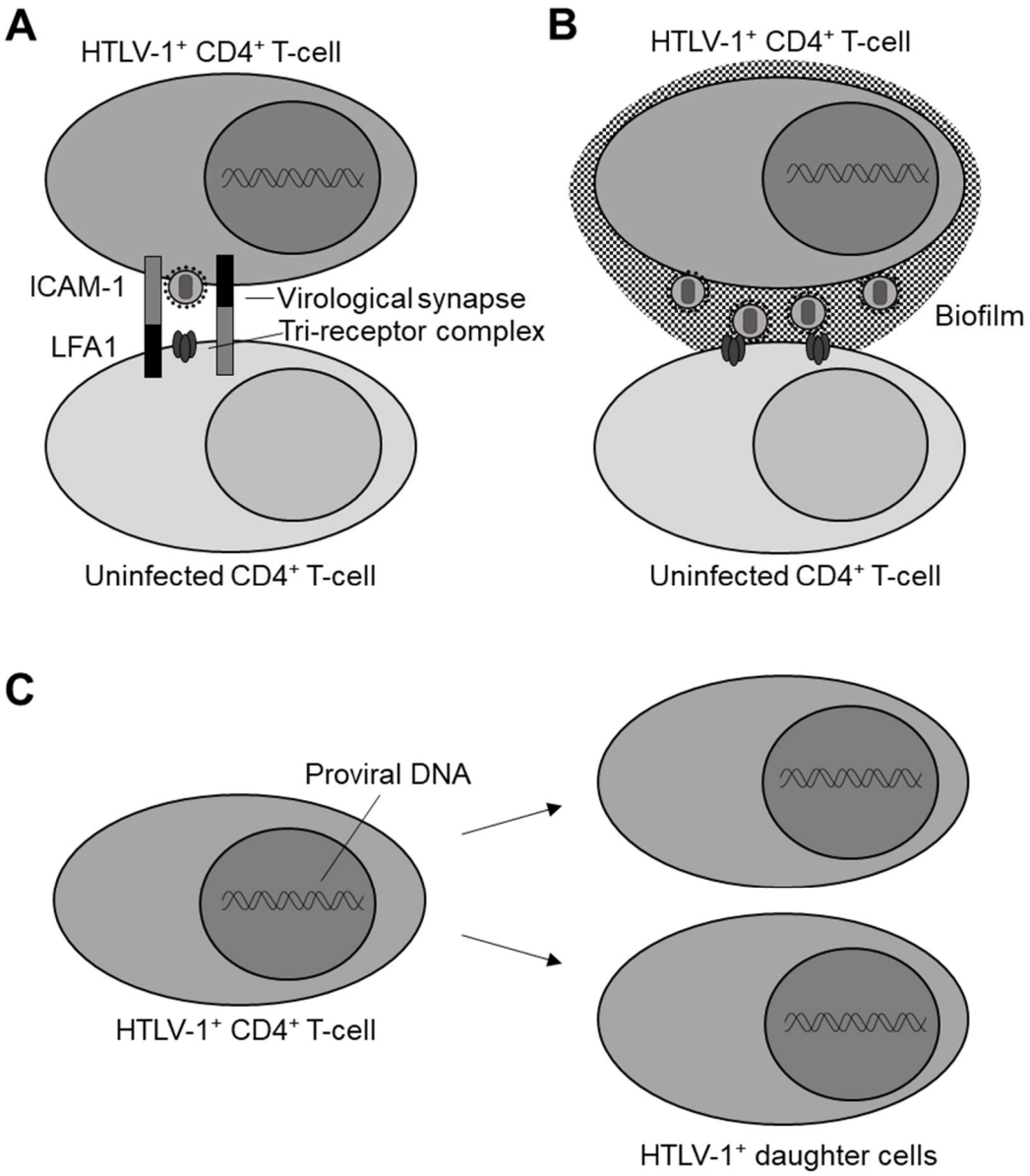

Figure 1.2: Routes of HTLV-1 cell-to-cell transmission. (A) Virological synapses, which are formed from cellular adhesion molecules ICAM-1 and LFA1, tether infected cells to target cells and provide a space into which viral particles bud, mature, and adhere to target cell tri-receptor complexes. **(B)** Virally-infected cells form an extracellular, carbohydrate-rich, biofilm-like matrix which concentrates and protects viral particles, while enhancing cell-to-cell transmission in conjunction with virological synapses. **(C)** Clonal expansion of HTLV-1-infected cells occurs when infected cells undergo cell division, and the cellular genome, complete with permanently-integrated proviral DNA, is duplicated and packaged into the daughter cell.

degradation, as cellular tRNAs are suspected to prime reverse transcription[47,48]. Synthesis of the dsDNA genome from the ssRNA genome is carried out by the virally-packaged RT and Pol enzymes[49,50]. In the hypothesized model of reverse transcription, a cellular tRNA primes the synthesis of a negative sense DNA strand (**Figure 1.3.A**) to form a RNA-DNA heteroduplex (**Figure 1.3.B**), followed by the degradation of the positive-sense RNA strand by RT RNAse H activity, leaving a negative sense ssDNA intermediate (**Figure 1.3.C**)[50]. The viral polymerase synthesizes the complementary positive sense DNA strand, resulting in dsDNA viral genome (**Figure 1.3.D**). During this process, the unique 5' (U5) and unique 3' (U3) untranslated regions are duplicated to create complete U3-R-U5 sequences that flank the viral DNA. These highly repetitive regions make up the 5' and 3' long terminal repeats (LTR), which contain important transcriptional *cis*-regulatory sequences[51–53].

Integrase interacts with the DNA termini at the U3 and U5 regions located on the 5' and 3' ends of the viral dsDNA to form the pre-integration complex (PIC) (**Figure 1.3.D**)[48,54]. The PIC is imported into the nucleus, possibly through nuclear pore complex (NPC) mediated transport, and IN facilitates strand transfer to permanently insert the viral dsDNA into the cellular genome. Integrated viral DNA will subsequently be referred to as the provirus. Most infected cells contain a single copy of the provirus, however about 10% of infected cells contain two proviral copies[55,56]. Although early evidence suggested that proviral integration sites are randomly located within the cellular genome, more recent findings support that the viral genome integrates into transcriptionally-active sites[20,57–61]. It is possible that integration into these sites confers

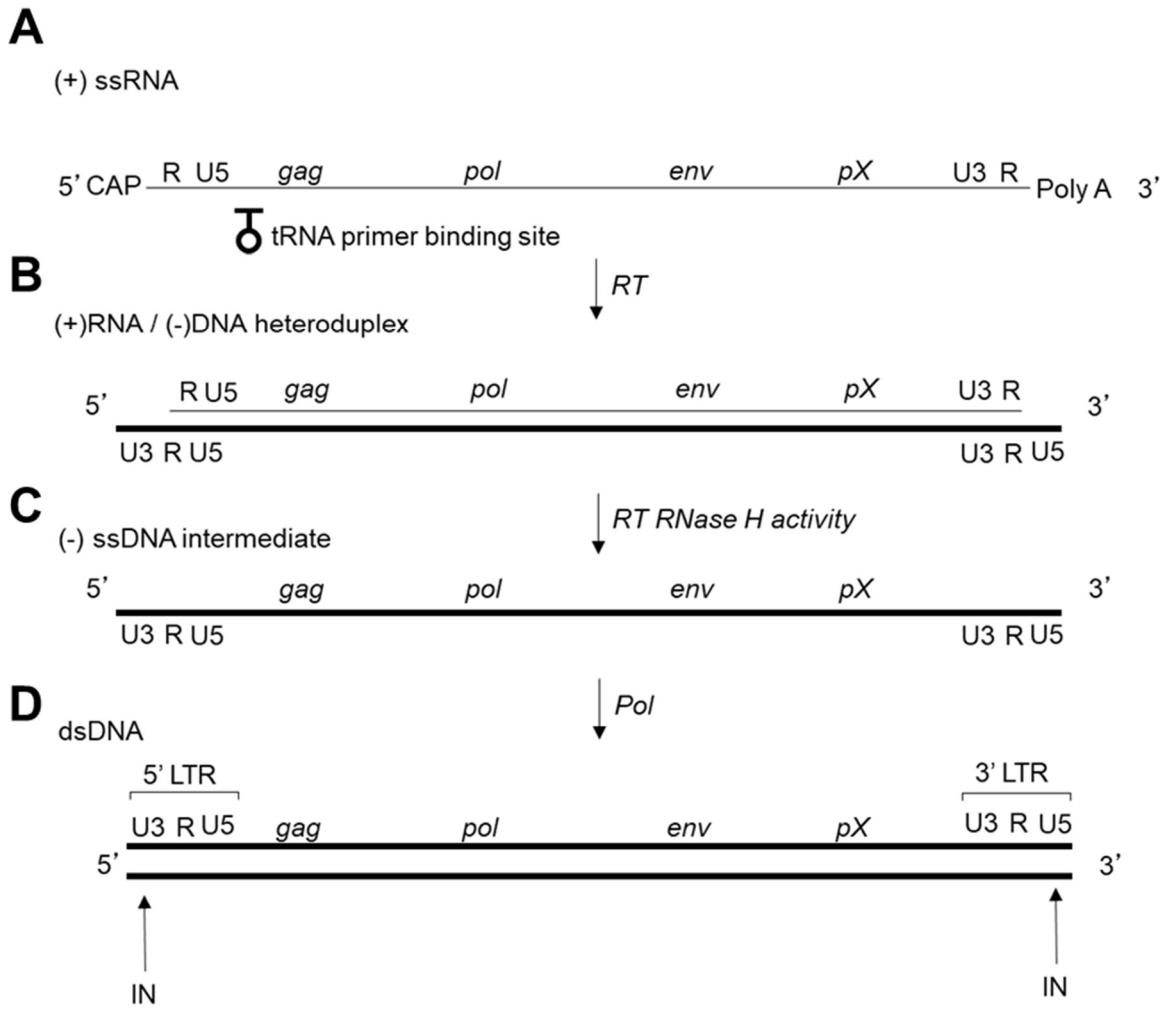

Figure 1.3: Retroviral reverse transcription and integration. The HTLV-1 positive-sense ssRNA genome (**A**) is reverse transcribed by pre-packaged viral reverse transcriptase (RT) using a cellular tRNA primer to form a (+)RNA/(-) DNA heteroduplex (**B**). Intrinsic Rnase H activity of RT degrades the (+) RNA strand (**C**), and the viral polymerase (Pol) synthesizes the complementary (+) DNA strand, forming a complete dsDNA genome (**D**). Viral integrase (IN) interacts with the termini at the U3 and U5 regions to facilitate integration into the host genome, forming the provirus.

a survival advantage to the infected cell, however it is unclear whether integration site alone specifically contributes to pathogenesis[14,56].

Proviral Gene Expression: HTLV-1 is classified as a complex retrovirus, indicating that in addition to encoding the simple retroviral structural genes Gag, Pro, Pol, and Env, it also contains a pX region that encodes regulatory and accessory viral proteins (**Figure 1.4**). Though our understanding of pX region-encoded proteins remains incomplete, emerging evidence supports that they are important for certain aspects of HTLV-1 infection[62,63]. HTLV-1 accessory proteins are proposed to play indirect roles in viral replication and infectivity. For instance, p12 is a hydrophobic protein that is reported to localize to endoplasmic reticulum and golgi membranes to affect intracellular calcium signaling. Meanwhile, p13 is reported to localize to mitochondrial membranes to induce depolarization and upregulate cellular respiration. Finally, p30 is a putative transcription factor which may influence cellular and viral gene expression early in infection[63–65]. Regulatory proteins, which include Transactivator X (Tax) and the HTLV-1 basic leucine zipper factor (HBZ), directly influence proviral gene expression. Tax is reported to upregulate proviral gene expression through an interaction with cellular transcription factor cAMP response element binding protein (CREB) and coactivators p300 and CREB-binding protein (CBP) to promote proviral gene expression at Tax-responsive elements (TxREs) located in the U3 region of the 5' LTR (**Figure 1.4**)[51–53,66–76]. Conversely, HBZ is reported to sequester cellular transcription factors and coactivators, including p300 and CREB, to negatively regulate transactivation of the 5' LTR (**Figure 1.4**)[77–82]. These two regulatory proteins have been extensively studied and will be discussed in more detail later in this chapter.

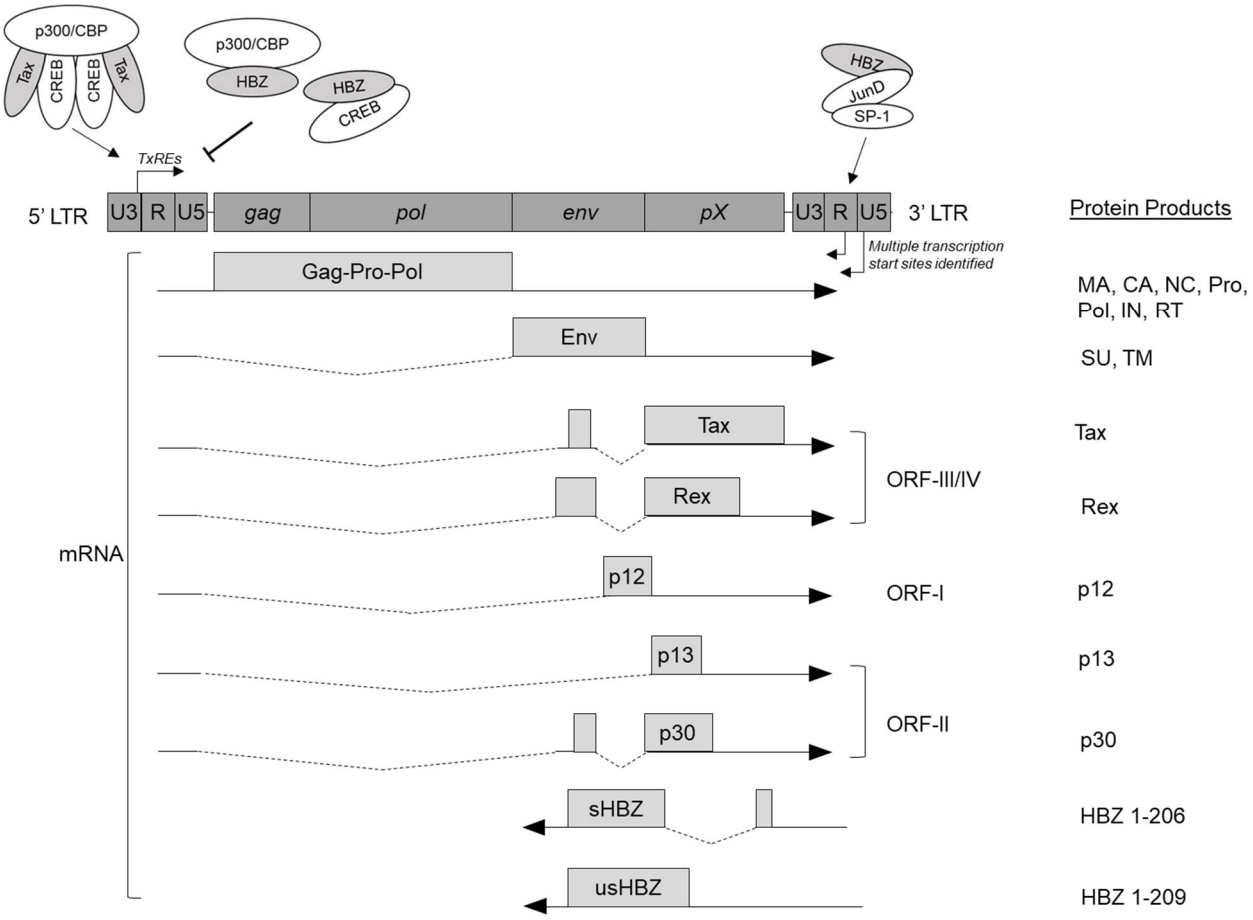

Figure 1.4: Expression of the HTLV-1 proviral genome. The HTLV-1 provirus is permanently integrated into the host cell genome at near-random locations by the actions of the viral integrase. The provirus is flanked on the 5; and 3' ends by a long terminal repeat region (LTR), which contains untranslated regions (U3, U5) and a region of repetitive sequence (R). Sense proviral transcription is upregulated at the 5' LTR by the viral regulatory protein Tax, in conjunction with cellular transcriptional regulators p300/CBP and CREB. Transcription from the 5' LTR produces one transcript encoding the Gag-Pro-Pol polyprotein. The transcript is singly spliced to produce the Env transcript. Viral accessory and regulatory proteins are encoded in the pX region and are expressed through complex alternative splicing. Antisense transcription is regulated by multiple transcriptional start sites in the 3' LTR and produces the viral regulatory protein HBZ in two forms: spliced (HBZ Sp1) and unspliced (HBZ US). HBZ interacts with cellular transcription factors JunD and SP-1 to enhance antisense transcription *via* SP-1 binding sites in the 3' LTR R and U5 regions. Additionally, HBZ downregulates sense proviral gene expression by sequestering p300/CBP and CREB away from Tax.

HTLV-1 encodes a great number of viral proteins within the span of approximately 8,200bp[83]. In order for all of its genes to be expressed, the virus utilizes a variety of transcriptional, transcript splicing, and post-translational mechanisms. Tax transactivates the transcription of a single, polycistronic transcript which must undergo extensive alternative splicing to produce singly and doubly spliced mRNAs (**Figure 1.4**). The full-length Gag-Pro-Pol transcript encodes three proteins: The Gag polyprotein, the Pol polyprotein, and the viral protease. Subsequent proteolytic cleavage of polyproteins creates the viral structural and enzymatic gene products MA, CA, NC, POL, IN, and RT (**Figure 1.4**)[48,84–86]. Complex transcript splicing patterns allow ribosomes to read four unique open reading frames (ORF I-IV) within the pX region during translation, producing Tax, Rex, p21, p30, p13, and p12 (**Figure 1.4**)[65,87]. Additionally, the virus also encodes a unique regulatory protein, HBZ, on its antisense strand[77,88–90]. Unlike the viral genes encoded on the sense strand of the provirus, HBZ transcription initiates from the 3' LTR, in which multiple transcriptional start sites in the R and U5 regions have been identified[91]. HBZ has been observed in an unspliced form (usHBZ, 209aa) and a slightly shorter, spliced form (sHBZ, 206aa) (**Figure 1.4**)[92–94]. Interestingly, the spliced form of HBZ has been observed to be more functional than the unspliced form, and its expression was also reported to be four times greater than that of the unspliced transcript in HTLV-1-infected cells. As such, the sHBZ is the more commonly studied variant and here, subsequent referral to HBZ implies the spliced variant[95,96].

Virion Assembly: After post-transcriptional processing of viral mRNAs is completed, the viral protein Rex interacts with Rex responsive elements (RxRE) in the U3 and R regions of the mRNA and facilitate nuclear export through nuclear pore complexes

(NPCs)[97–101]. Once viral transcripts reach the cytoplasm, free host ribosomes produce protein from doubly spliced transcripts, while membrane-bound ribosomes synthesize singly spliced transcripts to produce envelope proteins[48,85]. Envelope polyprotein precursors are glycosylated and proteolytically cleaved by cellular furin-like proteases as they traffic through the Golgi before they are secreted in their functionally active forms: surface glycoprotein (SU) and transmembrane glycoprotein (TM)[102]. Concurrently, viral genomic RNAs are also produced and exported from the nucleus. Though retroviral RNA trafficking mechanisms have yet to be elucidated, some evidence suggests that simple diffusion may be responsible[103]. The Gag and Pol polyproteins are trafficked to the cell membrane where they interact with genomic RNA to assemble new viral particles through complex Gag-Gag oligomerization. The virus buds through the host cell membrane, acquiring its outer envelope studded with SU and TM proteins[48].

After budding, retroviral particles are reported to undergo maturation in order to become fully infectious. During this process, the viral protease cleaves the Pol polyprotein to produce IN and Pol proteins, while the Gag polyprotein is cleaved to produce CA, MA, and NC proteins (**Figure 1.1**)[29,48,85,104]. Evidence supports that improper viral maturation results in the formation of a poorly defined core structure and poor infectivity. Development of infectious HTLV-1 viral particles is not well studied, and it remains unclear whether maturation is required. Interestingly, cryo-electron tomographic analysis of HTLV-1 virions showed that only 15% of new viral particles observed had a defined core structure, while 60% of observed virions had an undefined

core[29]. This evidence may help explain why cell-free HTLV-1 infectivity is so poor in comparison to other retroviruses

HTLV-1 and Human Disease: In HTLV-1-infected individuals, high proviral load in peripheral blood mononuclear cells (PBMCs) is reported to increase the risk of transmission and acquisition of an HTLV-1-associated disease[18,105–116]. HTLV is the causative agent of several diseases, including HAM/TSP, ATL, HTLV-1 associated uveitis, and HTLV-1-associated infectious dermatitis. Immune suppression has also been reported to increase the risk of developing opportunistic infections such as tuberculosis and strongyloidiasis. Higher frequencies of arthritis, fibromyalgia, urinary tract infections, and depression are also reported in HTLV-1-infected populations[7]. This review will focus only on the literature concerning ATL and HAM/TSP.

HTLV-1-Associated Myelopathy/ Tropical Spastic Paraparesis: HAM/TSP is a progressive neurodegenerative disorder which is characterized by spastic paraparesis, bowel and/or bladder dysfunction, and marked changes in lower limb sensory function[5,6,117]. HAM/TSP develops in an estimated 1% of HTLV-1-infected individuals and is associated with blood-borne transmission of the virus. HAM/TSP occurs more commonly in women rather than men, and a high proviral load remains the most important risk factor for pathogenesis. Additional risk factors include the presence of the HLA-DRB1*0101 allele and polymorphisms in genes which encode pro-inflammatory cytokines TNFα and IL-15[106,108,118–120]. Though the exact mechanism of pathogenesis remains unclear, the disease is thought to be immune-mediated. It has been proposed that HTLV-1 can infect glial cells, which may be targeted and lysed by HTLV-specific cytotoxic T-cells. Another hypothesis suggests that HTLV-1-infected leukocytes migrate

to the central nervous system (CNS) compartment, where they are also targeted by HTLV-specific $CD8^+$ T-cells; however, the release of pro-inflammatory cytokines may also damage neighboring CNS cells, a phenomenon known as the bystander effect[121,122]. Additional evidence supports that anti-HTLV antibodies cross-react with self-antigens in the CNS through a process known as molecular mimicry[123–125]. Finally, one transcriptional analysis study reports that HAM/TSP is associated with the overexpression of interferon-stimulated genes, however it is unclear whether pathogenesis is caused by, or merely the result of, changes in interferon-regulated gene expression[126,127].

Currently, there are no effective treatments that improve long-term patient condition, however some short-term improvements have been reported in patients treated with corticosteroids, plasmapheresis, intravenous gammaglobulin, anti-CD25 IL-2 signaling inhibitor, interferons, and nucleoside analogs[128–140]. Further study will be required to evaluate the long-term benefits of these treatments for HAM/TSP patients.

Adult T-cell Leukemia: The most severe HTLV-1-associated disease is ATL, an aggressive lymphoproliferative disorder that results from the expansion of HTLV-1-infected $CD4^+$ T-cells. ATL cells are highly migratory due, in part, to changes in the expression of cell surface adhesion proteins, and have been reported to infiltrate numerous tissue types[141–144]. Hypercalcemia is a major, and often fatal complication that is reported in 70% of ATL patients and is caused by an increase in the number of bone osteoclasts which promote increased bone resorption[145,146]. Though ATL occurs in fewer than 5% of HTLV-1 positive individuals, it remains exceedingly difficult to treat

with chemotherapeutics and anti-retroviral drugs; ATL patients typically succumb to the disease in a matter of months[147].

The development of ATL is associated with vertical transmission of the virus through breastfeeding[148–150]. ATL most commonly affects men and symptoms first appear in people aged 40 to 50 years old. Additional risk factors include high proviral load, high anti-HTLV-1 antibody levels, a history of infectious dermatitis, and smoking. Infected people who have a family history of ATL are also more likely to develop the disease, suggesting that some aspects of disease susceptibility may be hereditary[141,151,152]. Diagnosis of ATL is made when abnormally-shaped leukocytes with polylobulated nuclei are observed in peripheral blood and anti-HTLV-1 antibodies in the peripheral blood are detectable[153].

ATL severity is categorized into four clinical subtypes based upon lymphocyte count, the percent of atypical lymphocytes observed, lactate dehydrogenase levels, calcium levels, as well as the presence of certain symptoms including lymphadenopathy, ascites, pleural effusion, and lesions of the skin, lungs, liver, spleen, gastrointestinal tract, or central nervous system[7,154]. The least severe Smoldering and Chronic subtypes are slowly progressing manifestations of ATL which have survival rates ranging from one to five years. The most severe Lymphoma and Acute subtypes, which account for the most commonly diagnosed forms of ATL, are rapidly progressing leukemic manifestations with survival rates of four to ten months[7,147,154,155].

Classifying ATL subtypes help clinicians develop treatment plans for their patients. For example, patients diagnosed with smoldering and chronic ATL subtypes are typically not treated, but rather a “watchful waiting” protocol is employed and

chemotherapeutic treatment may be implemented as symptoms worsen[154,156,157]. However, after decades of clinical study, an effective standard treatment has yet to be implemented because current chemotherapeutic and antiretrovirals are ineffective for treating ATL for either the short- or long-term[153,155,158]. Patients with less severe symptoms, such as skin lesions or opportunistic infection, are treated with zidovudine (AZT), a nucleoside analog reverse transcriptase inhibitor, and interferon alpha (IFN-α). In addition to antiretrovirals, combination chemotherapeutic approaches are also used in patients with severe ATL subtypes. Possible regimen components include cyclophosphamide, doxorubicin, vincristine, prednisone, etoposide, dexamethasone, ranimustine, vindesine, and carboplatin[155].

For ATL patients who respond to therapy, allogeneic hematopoietic stem cell transplantation (allo-HSCT) may be recommended and has shown promising results for long term survival[155,159–161]. However, locating matching donors remains an obstacle to this approach. Furthermore, decreased transplant success rate is associated with increasing age, and ATL typically occurs in the later years of life. Importantly, allo-HSCT is recommended only for patients who respond well to initial chemotherapeutics, but not for non-responding patients. For these individuals, only supportive care can be given. As such, there is a great need to develop novel treatment options which are efficacious in non-responders. A number of clinical trials are currently ongoing to evaluate the efficacy of novel drugs in ATL patients. Classes of drugs under evaluation include antimetabolites, leukocyte-specific monoclonal antibodies, proteasome inhibitors, kinase inhibitors, immunomodulatory drugs, and HDAC inhibitors (**Table 1**).

Drug class	Drug name	Mechanism of Action
Antimetabolics	Cladribine	Purine nucleoside analogue; phosphorylated derivatives accumulate in lymphocytes to cause DNA damage and cell death.
	Clofarabine	Nucleoside metabolic inhibitor; DNA polymerase and ribonucleotide reductase inhibitor; disrupts mitochondrial membranes
	Pralatrexate	Folate analogue; dihydrofolate reductase inhibitor; competitive inhibitor of folylpolyglutamyl synthase
Monoclonal antibodies	Mogamulizumab	Anti-CCR4 MAb; reduces leukocyte migration, promotes antibody-dependent cytotoxicity (ADCC)
	Daclizumab	Anti-CD25 MAb; blocks IL-2 binding and subsequent signaling
	Brentuximab vedotin	Anti-CD30 MAb conjugated to cytotoxic agent monomethyl auristatin E (MMAE) via a protease cleavage linker; Binds CD30, is internalized, and toxin is cleaved and released into the cytoplasm.
	Alemtuzumab	Anti-CD52 MAb; promotes ADCC
Proteasome inhibitor	Bortezomib	Reversible 26S proteasome inhibitor; blocks degradation of NF-κB inhibitor IκBα to prevent activation of NF-κB pro-survival mechanisms
AKK inhibitor	Alisertib	Aurora K kinase inhibitor; causes G_2M arrest and impairs cell division to induce apoptosis
Immunomodulatory agents	Lenalidomide	Thalidomide analogue; inhibits proliferation and induces apoptosis in some hematopoietic tumor cells
Vaccines	Tax-DC	Autologous dendritic cells (DC) pulsed with Tax peptide (CTL epitopes); augments anti-HTLV-1 cytotoxic T-cell response.
	THV02	Lentiviral vectors encoding a polypeptide derived from Tax, HBZ, p12, and p30; Induces an anti-HTLV-1 cellular immune response in animal models.

Table 1.1: Novel ATL therapeutic targets. The table outlines new drugs, and their mechanisms of action, that are currently under investigation for the treatment of ATL.

Interestingly, two anti-HTLV-1 vaccines are also in the early stages of development. One vaccine approach is an autologous transfer of patient dendritic cells pulsed with Tax peptide fragments which correspond to cytotoxic T-cell recognized epitopes, and are expected to enhance the Tax-specific CTL response[162]. Secondly, the THV02 vaccine consists of lentiviral vectors which encode a unique HTLV-1 polypeptide composed of Tax, HBZ, p12, and p30 immunogenic peptide fragments. This peptide is expected to stimulate a robust cellular response against HTLV-1-infected cells and has shown some success in animal models[163]. These novel therapeutic approaches and vaccines have been extensively reviewed elsewhere[155]. However, it is important to consider that the majority of clinical trials for ATL patients take place primarily in Japan and fail to take into account differences in eastern and western HTLV strains and differences in population-specific risk factors. Even if these therapies show promise in eastern trails, further clinical data and trials that target patients in western endemic countries will be required to establish effective treatment plans in these regions.

A Model for ATL Development: The mechanisms by which HTLV-1 drives the progression of ATL are not completely understood. The current model of ATL development is divided into two phases: *de novo* viral infection and clonal expansion. Both of these mechanisms are important for increasing HTLV-1 proviral copy number.

The early stage in infection is dominated by *de novo* viral replication and cell-to-cell transmission of virions, which is important for expanding the diversity of HTLV-1-infected cell clones (**Figure 1.5**). Virally-infected clones are identified by proviral copy

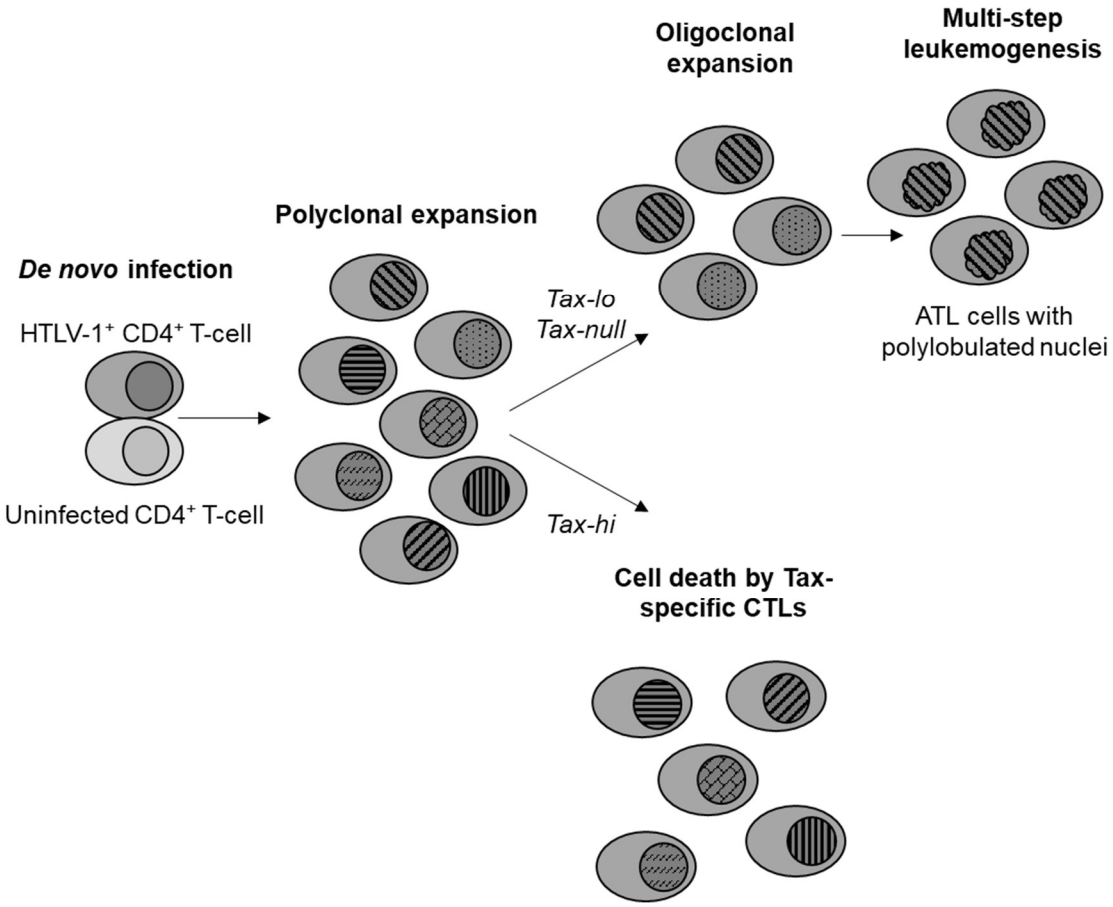

Figure 1.5: Clonal expansion of HTLV-1-infected lymphocytes. HTLV-1-infected cell clones are established through cell contact-dependent *de novo* infection and are differentiated though proviral integration site, denoted in this diagram by different nuclear fill patterns. Early in infection, the clonal pool is diverse, reflecting continued *de novo* infection. Proviral load concurrently increased through polyclonal expansion. Viral antigens, mainly Tax, prime a robust CTL response which target clones expressing high levels of Tax (Tax-hi). Clones expressing low levels of Tax (Tax-lo), or have silenced sense strand gene expression altogether (Tax-null), escape negative selection and continue to proliferate (oligoclonal expansion). Cellular longevity, increased proliferation, and the accumulation of genetic damage promote transformation in one clone, resulting in a leukemic phenotype (ATL).

number and proviral integration site[19,60]. Though integration site selection is not yet completely understood, the virus requires the open DNA conformation found in euchromatin[164,165]. Furthermore, retroviral integration is hypothesized to be influenced by host factors and be biased toward specific palindromic nucleotide motifs[58–60]. Notably, some clones exist in high abundance while others exist in low abundance. This may be due to the orientation of the provirus in its integration site, and whether it integrated within a coding region or close to transcriptional start site[61,164]. Interestingly, it is estimated that HTLV-1 infection can produce between 20,000 and 50,000 cellular clones in circulating blood, not considering clones that may be constrained to lymphoid tissues[166].

Although *de novo* replication is important for establishing HTLV-1 infection and the polyclonal pool of infected lymphocytes, it is also associated with increased viral antigen presentation and the priming of a robust cytotoxic T-cell (CTL) response (**Figure 1.5**). Anti-HTLV CTLs have been demonstrated to primarily recognize antigen derived from sense strand encoded proteins, mainly Tax[167]. However, the antisense protein HBZ does not elicit a similar immune response[168]. Therefore, it is expected that negative selection is primarily based upon Tax expression, resulting in the elimination of cell clones expressing moderate to high levels of Tax and the evasion of cell clones expressing little, or no Tax.

CTL immune evasion is mediated primarily by modulation of sense proviral transcription to reduce Tax expression. Some clones have been documented to introduce mutations into the Tax-encoding gene sequence within the proviral DNA, while others reduce Tax expression through the deletion or hypermethylation of the 5’

LTR[19,169–173]. The reduction in the level of Tax confers a survival advantage within host cells and experimental observations confirm that Tax transcripts are absent in over 60% of ATL cases. Furthermore, by maintaining these cells in culture to remove negative selective pressure, Tax expression is restored[170,174].

The surviving clonal population, or oligoclonal pool, exhibits survival advantages that allow them to persist and proliferate throughout infection (**Figure 1.5**)[14,19,175–178]. Clonal expansion of infected cells has been directly associated with ATL onset, supporting that this form of viral replication significantly contributes to pathogenesis (**Figure 1.5**)[110]. ATL is typically dominated by a single infected cell clone, which may originate from either a high abundance clone, or a low abundance clone[164,166]. In either case, the onset of disease is characterized by the rapid proliferation of a single clonal population, which comes to dominate the infection. However, in some cases of ATL, the dominant clone has been observed to be replaced by a secondary clone in a process known as clonal succession[179]. Therefore, multiple pathogenic clones may contribute to disease progression at different points throughout infection.

The progression of a single clone to a leukemic phenotype is proposed to be mediated by a multistep oncogenic process, requiring several pro-leukemogenic "hits"[166,180,181]. In this model, HTLV-1 infection serves as the first of a series of five to eight "hits" which cooperate to induce malignant transformation. Extensive work evaluating HTLV-1-meidated activation of cellular pro-oncogenic pathways suggests that subsequent "hits" result from viral manipulation of normal cellular processes which, in turn, drive disease progression[14,166,182]. The progression of some infected cell clones to malignancy may depend upon additional factors, such as the pattern of proviral gene

expression, which is likely strongly influenced by integration site, as well as clonal longevity[14,56,166].

The Role of HTLV-1 Regulatory Proteins Tax and HBZ in Transformation:

Extensive study of viral gene products has implicated both Tax and HBZ in oncogenesis. Though Tax and HBZ are important for coordinating proviral gene expression for *de novo* viral replication, clonal proliferation, and immune evasion, they are also reported to manipulate cellular gene expression. While this is generally thought to provide a favorable environment for viral replication and spread, it may also inadvertently activate pro-oncogenic mechanisms[14,183].

Though some evidence supports a role for Tax in HTLV-1-mediated oncogenesis, its contribution to transformation is still being evaluated. Tax is a potent transcriptional activator that, in addition to activating proviral gene expression, activates the expression of pro-proliferative cellular transcription factors ERG-1, ERG-2, Fra1, c-Jun, and JunD[184]. Tax has also been well documented to hyperactivate pro-survival canonical and non-canonical NF-κB pathways through the inhibition of negative control mechanisms located at multiple points in their respective signaling cascades[184–190]. A consequence of NF-κB hyperactivation is the overproduction enzymes which produce reactive nitrogen and oxygen species (RNOS)[191]. RNOS have been reported to accumulate within Tax-expressing cell lines, as well as in Tax-expressing HTLV-1-infected cell lines, likely in an NF-κB-dependent manner[192,193]. The accumulation of RNOS is well documented to cause damage to cellular structures, including DNA. Damage to cellular DNA is frequently observed in HTLV-1-transformed cells, which may result, in part, from the accumulation of intracellular RNOS[194]. Although DNA-damage

sensors typically function to detect genetic damage and trigger cell cycle arrest DNA-damage checkpoints, Tax has been reported to overcome checkpoint control mechanisms by upregulating the expression of cyclin D2, directly activating cyclin-dependent kinases (CDK), and repressing CDK inhibitors[187,195]. Furthermore, Tax attenuates the activation of some DNA damage repair pathways, including homologous recombination (HR), nucleotide excision repair (NER), base excision repair (BER), and mismatch repair (MMR)[195–199]. Considered as a whole, these reports support that Tax contributes to HTLV-1-mediated oncogenesis by initiating unrestrained cell cycle progression, directly and indirectly promoting the accumulation of genetic damage, and by activating pro-survival signaling pathways[200].

Though *in vitro* evidence supports that Tax plays an important role in oncogenesis, it is unlikely that it initiates transformation alone[201]. *In vitro* studies performed with rat primary fibroblasts indicated that Tax readily induces a transformed phenotype, resulting in cells that were resistant to apoptosis and were capable of forming tumors in mice[202–204]. To evaluate the role of Tax in HTLV-1-associated disease progression *in vivo*, Tax transgenic mouse models have been developed. In these various models, Tax expression has been demonstrated to cause spontaneous osteolytic bone lesions, induce granular lymphocytic leukemia, promote the onset of inflammatory diseases, induce hind limb paraparesis, and cause the development of a pre-T-cell leukemia/lymphoma[205–207]. However, work performed in human primary T-lymphocytes found that, unlike in rodent cells, transformation is a much rarer occurrence and that many of the pro-oncogenic functions of Tax, as described above, were only maintained in the presence of exogenous IL-2[201,208–212]. These data support

that Tax is, in actuality, a poor oncogene when acting alone and that Tax-mediated transformation may depend on other factors. Furthermore, Tax also serves as a major target of the host CTL response and its continued expression is only reported in less than 40% of freshly isolated ATL cells[167,170,174]. This evidence further supports that while Tax expression may contribute to the initiation of oncogenesis, its continued expression is not necessarily required for the development of a malignant phenotype.

HBZ is another viral regulatory protein that has been implicated in leukemogenesis and HTLV-1 disease progression. HBZ is encoded on the antisense strand of the provirus and its expression is regulated from the 3' LTR, which is not reported to acquire mutations or become methylated during infection (**Figure 1.4**)[77,213]. HBZ expression is maintained in all ATL cell lines and is observed to be expressed throughout all phases of HTLV-1 infection[95,96,214–216]. Additionally, experimental work supports that HBZ plays a major role in disease progression. Using an HBZ-transgenic mouse model, in which HBZ is expressed under a CD4 promoter, investigators demonstrated that HBZ produces symptoms consistent with disease progression, including increased $CD4^+$ T-cell count, increased prevalence of T-regulatory cells, the appearance of inflammatory lesions in the skin and lungs, and increased susceptibility to opportunistic infection[217–219]. Furthermore, HBZ expression has been recently linked to the development of osteolytic bone lesions; HBZ-expressing cells are reported to exhibit significantly increased expression of DKK1, a central mediator of bone resorption[220]. Additional work performed in an HBZ-transgenic mouse model shows the development of osteolytic bone disease, as evidenced by significant bone loss, increased bone-acting factors present in serum and increased expression of DKK1, as

well as two other bone resorption mediators RANKL and PTHrP, in HBZ-expressing splenic T-cells[221]. Finally, HBZ expression in transgenic mouse models also corresponds to the development of lymphoproliferative disease, including T-cell lymphomas and spontaneous hematopoietic cell tumors[217,221]. Though *in vitro* cellular immortalization studies found that HBZ expression alone is insufficient to induce transformation, its expression was found to be important for establishing infection within the host and for maintaining the survival of HTLV-1-infected cell populations[222,223].

HBZ is a transcriptional regulator characterized by three major domains: The N-terminal activation domain (AD), the central domain (CD), and the N-terminal basic leucine zipper (bZIP) domain (**Figure 1.6.A**). The activation domain contains two LXXLL-like motifs which facilitate HBZ's interaction with cellular coactivators p300 and CBP[82,224]. The central domain is important for the nuclear localization of HBZ, as it contains two nuclear localization signals. Likewise, the bZIP domain contains a third nuclear localization signal[225]. The bZIP domain is composed of a basic region, followed directly by a leucine zipper. Leucine zippers are comprised of a series of leucine heptad repeats and are common features of proteins in the bZIP transcription factor family, which includes the AP-1 family, the ATF/CREB family, the C/EBPG family, the CNC family, and the Maf family. The interaction between leucine residues is driven by their hydrophobicity, which facilitates heterodimerization among bZIP family members to form functionally-active transcriptional regulators (**Figure 1.6.B**). The basic region confers DNA-binding capability to the dimer, allowing for the recognition of AP-1 sites in gene promoters[226]. Importantly, HBZ dimerizes with some bZIP family proteins, but not all. For example, HBZ is reported to interact with ATF-1, ATF-2, ATF-7, c-Jun, JunB, JunD,

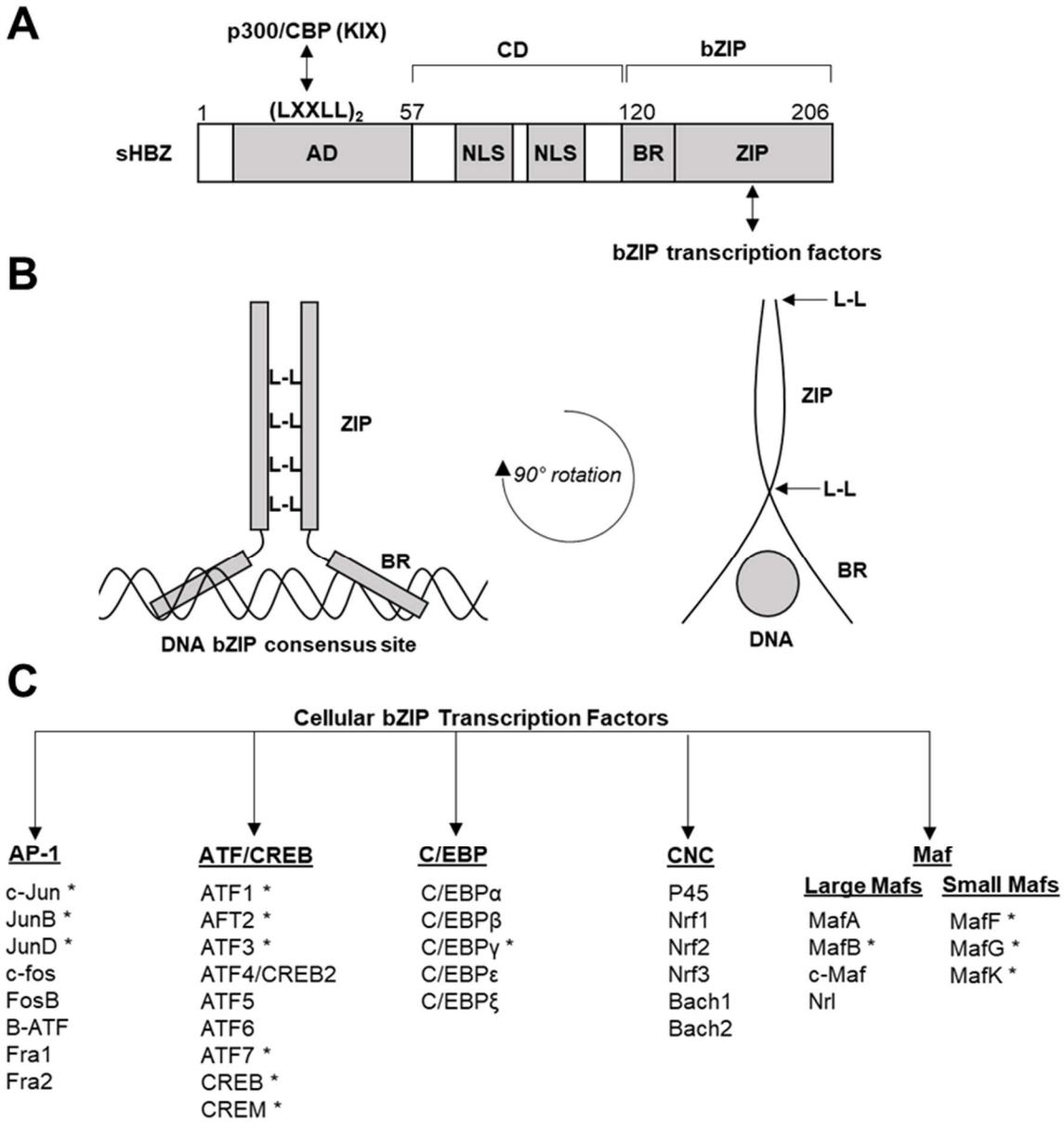

Figure 1.6: HBZ is a virally-encoded bZIP transcriptional regulator. (A) A schematic of the functional domains of HBZ. HBZ contains an N-terminal activation domain (AD), containing two LXXLL motifs ($LXXLL_2$) that interact with cellular coactivators p300/CBP via their KIX domain. The central domain (CD) contains two nuclear localization signals (NLS). The C-terminal basic region (BR) and leucine zipper motif (ZIP) compose the basic leucine zipper domain (bZIP), which selectively interacts with host cell bZIP transcription factors. **(B)** A schematic of a prototypical bZIP transcription factor dimer. The leucine residues (L) in the ZIP domain interact via hydrophobic interactions (L-L) to form an α-helical coiled-coil structure. Upon dimerization, the BRs undergo a conformational change which allows them to access the major groove of the DNA at a recognition site. A 90° rotation is shown to better depict the coiled-coiled ZIPs. **(C)** Human bZIP transcription factors are divided into 5 main families: Activator Protein 1 family (AP-1), Activating Transcription Factor/ cAMP Response Element Binding protein family (ATF/CREB), CCAAT Enhancer Binding Protein family (C/EBP), Cap'n'Collar family (CNC), and Musculoaponeurotic Fibrosarcoma family (Maf). * denotes that these proteins have been demonstrated to dimerize with HBZ.

CREB-1, MafG, and as reported in Chapter 3, MafF and MaK[78,79,81,227–230]. However, HBZ does not interact with Fos transcription factors, nor does it form stable homodimers[78,79]. Furthermore, its DNA-binding domain lacks the consensus sequence typically associated with DNA interactions (bb-bN-AA-b(C/S)R-bb)[78,81,225,231,232]. This evidence suggests that HBZ negatively regulates transcription by interacting with cellular bZIP transcription factors and sequestering them from their DNA-binding sites. Indeed, this hypothesis is supported by the observation that HBZ reduces transactivation at the proviral 5' LTR, which is achieved by (1) interacting with CREB to decrease its recruitment to TxREs in the 5' LTR, and (2) interacting with coactivators p300/CBP via their KIX domain to interfere with their ability to bind Tax (**Figure 1.4**)[77,81,82]. However, the exception to this hypothesis lies in the case of the HBZ-JunD-Sp1 complex, which is reported to activate transcription at the 3' LTR in an Sp-1-dependent manner (**Figure 1.4**)[233]. Furthermore, this complex was reported to exert control on cellular transcription by upregulating the expression of telomerase (hTERT)[228]. These reports suggest that HBZ has pleiotropic transcriptional activity, and further work is required to fully understand its impact of cellular gene expression.

HBZ Maintains Viral Persistence by Regulating Host Cell Proliferation and Survival: HBZ significantly contributes to clonal expansion of HTLV-1-infected lymphocytes by activating cell survival and proliferation pathways. HBZ expression is demonstrated to support cellular proliferation and survival *in vitro* and *in vivo*[93,229,234–239]. Pro-proliferative functions of HBZ include the inhibition of p53-dependent apoptosis, the activation of pro-survival pathways, and overcoming Tax/NF-κB-induced replicative senescence[240–245]. Interestingly, the bZIP domain of HBZ is believed to be important for

upregulating lymphocyte proliferation: antisense transcripts expressed by HTLV-2, HTLV-3, and HTLV-4 encode antisense proteins (AP-2, AP-3, AP-4) which lack the full bZIP domain and are unable to promote lymphoproliferation[246].

Interestingly, some reports also attribute HBZ mRNA transcripts with pro-proliferative functions. The majority of HBZ transcripts are retained in the nucleus, with only a small portion successfully transcribed. Experimental evidence suggests that nuclear HBZ mRNA may be important for epigenetic regulation of host cell gene expression[247]. Additionally, some findings implicate HBZ mRNA in the upregulation of cellular proliferation[93]. Importantly, little is known about HBZ mRNA function, therefore, the contribution of HBZ mRNA to disease progression is still widely debated.

Tax and HBZ Expression is Tightly Regulated to Maintain Viral Infection: Given that the *de novo* infection phase, the immune evasion phase, and the clonal expansion phase of infection exhibit different requirements for Tax and HBZ activity, it is expected that the expression of these proteins must be tightly regulated (**Figure 1.7**). Evaluation of leukemic cells isolated from ATL patients has shown that the production of sense proviral transcripts, which encode Tax, is suppressed in the majority of cases, but that antisense transcripts are consistently detectable. These finding were recently confirmed in single cell analysis of sense and antisense proviral transcripts[248,249]. The authors reported the continued presence of an antisense transcript, the expression of which was highly correlated with S and G_2/M phases of the cell cycle, possibly to ensure the successful portioning of HBZ protein into daughter cells. Conversely, sense transcripts were only detected in a small percentage of leukemic cells[248,249]. However, 5' LTR silencing is likely not permanent in most cell clones and reactivation may be

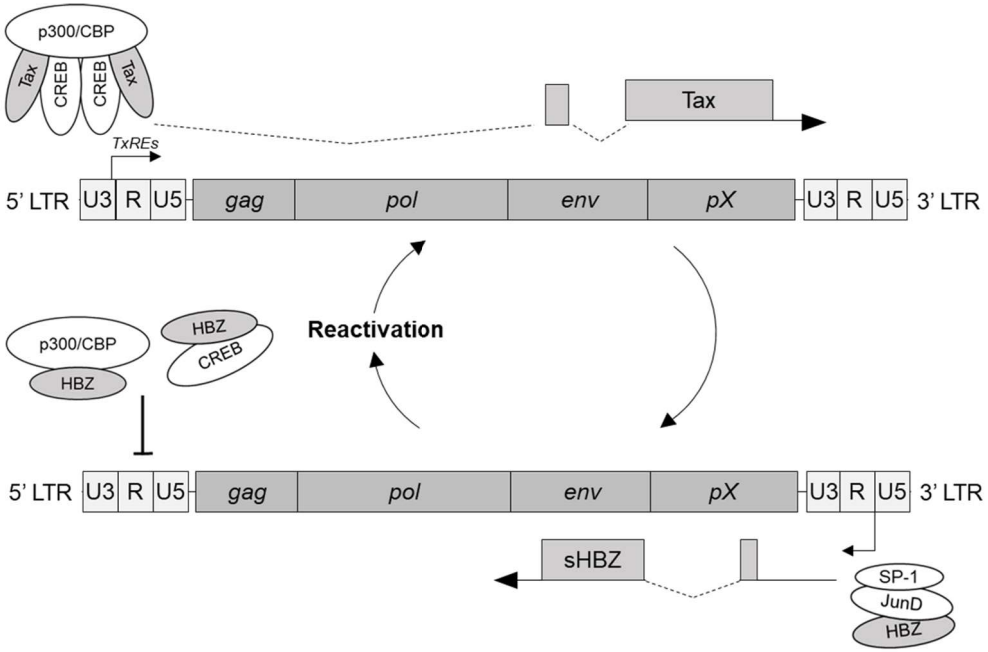

Prolonged Sense Transcription

NF-κB hyperactivation:
- Induces cellular senescence
- Produces ROS to further activate the 5'LTR

Inhibition of cellular checkpoints:
- Accumulation of genetic defects

CTL immune detection:
- Increased Tax levels allows the cell to be targeted by anti-Tax CTLs

Sustained Antisense Transcription:

Suppression of NF-κB:
- Prevents senescence

Immune evasion:
- Suppresses 5' LTR (Tax, p13) transcription
- Upregulates ROS detoxification to prevent 5' LTR reactivation*

Anti-apoptotic:
- Prevents DNA-damage induced cell death
- Prevents ROS-mediated cell death*
- Promotes accumulation of genetic defects*

Pro-proliferation signaling:
- Promotes clonal expansion

Figure 1.7: Proviral gene expression is extensively regulated. A model of proviral gene expression, regulated by the opposing transcriptional activities of Tax and HBZ. Sense transcription is upregulated primarily during early infection during *de novo* viral replication. Gene expression is regulated at the 5' LTR by Tax, p300/CBP, and CREB. Rare, sporadic reactivation of sense transcription has also been reported during later phases of infection. Antisense transcription is maintained throughout infection. Gene expression is regulated at the 3' LTR and is enhanced by HBZ, JunD, and SP-1. Outcomes of sense and antisense transcription are listed. *denotes processes which are investigated in more detail in chapters 2-3.

possible under certain cellular conditions[170,174,250]. Consistent with this hypothesis, the expression of sense transcripts was reported to be sporadically activated and deactivated independently of cell cycle progression[248,249]. It has been proposed that transient activation of Tax expression, known as a Tax transcriptional "burst", is required to activate viral replication for *de novo* infection and induce anti-apoptotic signaling which may play a role in promoting the continued survival of the infected cell population as a whole[249].

In summary, even though Tax was once thought to be the sole driver of leukemogenesis, a growing body of evidence suggests that HBZ may be playing a much more significant role. Given its continual expression, its manipulation of host gene expression, its roles in increasing cellular proliferation, as well as activities enhancing cellular longevity, HBZ likely increases the risk of developing pro-carcinogenic genetic abnormalities, which may ultimately contribute to ATL development. In light of this growing evidence, it was our goal to expand the understanding of the mechanisms utilized by HBZ to drive long-term viral persistence and activate pro-oncogenic events.

Specific Aims:

Aim 1: Evaluate the contribution of HBZ to host cell DNA damage responses and its role in the accumulation of genetic damage.

Rationale: Nuclear morphology is one of the main diagnostic markers of ATL. Leukemic cells are reported to contain polylobulated nuclei which arise from a variety of genetic aberrations, including gross chromosomal rearrangements stemming from double stranded DNA breaks. The HTLV-1-encoded oncoprotein Tax is well characterized to

induce genetic damage by increasing the production of reactive oxygen and nitrogen species, inhibiting DNA damage repair pathways, and bypassing cell cycle checkpoint control mechanisms. However, Tax expression is silenced in the majority of HTLV-1-infected cells, suggesting that virus-induced transformation depends upon additional factors. The virally-encoded protein HBZ contributes significantly to leukemogenesis. Unlike Tax, its expression is maintained throughout all phases of HTLV-1 infection and its activity is important for maintaining long-term survival and proliferation of infected cell clones. Preliminary evidence suggests that genetic damage is also associated with HBZ expression, suggesting the negative regulation of one or more DNA damage repair mechanisms. However, the effect of HBZ on DNA damage repair has not been assessed. Here, we aim to evaluate whether HBZ modulates the efficacy of DNA repair systems. Due to the contributions of double stranded DNA breaks to the development of the ATL phenotype, we will focus our analysis primarily upon the double-stranded DNA repair pathways homologous recombination (HR) and non-homologous end joining (NHEJ). Findings related to Aim 1 are presented in Chapter 2.

Aim 2: Assess the role of HBZ in the regulation of the cellular oxidative stress response.

Rationale: ATL cells are reported to harbor a high degree of drug resistance, rendering most chemotherapeutic strategies ineffective. Furthermore, the onset of multi-drug resistance in ATL patients is associated with aggressive disease progression and relapse. This suggests that HTLV-1 may manipulate cellular detoxification pathways to maintain the survival of the infected population. The virally-encoded oncoprotein HBZ is expressed consistently throughout infection and its activity is important for protecting

host cells from the induction of apoptosis and replicative senescence, thereby maintaining clonal proliferation of HTLV-1-infected cell populations. In many other cancer types, the expression of cytoprotective antioxidant genes is constitutively activated, promoting drug and radiation resistance, and negatively influencing patient outcome. Because HBZ is so important for maintaining the prolonged survival of infected cells, we questioned whether the transcriptional activities of HBZ influence the cellular antioxidant response as a cytoprotective mechanism. Here, we aim to evaluate the expression of antioxidant response genes in HBZ-expressing cells and determine if the cellular antioxidant response is important for host cell survival or proliferation. Findings related to Aim 2 are presented in Chapter 3.

Chapter 2

The HTLV-1 basic leucine zipper factor (HBZ) attenuates repair of double-stranded DNA breaks *via* non-homologous end joining (NHEJ)

Rushing AW[1], Hoang K[1], Polakowski N[1], and Lemasson I[1].

[1] Brody School of Medicine, Department of Microbiology and Immunology, East Carolina University, Greenville, NC, USA.

Abstract

Adult T-cell leukemia (ATL) is a fatal malignancy of $CD4^+$ T-cells infected with human T-cell leukemia virus type I (HTLV-1). ATL cells often exhibit random gross chromosomal rearrangements that are associated with the induction and improper repair of double-stranded DNA breaks (DSBs). The viral oncoprotein Tax has been reported to impair DSB repair, but is not shown to be consistently expressed throughout all phases of infection. The viral oncoprotein HTLV-1 basic leucine zipper factor (HBZ) is consistently expressed prior to and throughout disease progression, but it is unclear whether it also influences DSB repair. We report that HBZ attenuates DSB repair by non-homologous end joining (NHEJ), but not by homologous recombination (HR), in a manner dependent upon the basic leucine zipper (bZIP) domain. HBZ was found to interact with two vital members of the NHEJ core machinery, Ku70 and Ku80, and to be recruited to DSBs in a bZIP-dependent manner. We observed that HBZ expression also resulted in a bZIP-dependent delay in DNA-PK activation. Though Tax is reported to interact with Ku70, we did not find Tax expression to interfere with HBZ:Ku complex formation. However, as

Tax was reported to saturate NHEJ, we found this effect masked HBZ's attenuation of NHEJ. Overall, these data suggest that DSB repair mechanisms are impaired not only by Tax, but also by HBZ, and show that HBZ expression may significantly contribute to the accumulation of chromosomal abnormalities during HTLV-1 mediated oncogenesis.

Importance

Human T-cell leukemia virus type 1 (HTLV-1) infects 15-20 million people worldwide. Approximately 90% of infected individuals are asymptomatic and may remain undiagnosed, increasing the risk that they will unknowingly transmit the virus. Viral infection will cause about 5% of the HTLV-1 positive population to develop Adult T-cell Leukemia (ATL), a fatal disease that is not highly responsive to treatment. Though ATL development remains poorly understood, two viral proteins, Tax and HBZ, have been implicated in driving disease progression by manipulating host cell signaling and transcriptional pathways. Unlike Tax, HBZ expression is consistently observed in all infected individuals, making it important to elucidate the specific role of HBZ in disease progression. Here, we present evidence that HBZ could promote the accumulation of double-stranded DNA breaks (DSB) through the attenuation of the non-homologous end joining (NHEJ) repair pathway. This effect may lead to genome instability, ultimately contributing to the development of ATL.

Introduction

Genetic instability is a prominent feature in cellular transformation and is characterized by the accumulation of abnormalities in chromosomal number and

structure which may result in changes to tumor-suppressor or proto-oncogene expression[251,252]. Stability of the genome is particularly threatened by double-stranded DNA breaks (DSBs), which are acquired from both endogenous and exogenous sources[253,254]. Upon recognition of a DSB, DNA damage response checkpoint mechanisms arrest the cell cycle, and repair is initiated. While a failure in DSB repair can lead to apoptosis, incorrect repair poses a great risk for the introduction of mutations and gross chromosomal rearrangements, which may contribute to carcinogenesis[251,253,255–257]. Generally, two distinct repair mechanisms are used to process and seal DSBs: homologous recombination (HR) and non-homologous end joining (NHEJ).

HR is a template-dependent repair mechanism most active during S-phase in which a damaged region is repaired using the homologous region of the intact sister chromatid as a template for DNA synthesis[258–260]. Though this process may preserve the fidelity of the sequence spanning the break site, frequent repetition in the genome creates the possibility that the incorrect template sequence will be used to prime repair, which may result in genomic rearrangement[261].

NHEJ is a template-independent repair mechanism that is active during all phases of the cell cycle and consists of a classical pathway (C-NHEJ) and an alternative pathway (Alt-NHEJ)[262]. Alt-NHEJ is the lesser understood of the two pathways, but is reported to utilize areas of microhomology to mend DNA lesions *via* the enzymatic activities of the MRN complex and PolΘ[263]. Conversely, C-NHEJ mends DNA breaks lacking homology by either directly ligating compatible DSBs (NHEJ-C) or facilitating endonucleolytic processing prior to ligation in the case of incompatible DSBs

(NHEJ-I). In each case, repair is initiated by Ku70 and Ku80, which bind and stabilize the DNA termini. Phosphatidylinositol-3-kinase-like kinase (PIKK) family member DNA Protein Kinase (DNA-PK), which is composed of the catalytic subunit (DNA-PKcs) and the Ku heterodimer, then bridges the break and phosphorylates a number of NHEJ repair proteins (**Figure 2.1**). Though DNA-PK activity is critical for repair, the significance of its kinase activity remains unclear since the phosphorylation of NHEJ targets is not required for successful repair[264]. The exception is the autophosphorylation of DNA-PK at Ser2056, which is critical for successful DSB repair[265]. Ser2056 autophosphorylation induces a conformational change within the enzyme that releases it from the DNA and allows ligation enzymes, XRCC4 and Ligase IV, to access and seal the break[265–269]. Failure to phosphorylate Ser2056 is reported to stabilize DNA-PK on the lesion, preventing ligation and the completion of NHEJ[269]. In this way, DNA-PK is hypothesized to prevent premature ligation and coordinate the later stages of NHEJ[270]. In addition to serving as a critical regulator of DSB repair, DNA-PK activity is also linked to the activation of p53-dependent apoptosis in response to unrepaired DNA damage[271–277].

Defects in DSB repair pathways and cell cycle checkpoint control are clearly associated with an increased risk for developing solid tumors and hematological malignancies[253]. Adult T-cell Leukemia/ Lymphoma (ATL) is a fatal malignancy of $CD4^+$ T-cells caused by a lifelong infection with human T-cell leukemia virus type I (HTLV-1)[2,278,279]. Approximately 5% of HTLV-1-positive individuals develop ATL, though the process by which this disease occurs remains poorly understood. ATL development

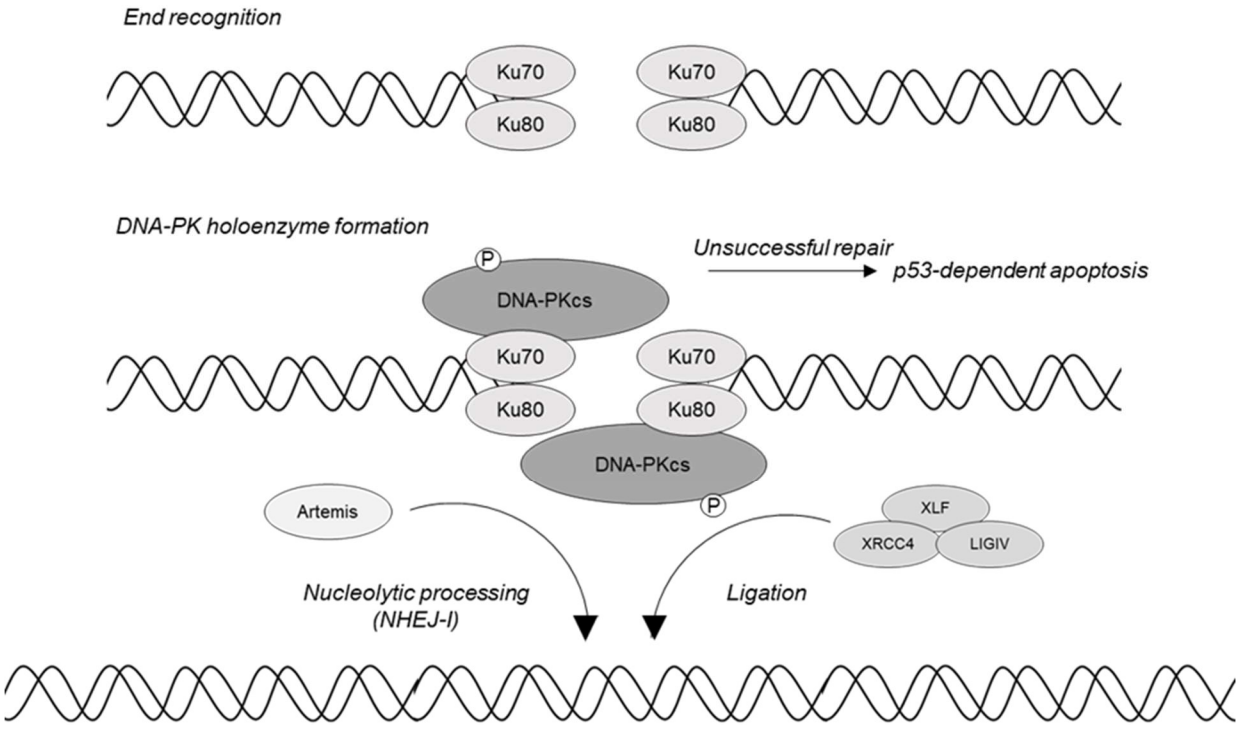

Figure 2.1: A model of NHEJ-mediated repair. DSB end recognition is facilitated by Ku70:Ku80 heterodimers, which bind and stabilize the lesion. The DNA protein kinase catalytic subunit (DNA-PKcs) is recruited to each Ku dimer, where it is believed to play an important role in synaptic end bridging and may serve as a scaffolding protein. Phosphorylation is important for the regulation of DNA-PK activities. Here, we focus on autophosphorylation of Ser2056, a marker for DNA-PK activation. Though its functions are not well understood, DNA-PK may play a role in coordinating the recruitment and activation of NHEJ endonuclease and ligation machinery. The endonucleolytic activities of Artemis may be particularly important for the processing of incompatible DSBs (NHEJ-I). Unsuccessful repair of DSBs is hypothesized to promote p53-dependent apoptosis through DNA-PK activity.

is likely driven by a multi-step oncogenic process, as evidenced by the extended length of time required for pathogenesis to occur, the limited number of infected individuals who develop the disease, and by the accumulation of seemingly random genetic abnormalities in infected cells[181]. Karyotyping of ATL cells isolated from patients reveal that chromosomal structural and numerical abnormalities are consistently present, but that these aberrations are not necessarily conserved among patients[280].

HTLV-1 encodes two proteins that have been reported to drive oncogenesis: Transactivator X (Tax) and HTLV-1 basic leucine zipper factor (HBZ). Tax expression induces genetic instability by promoting multinucleation, chromosomal aneuploidy, and telomere attrition[281–285]. Tax is also reported to induce DSBs through production of reactive oxygen species (ROS) as a result of constitutive NF-κB activation, upregulation of nitric oxide synthase (iNOS) expression leading to increased nitric oxide (NO) production, and inhibition up to 80% of HR to cause saturation of classical NHEJ and prevent the repair of newly acquired DSBs[192,193,197]. Additionally, Tax promotes dephosphorylation of the ATM kinase *via* the WIP1 phosphatase which leads to a bypass of the G_2/M DNA damage response checkpoint and accelerates cellular replication[286–292].

Although Tax is well-established to play a significant role in creating genomic instability, and its expression is sufficient to induce leukemogenesis in Tax transgenic mouse models, it remains unclear whether oncogenesis in humans is dependent upon additional factors[205–207]. IL-2-dependent, Tax-mediated immortalization of human primary $CD4^+$ T-cells is possible, but it is a highly inefficient and rare event[201]. Furthermore, many ATL cell clones exhibit a loss of Tax expression through mutation,

methylation, or deletion of the 5' Long Terminal Repeat (LTR), and cells which retain Tax expression exhibit only short bursts of sense proviral transactivation[170,200,248,249,293].

Unlike Tax, expression of the antisense-encoded *hbz* gene, which is regulated by the 3' LTR, is retained throughout infection[77,91,93,222,294–298]. HBZ exhibits a variety of pro-oncogenic properties that include stimulating cellular proliferation, accelerating cell cycle progression through upregulation of E2F-mediated transcription, and suppressing apoptosis[223,229,239,243,299]. Though little is known about whether HBZ contributes to the accumulation of chromosomal abnormalities, one study reports that ectopic HBZ expression increases the frequency of DNA breaks[239]. Furthermore, HBZ-expressing cells exhibit increased sensitivity to DSBs induced by etoposide-mediated topoisomerase II inhibition and delayed onset of DNA damage-induced G_2/M arrest[240,300]. These findings led us to question whether sensitivity to DSBs in HBZ-expressing cells is the result of a defect in one or more mechanisms of DSB repair.

We report that HBZ attenuates NHEJ of both compatible and incompatible DSBs, but that it does not significantly alter HR. We observed that HBZ interacts with NHEJ-initiating proteins Ku70 and Ku80 through its bZIP domain, and that it is recruited to DSB sites *in vitro* in a bZIP-dependent manner. Though we did not find the interaction shared between DNA-PKcs and Ku70 to be affected by HBZ, we observed that autophosphorylation at Ser2056 is delayed, also in a bZIP-dependent manner, suggesting that HBZ interferes with the activation of DNA-PK kinase activity in response to DNA damage. Though Tax is reported to interact with Ku70, it did not interfere with the formation of the HBZ:Ku complex. Additionally, Ku protein levels are retained in HTLV-1 infected cell lines which express little to no Tax, although they are reduced in

cells with high levels of Tax expression as previously reported[301]. Interestingly, HBZ-mediated attenuation of NHEJ was masked by the co-expression of Tax, which enhanced NHEJ activity. Together, these findings suggest that DSB repair mechanisms are impaired not only by Tax, but also by HBZ, and show that HBZ may contribute to the accumulation of DSBs and chromosomal abnormalities over the course of HTLV-1 infection, especially in infected cell clones that no longer express Tax consistently.

Results

HBZ attenuates repair of double-stranded DNA breaks through NHEJ, but not HR:

To investigate whether HBZ impacts the repair of DSBs, we used previously described classical NHEJ and HR repair reporter vectors to quantify successful repair in HBZ-expressing cells and empty vector control cells (**Figure 2.2.A-B**)[302,303]. Briefly, the NHEJ reporter plasmids encode one copy of the GFP reporter gene interrupted by a 3kb *PEM1* gene intron. Within the intron lies an adenoviral (AV) exon flanked by I-SceI restriction endonuclease sites. The NHEJ-compatible break (NHEJ-C) reporter plasmid has two I-SceI restriction sites in the direct orientation that, upon digestion, create two compatible ends that do not require additional nucleolytic processing prior to ligation (**Figure 2.2.A**). The NHEJ-incompatible break (NHEJ-I) plasmid has two inverted I-SceI sites that generate incompatible ends, requiring nucleolytic processing prior to ligation (**Figure 2.2.A**). Excision of the AV exon during repair followed by splicing of the transcript results in GFP expression, which is quantified by flow cytometry. The HR reporter pDR-GFP encodes a full-length copy and a 5’ and 3’ truncated copy of GFP

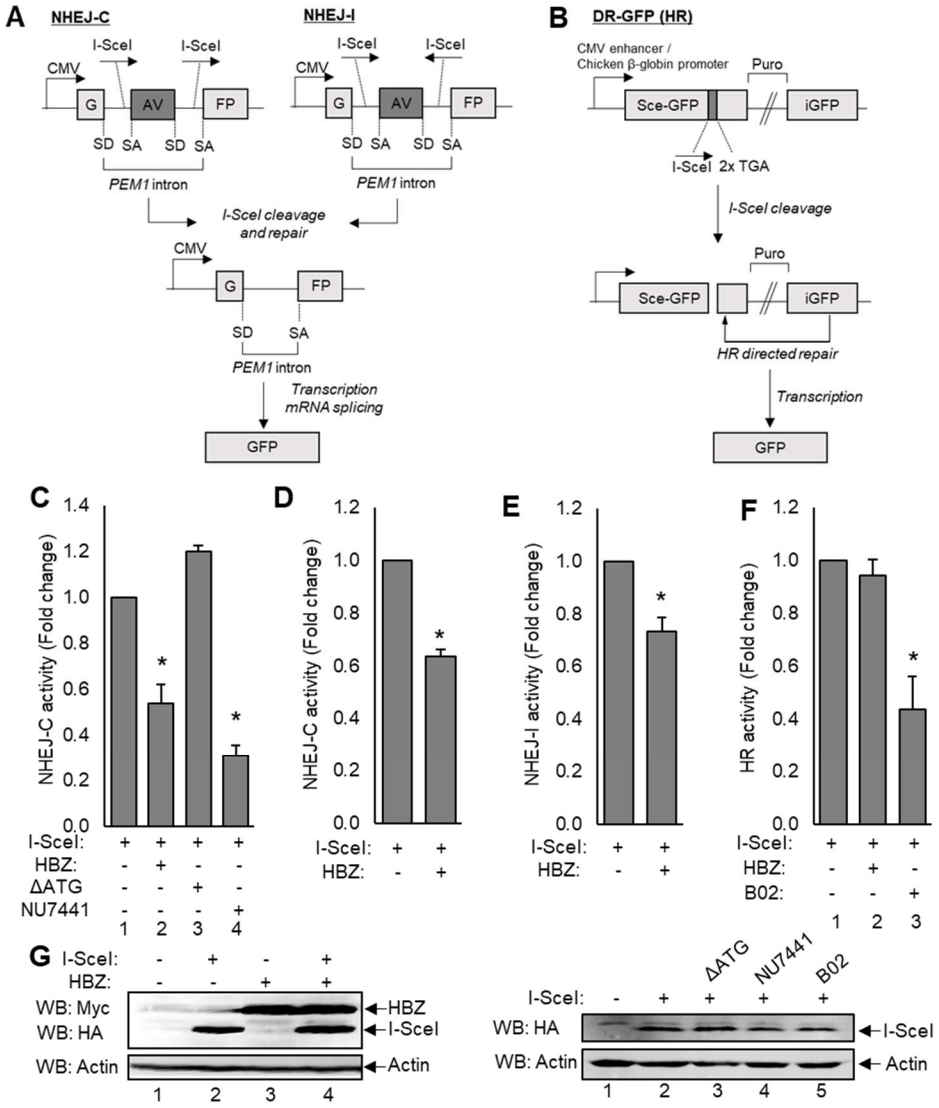

Figure 2.2: GFP reporter-based DSB repair vectors reveal that HBZ attenuates NHEJ-C and NHEJ-I, but not HR. (A) Schematics of the reporter vectors used to measure NHEJ of compatible DSBs (NHEJ-C) and NHEJ of incompatible breaks (NHEJ-I), both part of the classical NHEJ pathway, are shown. The GFP reporter gene is separated by the *PEM1* gene intron containing an adenoviral (AV) exon flanked by two I-SceI restriction sites in a direct orientation (NHEJ-C) or an indirect orientation (NHEJ-I). Cleavage at these sites results in excision of the AV exon and repair by NHEJ. The *PEM1* intron is spliced out of the transcript at the splice donor (SD) site and splice acceptor (SA) site, resulting in an uninterrupted GFP-encoding transcript. **(B)** A schematic of the reporter vector used to measure HR is shown. This vector contains one complete copy of the GFP reporter gene (Sce-GFP) and a truncated copy of GFP that serves as a template for repair (iGFP), which are separated by a puromycin resistance cassette (Puro). Eleven base pairs were deleted from the Sce-GFP cDNA sequence and replaced with one I-SceI restriction site and two in-frame stop codons. This missing sequence ensures that template-dependent repair must occur to result in the production of a full length GFP gene. **(C)** HEK 293T cells were transfected with a total of 6μg of plasmid DNA (2μg pSG-I-SceI-HA, 2μg pcDNA-HBZ-Myc-His, 2μg pcDNA-ΔATG-Myc-His, 2μg NHEJ-C reporter). Where indicated, cells were treated with 2μM NU7441 for 24hrs. Cells were collected for flow cytometric analysis of GFP expression as outlined in the Materials and Methods. Data was collected from 20,000 individual events and is shown as fold change from maximum repair activity (I-SceI+ reporter). HBZ data is an average of ten independent experiments, ΔATG data is an average of three independent experiments, and NU7441 is an average of 3 independent experiments. Error bars represent SEM (Student's t-test, * $p \leq 0.05$). **(D)** Jurkat cells were electroporated with a total of 6μg of plasmid DNA (2μg pSG-I-SceI-HA, 2μg pcDNA-HBZ-Myc-His, 2μg NHEJ-C reporter) and analyzed for GFP expression as outlined in C. Data shown are an average of two independent experiments and error bars indicate SEM (Student's t-test, *$p \leq 0.05$). **(E)** HEK 293T cells were transfected with a total of 6μg of plasmid DNA (2μg pcDNA-HBZ-Myc-His, 2μg NHEJ-I reporter) and analyzed as outlined above. Data shown are an average of five independent experiments and error bars represent SEM (*Student's t-test, * $p \leq 0.05$). **(F)** HEK 293T cells were transfected with a total of 6μg of plasmid DNA (2μg pcDNA-HBZ-Myc-His, 2μg DR-GFP reporter) and treated with 20μM B02 for 24hrs where indicated. Data shown are an average of three independent experiments and error bars represent SEM (*Student's t-test, * $p \leq 0.05$). **(G)** Western blots of cellular protein extracts (30-60μg) were used to confirm transfections in HEK 293T cells using the indicated antibodies.

separated by 3.7kb containing a puromycin cassette. Eleven base pairs were deleted from full-length GFP cDNA sequence and replaced with an I-SceI site and 2 in-frame stop codons (Sce-GFP) (**Figure 2.2.B**). Once digested, HR machinery use the truncated internal GFP (iGFP) sequence as the template for repair, thereby replacing the missing nucleotides to allow expression of the full length fluorescent product.

To determine whether HBZ influences the NHEJ of compatible DNA breaks, we transfected HEK 293T cells with the NHEJ-C reporter, the I-SceI expression vector, and either pcDNA-HBZ-Myc-His, or the empty vector (**Figure 2.2.C**). Since the HBZ transcript has been reported to have functions unique from the HBZ protein, we also evaluated whether the HBZ transcript affects NHEJ-C using the pcDNA-HBZ-ΔATG expression vector (lane 3). Additionally, one group of cells was treated with the NHEJ inhibitor NU7441, an inhibitor of DNA-PK enzymatic activity, to serve as a control for this assay (lane 4)[304]**.** We observed that HBZ expression significantly attenuated NHEJ-C activity, as did treatment with NU7441. We noted that attenuation was mediated by the HBZ, but not the HBZ mRNA. Furthermore, we confirmed that HBZ attenuates NEHJ-C similarly in Jurkat T-cells (**Figure 2.2.D**). We also evaluated the efficiency of NHEJ of incompatible DNA breaks (NHEJ-I) and found that HBZ also significantly attenuates NHEJ-I activity (**Figure 2.2.E**). Finally, we assessed whether HBZ affects the HR pathway (**Figure 2.2.F**). HEK 293T cells were transiently transfected with the DR-GFP reporter plasmid, and either pcDNA-HBZ-Myc-His (lane 1) or the empty vector (lane 2). Additionally, one group of cells was treated with the HR inhibitor B02 as a control for this assay (lane 3)[305]. We observed that HBZ failed to affect the efficiency of HR.

HBZ interacts with Ku70 and Ku80 *via* the bZIP domain: HBZ is reported to interact with a number of nuclear proteins to exert control over cellular processes. We questioned whether HBZ attenuates NHEJ through an interaction with cellular DNA repair machinery. To investigate novel HBZ-binding partners, we performed a preliminary proteomic screen in which we evaluated binding partners of affinity-purified HBZ protein complexes. Briefly, HBZ-containing protein complexes were immunoprecipitated from HeLa cells stably transfected with the pCMV-HBZ-FLAG expression vector. The FLAG-epitope tag, located on the C-terminal end of HBZ, allowed for FLAG immunoprecipitation-mediated purification of HBZ-containing protein complexes. Eluted proteins were subsequently identified by liquid chromatography tandem mass spectrometry (LC-MS/MS). To account for possible non-specific protein interactions with the anti-FLAG antibody, the immunoprecipitation was also performed using protein extracts from cells containing the empty vector control (pCMV-3Tag-8). In validation of our screen, we identified peptide fragments unique to HBZ, as well as several previously reported HBZ-interacting proteins, including p300/CBP[82,224,241], c-Jun[78], JunB[78], JunD[228], ATF-1[81], ATF-7 (unpublished), CREB-1[81], CREM[81], and C/EBPG[229] (**Figure 2.3.A**). Interestingly, the analysis also indicated that HBZ interacts with NHEJ proteins Ku70 and Ku80.

Upon sensation of a DNA break, Ku70 and Ku80 form a dimer and bind to DSBs and initiate NHEJ by recruiting the DNA-PK catalytic subunit (DNA-PKcs) to these sites. We confirmed the interaction of HBZ with Ku70 and Ku80 using co-immunoprecipitation with lysates from HEK 293T cells transiently overexpressing HBZ-Myc-His, FLAG-Ku70,

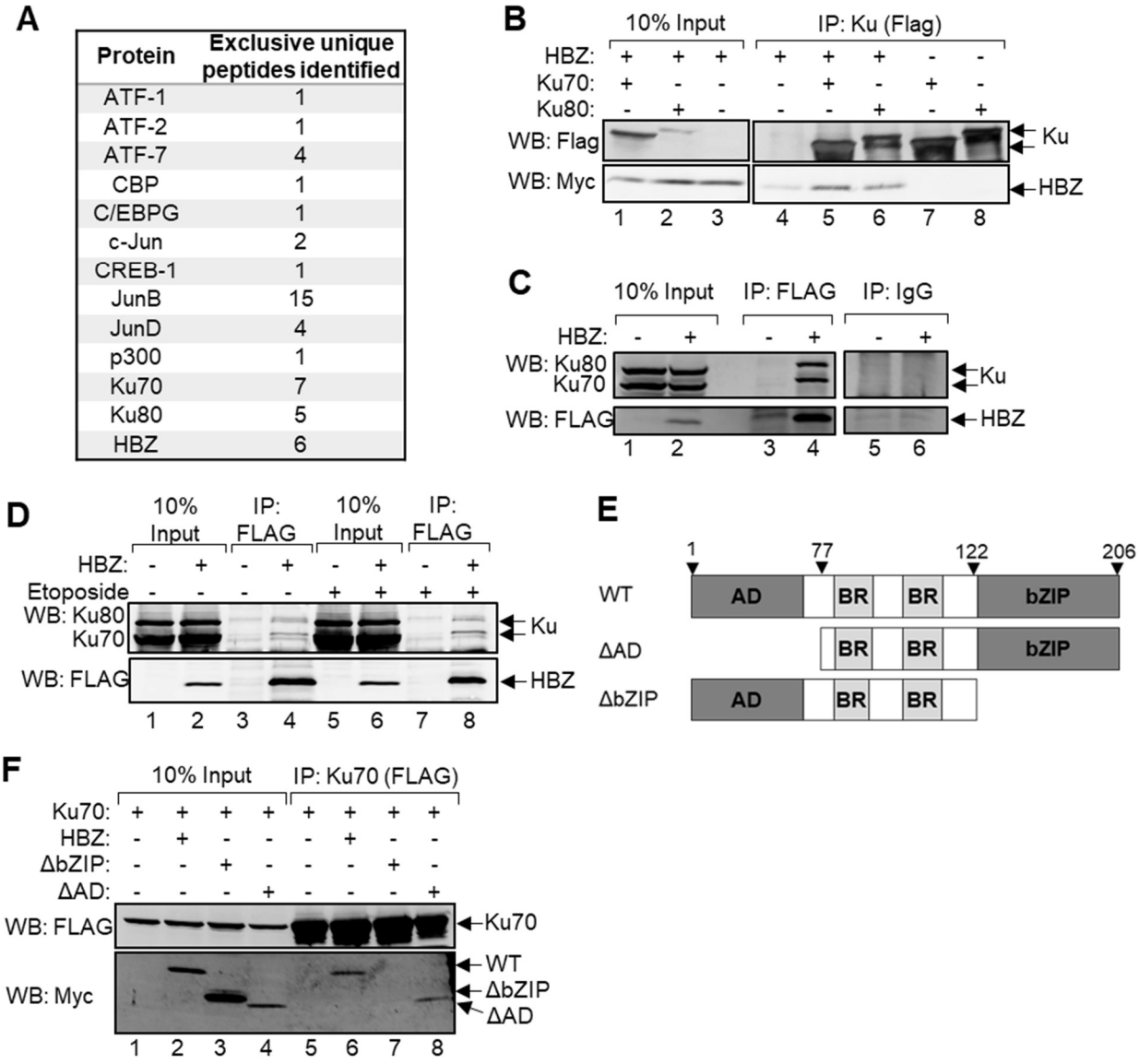

Figure 2.3:HBZ interacts with Ku through its bZIP domain. (A) A table outlining previously reported HBZ-interacting partners, as well as novel HBZ-interacting proteins Ku70 and Ku80, that were recovered from HBZ-FLAG immunoprecipitation and identified by LC-MS/MS. Proteins shown are unique to HBZ-FLAG samples and were identified with 99% probability. The data is representative of one independent experiment and the number of peptides identified are shown. **(B)** HEK 293T cells were transfected with 12µg of plasmid DNA (4µg pEGFP-Ku70-FLAG, 4µg pEGFP-Ku80-FLAG, 8µg pcDNA-HBZ-Myc-His) for 48 hours. Anti-FLAG antibody was used to immunoprecipitate FLAG-Ku70 and FLAG-Ku80 from 300µg of protein extracts. Eluates (lanes 4-8) and 30µg of protein input (lanes 1-3) were analyzed by Western blot using the indicated antibodies. **(C)** Endogenous Ku70 and Ku80 were co-immunoprecipitated with HBZ-FLAG from 500µg of total protein harvested from HeLa cells stably transfected with pCMV-HBZ-FLAG or the empty vector. FLAG immunoprecipitation (IP) eluates (lanes 3-4) and 30µg of protein inputs (lanes 1-2) were analyzed by Western blot using the indicated antibodies. An immunoprecipitation with rabbit IgG was concurrently performed (lanes 5-6). **(D)** Per IP, three sets of MT-2 cells ($3x10^6$) in 300µL serum-free RPMI were electroporated with 15µg of pCMV-HBZ-FLAG or the empty vector in 0.4 cm cuvettes (pulse=200V, 975uF, ∞Ω). Where indicated, cells were treated for 5hrs with 50µM etoposide. Anti-FLAG immunoprecipitations were performed with 500µg of cell lysate. Eluates and 10% protein inputs were analyzed by Western blot using the indicated antibodies. **(E)** A schematic of wild type HBZ (WT) and HBZ truncation mutants (ΔAD, ΔbZIP) used throughout this study. HBZ contains an N-terminal activation domain (AD), centrally located basic regions (BR), and a C-terminal basic leucine zipper (bZIP) domain. **(F)** HEK 293T cells were transfected with 12µg of plasmid DNA (4µg pEGFP-Ku70-FLAG, 4µg pcDNA-HBZ-Myc-His, 8µg pcDNA-HBZ-ΔAD-Myc-His, 4µg pcDNA-HBZ-ΔbZIP-Myc-His). Ku70-FLAG was immunoprecipitated from 300µg of protein extracts using anti-FLAG antibody. Eluates (lanes 5-8) and 30µg of protein inputs (lanes1-4) were analyzed by Western blot using the indicated antibodies.

and FLAG-Ku80. Ku proteins, which each contain an N-terminal FLAG tag, were immunoprecipitated with anti-FLAG antibody, and the eluates were analyzed by Western blot for the presence of HBZ by probing for its C-terminal Myc tag (**Figure 2.3.B**). HBZ was also confirmed to interact with endogenous Ku70 and Ku80 in which, lysates from HeLa cell lines stably expressing HBZ-FLAG, or transfected with the empty vector, were used to immunoprecipitate endogenous Ku70 and Ku80 protein complexes using anti-FLAG antibody (**Figure 2.3.C**). Again, we observed that both Ku70 and Ku80 co-immunoprecipitated with HBZ. Finally, to confirm that HBZ and Ku proteins interact within the context of the HTLV-1-infected T-cell, MT-2 cells were electroporated with pCMV-HBZ-FLAG or the empty vector, and HBZ was immunoprecipitated using anti-FLAG antibodies (**Figure 2.3.D**). We observed that endogenous Ku70 and Ku80 co-immunoprecipitated with HBZ (lane 4). To determine if the interaction would be enhanced by the induction of DNA breaks, we treated electroporated cells with the topoisomerase II inhibitor etoposide for five hours to induce the accumulation of DSBs (lanes 5-8). However, we did not observe that etoposide treatment greatly enhanced HBZ:Ku complex formation, suggesting that these interactions may occur independently of DNA damage.

HBZ is characterized by three major regions (**Figure 2.3.E**): the N-terminal activation domain (AD) that directly interacts with cellular coactivators and histone acetyltransferases[82,224,240,241], the central basic regions (BR) that facilitate nuclear localization[225], and the C-terminal basic leucine zipper (bZIP) motif that mediates interactions between HBZ and cellular bZIP transcription factors[78,81,227–229]. To determine which of these regions is important for facilitating the interaction with Ku, we

performed immunoprecipitations with cell lysates from HEK 293T cells that transiently overexpressed FLAG-tagged Ku70 and either wild type HBZ (HBZ-WT), HBZ-ΔAD, or HBZ-ΔbZIP (**Figure 2.3.F**). Deletion of the HBZ AD did not prevent HBZ from interacting with Ku70 (lane 8), but deletion of the bZIP domain abolished the interaction (lane 7), indicating that the bZIP domain facilitates the HBZ:Ku interaction.

HBZ does not impair Ku-mediated DSB end recognition: To assess the importance of DNA contact in the formation of the HBZ:Ku complex, we tested whether degrading DNA *via* endonuclease activity would affect these protein interactions. We immunoprecipitated Ku70-FLAG from HEK 293T cells co-transfected with HBZ-Myc-His. Cell lysates were split in half, and one set was treated with the endonuclease, benzonase, while the other remained untreated (**Figure 2.4.A**). The results show that the interaction between Ku70 and HBZ is maintained in endonuclease-treated cell lysates, indicating that the stability of this protein complex is not DNA-dependent.

These findings led us to question whether HBZ prevents Ku-mediated DSB end recognition. *In vitro* DNA-binding assays have been extensively used to characterize interactions between NHEJ core machinery and DNA termini[306–311]. Using this technique, we tested whether HBZ influences the recruitment of Ku70 or Ku80 to DSBs. Biotinylated, double-stranded, blunt-end DNA fragments (35bp) were immobilized on streptavidin-coupled beads and incubated with nuclear extracts from HEK 293T cells transiently overexpressing Myc-His-tagged HBZ-WT, HBZ-ΔAD, or HBZ-ΔbZIP. Proteins captured by the immobilized DNA were eluted and analyzed by Western blot to determine if HBZ influences Ku recruitment and, if so, which domain of HBZ is

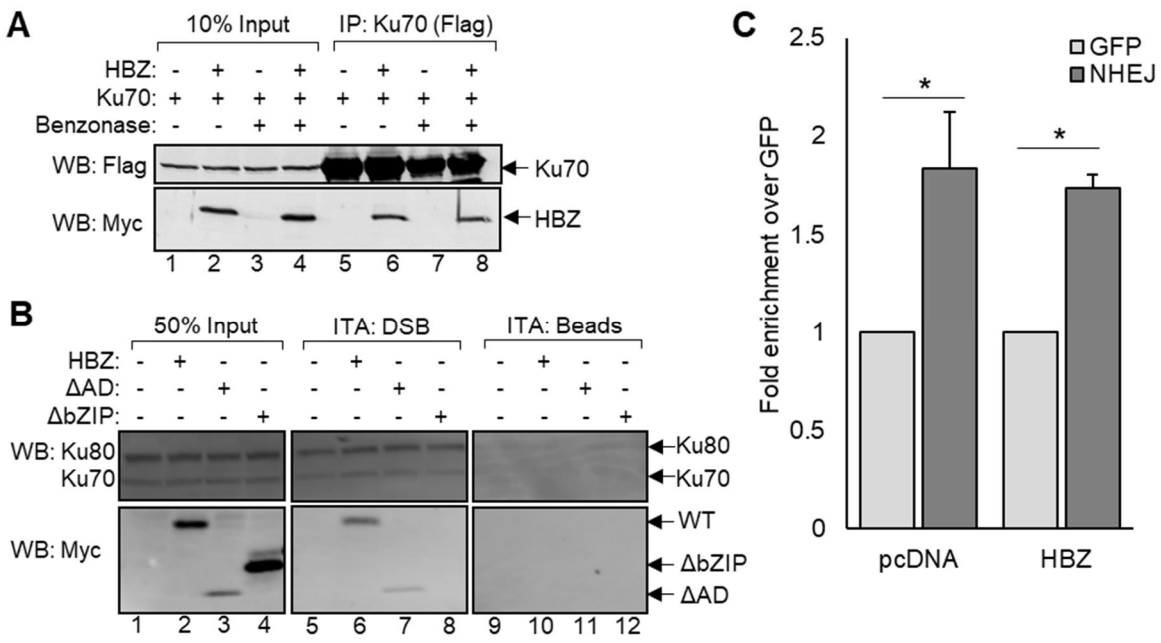

Figure 2.4: HBZ is recruited to DSBs in a Ku-dependent manner. (A) HEK 293T cells were transfected with 12μg of plasmid DNA (4μg pEGFP-Ku70-FLAG, 8μg pcDNA-HBZ-Myc-His). Protein extracts were divided and were either treated with 250U of benzonase for 45 minutes or were left untreated. FLAG-Ku70 was immunoprecipitated from approximately 3mg of protein using anti-FLAG antibodies. Eluates (lanes 5-8) and 10% of the input protein (lanes 1-4) were analyzed by Western blot using the indicated antibodies. **(B)** HEK 293T cells were transfected and nuclear proteins were harvested as described in the Materials and Methods. Nuclear protein (10μg) was incubated with an immobilized, blunt ended, double-stranded DNA fragment (ITA:DSB), or with unbound resin (ITA:Beads). Eluates and 5μg of protein inputs (50% input) were analyzed by Western blot using the indicated antibodies **(C)** HeLa cells stably transfected with pcDNA-HBZ-Myc-His or the empty vector, were co-transfected with the NHEJ-C reporter and the I-SceI expression vector. Chromatin immunoprecipitation assays were performed using the indicated antibodies. Primers specific for the NHEJ-C reporter, or for an internal GFP sequence were used to amplify precipitated DNA. Data shown is an average of four independent experiments and represents fold change in Ku70 enrichment in the I-SceI cut site (NHEJ) relative to Ku70 enrichment at the internal GFP sequence (GFP). Error bars represent SEM (Student's t-test, * $p \leq 0.05$).

responsible for this activity (**Figure 2.4.B**). The results indicate that HBZ neither promoted, nor impaired Ku recruitment to DNA termini (lane 6). Interestingly, we noted that HBZ-WT and HBZ-ΔAD were recruited to the DNA (lane 6-7), but that HBZ-ΔbZIP was not (lane 8). These findings indicate that the bZIP domain of HBZ is important for its recruitment to DSBs, as well as for facilitating its interaction with Ku, suggesting that HBZ is recruited to DNA lesions in a Ku-dependent manner.

As an alternative approach, we performed chromatin immunoprecipitation to evaluate Ku70 recruitment to DSBs *in vivo*. For these assays, stable HeLa cell lines containing the HBZ-expression vector pcDNA-HBZ-Myc-His or the empty vector (pcDNA) were transiently transfected with the NHEJ-C reporter plasmid and the I-SceI expression plasmid. After approximately 24 hours, Ku70-bound chromatin fragments were immunoprecipitated. ChIP PCR was performed using primers recognizing the NHEJ reporter I-SceI cut site, or recognizing an internal GFP sequence, and data are presented as a function of Ku70 enrichment at the internal GFP site (**Figure 2.4.C**). We observed that Ku70 was significantly enriched at the NHEJ I-SceI cut site (NHEJ) in both the empty vector cell line and in the HBZ-expressing cell line, as compared to Ku70 enrichment at the internal GFP site. Furthermore, consistent with our previous results, we did not observe HBZ expression to significantly alter Ku70 recruitment.

The bZIP domain of HBZ is important for the attenuation of NHEJ: We next addressed whether the interaction between HBZ and Ku contributes to HBZ-mediated attenuation of NHEJ. Because our findings support that HBZ interacts with Ku *via* its bZIP domain, we hypothesized that HBZ mutants lacking this region would be unable to

attenuate NHEJ-C. HEK 293T cells were transiently transfected with the NHEJ-C reporter plasmid, the I-SceI restriction enzyme expression plasmid, and either HBZ-WT, HBZ-ΔAD, or HBZ-ΔbZIP, and were analyzed 48 hours post-transfection for successful NHEJ-mediated repair (**Figure 2.5**). We observed that the bZIP truncation mutant was incapable of NHEJ attenuation (lane 3). Conversely, the AD truncation mutant inhibited NHEJ similarly to WT HBZ (lane 4). In our hands, HBZ-ΔAD protein levels observable by Western blot are typically lower than the levels of other HBZ proteins. We found that by transfecting increased amounts of the HBZ-ΔAD expression vector, NHEJ-C was attenuated even further (lane 5). Together, these data support that the bZIP domain of HBZ is a potent negative regulator of NHEJ activity.

HBZ impairs etoposide-induced DNA-PK autophosphorylation: Because we did not find HBZ to inhibit the recruitment of Ku70 or Ku80 to DNA termini *in vitro*, or to reduce the level of chromatin-bound Ku70 *in vivo*, it is unlikely that HBZ attenuates NHEJ at the DSB recognition step. Therefore, we hypothesized that HBZ modulates Ku-dependent processes that occur after recognition of DNA termini. DNA-PK holoenzyme recruitment and activation is believed to be important for facilitating synaptic end bridging and preventing premature DNA processing[312]. To determine if DNA-PK activities are impacted by HBZ, we first tested whether HBZ impedes the interaction between Ku70 and DNA-PKcs by immunoprecipitating Ku70 from HEK 293T cell lysates transiently overexpressing FLAG-Ku70 and HBZ-Myc-His. Prior to immunoprecipitation, cells were treated with 50μM etoposide to stimulate DNA-PK complex formation (**Figure 2.6.A**). The data show that DNA-PKcs is co-immunoprecipitated with Ku70 in cells transfected

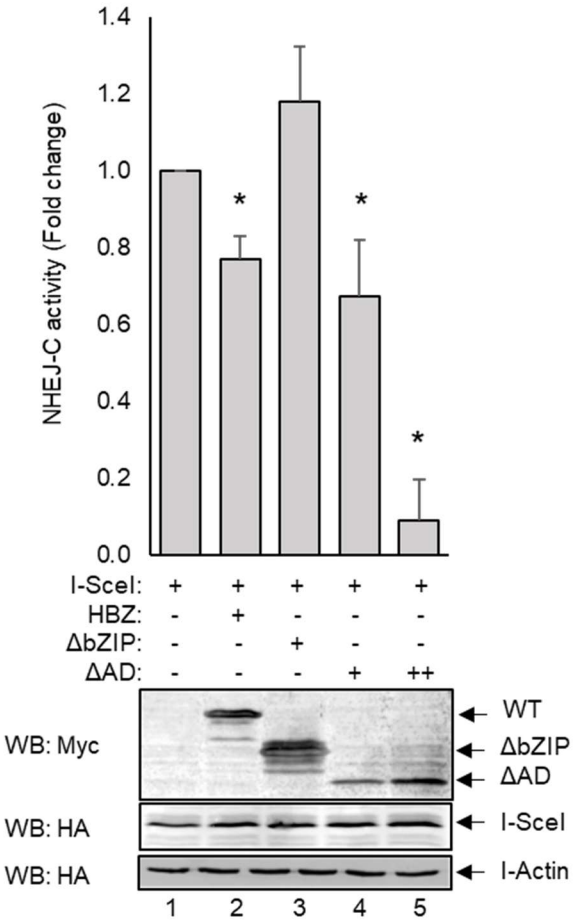

Figure 2.5: The bZIP domain of HBZ is important for the attenuation of NHEJ. HEK 293T cells were transfected with a total of 6-8μg of plasmid DNA (2μg pSG-I-SceI-HA, 2μg pcDNA-HBZ-Myc-His, 2μg pcDNA-HBZ-ΔbZIP-Myc-His, 2-4μg pcDNA-HBZ-ΔAD-Myc-His, and 2μg of the NHEJ-C reporter). GFP expression was detected by flow cytometry, and the fold change in NHEJ-C activity was calculated from 20,000 events. Data are an average of three independent experiments and error bars represent SEM (*Student's t-test, $p \leq 0.05$). Protein was extracted from the remaining transfected cells and was analyzed by Western blot using the indicated antibodies to confirm successful transfections.

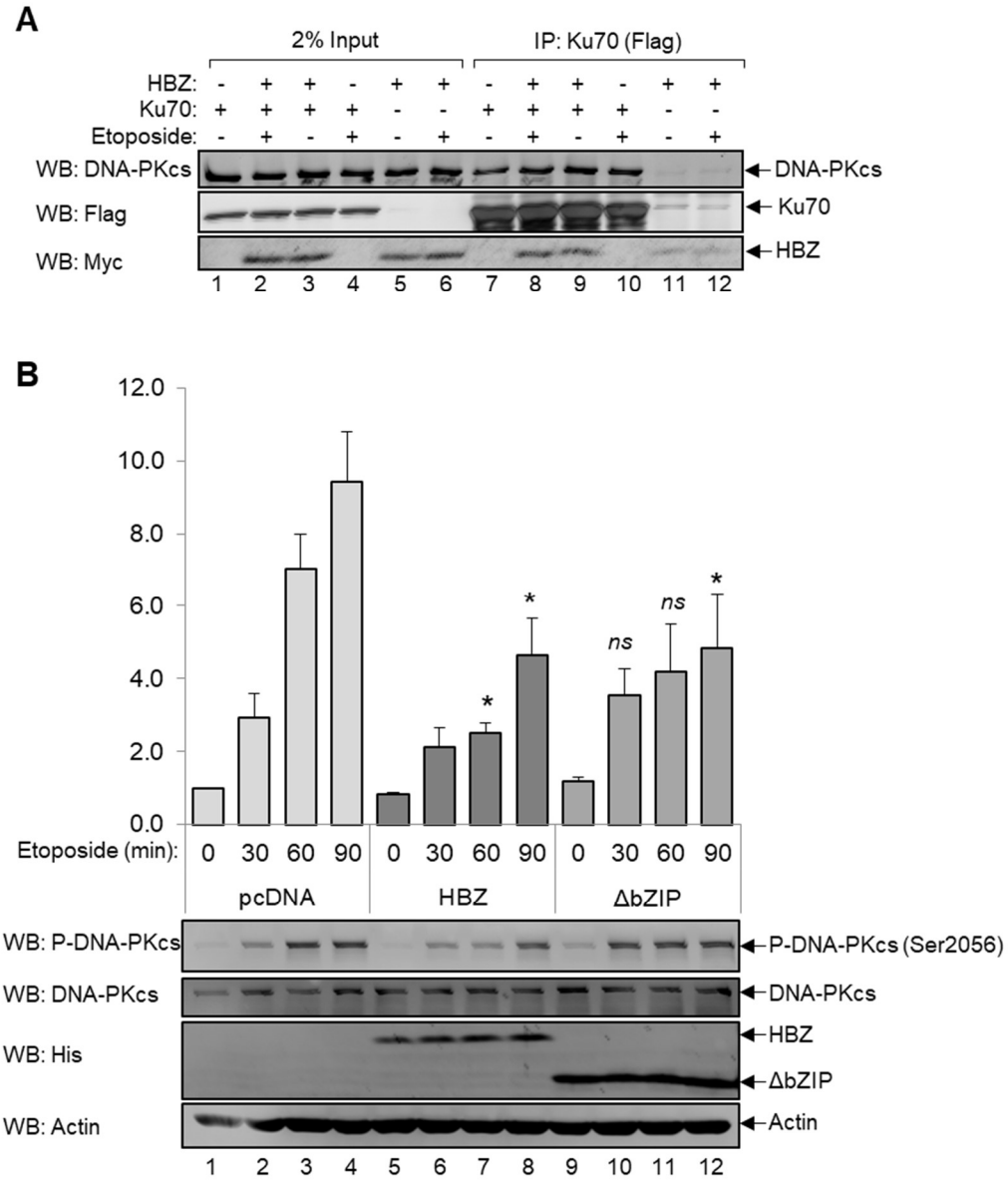

Figure 2.6: HBZ interferes with etoposide-induced DNA-PK autophosphorylation. (A) HEK 293T cells were transfected with 12µg of plasmid DNA (6µg pEGFP-Ku70-FLAG, 6µg pcDNA-HBZ-Myc-His, 6µg pcDNA 3.1) for 24 hours. Cells were treated with 50µM etoposide or equivalent amounts of DMSO for 5 hours before protein was extracted. FLAG-Ku70 was immunoprecipitated from 1mg of protein using anti-FLAG antibodies. Eluates (lanes 7-12) and 20µg of protein inputs (lanes 1-6) were analyzed by Western blot using the indicated antibodies. **(B)** HeLa clones stably transfected with an empty vector (lanes 1-4), pcDNA-HBZ-Myc-His (lanes 5-8), or pcDNA-HBZΔbZIP-Myc-His (lanes 9-12) were treated with 50µM etoposide over a 90-minute time course. Protein was extracted and 30µg of each were analyzed by Western blot using the indicated antibodies. Changes in DNA-PKcs autophosphorylation, relative to a constant, non-specific band, were quantified by densitometric analysis of Western blots from three independent experiments. Error bars represent SEM (Student's t-test, * $p \leq 0.05$, *ns* indicates not significant).

with the empty vector and in cells expressing HBZ, indicating that HBZ does not impair formation of the DNA-PK holoenzyme. Likewise, co-immunoprecipitation of DNA-PKcs with endogenous Ku70 in HeLa cell lines stably expressing HBZ-Myc-His or containing the empty vector confirmed that HBZ does not impair DNA-PK holoenzyme formation (data not shown).

Activation of DNA-PK kinase activity is dependent upon phosphorylation of several residues and is reported to be critical for the completion of NHEJ[269,313–317]. Though DNA-PK is phosphorylated by a number of other kinases, Ser2056 has been identified as a *bona fide* autophosphorylation site that is important for destabilizing DNA-PK from its position at the DNA break prior to ligation, a step critical to the completion of NHEJ[265,269]. We tested whether HBZ impairs DNA-PK Ser2056 autophosphorylation by treating HeLa cells stably transfected with pcDNA-HBZ-Myc-His or the empty vector with 50μM etoposide over a 90-minute time course (**Figure 2.6.B**). Cells were processed at 30-minute intervals, and lysates were treated with phosphatase inhibitors to prevent protein dephosphorylation. Proteins were analyzed by Western blot, and the P-DNA-PK band volume was quantified (ImageQuant) and normalized against a non-specific, constant band appearing on the same blot. We observed that in HBZ-expressing cells (lanes 5-8), the level of phosphorylated DNA-PK was significantly reduced, but not depleted, at the 60-minute and 90-minute time points (lanes 7-8) when compared to the level of phosphorylated DNA-PK at the same time points in empty vector cells (lane 3-4).

These data suggest a delay in the maximum activation of DNA-PK in HBZ-expressing cells. Analysis of P-DNA-PK HeLa cells lines stably expressing the HBZ-

ΔbZIP truncation mutant showed that autophosphorylation levels at the 30-minute and 60-minute timepoints (lanes 10-11) were not significantly altered as compared to the empty vector cells. However, these cells exhibited a reduction in DNA-PK autophosphorylation at the 90-minute timepoint (lane 12), suggesting that maximum DNA-PK activity may be impaired. Overall, our findings indicate that HBZ reduces DNA-PK autophosphorylation, suggesting a reduction in its maximum activation in a manner which is partially dependent upon the bZIP domain.

Ku simultaneously forms complexes with HBZ and Tax to differentially modulate NHEJ activity: The HTLV-1 encoded protein Tax also dysregulates NHEJ through a diverse set of mechanisms that may impact the effect of HBZ on this repair pathway. We addressed this possibility by first evaluating Ku70 and Ku80 protein levels in a panel of HTLV-1-infected and uninfected T-cell lines, as Tax was reported to reduce the expression of these proteins (**Figure 2.7.A**)[301]. Western blot analysis of cell lysates show that the virally-infected cells retain expression of the Ku proteins (lanes 8-14), suggesting that the effect of HBZ on NHEJ remains relevant in the presence of Tax. In corroboration with previous findings[301], infected cells with high Tax expression(lanes 8-12) displayed a reduction in Ku protein levels when compared to HTLV-1-infected cells expressing little to no Tax (lanes 13-14).

Tax was also reported to interact with Ku70[287], leading us to question whether Tax impedes the interaction between HBZ and Ku70 in cells co-expressing Tax and HBZ. To

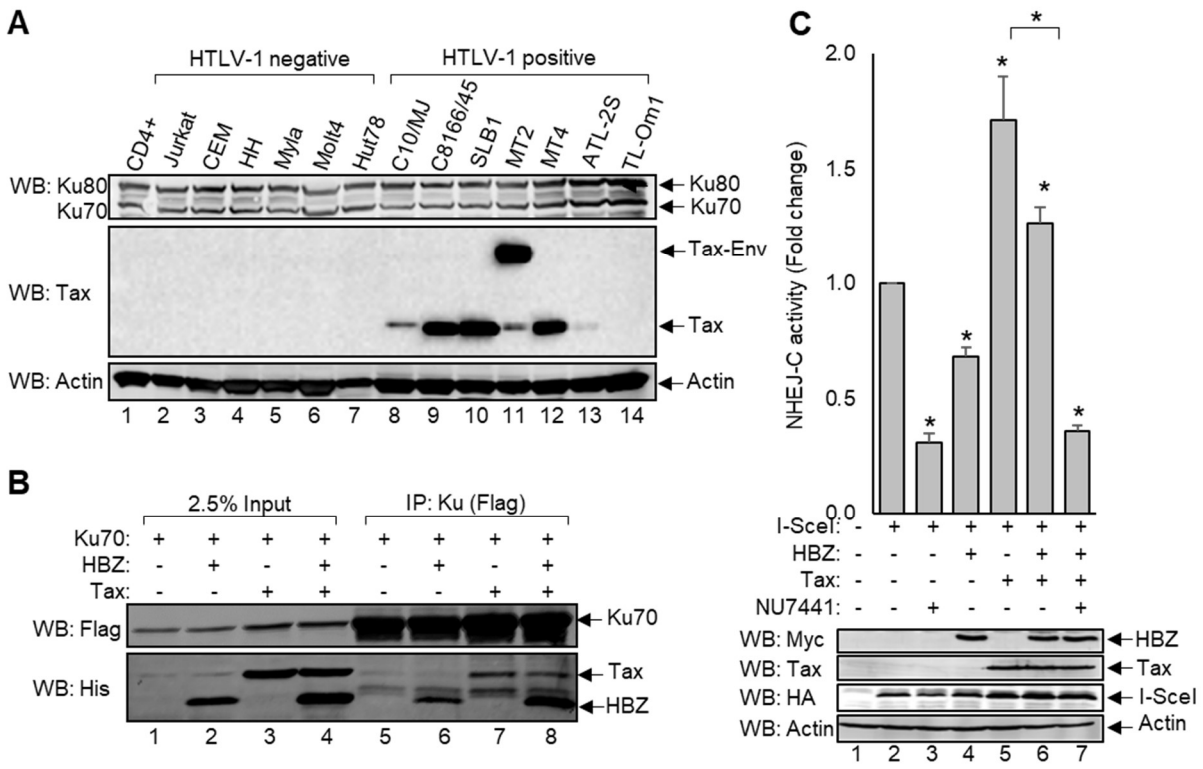

Figure 2.7: Ku simultaneously forms complexes with HBZ and Tax to differentially modulate NHEJ activity. (A) Protein extracts (15µg) from activated primary $CD4^+$ T-cells (anti-CD3, anti-CD28), as well as uninfected and HTLV-1-infected T-cell lines were analyzed by Western blot using the indicated antibodies. **(B)** HEK 293T cells were transfected with 12µg of plasmid DNA (3µg pEGFP-Ku70-FLAG, 6µg pcDNA-HBZ-Myc-His, 3µg pSG-Tax-His). FLAG-Ku70 was immunoprecipitated from 2mg of protein using an anti-FLAG antibody. Eluates (lanes 5-8) and 50µg of protein inputs (lanes 1-4) were analyzed by Western blot using the indicated antibodies. **(C)** HEK 293T cells were transfected with 7µg of plasmid DNA (2µg pSG-I-SceI-HA, 2µg pSG-HBZ-Myc, 1µg pSG-Tax-His, 2µg NHEJ-C reporter). Where indicated, cells were treated with 2µM NU7441 for 24hrs. GFP expression was detected by flow cytometry, and the change in NHEJ-C activity was calculated from 20,000 events. NU7441 and HBZ+Tax+NU7441 data are an average of three independent experiments, and remaining data are an average of six independent experiments. Error bars represent SEM (Student's t-test, * $p \leq 0.05$). Protein was extracted from the remaining transfected cells and 60µg of each sample was analyzed by Western blot using the indicated antibodies to confirm transfections. Lane 1 in the Western blot is a negative transfection control (I-SceI negative) and is not represented in the above NHEJ-C activity quantitation.

address this possibility, Ku70 was immunoprecipitated from HEK 293T cell lysates transiently overexpressing FLAG-Ku70, HBZ-Myc-His, and Tax tagged with a C-terminal 6x His epitope tag (**Figure 2.7.B**). We observed that Tax and HBZ both co-immunoprecipitated with Ku70 when expressed alone (lanes 6-7), or in combination (lane 8). Given that the Ku proteins are abundantly expressed, these data support that that neither protein influences the interaction of the other with Ku70.

Finally, Tax was reported to repress the HR repair pathway, leading to the saturation of NHEJ to compensate for the lost repair mechanism[197,287]. To determine how the co-expression of Tax and HBZ affects NHEJ repair, we evaluated the efficiency of NHEJ using the flow cytometric NHEJ reporter assay in HEK 293T cells transiently expressing the NHEJ-C reporter, the I-SceI restriction enzyme, and a combination of HBZ and Tax (**Figure 2.7.C**). We observed that HBZ attenuates NHEJ-C when expressed alone (lane 4) and when Tax was expressed alone (lane 5), we observed that it significantly enhanced NHEJ-C activity, which may be consistent with some of the previously reported activities of Tax[197,287]. Interestingly, when HBZ and Tax were co-expressed (lane 6), HBZ was observed to significantly reduce Tax-mediated enhancement of NHEJ. However, this activity still remained above basal levels indicating that HBZ only able to partially mitigate Tax-mediated activation of NHEJ-C. Finally, the DNA-PK inhibitor NU7441 significantly inhibited NHEJ-C activity regardless of Tax and HBZ expression, validating the assay results (lane 7). These data suggest that HBZ may work against Tax to attenuate NHEJ in infected cell populations co-expressing both viral proteins.

Discussion

The accumulation of genetic abnormalities is a hallmark of ATL cells and arises, in part, from inadequate repair of DSBs. Here, we analyzed the degree to which HBZ influences DSB repair to contribute to genetic instability. We report that HBZ significantly attenuates NHEJ-C and NHEJ-I repair activity, but not DSB repair *via* the HR mechanism. In line with these observations, we report novel interactions between HBZ and NHEJ-initiating proteins Ku70 and Ku80, which form dimers at DNA breaks to stabilize the lesion. Further characterization of HBZ:Ku interactions revealed that the bZIP domain of HBZ is required. Interestingly, the bZIP domain was also found to be required for the suppression of NHEJ-C, suggesting that attenuation may be related to its interaction with Ku proteins. Though the HBZ:Ku complex can form independently of DNA contact, we noted that HBZ does not appear to negatively impact Ku recruitment to DSBs. Rather, our findings support that HBZ accompanies Ku to DNA termini *in vitro*, also in a bZIP-dependent manner, suggesting that NHEJ is not attenuated by impaired DSB recognition.

Ku70 and Ku80 form the DNA-binding component of the DNA-PK holoenzyme. Once bound to a DNA break, Ku proteins recruit the DNA-PK catalytic subunit, which possesses kinase activity, to provide additional stability and coordinate repair. We observed that, though HBZ forms a complex with Ku, it does not appear to disrupt the interaction between Ku70 and DNA-PKcs. However, we noted that etoposide-induced DNA-PK autophosphorylation at Ser 2056 was impaired by HBZ, potentially indicating attenuated kinase activity (**Figure 2.8**).

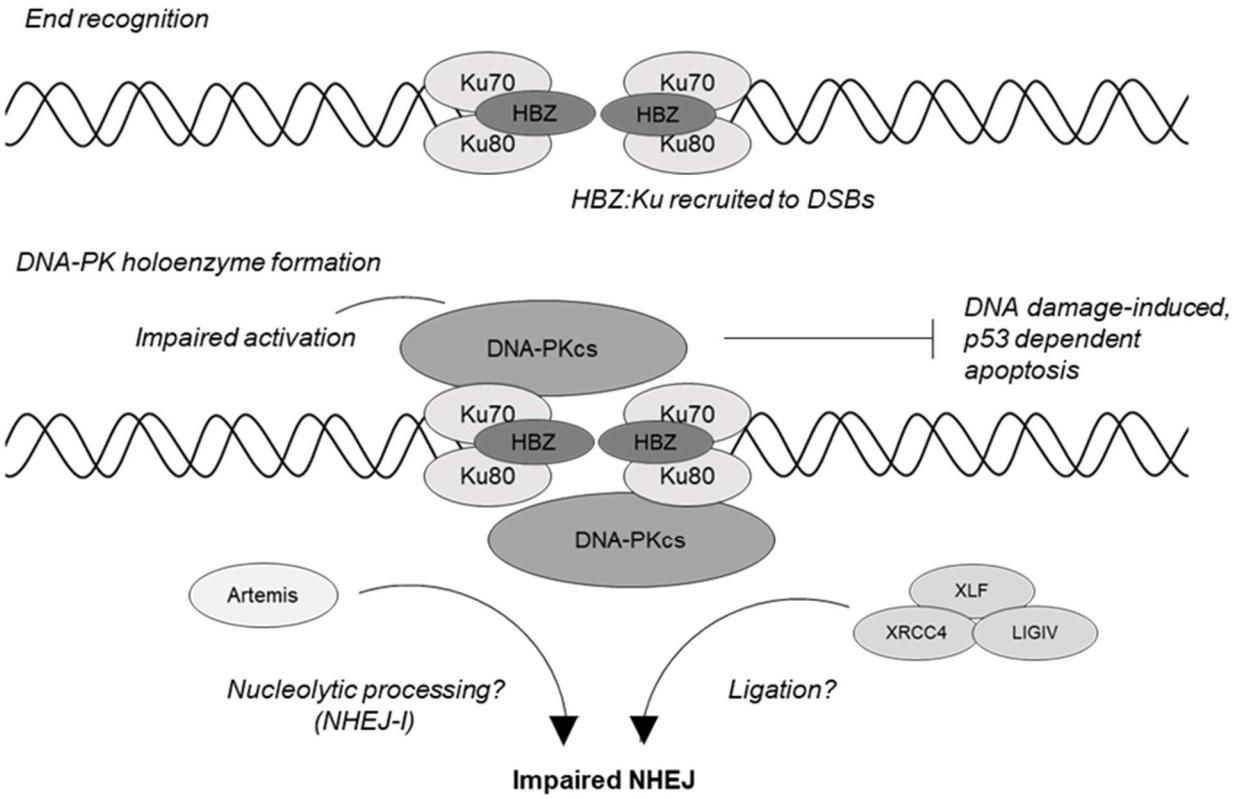

Figure 2.8: A proposed model for HBZ-mediated downregulation of NHEJ activity. We propose that HBZ interacts with Ku70:Ku80 heterodimers, possibly in a single complex, which is recruited to the DNA lesions. Though our data do not support that the presence of HBZ impairs the recruitment of DNA-PK to the break site, we observed that HBZ expression results in reduced autophosphorylation of DNA-PK, indicating impaired kinase activity. Several outcomes are possible, including impaired recruitment and/or activation of endonuclease and ligation machinery and increased stability of DNA-PKcs at the lesion, all of which have negative implications for NHEJ completion. Furthermore, we propose that HBZ-mediated impairment of DNA-PK kinase activity may block DNA-damage-induced pro-apoptotic signaling to p53 to enhance host cell survival and reduce sensitivity to DNA-damaging agents.

Activation of DNA-PK is initiated by DNA contact and phosphorylation of specific serine and threonine residues. Phosphorylation of Thr2609 is reported to be important for inducing a conformational change in the enzyme to promote DNA end processing, while phosphorylation of Ser2056 is reported to promote destabilization of DNA-PK from the lesion to allow repair to be completed[315]. Currently, Ser2056 is the only *bona fide* autophosphorylation site characterized in DNA-PK, as other sites are also targeted by additional PIKK family kinases. Furthermore, phosphorylated Ser2056 is accepted as a marker of DNA-PK activation and is associated with the completion of NHEJ[265–269]. We postulate that HBZ-mediated reduction of DNA-PK autoactivation indicates that DNA-PK is stabilized at DSBs, potentially negatively impacting later steps in NHEJ (**Figure 2.8**).

We also evaluated DNA-PK autophosphorylation in response to irradiation (IR), as both IR and etoposide have been reported to strongly induce the phosphorylation of Ser2056[265]. However, we did not observe strong DNA-PK activation in irradiated cells. Though IR and etoposide are both commonly used to induce DSBs, the toxicity of etoposide-induced breaks, as measured by H2AX phosphorylation, is much lower than the toxicity of IR-induced DSBs[318,319]. Increased toxicity of IR-induced lesions may explain why we were unable to replicate our results using this method of DNA damage induction.

Once activated, DNA-PK is demonstrated to phosphorylate a number of targets involved in NHEJ, including Artemis[320], AKT[321], H2AX[273], Ku70 and Ku80[322], XRCC4[323], XLF[324], and Ligase IV[325]; however, at this stage, the biological importance of these modifications remains largely unclear. Though the exact function of DNA-PK in NHEJ is not yet well defined, DNA-PK activity is essential for NHEJ, as the inhibition of kinase

activity sensitizes cells to DNA damage-induced cell death[314,326–330]. We question whether defective DNA-PK activation may have implications for the recruitment and activation of downstream NHEJ repair enzymes. A preliminary, qualitative analysis of chromatin-bound NHEJ enzymes after the induction of DSBs by etoposide treatment showed no noticeable differences in recruitment of the nuclease or ligation machinery (data not shown), however this method does not account for the presence of these enzymes elsewhere on the chromatin. Additionally, others have reported disparities between NHEJ-C and NHEJ-I in terms of the enzymes required for completion. Therefore, altered regulation of these enzymes could account for the differences in NHEJ-I and NHEJ-C efficiencies we observed in HBZ-expressing cells. Further investigation into the recruitment, phosphorylation patterns, and enzymatic activity of these enzymes is warranted to determine if HBZ negatively impacts their function in DSB repair.

In addition to its role in NHEJ-mediated DSB repair, DNA-PK activation has been characterized as a pro-apoptotic mechanism through which DNA damage induces the activation of the p53-dependent apoptosis cascade[271]. The pro-apoptotic signaling activity of p53 is tightly regulated by post-translational modifications, including acetylation and phosphorylation. Previous reports indicate that p53 is a phosphorylation target of DNA-PK, and that DNA-PK forms a complex with p53 on the DNA of cells treated with the nucleoside analogue gemcitabine, where it is postulated to act as a DNA damage sensor and provide pro-apoptotic signaling[274–276]. Additionally, DNA-PK is reported to phosphorylate the histone methyltransferase EZH2 to reduce its activity and promote DNA damage-induced apoptosis in T-cells[277]. Finally, DNA-PK is robustly

activated in apoptotic cells and phosphorylates H2AX during apoptotic DNA fragmentation[273]. Together, these findings support the role of DNA-PK as a pro-apoptotic DNA damage sensor. Here, we report that HBZ expression reduced DNA-PK activation in a bZIP-dependent manner. Our group has previously reported that HBZ reduces p53 acetylation *via* its interaction with cellular acetyltransferases, conferring resistance to etoposide-induced apoptosis[240,241]. Given that DNA-PK has been demonstrated to phosphorylate p53 *in vitro*, it is possible that HBZ-mediated impairment of DNA-PK kinase activity also contributes to the resistance to DNA damage-induced apoptosis. Interestingly Tax has also been demonstrated to impair p53 pro-apoptotic signaling by upregulating WIP1 phosphatase activity[286]. However, once Tax expression is lost due to negative regulation of 5' LTR transcription, it is expected that HBZ-modulation of p53 post-translational modifications is of critical importance for maintaining the continued survival of the host cell. It is possible that the downregulation of DNA-PK activation may represent another mechanism through which HBZ maintains the continued survival of the infected cell population.

Tax expression is important for facilitating *de novo* viral replication during early stages of infection. However, its expression is reported to be silenced in the majority of ATL cells at later stages, likely as a consequence of cytotoxic T-cell (CTL) evasion. However, some studies report the sporadic reactivation of 5' LTR transcription in a very small percentage of ATL cells. Conversely, expression of *hbz* transcripts was reported to be maintained in a cell cycle-dependent manner[248,249]. Interestingly, ATL patients exhibit a constant anti-Tax CTL response, supporting a constant, but perhaps low level, Tax immune challenge. These findings suggest that in some infected cell clones, Tax

and HBZ expression may briefly overlap, so it is important to understand how these viral proteins work in conjunction to regulate DNA damage repair. Tax has been demonstrated to reduce the efficiency of NHEJ through a reduction in Ku protein levels, as evidenced by a reduction in Ku expression in HTLV-1-infected cell lines C8166 and MT4, both of which express high levels of Tax[301]. Analysis of additional infected cell lines, some expressing little to no Tax, showed that while Ku expression was fairly consistent between uninfected and infected T-cell lines, infected cells with little or no Tax exhibited a slight increase in Ku70 and Ku80 protein levels. Though these data confirm that continued Tax expression somewhat reduces the level of Ku, it is unclear whether transient Tax expression will result in the same level of repression.

Additional evidence suggests that Tax saturates the NHEJ pathway through its interaction with DNA-PK and Ku70, resulting in an inability to repair newly acquired DSBs[287]. We found that when co-expressed, Tax and HBZ each maintain their respective interactions with Ku70, supporting that Tax:Ku and HBZ:Ku complexes form concurrently during instances in which Tax and HBZ are co-expressed.

Taken as a whole, these observations led us to question how HBZ and Tax concurrently modulate DSB repair activities. We observed that NHEJ-C activity was enhanced in Tax-expressing cells, and that Tax expression masked HBZ-mediated attenuation. These findings, in combination with evidence from previous reports, suggest that the preferred mechanism of DSB repair in HBZ^+ Tax^+ cells may be NHEJ, but that when Tax expression is silenced, the preferred repair mechanism may be HR. HR is a cell cycle dependent DSB repair mechanism that is active only during S and G_2/M phases. Therefore, increased rates of HR-dependent repair have been reported in

rapidly-proliferating cells, including some cancer cell types. Interestingly, the increased frequency of HR has been implicated in increased risk for chromosomal translocations and loss of heterozygosity, a major risk factor for carcinogenesis[261]. HBZ pro-proliferative activities have been implicated in maintaining clonal expansion and driving aggressive lymphoproliferation in ATL. Though we observed HR to be unaffected by HBZ expression, it is unclear whether HR represents a pro-leukemogenic mechanism in the context of the HTLV-1-infected cell. Further work will be required to delineate how Tax and HBZ affect the selection of DSB repair in primary ATL cells, and whether increased dependence of HR-mediated repair in HBZ-expressing cells contributes to disease progression.

Materials and Methods

Cell lines, cell culture, and treatments: HEK 293T cells were cultured in Dulbecco's Modified Eagle's Medium (DMEM) supplemented with 10% fetal bovine serum, 2mM L-glutamine, 100U/ml penicillin, and 50µg/mL streptomycin. Clonal HeLa-pCMV and HeLa-pCMV-HBZ-FLAG[240] were cultured in spinner flask suspensions in Minimum Essential Medium supplemented with 5% newborn calf serum, 3% fetal bovine serum, 2mM L-glutamine, 1X MEM non-essential amino acids solution, 1mM sodium pyruvate, 100U/ml penicillin, 50µg/mL streptomycin, and 0.2mg/mL hygromycin B (Invitrogen). Clonal HeLa-pcDNA, HeLa-pcDNA-HBZ-Myc-His, and HeLa-pcDNA-HBZ-ΔbZIP-Myc-His cell lines were maintained in supplemented DMEM and were maintained under selection with 0.5mg/mL geneticin (ThermoFisher). T-cell lines were maintained in either supplemented Iscove's Modified Dulbecco's Medium (IMDM) or supplemented Roswell

Park Memorial Institute (RPMI) medium. To inhibit NHEJ repair activity, cells were treated the DNA-PK inhibitor NU7441 (2μM) for 24hrs. To inhibit HR repair activity, cells were treated with the RAD51 inhibitor B02 (20μM) for 24hrs. To induce the accumulation of DSBs, cells were treated with 50μM of etoposide (Sigma-Aldrich) in DMSO for the indicated amount of time.

Plasmids and Antibodies: The following HBZ mammalian expression plasmids have been described: pcDNA-HBZ Sp1-Myc-His (aa 1-206)[91], pcDNA-HBZ-ΔAD-Myc-His (aa 77-206)[227], pcDNA-HBZ-ΔbZIP-Myc-His (aa 1-130)[81], pcDNA-HBZ-ΔATG-Myc-His[220], pCMV-HBZ-FLAG[240], pSG-HBZ-Myc[220], and pSG-Tax-His[298], pCMV-HBZ-FLAG[240]. Plasmids pEGFP-C1-FLAG-Ku70 and pEGFP-C1-FLAG-Ku80 were gifts from Steve Jackson (Addgene plasmids #46957 and #46958)[331]. NHEJ-C and NHEJ-I reporter plasmids were provided by Vera Gorbunova[332]. pDR-GFP was a gift from Maria Jasin (Addgene plasmid #26475)[303]. I-SceI-HA was amplified from pCBASceI, also a gift from Maria Jasin (Addgene plasmid #26477)[333] using a 5' BamHI primer and a 3' BglII primer (sequences available upon request) and subcloned into the pSG5 vector (Agilent Technologies) *via* BamHI, BglII digestion to construct pSG-I-SceI-HA. Empty vector plasmid pCMV-3Tag-8 was purchased from Agilent Technologies and pcDNA3.1 (+)/ Myc-His A was purchased from Invitrogen.

The following antibodies were used: anti-FLAG M2 (Sigma-Aldrich F3165), anti-Myc clone 4A6 (EMD Millipore 05-724), anti-His H-15 (Santa Cruz Biotechnology sc-803), anti-Actin clone C4 (EMD Millipore MAB1501), anti-DNA-PKcs (Cell Signaling #4602), anti-DNA-PKcs phospho-S2056 (Abcam ab18192), anti-Ku70 D10A7 (Cell

Signaling #4588), anti-Ku70 (Santa Cruz scb0917), and anti-Ku80 C48E7 (Cell Signaling #2180), anti-phospho-histone H2A.X Ser139 (EMD Millipore #07-164), anti-histone H3 (EMD Millipore #06-755). Anti-HBZ serum was generously provided by Jean-Michel Mesnard [77], and Tax monoclonal antibody (hybridoma 168B17-46-92) was obtained from the National Institutes of Health AIDS Research and Reference Reagent Program.

Identification of HBZ-binding proteins by liquid chromatography tandem mass spectrometry (LC-MS/MS): HeLa-S3 cells electroporated with pCMV-3Tag-8 or pCMV-HBZ-FLAG were cultured under hygromycin selection. Stably transfected clones were isolated and expanded to spinner flask suspension culture under continual hygromycin selection. $8x10^6$ cells were pelleted at 350xg for 3 min at 4°C, washed in 1x PBS, and resuspended in 1mL RIPA buffer (50mM Tris [pH 8.0], 1% Triton X-100, 100mM NaCl, 1mM $MgCl_2$, 400nM TSA, 2µg/mL leupeptin, 5µg/mL aprotinin, 1mM PMSF, and 1mM benzamidine). Cells were vortexed briefly, and incubated on ice for 20 minutes. Lysates were centrifuged at 16,000xg for 15 minutes at 4°C and soluble protein supernatant was isolated and quantified by Bradford protein assay (Bio-Rad). Equalized cell lysates were pre-cleared and HBZ-FLAG protein complexes were immunoprecipitated using anti-FLAG M2 magnetic resin (Sigma-Aldrich M8826): 40µL resin slurry was washed twice in 1X TBS+ (2µg/mL leupeptin, 5µg/mL aprotinin, 1mM PMSF, and 1mM benzamidine) and incubated with equalized protein extracts for approximately 16 hours. Resin was washed four times in 1X TBS+ and protein complexes were eluted by FLAG peptide competition using 0.5µg/µL FLAG peptide (Sigma-Aldrich F3290) in 100µL 1X TBS+ for

30 minutes. Eluates were run partially through an SDS-PAGE gel and total protein bands were excised for in-gel digestion. Gel pieces were washed first in 50mM ammonium bicarbonate (AMBIC), then in acetonitrile. Samples were reduced with 10mM DTT in 50mM AMBIC for 30 minutes at 56°C, washed in acetonitirile, alkylated with 55mM iodoacetamide in 50mM AMBIC for 20 minutes, washed in 50mM AMBIC, then washed in acetonitrile. Gel pieces were dried by speed vacuum centrifugation. Protein was digested in-gel using trypsin (Promega) in a 0.01% ProteaseMax/ 50mM AMBIC solution at a 1:30 enyzme:protein ratio. Digestion was halted using formic acid and peptides were extracted by covering the gel pieces with 60% acetonitrile/ 0.1% trifluoroacetic acid followed by sonication. Peptides were analyzed by liquid chromatography tandem mass spectrometry (LC-MS/MS) (Q-Exactive Hybrid Quadrupole-Orbitrap Mass Spectrometer, UC Davis Proteomics Core Facility). Tandem mass spectra were matched with peptide sequences by X! Tandem (Global Proteome Machine Organization) using the Uniprot_20140422_W_VRKr database assuming the digestion enzyme tryspin. X! Tandem was searched with a fragment ion mass tolerance of 20 ppm and a parent ion tolerance of 20 ppm. Fixed modifications included cysteine carbamidomethylation. Variable modifications included Glu->pyro-Glu of the N-terminus, ammonia loss of the N-terminus, Gln->pyro-Glu of the N-terminus, deamidated asparagine and glutamine, oxidation of methionine and tryptophan, dioxidation of methionine and tryptophan, and acetylation of the N-terminus. Scaffold version Scaffold_4.7.3 (Proteome Software Inc.) was used to validate and accept MS/MS-based protein identifications. Protein identifications were accepted at a False Discovery Rate of less than 1%, a probability of $\geq$99%, and with at least 3 identified peptides with a

maximum of 1 missed cleavage. To exclude the possibility of non-specific interactions of cellular proteins with anti-FLAG antibody, proteins which were identified in the empty vector (pCMV-3Tag-8) samples were excluded from analysis, leaving proteins that were only identified in the pCMV-HBZ-FLAG samples. Proteins unique to HBZ-FLAG samples were manually annotated based on function. Data is representative of one independent experiment and is available upon request.

Co-immunoprecipitation: HEK 293T cells ($2x10^6$) were transiently transfected using TurboFect (ThermoFisher) according to the manufacturer's instructions. Where, applicable, etoposide treatment (50μM) (Sigma-Aldrich) was carried out 4-5 hours prior to harvesting protein extracts. Protein extracts were prepared 24-48 hours post-transfection. For nuclease-treated samples, 250U benzonase (Sigma-Aldrich) was added to cell lysates before immunoprecipitation. For co-immunoprecipitations performed with anti-FLAG M2 magnetic resin (Sigma Aldrich M8826), 15μL of resin slurry was washed twice in RIPA buffer and incubated with the indicated amount of protein extract for approximately 16 hours at 4°C. Resin was washed four times in RIPA buffer and bound proteins were eluted by SDS dye and resolved by SDS-PAGE and Western blot. Immunoprecipitations performed with MT-2 cells were performed as follows: Per IP, three sets of MT-2 cells ($3x10^6$) in 300μL serum-free RPMI were electroporated with 15μg of pCMV-HBZ-FLAG or the empty vector in 0.4 cm cuvettes (pulse=200V, 975uF, ∞Ω). Where indicated, cells were treated for 5hrs with 50μM etoposide. Anti-FLAG immunoprecipitations were performed with 500μg of cell lysate. All eluates were analyzed by SDS-PAGE and Western blotting using the primary

antibodies listed in the figure legends. All blots were developed using Pierce ECL Plus chemiluminescence substrate (ThermoFisher), and visualized with a Typhoon 9410 (GE Healthcare).

NHEJ repair assays and flow cytometry: HEK 293T cells ($6x10^5$) were transiently transfected (TurboFect) with 6-7µg of DNA consisting of a mixture of DNA repair reporter vector (NHEJ-C, NHEJ-I, or DR-GFP), pSG-I-SceI-HA, as well as the Tax and HBZ expression vectors described in the figure legends. Where indicated, cells were treated with 2µM NU7441 or 20µM B02 (Selleckchem) for 24hrs. At 48 hours post-transfection, cells were pelleted, washed twice in 1x PBS, and resuspended in ice-cold 1x PBS for flow cytometric analysis. Live cell populations were analyzed for GFP expression using an LSRII flow cytometer (BD Biosciences). Data were analyzed using FlowJo (FlowJo, LLC). Transfections groups consisted of a reporter vector alone, a reporter vector + the I-SceI expression plasmid (reporter + I-SceI), and a reporter vector + I-SceI expression plasmid + protein of interest expression vectors (e.g. Tax and/or HBZ). For each experiment, background GFP levels were measured from reporter only cells and was subtracted from all other transfection groups. Maximum GFP expression (reporter + I-SceI) was set to 1 and data are displayed as fold change relative to reporter + I-SceI group GFP expression. Fold change changes in the total number of cells within the live cell population that are GFP-positive. Western blot was used to confirm expression of transfected plasmids using the antibodies indicated in the figures.

Nuclear protein extraction and *in vitro* immobilized DNA-binding assays: Nuclear protein extracts were prepared as follows: $8x10^6$ HEK 293T cells were transfected by calcium phosphate transfection with 50µg-100µg of plasmid DNA as indicated in the figure legend (50µg pcDNA3.1, 50µg pcDNA-HBZ-Myc-His, 100µg pcDNA-HBZ-ΔAD-Myc-His, 50µg pcDNA-HBZ-ΔbZIP-Myc-His, 50µg pcDNA-HBZ-ΔZIP) and nuclear protein was harvested 48 hours post-transfection using a previously described method[334,335]. Supernatants were collected and dialyzed for approximately 16 hours against 0.1M HM (50mM HEPES [pH7.9], 100mM KCl, 20% glycerol, 12.5mM $MgCl_2$, 1mM EDTA, 0.025% Tween, 1mM DTT). Nuclear protein concentration was quantified by Bradford protein assay (Bio-Rad).

Variations of the immobilized DNA template have been used to analyze binding of NHEJ proteins to DNA termini[306–311]. We performed our immobilized DNA-binding assays as previously described with only minor modifications[336]. Per reaction, 2pmol of biotinylated double-stranded DNA 35bp in length was bound to 15µL M-280 streptavidin-coupled Dynabeads (Invitrogen) according to the manufacturer's instructions. DNA-bound resin was blocked for one hour in ITB (20mM HEPES [pH 7.9], 0.2mM EDTA, 100mM KCl, 6.25mM $MgCl_2$, 10mM $ZnSO_4$, 20% glycerol, 0.01% Triton X-100, 5% BSA, 0.2mM PMSF, 1mM benzamidine, 10µg/mL aprotinin, 10µg/mL leupeptin, 1mM DTT) with 5% BSA. The resin was cleared and loaded with 10µg of nuclear protein extracts in a total volume of 500µL of ITB/ 5% BSA and rocked for 2 hours at 4°C. Resin was washed four times in ITB without BSA and protein was eluted with SDS dye and resolved by SDS-PAGE and Western blot.

Chromatin immunoprecipitation assays (ChIP): HeLa cell lines stably transfected with pcDNA 3.1, pcDNA-HBZ-Myc-His, or pcDNA-HBZ-ΔATG were plated at $1x10^7$ and were transiently transfected with 10μg of the NHEJ reporter vector and 10μg of the I-SceI expression plasmid. Twenty-four hours post-transfection, the chromatin was crosslinked by adding 1% formaldehyde to the media for 10 min at 37°C, followed by the addition of 0.125M glycine to quench the reaction. Cells were collected with a cell scraper, pelleted at 350xg, and washed in 1X PBS. The remainder of the ChIP assay was performed using the Zymo Spin ChIP Kit (Zymo Research) according to the manufacturer's instructions. For each ChIP reaction, 20μg of crosslinked chromatin was diluted to a final volume of 1mL in ChIP chromatin dilution buffer provided in the kit, and was incubated with 5μg of the appropriate antibody for approximately 16 hrs. Immunoprecipitation was performed using anti-Ku70 A-9 (Santa Cruz scb0917) or pre-immune rabbit serum (IgG). ChIP DNA was purified according to the kit protocol and was eluted in a total volume of 50μL. Real-time PCR and data analysis were performed as described previously[81]. PCR primers targeted a region of DNA sequence neighboring the NHEJ-C I-SceI cleavage site, or an uncleaved region of the reporter plasmid (GFP). Primer sequences are available upon request. Standard curves were generated for primer sets using fivefold serial dilutions of each input DNA from the ChIP and were included on each experimental plate. PCR efficiencies ranged from 95 to 105%, with correlation coefficients greater than 0.99. Quantitation was performed by comparing threshold cycle values for co-immunoprecipitated DNA to the threshold cycle value for the input DNA in each ChIP[337]. Ku70 enrichment for each experiment was normalized against IgG. Fold change was calculated by dividing values for the NHEJ cut

site primer set to the uncut GFP primer set. Therefore, data shown represent fold change in Ku70 binding compared to the uncut region of the reporter plasmid. Significance was calculated using the Student's t-test (*$p \leq 0.05$) and error bars represent SEM.

Acknowledgements and Funding:

We would like to acknowledge Torsten Wurm for his preliminary work on this project. We would also like to thank Stephanie Nguyen, Chyna Johnson, Kayla DeOca, and Alicia Kwon for their assistance. Funding for this study was provided by the National Institute of Health's National Cancer Institute (NIH/NCI CA128800) to IL. The funding agency had no role in the study design, data collection and interpretation, or the decision to submit the work for publication.

Chapter 3

The HTLV-1 basic leucine zipper factor (HBZ) upregulates the expression of antioxidant Heme Oxygenase I and promotes detoxification of reactive oxygen species

Amanda W. Rushing[1], Blake Rushing[2], Kimson Hoang[1], Stephanie V. Sanders[1], Jean-Marie Péloponèse Jr[3], Nicholas Polakowski[1], and Isabelle Lemasson[1]

[1] Department of Microbiology and Immunology, Brody School of Medicine, East Carolina University, Greenville, North Carolina, United States of America

[2] Department of Pharmacology and Toxicology, Brody School of Medicine, East Carolina University, Greenville, North Carolina, United States of America

[3] Institut de Recherche en Infectiologie de Montpellier, Montpellier, France

Abstract

HTLV-1 establishes lifelong, chronic infection and is the etiological agent of Adult T-cell Leukemia (ATL) and HTLV-1-asociated myelopathy/ tropical spastic paraparesis (HAM/TSP). The viral regulatory proteins Tax and HBZ are important for disease progression and each are reported to play roles in maintaining HTLV-1 infection and leukemogenesis. Tax is reported to stimulate the production of toxic reactive oxygen and nitrogen species (RNOS) that can induce DNA damage, replicative senescence,

and apoptosis. It is unclear how HTLV-1-infected cells overcome Tax-mediated production of RNOS, however HBZ has been demonstrated to be essential for maintaining the continued survival and proliferation of the infected cell population. We report that HBZ upregulates the expression of certain antioxidant genes, including Heme Oxygenase I (HMOX-1), a heme-metabolizing enzyme which is important for maintaining cellular homeostasis and protecting against stress-induced apoptosis. Here, we provide evidence supporting that HMOX-1 upregulation is facilitated by HBZ and small Maf (sMaf) heterodimers, which we found to be recruited to antioxidant response elements (AREs) in the HMOX-1 promoter *in vitro* and *in vivo*. Furthermore, we found transactivation at AREs to be significantly upregulated in HBZ-expressing cells. We also present evidence supporting that HBZ expression confers resistance to stress-induced cell death, and attenuates Tax-induced oxidative stress. These findings suggest an additional mechanism through which HBZ contributes the long-term survival and proliferation of HTLV-1-infected cell populations within the host.

Introduction

The accumulation of reactive oxygen and nitrogen species (RNOS) can induce damage to cellular structures, including genetic material. Oxidative DNA damage can result in cell cycle arrest, the induction of replicative senescence, and initiation of apoptosis[338,339]. To avoid these outcomes, the antioxidant response is activated to induce the expression of free radical- and metal-scavenging enzymes to detoxify free radicals and restore cellular homeostasis. The induction of the antioxidant response is largely regulated by small musculoaponeurotic fibrosarcoma proteins MafF, MafG, and

MafK, along with the Cap'n'Collar (CNC) transcription factor NF-E2-related factor 2 (Nrf2). Upon sensation of oxidative stress, small Mafs (sMafs) heterodimerize with Nrf2 to promote stable DNA-binding at antioxidant response elements (AREs) in the promoters of antioxidant genes, resulting in transcriptional upregulation[340–343]. Though the upregulation of antioxidant enzymes is an important cancer-prevention mechanism, constitutive overexpression of these proteins is reported in a variety of malignancies, where they are associated with the development of drug and radiation resistance, increased metastasis, and poor patient outcome[344–349].

Human T-cell leukemia virus type I (HTLV-1) is a human retrovirus that preferentially infects $CD4^+$ T-cells and establishes a persistent, lifelong infection. While the majority of HTLV-infected individuals remain asymptomatic carriers, HTLV-1 may also cause lymphoproliferative and inflammatory diseases. HTLV-1-associated myelopathy/tropical spastic paraparesis (HAM/TSP) is a chronic inflammatory condition that causes severe demyelination of the spinal cord[5,6]. Though pathogenesis is not yet definitively understood, evidence suggests that anti-HTLV-1 cytotoxic T-cells (CTLs) target infected lymphocytes that have crossed the blood-brain barrier, resulting in increased pro-inflammatory cytokine production and damage to the surrounding nervous tissue[121,132,350]. Adult T-cell leukemia (ATL) is a highly aggressive lymphoproliferative disorder that affects about 5% of HTLV-1 carriers[2–4,7]. Like HAM/TSP, the mechanisms that drive ATL progression remain unclear, however pathogenesis is closely associated with the activities of two, pro-oncogenic viral regulatory proteins, Tax and the HTLV-1 basic leucine zipper factor (HBZ)[96,213,223,351,352].

Tax and HBZ have each been demonstrated to play varying roles in regulating proviral gene expression, promoting cellular proliferation, and inhibiting apoptosis.

Tax is reported to be essential for *de novo* viral replication and transmission, as well as for preventing the induction of apoptosis[41,353]. Paradoxically, it has also been demonstrated to induce the production of RNOS through the hyperactivation of canonical and non-canonical NF-κB pathways, as well as by upregulating the expression of inducible nitric oxide synthase (iNOS)[184–189,191–193,354,355]. Furthermore, the viral accessory protein p13 has been observed to localize to inner mitochondrial membranes to induce membrane depolarization, upregulate respiration, and greatly enhance the production of ROS[356–360].

Given the immunogenicity of Tax, the expression of sense strand-encoded viral genes is silenced in the majority of ATL cells through mutation, hypermethylation, or transcriptional repression of the 5' long terminal repeat (LTR)[19,169–173,361]. Unlike Tax and p13, HBZ is encoded on the antisense strand and is consistently expressed throughout HTLV-1 disease progression[93,96,214,351,362]. HBZ has been extensively characterized to have pro-survival functions and its expression is critical for maintaining the continued proliferation of HTLV-1-infected cells. Notably, HBZ is reported to prevent the induction of apoptosis, rescue host cells from NF-κB-induced senescence, and promote immune evasion by downregulating transcription at the 5' LTR [93,234,236–238,240,243–245]. These reports confirm that HBZ plays a variety of cytoprotective roles within the host cell, possibly as a means of promoting long-term viral persistence. However, its involvement in the response to Tax- and p13-induced oxidative stress is

unknown. We questioned whether HBZ modulates the host cell antioxidant response to regulate homeostasis and maintain survival and proliferation of infected cell clones.

We report that HBZ expression results in the transcriptional activation of several antioxidant response genes known to be regulated by Nrf2:sMaf complexes, including Heme Oxygenase I (HMOX-1), which we found to be increased at the transcript, protein, and functional levels. HMOX-1 is a prototypical antioxidant enzyme that safely catalyzes the degradation of heme to protect against stress-induced apoptosis **(Figure 3.1)**[363–366]. Interestingly, HMOX-1 overexpression is reported in a variety of malignant tissues and may contribute to the development of drug resistance[367–371]. Because HMOX-1 is associated with cancer cell survival, and its function and transcriptional regulation are well understood, we used this gene as a model for evaluating HBZ-mediated transcriptional manipulation of the antioxidant response.

Here, we confirmed the leucine zipper-dependent interaction between HBZ and MafG[230], and report similar interactions between HBZ and MafF and MafK. Interestingly, enhanced HMOX-1 expression was found to be dependent upon the basic leucine zipper (bZIP) domain of HBZ, suggesting that interactions with sMafs may be important for upregulation. Analysis of the DNA-binding capabilities of the HBZ:sMaf complex supports its recruitment to AREs found in the HMOX-1 promoter *in vitro and in vivo*. Furthermore, AREs were found to be transactivated in HBZ-expressing cells in a bZIP-dependent manner. Finally, we confirmed the role of Tax in upregulating levels of intracellular ROS and report that HBZ functions in a cytoprotective capacity by reducing Tax-induced oxidative stress and by promoting cell survival in response to oxidation. These findings support that HBZ enhances the induction of HMOX-1, and perhaps a

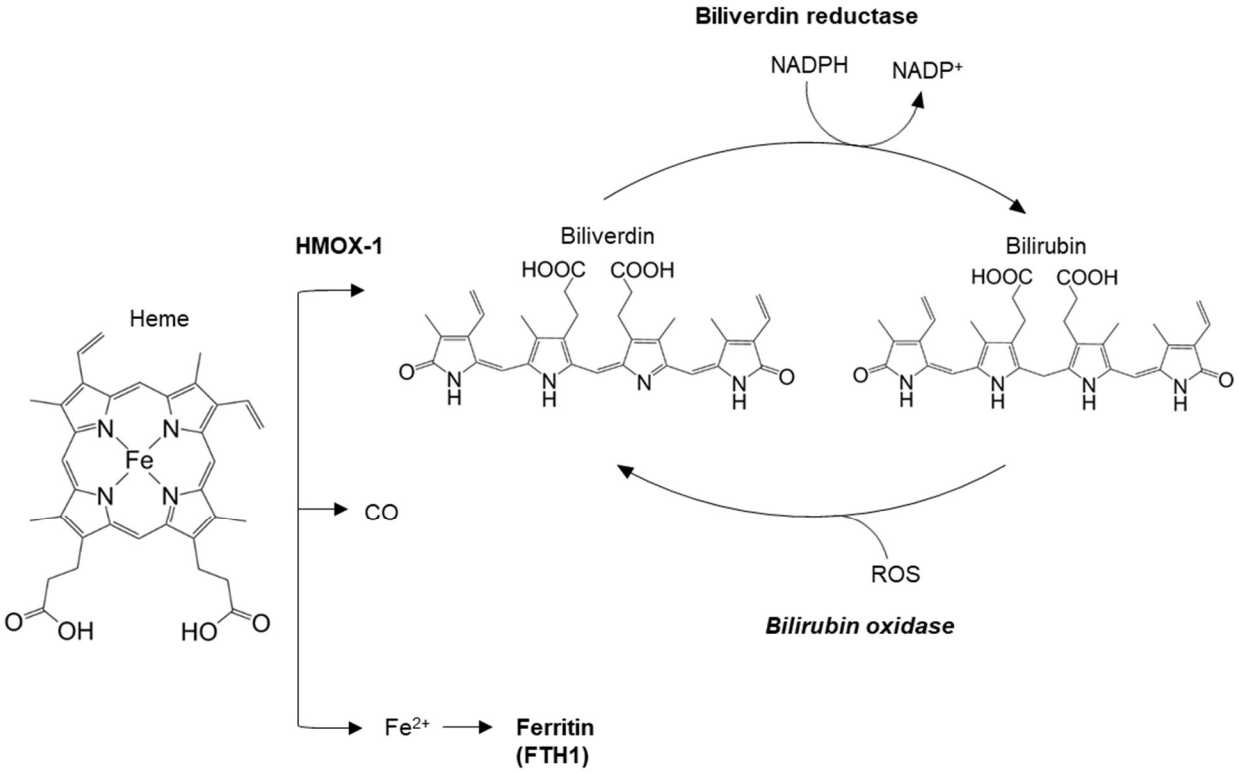

Figure 3.1: HMOX-1 metabolizes heme to prevent iron-induced toxicity. Heme (iron protoporphyrin IX) is released from hemoproteins that become damaged. HMOX-1 is upregulated in response to rising levels of intracellular heme, as well as in response to other sources of oxidative stress. HMOX-1 enzymatically cleaves the protoporphyrin ring to create biliverdin, carbon monoxide (CO), and free ferrous iron (Fe^{2+}). Ferrous iron is scavenged by Ferritin and biliverdin is reduced to bilirubin. Bilirubin may be oxidized by reactive oxygen species (ROS) to form biliverdin, a putative ROS sink. HMOX activity assays performed in this study utilize the enzyme bilirubin oxidase from *Myrothecium verrucaria* to convert bilirubin into biliverdin for quantification.

larger antioxidant response, potentially as a means of overcoming oxidative stress induced by Tax. We propose that this activity likely promotes long-term cell survival and may contribute to viral persistence in the host.

Results

Genes in the Nrf2-ARE pathway are upregulated in HBZ-expressing cells: HBZ has been reported to alter cellular gene expression by affecting the functions of transcriptional regulators, but the physiological impact of these changes remains poorly understood. To evaluate HBZ-induced changes in gene expression on a large scale, we performed a microarray analysis of transcripts in a clonal HeLa cell line stably expressing HBZ-Myc-His, compared to transcripts found in empty vector-transfected cells. Gene transcripts that were upregulated in HBZ-expressing cells were manually annotated by function and preliminary analysis suggested that several antioxidant stress response genes are among those upregulated as a result of HBZ expression. To evaluate if the transcription of these genes is regulated by the activity of the Nrf2:sMaf complex at promoter AREs, we compared our data to Nrf2 and sMaf ChIP-seq data sets reported by other groups[372–375]. We found that HBZ expression resulted in the upregulation of Nrf2:sMaf-regulated genes HMOX-1, FTH1, SQSTM1, PIM1, and TNFRSF1A. We confirmed our findings by quantifying transcript levels of these genes in HeLa cells stably expressing HBZ-Myc-His as compared to empty vector-transfected cells (**Figure 3.2**).

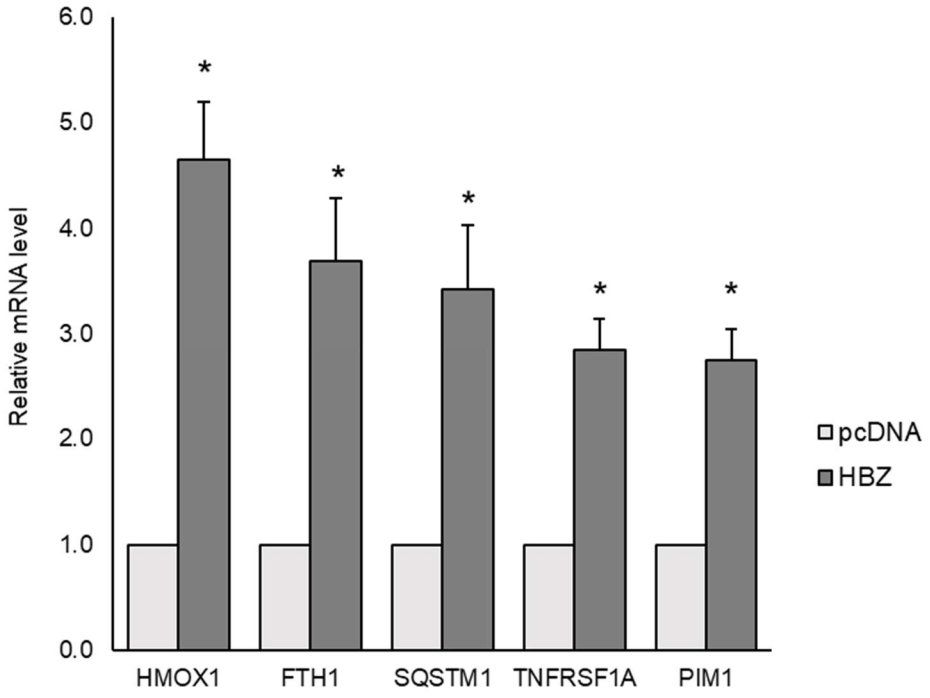

Figure 3.2: Antioxidant response genes are upregulated in HBZ-expressing cells. qRT-PCR was used to quantify select antioxidant response gene transcripts in HeLa cells stably transfected with pcDNA-HBZ-Myc-His (HBZ) or the empty vector (pcDNA). For HMOX-1, data is an average of seven independent experiments. For FTH1, SQSTM1, TNFRSF1A, and PIM1, the data are an average of four independent experiments. For all data, error bars indicate SEM (Student's t-test, * $p \leq 0.05$).

HMOX-1 is upregulated in HTLV-1-infected T-cells: HMOX-1 is a well-characterized antioxidant enzyme that is upregulated in response to a wide variety of cellular stressors, including its substrate heme, and ROS-producing compounds such as hydrogen peroxide (H_2O_2)[363]. Because HMOX-1 is emerging as a potential prognostic marker for certain cancers, and because transcriptional regulation of HMOX-1 is well understood, we focused our analysis on this gene[366]. We next quantified HMOX-1 transcripts in a panel of HTLV-1-infected and uninfected T-cell lines. Uninfected cells in this panel included T-acute lymphoblastic leukemia (T-ALL) cell lines Jurkat and CEM, as well as primary $CD4^+$ and anti-CD3, anti-CD28 activated $CD4^+$ T-cells, as activation has been shown to increase HMOX-1 transcription[376]. HTLV-1-infected T-cell lines included MT-2, which were established *in vitro*, and ATL-2s and TL-Om1, which were established *in vivo* and derived from ATL patients (**Figure 3.3.A)**. Although all three infected cell lines express HBZ, TL-Om1 are deficient in Tax expression due to hypermethylation of the 5' LTR[172]. We observed that HMOX-1 transcripts were increased in activated primary $CD4^+$ T-cells, and in all three infected cell lines, even in the absence of Tax expression (TL-Om1), supporting that HBZ is primarily responsible for upregulating expression.

We next confirmed that the increase in HMOX-1 transcripts we observed corresponds to an increase in protein levels. Because HMOX-1 is primarily localized to the endoplasmic reticulum membrane, we analyzed the membrane-bound protein fraction of HTLV-1-infected T-cells for HMOX-1 protein levels[365]. Voltage-dependent anion-selective channel protein (VDAC) is also found in the membrane-bound protein fraction and was used as a loading control for these experiments. We observed HMOX-

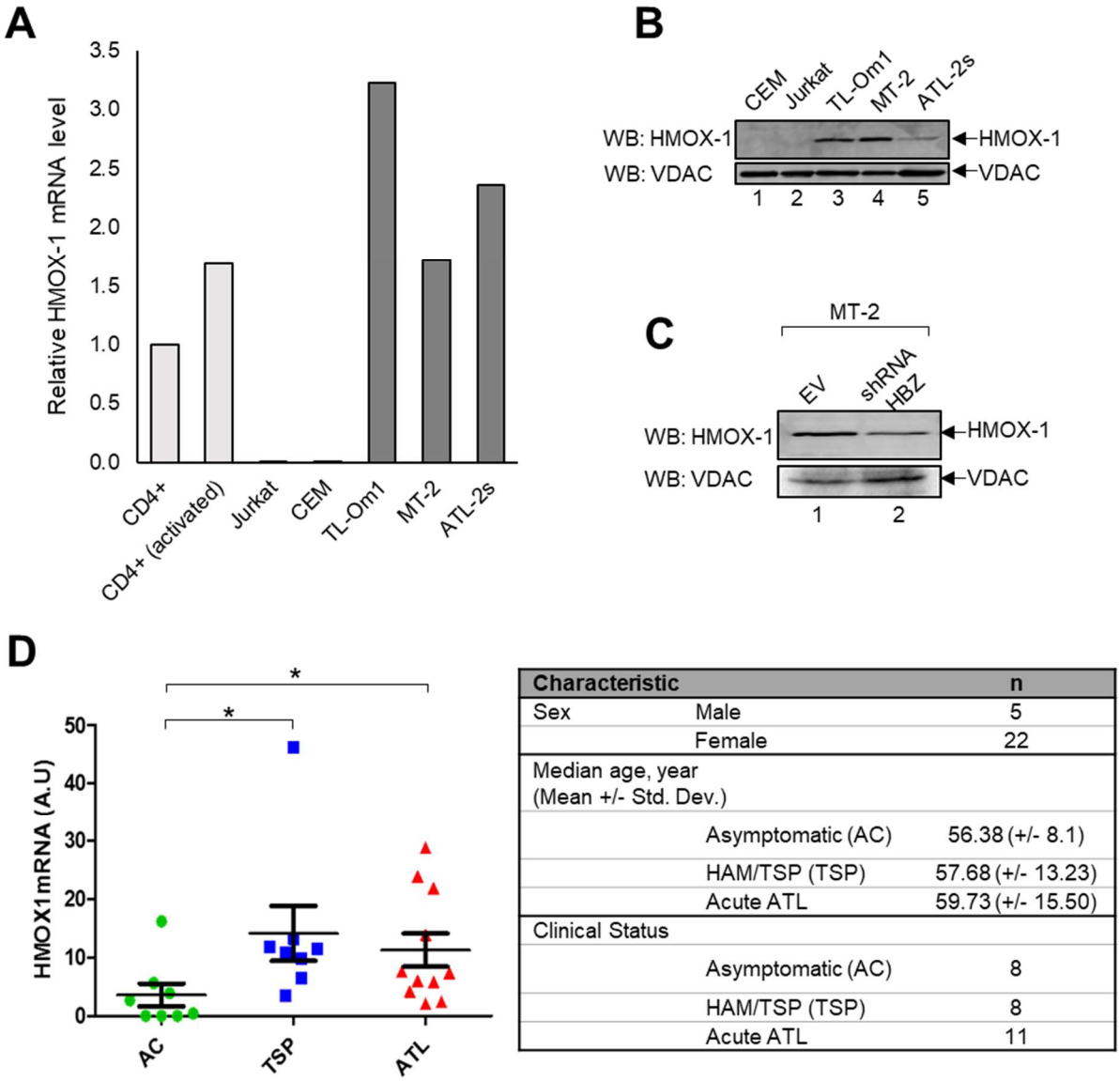

Characteristic		n
Sex	Male	5
	Female	22
Median age, year (Mean +/- Std. Dev.)		
	Asymptomatic (AC)	56.38 (+/- 8.1)
	HAM/TSP (TSP)	57.68 (+/- 13.23)
	Acute ATL	59.73 (+/- 15.50)
Clinical Status		
	Asymptomatic (AC)	8
	HAM/TSP (TSP)	8
	Acute ATL	11

Figure 3.3 HMOX-1 transcripts are upregulated HTLV-1-infected T-cells. (A) HMOX-1 transcripts were quantified in uninfected T-cell lines (Jurkat, CEM, $CD4^+$, activated $CD4^+$) and HTLV-1-infected T-cell lines (1185, TL-Om1, MT-2, ATL2-S). Data shown is from one experiment performed in triplicate and is representative of three independent experiments. **(B)** Membrane-bound HMOX-1 protein levels in uninfected T-cell lines (Jurkat,CEM) and HTLV-1-infected T-cell lines (TL-Om1, MT-2, ATL-2s). A total of 60 µg of protein was analyzed by Western blot using the indicated antibodies. **(C)** Membrane-bond HMOX-1 protein levels (90 µg) were evaluated in MT-2 cells stably transected with an shRNA against HBZ (shHBZ), or the empty vector (EV). **(D)** HMOX-1 transcript levels were evaluated in $CD8^+$-depleted PBMCs isolated from asymptomatic carriers (AC), HAM/TSP patients (TSP), and acute ATL patients (ATL). Patient information is shown in the table. Error bars indicate standard deviation (Student's t-test, * $p \leq 0.05$)

1 protein levels to be consistent with HMOX-1 transcript levels (**Figure 3.3.B**). To further confirm the role of HBZ in upregulating HMOX-1 at the protein level, we compared membrane-bound HMOX-1 protein levels in MT-2 cells transfected with shRNA that targets HBZ (shRNA HBZ) or transfected with the empty vector (EV) (**Figure 3.3.C**)[377,378]. We observed that HMOX-1 protein was reduced in shRNA HBZ-transfected cells as compared to EV.

We next evaluated whether there was any correlation between HMOX-1 expression and HTLV-1-associated diseases in patients. We compared transcripts between $CD8^+$ T-cell depleted PBMCs isolated from a small group of acute ATL patients (n=8), HAM/TSP patients (n=8), and asymptomatic carriers (n=11) (**Figure 3.3.D**). On average, HMOX-1 transcripts were observed to be upregulated in the ATL patient group and in the HAM/TSP patient group when compared to asymptomatic carriers. This preliminary analysis of HTLV-1-infected individuals suggests that HMOX-1 overexpression may be related to disease progression.

Finally, to evaluate the enzymatic activity of HMOX-1 in HBZ-expressing cell lines, we used liquid chromatography mass spectrometry (LC-MS) to quantify biliverdin levels, the main product of HMOX-1-mediated heme metabolism (**Figure 3.1**)**.** Perplexingly, the data showed that HeLa cells stably expressing HBZ did not exhibit a significant change in HMOX-1 activity until they were exposed to oxidative conditions by H_2O_2 treatment. Stressed HBZ-expressing cells exhibited significantly higher levels of biliverdin when compared to empty vector-transfected cells (**Figure 3.4.A**). When we analyzed HMOX-1 transcripts from H_2O_2-treated cells, we saw that though exposure to oxidative stress induced HMOX-1 expression in both cell lines, significantly higher

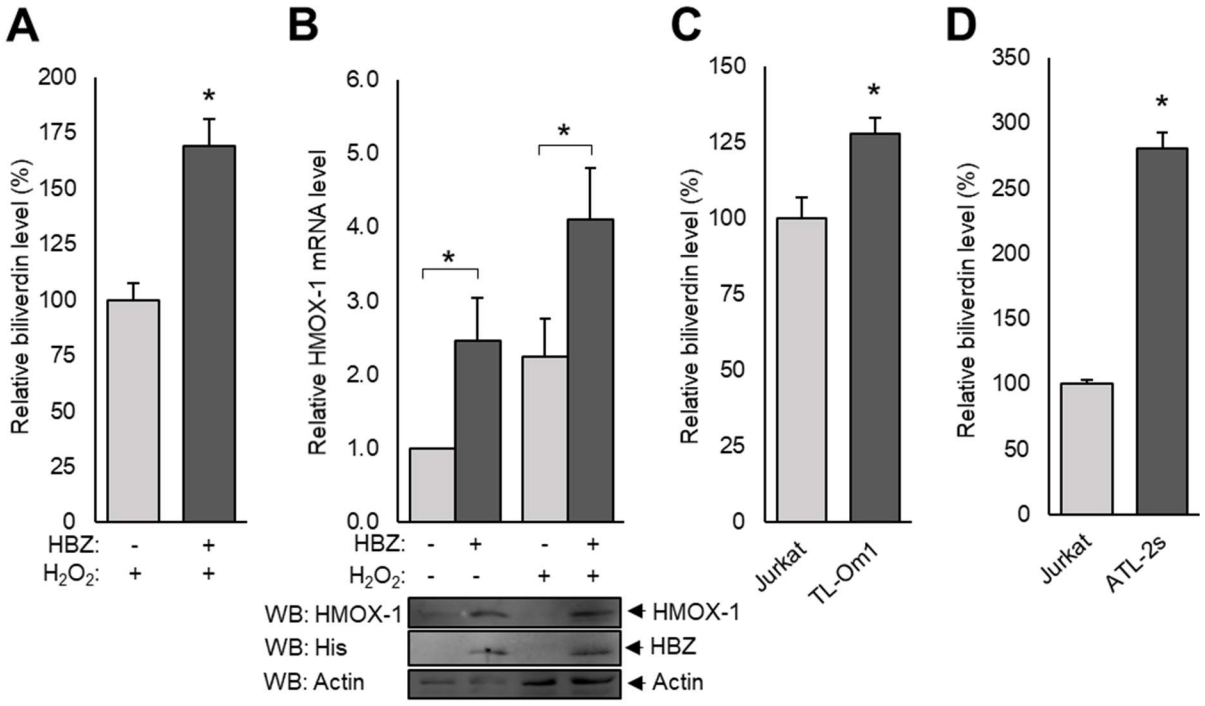

Figure 3.4: HMOX-1 enzymatic activity is coordinately upregulated in HBZ-expressing cells. (A) HeLa cells stably expressing HBZ-Myc-His or containing the empty vector were treated with 200μM H_2O_2 for four hours in low serum media (0.5% FBS) before whole cell protein was isolated and enzymatic reactions were performed as indicated in the Materials and Methods. To determine HMOX1- activity, biliverdin peak area was calculated in each sample relative to the biliverdin d_4 internal standard peak area. Data was normalized to empty vector cells and represents the percent increase in HMOX-1 activity. Data is an average of six independent experiments and error bars indicate SEM (Student's t-test, * $p \leq 0.05$). (**B**) HMOX-1 mRNA transcripts were analyzed in HeLa cells (HBZ-Myc-His and empty vector) treated with 200μM H_2O_2, or with the vehicle control (PBS), for four hours in low serum media (0.5% FBS). Data is an average of three independent experiments and error bars represent SEM (Student's t-test, * $p \leq 0.05$). Whole cell protein was harvested from an identically-treated cell set and 60μg of each was analyzed by Western blot using the indicated antibodies. **(C-D)** Jurkat and TL-Om1 (C), as well as Jurkat and ATL-2s (D) T-cell lines were equalized for protein content, and cellular extracts were used to assess HMOX-1 enzymatic activity. Biliverdin peak area was calculated in each sample relative to the biliverdin d_4 internal standard peak area. Data was normalized to uninfected Jurkat cells and represents the percent increase in HMOX-1 activity. Data is an average of four independent experiments and error bars represent SEM (Student's t-test, * $p \leq 0.05$).

activation was observed in HBZ-expressing cells, possibly indicating a more robust antioxidant response (**Figure 3.4.B**). Analysis of HMOX-1 enzyme activity in HTLV-1-infected T-cell lines TL-Om1 (**Figure 3.4.C**) and ATL-2s (**Figure 3.4.D**) showed that each cell type exhibited a significant increase in biliverdin production when compared to uninfected Jurkat T-cells. Taken together, these data support that HMOX-1 transcript levels, protein levels, and enzymatic activity are all upregulated in cells which express HBZ, as well as in HTLV-1-infected T-cell lines.

HBZ interacts with key regulators of the antioxidant response: HBZ is well characterized to interact with cellular transcription factors to alter their functions[78,79,81,227,229,230,379]. We hypothesized that HBZ modulates the expression of HMOX-1 by interacting with its transcriptional regulators to directly or indirectly affect expression. HMOX-1 expression is known to be extensively regulated by sMaf:Nrf2 heterodimers[366]. Interestingly, a previous report indicates that HBZ interacts with one of the sMafs, MafG[230]. A preliminary proteomic analysis of HBZ-binding partners confirmed the interaction between HBZ and MafG and also identified interactions between HBZ and MafF and MafK (**Figure 3.5.A**). We also identified several known HBZ-binding partners in our screen, validating our approach.

The sMaf family of transcription factors are essential for the regulation of antioxidant response genes[342,373,380,381]. Small Mafs are postulated to be functionally redundant and are reported to form homodimeric complexes at AREs in gene promoters to repress transcription[382,383]. Additionally, sMafs heterodimerize with CNC bZIP transcription factors for additional regulatory activity (**Figure 1.6.C**)[384–387]. Interestingly,

A

Protein	Exclusive unique peptides identified
ATF-1	1
ATF-2	1
ATF-7	4
CBP	1
C/EBPG	1
c-Jun	2
CREB-1	1
JunB	15
JunD	4
MafF	3
MafG	5
MafK	6
p300	1
HBZ	6

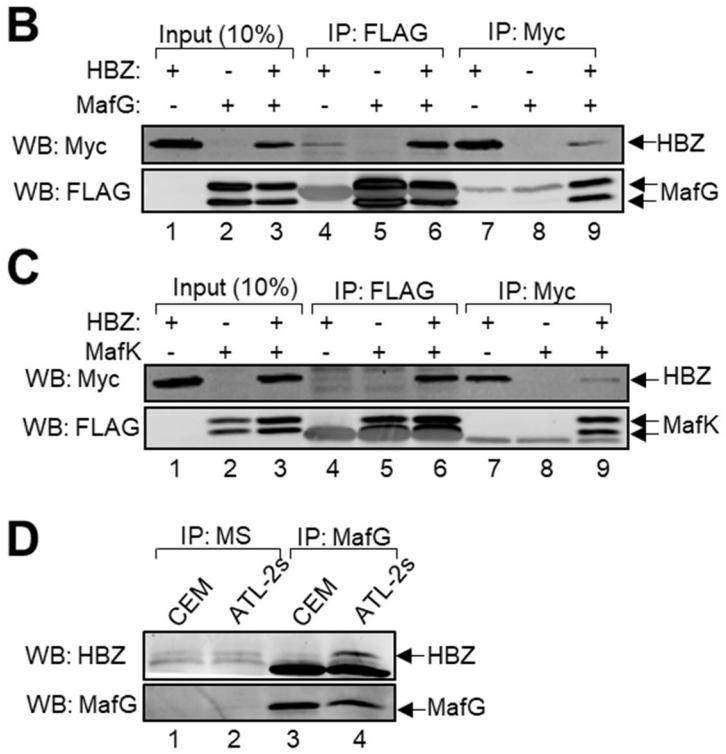

Figure 3.5: HBZ co-immunoprecipitates with the small Maf transcriptional regulators. (A) A preliminary proteomic screen for novel HBZ-binding partners confirmed MafG and identified MafF and MafK as HBZ-interacting bZIP transcription factors. Known binding partners of HBZ were identified in this screen, validating our method. Protein identifications were accepted at a False Discovery Rate of less than 1%, a probability of >99%, and the number of unique peptides identified for each protein is shown. **(B)** HEK 293T cells were transiently transfected with 12µg of plasmid DNA (6µg pCMV-MafG-FLAG, 6µg pcDNA-HBZ-Myc-His). HBZ was immunoprecipitated from 300µg of cell lysates by anti-Myc antibody (IP:Myc) and MafG was immunoprecipitated from 300µg cell lysates by anti-FLAG antibody (IP: FLAG). Eluates (lanes 4-9) and input protein samples (lanes 1-3) were analyzed by Western blot using the indicated antibodies. **(C)** HEK 293T cells were transiently transfected with 12µg of plasmid DNA (6µg pCMV-MafK-FLAG, 6µg pcDNA-HBZ-Myc-His). HBZ was immunoprecipitated from 300µg of cell lysates by anti-Myc antibody (IP:Myc) and MafK was immunoprecipitated from 300µg of cell lysates using anti-FLAG antibody (IP: FLAG). Eluates (lanes 4-9) and input protein samples (lanes 1-3) were analyzed by Western blot using the indicated antibodies. **(D)** MafG was immunoprecipitated (IP:MafG) from 2mg ATL-2s and CEM cell. Mouse serum was used as a negative immunoprecipitation control (IP:MS). Eluates were analyzed by Western blot using the indicated antibodies.

CNC and Bach proteins are unable to stably bind DNA without first dimerizing with a small Maf, supporting the importance of the sMafs in the regulation of the antioxidant response[342,387,388].

We confirmed the interactions between HBZ and sMafs using co-immunoprecipitation in which FLAG-tagged sMafs (MafG-FLAG, MafK-FLAG) were transiently coexpressed with HBZ-Myc-His in HEK 293T cells, and immunoprecipitated from cell lysates using anti-FLAG antibody (**Figure 3.5.B-C**). Additionally, endogenous HBZ and small Mafs were found to co-immunoprecipitate from HTLV-1-infected T-cell lysates, supporting that the interaction also occurs within the context of the HTLV-1-infected cell (**Figure 3.5.D**).

HBZ interacts with small Mafs through direct dimerization of the ZIP domains: Our next goal was to further characterize the HBZ:sMaf interaction. Work from Keating's group showed that purified recombinant HBZ-bZIP interacts with MafG and is recruited to sMaf DNA-binding sites in *in vitro* gel shift assays[230]. We wanted to confirm the sMaf interaction with full-length HBZ and determine if the interaction could occur independently of DNA contact. We performed GST pulldown assays in which recombinant purified 6xHis-tagged MafF was incubated with GST-tagged HBZ, or GST-tagged MafG as a positive control for binding (**Figure 3.6.A**). The results indicate that MafF interacts with GST-HBZ directly, as it does with GST-MafG, independently of DNA-contact.

Small Maf dimerization is reported to be dependent upon direct ZIP motif interactions[389]. To determine which domain of HBZ is important for mediating its

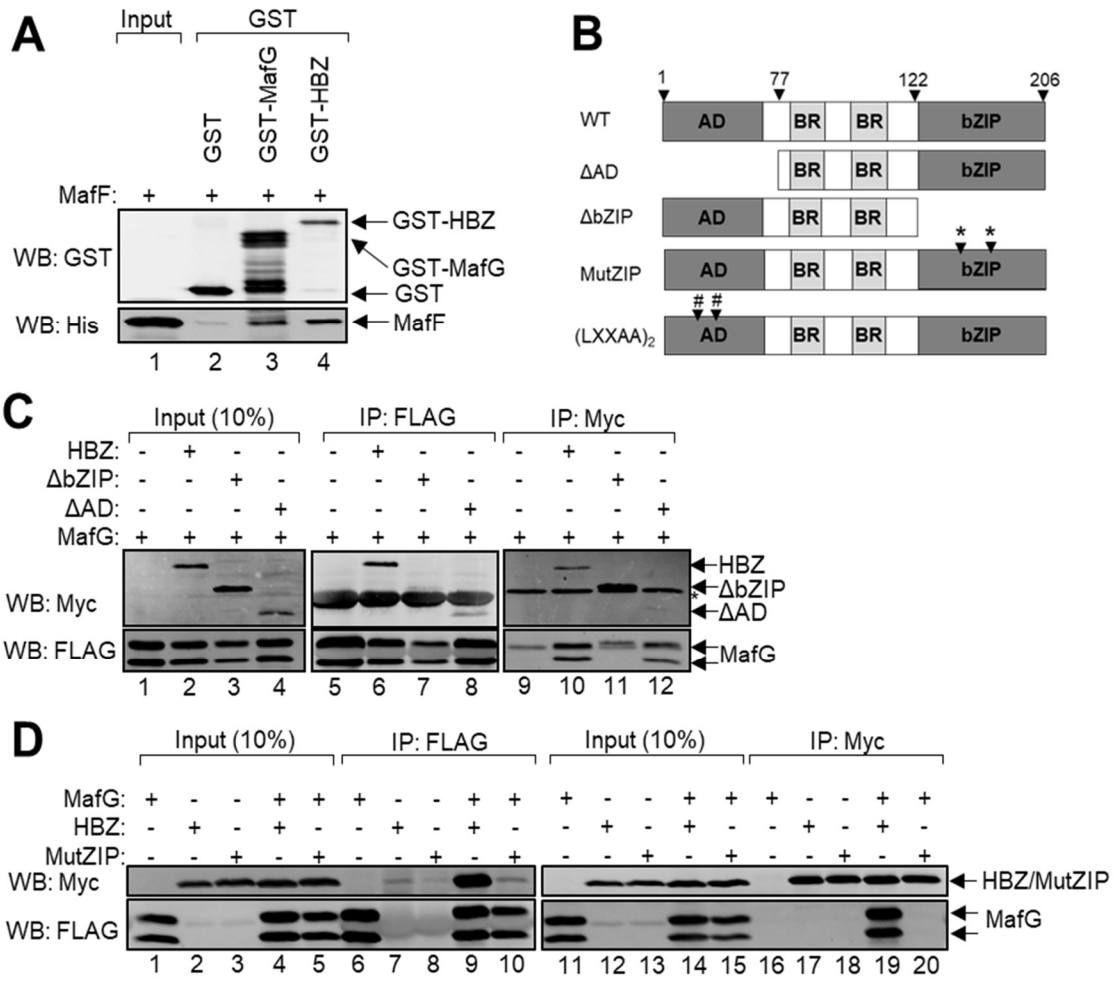

Figure 3.6: HBZ interacts with sMafs through dimerization of the ZIP domains. (A) Recombinant GST fusion proteins (50pmol) were pre-bound to glutathione-conjugated agarose, then incubated with 30pmol purified recombinant MafF-6xHis (lane 1). Bound protein was eluted (lanes 2-4) and analyzed by Western blot with the indicated antibodies. **(B)** Schematics of wild type HBZ (WT), the activation domain truncation mutant (ΔAD), and the basic leucine zipper truncation mutant (ΔbZIP). Point mutants include the leucine zipper point mutant (MutZIP), in which L→C substitutions are indicated (*), and the activation domain point mutant ($LXXAA_2$) in which LXXLL→LXXAA substitutions are indicated (#). **(C)** HEK 293T cells transiently transfected with a total of 12μg of plasmid DNA (3μg pCMV-MafG-FLAG, 9μg pcDNA-HBZ-Myc-His, 9μg pcDNA-HBZΔAD-Myc-His, 9μg pcDNA-HBZΔbZIP). MafG-FLAG was immunoprecipitated from 300μg of cell lysates using anti-FLAG antibody (lanes 5-8). HBZ-WT and HBZ truncation mutants were immunoprecipitated from 300μg of cell lysates using anti-Myc antibody (lanes 9-12). Inputs (lanes 1-4) and eluates were analyzed by Western blot using the indicated antibodies (* denotes a non-specific band which results from immunoprecipitation). **(D)** HEK 293T cells were transiently transfected with a total of 12μg plasmid DNA (1μg pCMV-MafG-FLAG, 6μg pcDNA-HBZ-Myc-His, 6μg pcDNA-HBZ-MutZIP-Myc-His). MafG-FLAG was immunoprecipitated from 300μg of cell lysates using anti-FLAG antibody (lanes 6-10). HBZ WT and HBZ-MutZIP was immunoprecipitated from 300μg of cell lysates using anti-Myc antibody (lanes 16-20). Inputs (lanes 1-5, 11-15) and eluates were analyzed by Western blot using the indicated antibodies.

interaction with sMafs in the cellular context, we performed co-immunoprecipitation assays with HEK 293T cell lysates overexpressing wild type HBZ (HBZ WT), or one of two HBZ truncation mutants: HBZ-ΔAD or HBZ-ΔbZIP (**Figure 3.6.B**). Anti-FLAG immunoprecipitation of MafG-FLAG, as well as the reciprocal anti-Myc immunoprecipitation of Myc-tagged HBZ proteins, showed that deletion of the bZIP domain abolishes the HBZ:sMaf interaction (**Figure 3.6.C**, lane 7&11). To confirm sMaf specificity for the leucine zipper, further experiments were performed with the HBZ-MutZIP point mutant, which harbors L→C substitutions in the second and fourth leucine heptad repeats that are demonstrated to abolish HBZ interactions with bZIP transcription factors (**Figure 3.6.B**)[377]. In these assays, MafG failed to interact with HBZ-MutZIP, confirming that the HBZ:sMaf interaction is mediated by the ZIP motif (**Figure 3.6.D**).

HBZ:sMaf dimers are recruited to consensus AREs *in vitro*: CNC family proteins, including the transactivator Nrf2 and closely related transcriptional repressor Bach1, regulate antioxidant gene expression by controlling transactivation at AREs. However, these proteins do not form stable homodimers, preventing them from binding AREs. Therefore, sMafs are an obligate binding partner that strongly tethers CNC proteins to ARE sites[383]. Similarly, HBZ does not form stable homodimers, leading us to question whether HBZ utilizes sMafs to facilitate its recruitment to AREs. To assess the DNA-binding capabilities of HBZ and sMafs, we performed electrophoretic mobility shift assays (EMSA). A previous report used EMSA to demonstrate that MafG binds to the ARE consensus, and that this complex was shifted with the addition of HBZ bZIP,

indicating that the HBZ bZIP and MafG bind AREs *in vitro*[230]. However, it is unclear whether full-length HBZ is recruited to these sites in a similar manner. To address this, we performed EMSA using ^{32}P-labeled double-stranded oligonucleotides which contain the ARE consensus sequence. As a negative control, we used a mutated ARE sequence in which core-flanking GC dinucleotides, which are important for sMaf binding, were substituted (**Figure 3.7.A**)[390]. We first validated our experimental approach by evaluating sMaf binding to the ARE and to the ARE MT probes (**Figure 3.7.B**). As previously reported, we found that MafG binds to the ARE probe strongly (lane 2), likely in the form of a homodimer, but fails to interact strongly with the ARE MT (lane 4). We next assessed the ARE-binding ability of MafG and full-length HBZ, as well as the ARE-binding ability of MafG and HBZ-AD, a bZIP domain-deficient mutant (**Figure 3.7.C**). As expected, we found that HBZ and HBZ-AD alone fail to bind the ARE consensus probe (lanes 3-4). However, when HBZ and MafG were incubated together, we noted the intensity of the MafG:ARE band was greatly enhanced (lane 6), but not in reactions with HBZ-AD (lane 5). We took the enhanced band intensity to indicate the formation of the HBZ:sMaf complex that binds strongly at the ARE in a bZIP-dependent manner, supporting the observations reported by Keating's group[230].

To confirm the presence of HBZ at AREs *in vitro*, we performed immobilized DNA-binding assays. To evaluate sMaf and HBZ binding in a cellular context, we incubated streptavidin:biotin-immobilized ARE probe or ARE MT probe with nuclear protein extracts from HEK 293T cells overexpressing MafG-FLAG and HBZ-Myc-His (**Figure 3.7.D**). As expected, we found that MafG binds the ARE consensus in the absence of HBZ (lane 4), and in the absence of MafG overabundance, HBZ fails to

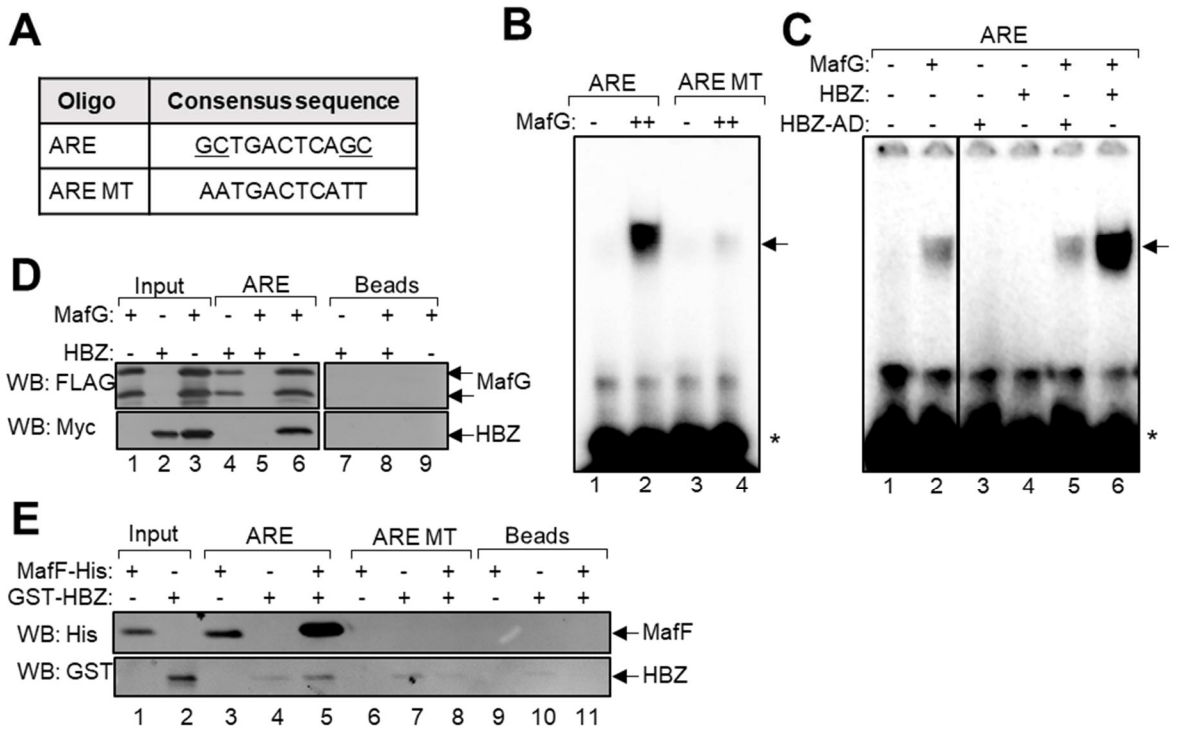

Figure 3.7: HBZ and MafG are recruited to consensus ARE sites *in vitro*: (A) Consensus sMaf-binding ARE sequence flanked by GC-dinucleotides (underlined). Point mutations in the flanking regions prevent sMaf binding (ARE MT). **(B)** Purified recombinant MafG-His (1nM) was incubated with the indicated radiolabeled probes for 1hr and DNA:protein complexes were separated using gel electrophoresis. **(C)** Purified recombinant MafG-His (0.5nM), GST-HBZ (50nM), and GST-HBZ-AD (50nM) were incubated together for 1hr, then incubated with the indicated radiolabeled probes for 1hr. DNA:protein complexes were separated using gel electrophoresis. For B and C, arrows denote the band of interest, and * denotes unbound probe. **(D)** HEK 293T cells were transiently transfected with 50µg plasmid DNA (25µg pcDNA-HBZ-Myc-His, 25µg pCMV-MafG-FLAG) by calcium chloride transfection. Nuclear protein was harvested and dialyzed as described in the Materials and Methods. Nuclear protein (10µg) was incubated with immobilized oligonucleotides (ARE), or with streptavidin beads alone (Beads), and bound proteins were eluted and analyzed by Western blot using the indicated antibodies. **(E)** Purified recombinant GST-HBZ (8pmol) and MafG-His (4pmol) were incubated with immobilized oligonucleotide probes (ARE, ARE MT), or with streptavidin beads alone. DNA-bound proteins were eluted and analyzed by Western blot using the indicated antibodies.

interact with the ARE consensus (lane 5), possibly because of competition with CNC and Bach transcription factors for endogenous sMaf binding. When MafG and HBZ were overexpressed together, HBZ was observed to bind the ARE consensus site (lane 6), and consistent with our EMSA results, MafG binding to the ARE appeared to be enhanced in the presence of HBZ. These data support that the HBZ:sMaf complex binds AREs with strong stability.

To confirm that sMafs are sufficient to facilitate the recruitment of HBZ to the ARE consensus site, we performed similar immobilized DNA-binding assays with purified recombinant proteins, GST-HBZ and MafF-His, rather than nuclear protein extracts (**Figure 3.7.E**). Again, we observed that MafF binds to the ARE consensus (lane 3) and that its binding is enhanced in the presence of HBZ (lane 5). We also observed that GST-HBZ interacts with the ARE oligo above background levels when MafF is present in the reaction (lanes 4, 5). Mutation of the ARE GC-dinucleotide flanking regions (ARE MT) abolished MafF binding, and returned HBZ binding to background levels (lanes 6-8). Taken together, these data indicate that HBZ and sMafs bind directly and specifically to AREs in an sMaf-dependent manner, supporting that sMafs tether HBZ to ARE sites *in vitro*.

HBZ binding is enriched at AREs in the HMOX-1 promoter: We next wanted to evaluate whether HBZ:sMaf complexes are recruited specifically to the *hmox1* promoter. According to previously reported MafK ChIP-seq data, MafK binds to two major sites in the *hmox1* promoter, which we have termed the “distal” and “proximal” binding sites (**Figure 3.8.A**)[374]. The distal site contains three ARE sites (distal 1-3) while

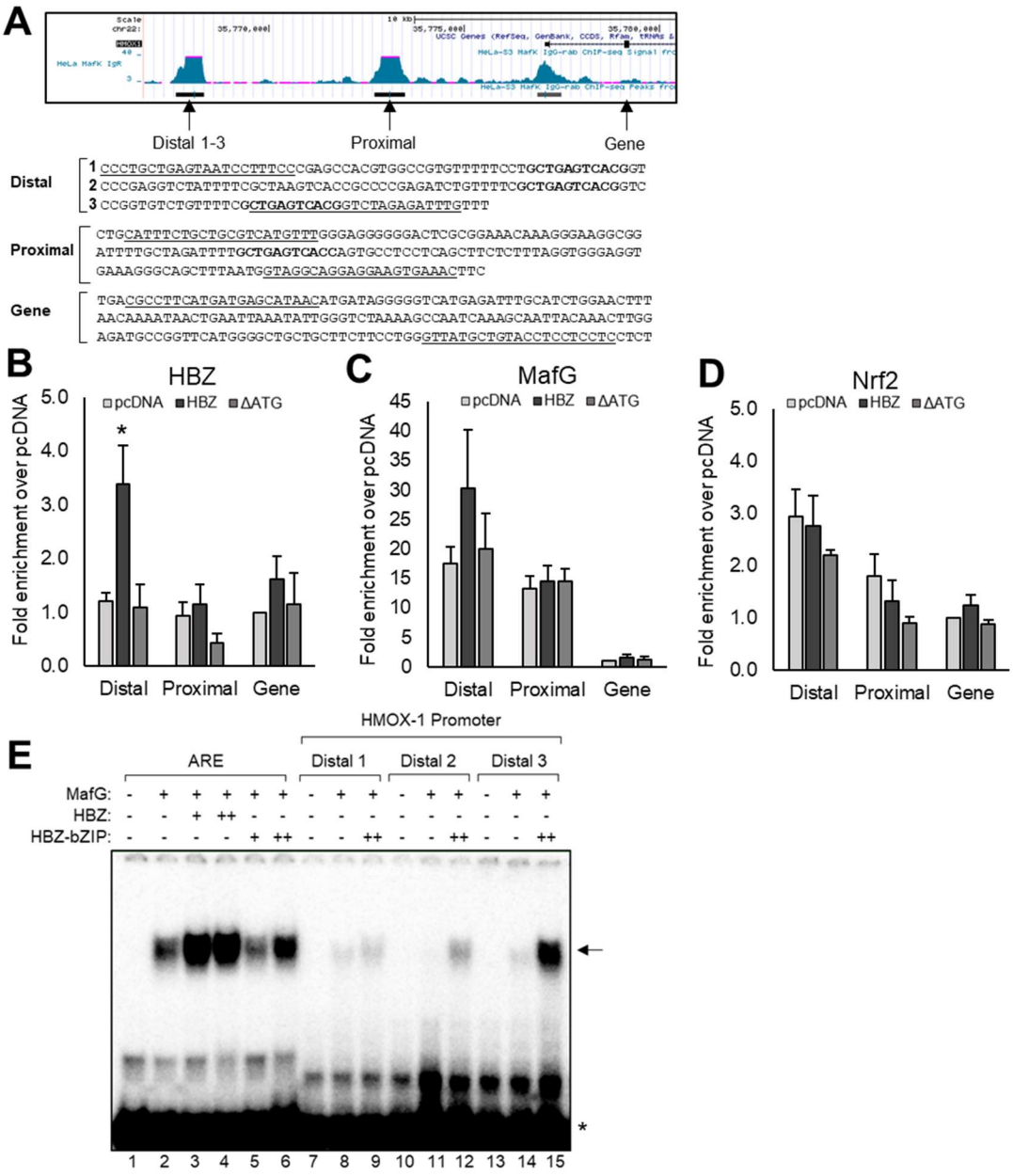

Figure 3.8: Chromatin-bound HBZ is enriched at AREs located in the distal *hmox1* promoter. . (A) A schematic of the HMOX-1 promoter MafK binding sites (USC Genome Browser). For EMSA assays, AREs within the distal (distal 1-3) and proximal MafK binding site were selected to evaluate the DNA-binding capabilities of HBZ:sMaf complexes (**bolded sequences**). For ChIP assays, ChIP primers (underlined sequences) were designed to flank the AREs identified within these MafK binding sites. As a negative control, we included a primer set (underlined sequences) designed for a region located within the HMOX-1 gene where MafK is not reported to bind. For all figures, chromatin was crosslinked, sheared, and purified from $1x10^7$ HeLa cells stably expressing HBZ-Myc-His, HBZ-ΔATG, or containing the empty vector (pcDNA). Sheared chromatin was quantified and 200µg was used for each immunoprecipitation reaction. (**B**) Anti-His antibody (5µg) was used to immunoprecipitate HBZ-Myc-His-bound chromatin fragments. Data shown is an average of three independent experiments and error bars represent SEM (Student's t-test, * *p<0.05*). **(C)** Anti-MafG antibody (2.5-5µg) was used to immunoprecipitate MafG-bound chromatin fragments. Data shown is an average of 3 independent experiments and error bars represent SEM. **(D)** Anti-Nrf2 antibody (5µg) was used to immunoprecipitate Nrf2-bound chromatin fragments. Data shown is an average of three independent experiments and error bars represent SEM. **(E)** Purified recombinant MafG-His (0.5nM), GST-HBZ (50nM), and T7-HBZ-bZIP (50nM) were incubated together for 1hr, then with the indicated radiolabeled probes for 1hr. DNA:protein complexes were separated using gel electrophoresis. The arrow denotes the bands of interest, and * denotes unbound probe.

the proximal MafK binding site contains one ARE. To determine whether HBZ:sMaf heterodimers are recruited to the *hmox1* promoter *in vivo*, we performed ChIP to assess the levels of HBZ, MafG, and Nrf2 bound to the proximal and distal MafK-binding sites. Here, we used HeLa cells that stably express HBZ WT, HBZ-ΔATG, or contain the empty vector (pcDNA). Importantly, the HBZ-ΔATG expression vector produces the HBZ mRNA transcript, but not the HBZ protein, allowing us to evaluate possible effects specific to the HBZ transcript[377]. Purified DNA was analyzed by quantitative ChIP PCR using primers which recognize the distal and proximal *hmox1* promoter ARE sites, as well as a primer that recognizes an intergenic region of *hmox1* as a negative control (**Figure 3.8.A**). Interestingly, we found that HBZ binding was significantly enriched in the distal *hmox1* promoter when compared to the empty vector intergenic location (**Figure 3.8.B**). MafG binding was similarly enhanced at the distal promoter in HBZ-expressing cells (**Figure 3.8.C**). Though MafG enrichment was not statistically significant among our experimental replicates, we speculate that the enhanced binding we observed is likely biologically relevant since sMafs are well documented to be critical regulators of HMOX-1 gene expression[383,391,392]. We also evaluated levels of chromatin-bound Nrf2 to determine if HMOX-1 induction is related to the transcriptional activity of Nrf2 (**Figure 3.8.D**). Nrf2 binding was observed to be similar at the distal and proximal *hmox1* promoters among all three cell types, providing evidence that HBZ-mediated transcriptional upregulation occurs independently of Nrf2 activity

To evaluate which ARE in the distal *hmox-1* promoter is bound by the HBZ:sMaf complex, we performed EMSA by incubating purified recombinant MafG-His and T7-HBZ-bZIP with oligonucleotide probes that correspond with the distal 1, distal 2, and

distal 3 sites (**Figure 3.8.E**). The data indicate that MafG homodimers bind weakly to the distal 1 and distal 2 probes (lane 8,11), and that binding is enhanced by the presence of the HBZ-bZIP domain (lane 9,12). MafG homodimers also bound to the distal 3 probe (lane 14), but MafG binding was greatly enhanced by the HBZ-bZIP, indicating the formation of a MafG:HBZ complex (lane 15). Overall, these data support that the sMaf:HBZ complex is an important transcriptional regulator of *hmox1* gene expression from the distal sMaf binding site.

Coactivators p300/CBP are recruited to the HBZ:sMaf complex: The interactions between HBZ and cellular coactivators p300/CBP have been extensively characterized in previous reports[82,224]. Although sMafs do not contain an activation domain, they have been reported in protein complexes with coactivators p300 and CBP facilitated by the activation domain of Nrf2[382,393]. We questioned whether HBZ similarly facilitates complex formation with sMafs and p300/CBP. We co-immunoprecipitated MafG-FLAG from HEK 293T cell lysates overexpressing HBZ-Myc-His and expressing endogenous levels of p300 and CBP (**Figure 3.9**). As expected, we found that both p300 and CBP fail to co-immunoprecipitate with MafG in the absence of HBZ (lane 4). However, both coactivators co-immunoprecipitated with MafG in cell lysates that also contained HBZ (lane 6). These observations support a model in which HBZ interacts with sMafs through its bZIP domain and recruits p300/CBP to the complex, likely through its activation domain.

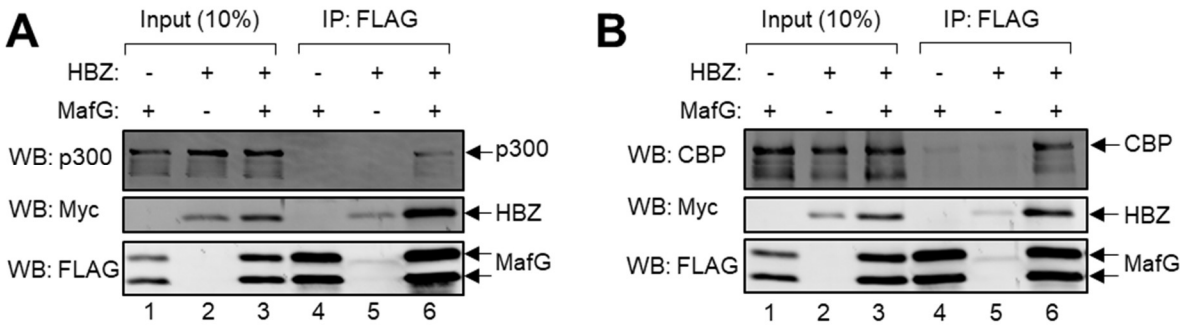

Figure 3.9: Cellular coactivators p300/CBP are recruited to the HBZ:sMaf complex. (A) HEK 293T cells were transiently transfected with 12µg plasmid DNA (1µg pCMV-MafG-FLAG, 6µg pcDNA-HBZ-Myc-His) and MafG-FLAG was immunoprecipitated from 300µg of cell lysates using anti-FLAG antibody (IP:FLAG, lanes 4-6). Eluates and input samples (lanes1-3) were analyzed by Western blot using the indicated antibodies. **(B)** HEK 293T cells were transiently transfected with 12µg plasmid DNA (1µg pCMV-MafG-FLAG, 6µg pcDNA-HBZ-Myc-His) and MafG-FLAG was immunoprecipitated from 300µg of cell lysates using anti-FLAG antibody (IP:FLAG, lanes 4-6). Eluates and input samples (lanes1-3) were analyzed by Western blot using the indicated antibodies.

HBZ expression activates transcription of an ARE luciferase reporter plasmid:

The DNA-binding capabilities of the HBZ:sMaf complex, paired with its recruitment to AREs *in vivo*, and the presence of cellular coactivators within the complex, suggest the possibility that this protein complex may function to transactivate gene expression. To evaluate the transcriptional activity of HBZ at ARE sites, we constructed a luciferase reporter plasmid containing four consensus ARE repeats, pGL-4xARE-Luc (**Figure 3.10.A**). The reporter vector, pGL4.26, was also studied to account for transactivation at the minimal promoter (minP). The 4xARE and minP reporters were transfected in Jurkat T-cells, along with expression vectors for HBZ, HBZ-MutZIP, or the empty vector (pSG5) (**Figure 3.10.B**). Background luciferase activity of the minP reporter was subtracted from luciferase activity of the 4xARE reporter. The results indicate that HBZ significantly activates transcription of the 4xARE promoter construct, but that HBZ-MutZIP was unable to do so. These data suggest that HBZ either directly or indirectly activates transcription at AREs and that the bZIP domain is critical for this function.

To help determine whether the observed transcriptional activation is dependent upon sMaf activity, we performed similar luciferase reporter assays with the addition of the Nrf2 dominant negative mutant (Nrf2-DN). The Nrf2-DN mutant has a deletion in the activation domain, but its ability to interact with sMafs and bind to AREs is maintained, resulting in repression of ARE transactivation (**Figure 3.11.C**)[394]. Co-immunoprecipitation experiments confirm that Nrf2-DN successfully interacts with MafG-FLAG (**Figure 3.10.D**). When Nrf2-DN was expressed in luciferase reporter assays (**Figure 3.10.E**), mild transcriptional activation of the 4xARE promoter was observed, perhaps reflecting Nrf2-DN-mediated sequestration of sMafs and a coordinating

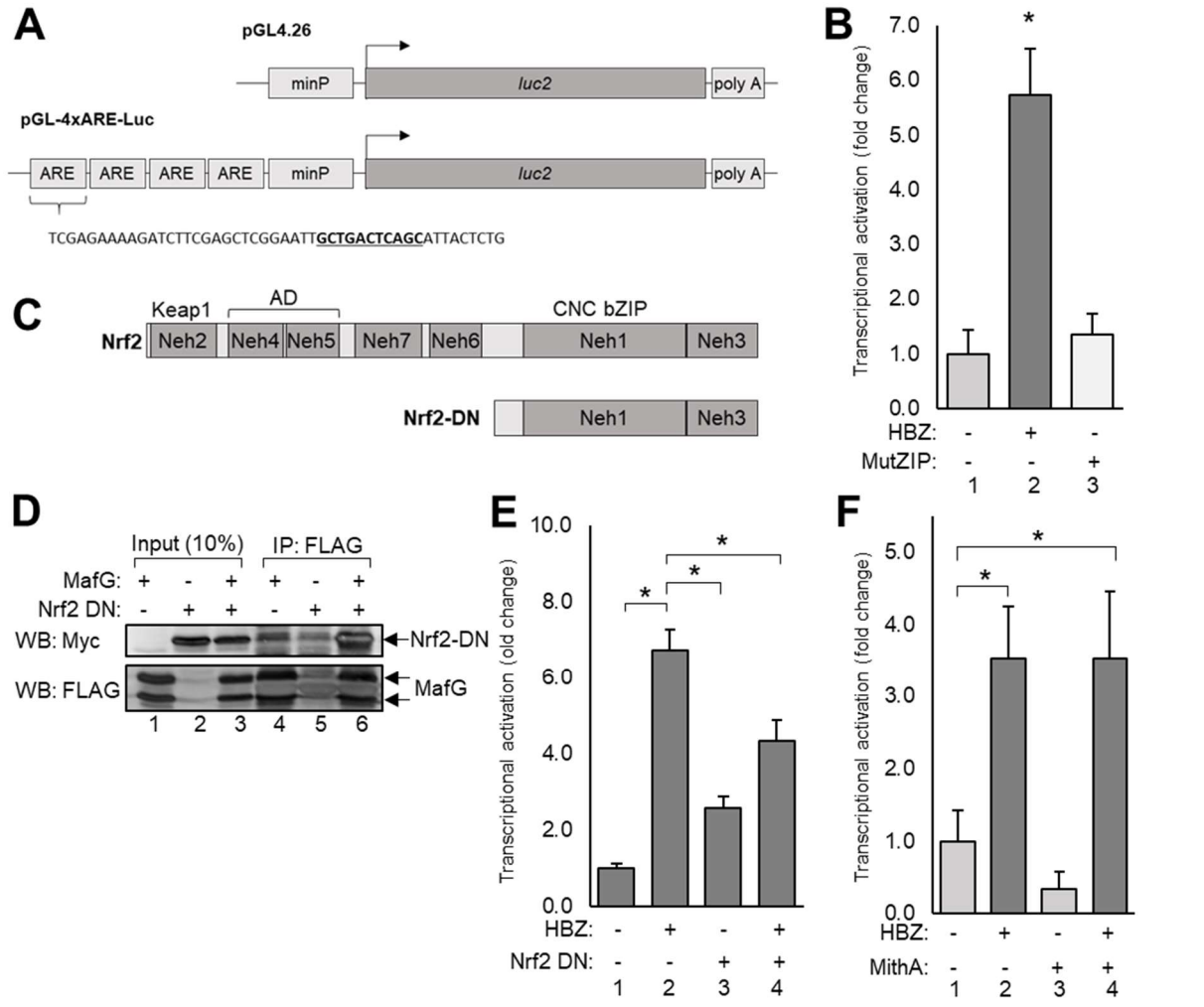

Figure 3.10: HBZ expression activates transcription of an ARE luciferase reporter. (A) A schematic of the reporter vectors used to evaluate the transcriptional activity of HBZ at ARE consensus sites. The pGL2.46 empty vector contains a minimal promoter (minP) controls the expression of the luciferase reporter gene (*luc2*). The pGL-4xARE-Luc reporter vector contains four repeats of the consensus ARE sequence upstream of the minimal promoter and luciferase reporter gene. **(B)** Jurkat cells were transfected with a total of 1µg plasmid DNA (250ng pSG-HBZ-Myc, 250ng pSG-HBZ-MutZIP-Myc, 100ng pGL4.26, 100ng pGL-4xARE-Luc). Cell lysates were harvested 48 hours post-transfection and luciferase activity was quantified. Background luciferase activity was calculated using the pGL4.26 vector. Data shown is an average of three independent experiments. Error bars represent SEM (Student's T-test, * $p \leq 0.05$). **(C)** A schematic of wild type Nrf2 which contains the Keap1 binding site Nrf2-ECH homology domain 2 (Neh2), the activation domain (Neh4 and Neh5), and the Cap'n'Collar basic leucine zipper domain (CNC bZIP, Neh1). **(D)** HEK293T cells were transfected with a total of 12µg of plasmid DNA (6µg pCMV-MafG-FLAG, 6µg pcDNA-Nrf2-DN-Myc). MafG-FLAG was immunoprecipitated from 300µg of cell lysates using anti-FLAG antibody (IP:FLAG) and Nrf2-DN-Myc was immunoprecipitated from 300µg of cell lysates using anti-Myc antibody (IP: Myc). FLAG IP eluates (lanes 4-6), Myc IP eluates (lanes 7-9), and protein inputs (10%) were analyzed by Western blot using the indicated antibodies. **(E)** Jurkat cells were transfected with a total of 1µg plasmid DNA (250ng pSG-HBZ-Myc, 250ng pcDNA-Nrf2-DN-Myc, 100ng pGL4.26, 100ng pGL-4xARE-Luc). Cell lysates were harvested 48hrs post-transfection and luciferase activity was quantified. Background luciferase activity was calculated using the pGL4.26 vector. Data shown is an average of three independent experiments. Error bars represent SEM (Student's T-test, * $p \leq 0.05$). **(F)** Jurkat cells were transfected with a total of 1µg plasmid DNA (250ng pSG-HBZ-Myc, 100ng pGL4.26, 100ng pGL-4xARE-Luc).At 24 hours post-transfection, cells were treated with 50µM Mithramycin A or the vehicle control (DMSO) for an additional 24hrs. Cells lysates were harvested and luciferase activity was quantified. Background luciferase activity was calculated using the pGL4.26 vector. Data shown is an average of three independent experiments. Error bars represent SEM (Student's T-test, * $p \leq 0.05$).

decrease in the number of sMaf homodimeric repressor complexes present (lane 3). When co-expressed with HBZ, we observed that Nrf2-DN expression significantly reduced HBZ-mediated transactivation of the 4xARE promoter (lane 4), supporting that HBZ-mediated transactivation occurs specifically at sMaf:Nrf2 binding sites and may be dependent upon the availability of sMafs.

Previous work showed that HBZ forms a complex with JunD and housekeeping transcription factor Sp1, which has been demonstrated to be recruited to GC-rich Sp1-binding sites to enhance transcription[228,233]. To evaluate whether HBZ-mediated transactivation of the ARE reporter is dependent upon Sp1 activity, we performed luciferase assays in which Jurkat T-cells were transfected with HBZ or the empty vector, and subsequently treated with the Sp1-binding inhibitor mithramycin A for 24 hours (**Figure 3.10.F**). We observed that mithramycin A treatment did not significantly affect basal expression of the reporter (lane 1,3), nor did it significantly reduce HBZ-mediated ARE transactivation (lane 2,4), supporting that HBZ-mediated ARE transactivation occurs independently of Sp1.

To help confirm these results *in vivo*, we analyzed HMOX-1 transcripts from HeLa cell lines stably expressing WT HBZ, HBZ-$(LXXAA)_2$, HBZ-MutZIP, or HBZ-ΔATG (**Figure 3.11.A**). The HBZ-$(LXXAA)_2$ mutant contains A→L mutations in the LXXLL motifs which abrogate the interaction between HBZ and coactivators p300/CBP (**Figure 3.6.B**)[82]. In our analysis, we observed that neither HBZ-$(LXXAA)_2$ nor HBZ-MutZIP increased the quantity of HMOX-1 transcripts, supporting that HBZ's interaction with p300/CBP through its activation domain, and its interaction with sMafs through the bZIP domain are both required to enhance HMOX-1 expression *in vivo*. Some activities of

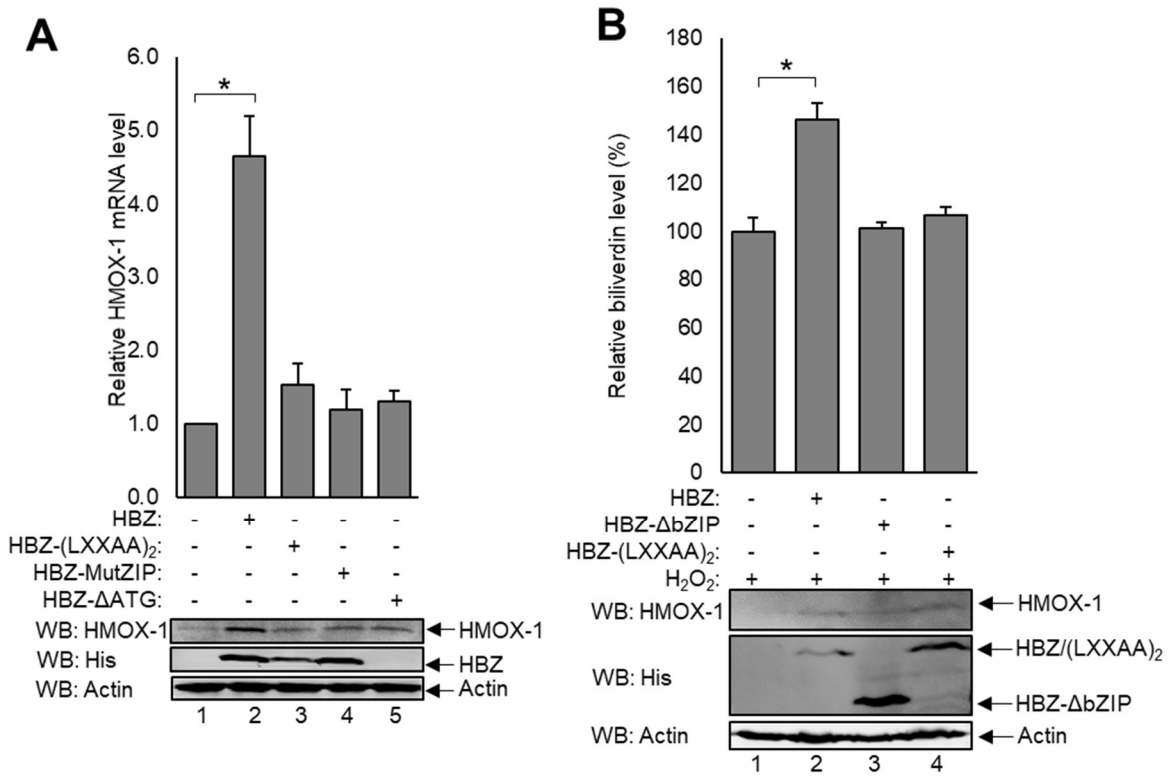

Figure 3.11: HBZ-mediated upregulation of HMOX-1 gene expression is dependent upon the activities of both the activation domain and bZIP domain. (A) qRT-PCR was used to quantify HMOX-1 transcripts in HeLa cells stably transfected with the indicated WT or mutated HBZ expression plasmid. Data is an average of three independent experiments and error bars indicate SEM (Student's t-test, * $p \leq 0.05$). **(B)** HMOX-1 enzymatic activity was measured in HeLa cells stably transfected with wild type HBZ (pcDNA-HBZ-Myc-His) or HBZ mutants (pcDNA-HBZ-ΔbZIP, pcDNA-HBZ-$(LXXAA)_2$. Cells were treated with 200μM H_2O_2 in low serum media (0.5% FBS) for four hours before cellular protein was isolated and analyzed for HMOX activity. Data is an average of three independent experiments and error bars show SEM (Student's t-test, * $p \leq 0.05$). A 60μg aliquot of each protein extract was reserved and analyzed by Western blot using the indicated antibodies.

HBZ have been attributed specifically to HBZ mRNA[93,239], however we did not observe HMOX-1 transcripts to be affected in HBZ-ΔATG cells (**Figure 3.11.A**). Further analysis of HMOX-1 enzymatic activity in HeLa cells expressing the HBZ bZIP truncation mutant, HBZ-ΔbZIP, and the HBZ activation domain point mutant, HBZ-$(LXXAA)_2$, confirmed that both the activation domain and bZIP domain are required for increased enzymatic activity (**Figure 3.11.B**).

HBZ expression corresponds with nuclear export of Bach1, but not with Nrf2 stabilization: An important step in the induction of the antioxidant response is the de-repression of AREs. ARE repression is maintained by sMaf homodimers and by sMaf:Bach1 heterodimers[382,395]. Upon oxidation, Bach1 is reported to be bound by heme, destabilizing it from the DNA[384,396]. This leads to nuclear export and proteolytic degradation. To evaluate if HBZ expression correlates with increased Bach1 de-repression, we stabilized cellular proteins by treating cells with the protease inhibitor MG132, and qualitatively analyzed nuclear and cytoplasmic Bach1 protein levels by Western blot (**Figure 3.12.A**). In HeLa cells lines stably expressing HBZ, we found an increase in the intensity of the cytoplasmic Bach1 band compared to empty vector-transfected cells (lanes 1-2). Analysis of Bach1 localization in HTLV-1-infected TL-Om1 cells showed a similar decrease in nuclear Bach1 (lane 4), as well as a coordinating increase in cytoplasmic Bach1 (lane 2), as compared to Jurkat cells, in which Bach1 was primarily found in the nuclear fraction (lane 3). These findings support that HBZ-mediated transactivation at AREs is accompanied by Bach1 de-repression.

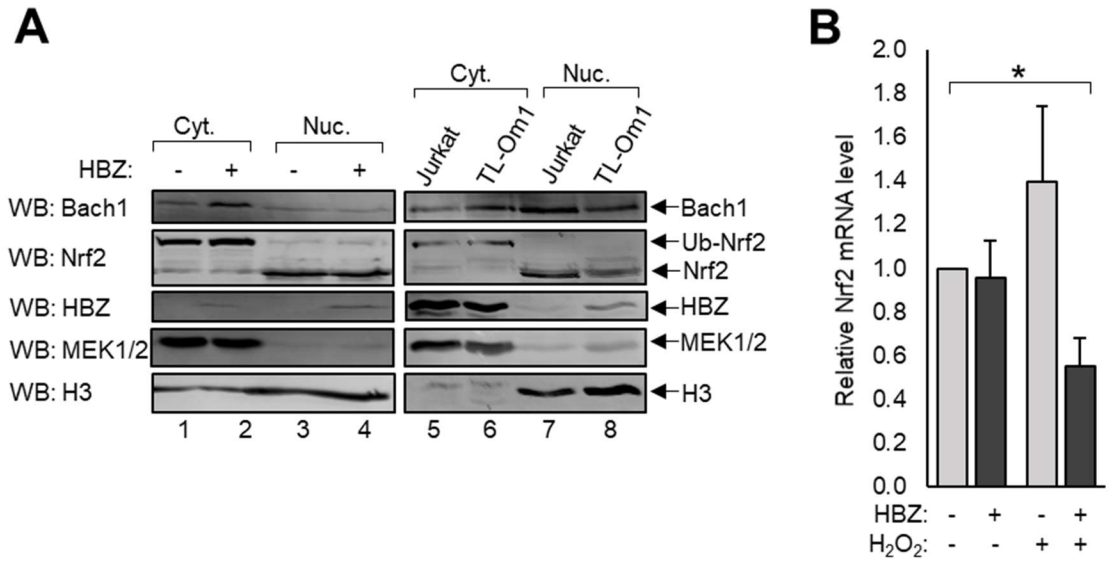

Figure 3.12: HBZ expression corresponds with nuclear export of Bach1, but not with Nrf2 nuclear import. (A) Nuclear and cytoplasmic protein fractions were harvested from HeLa cells stably expressing HBZ-Myc-His, or transfected with the empty vector, as well as from uninfected Jurkat T-cells and HTLV-1-infected TL-Om1 cells. Protein fractions (30µg) were analyzed by Western blot using the indicated antibody. MEK1/2 was used as a cytoplasmic marker, and histone H3 was used as a nuclear marker. (**B)** Nrf2 transcript levels in HeLa cells stably expressing HBZ-Myc-His or stably transfected with the empty vector were quantified by qRT-PCR. Cells were treated with either 200µM H_2O_2 or with the vehicle control (PBS). Data is an average of three independent experiments and error bars represent SEM (Student's t-test, * $p \leq 0.05$).

The upregulation of antioxidant response genes is reported to require the stabilization and nuclear import of the Nrf2 transcriptional activator. Under homeostatic conditions, Nrf2 is found primarily in the cytoplasm, where it remains bound by the Keap1-Cullin3 E3-ubiquitin complex and is rapidly proteolytically degraded. Oxidation of the Keap1 complex by free radicals results in the release and stabilization of Nrf2, allowing it to accumulate in the nucleus[341]. Our ChIP analysis did not show increased recruitment of Nrf2 to the HMOX-1 promoter in HBZ-expressing cells (**Figure 3.8.D**). To further confirm that HBZ-dependent ARE transactivation occurs independently of Nrf2 activity, we qualitatively assessed the levels of cytoplasmic and nuclear Nrf2 in HBZ-expressing cells compared to empty vector-transfected cells (**Figure 3.12.A**). We did not observe HBZ expression to noticeably increase nuclear Nrf2 levels (lane 4). Furthermore, the majority of Nrf2 in the cytoplasm was observed at a higher molecular weight, suggesting a polyubiquitinylated form of Nrf2 (lane 2). Analysis of Jurkat (lane 5,7) and TL-Om1 (lane 6,8) cells showed similar results. Taken together, these data support that HBZ expression does not correspond with Nrf2 stabilization and nuclear import.

Finally, transactivation of Nrf2 has also been reported to occur in response to oxidative stress[397–399]. We next tested whether exposure to oxidative stress upregulates Nrf2 gene expression in HBZ-expressing cells (**Figure 3.12.B**). We quantified Nrf2 transcripts in HeLa cell lines stably expressing HBZ, or transfected with the empty vector control. To induce stress, cells were treated with 200μM H_2O_2 four hours prior to RNA extraction. Basal Nrf2 expression was observed to be similar in vehicle-treated cell lines (lanes 1-2), and though we observed that Nrf2 was significantly upregulated in

stressed empty vector cells (lane 3), we failed to observe a similar increase in HBZ-expressing cells (lane 4).

HBZ has cytoprotective activity during oxidative stress: HMOX-1 activity has been demonstrated to confer resistance to cellular stressors, including its substrate heme, as well as to some ROS-inducing chemotherapeutic agents. HTLV-1-infected T-cells are characterized by increased resistance to a variety of stress-inducing chemotherapy agents including cisplatin, doxorubicin, and etoposide[400–403]. We hypothesized that HBZ upregulates the expression of antioxidant genes to promote cell survival during exposure to oxidative stress. To evaluate the cytoprotective effects of HBZ, we performed cell viability assays, in which HeLa cells stably expressing HBZ or containing the empty vector were treated with 40μM hemin to induce iron-mediated oxidative stress (**Figure 3.13.A**). We observed that cells transfected with the empty vector exhibited a significant reduction in viability when treated with hemin, but that the survival of HBZ-transfected cells remained unaffected, supporting that HBZ plays a cytoprotective role during oxidative stress.

Previous reports using fluorescence microscopy and flow cytometric approaches have shown that Tax expression results in increased intracellular RNOS, which is likely due to constitutive activation of NF-κB signaling and the induction of iNOS[192,193,354]. Our work demonstrates that HBZ robustly activates the expression of antioxidant genes, and we propose that this activity plays a role in protecting the host cell from Tax-induced oxidation. Using LC-MS, we quantified the cellular glutathione redox state of cells expressing combinations of Tax and HBZ. Glutathione is an abundant non-enzymatic

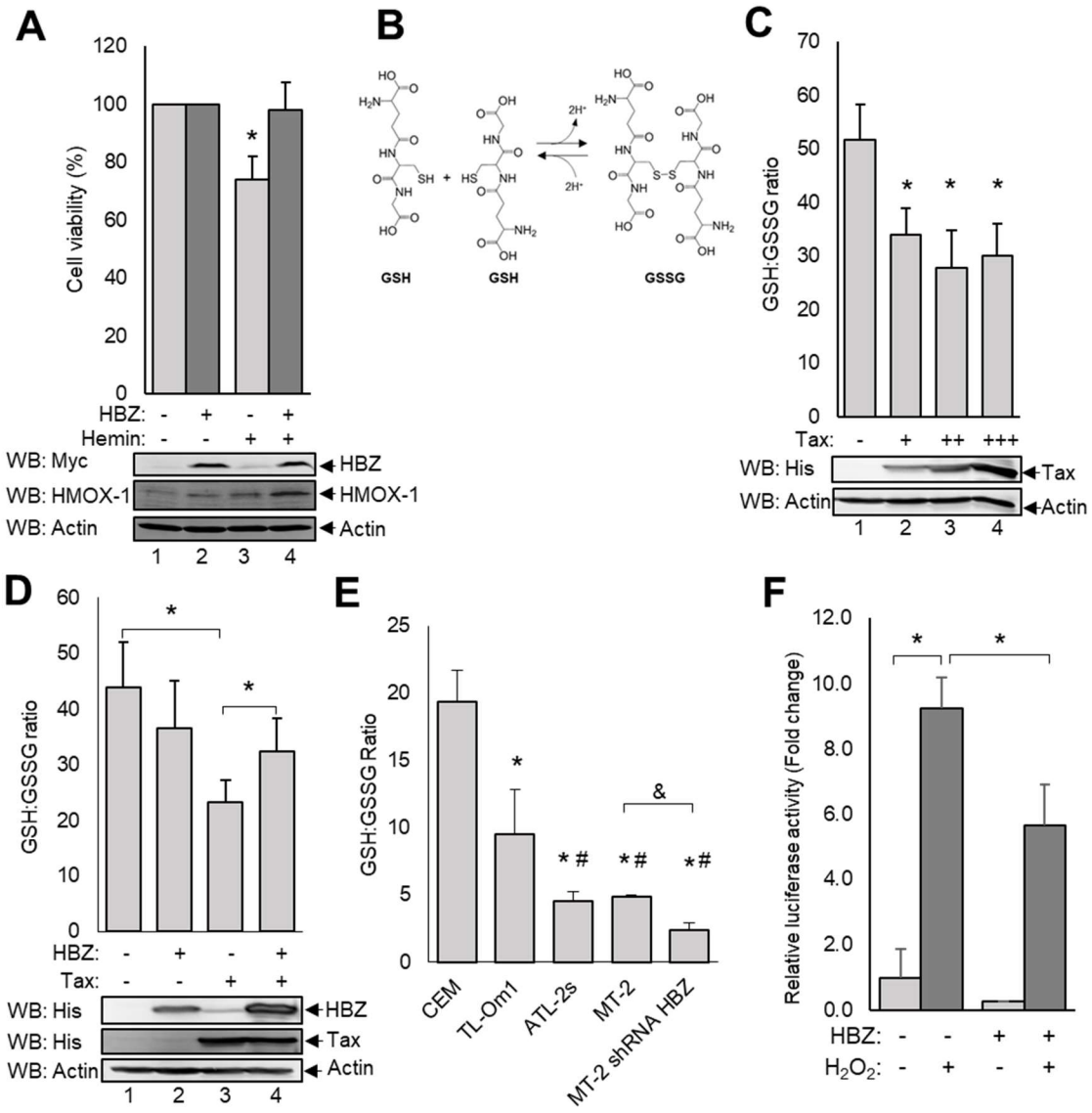

Figure 3.13: HBZ expression overcomes Tax-mediated production of ROS and has a cytoprotective effect. **(A)** HeLa cells stably expressing HBZ-Myc-His or containing the empty vector were plated at a density of $2.5x10^4$ in 96 well plates and allowed to adhere overnight. The following day, cell media was replaced with low serum media (0.05% serum) supplemented with 40μM hemin or DMSO. Treatments were carried out for approximately 24 hours and cell viability assays. Data is an average of three independent experiments and error bars represent SEM (Student's t.test, *$p \leq 0.05$). **(B)** A schematic of the conversion of reduced glutathione (GSH) to the oxidized form, glutathione disulfide (GSSG). **(C)** GSH:GSSG ratio was calculated in HEK 293T cells transiently transfected with increasing amounts of pSG-Tax-His for a total of 6μg plasmid DNA. Data is an average of three independent experiments and error bars represent SEM (Student's t-test, * $p \leq 0.05$). **(D)** GSH:GSSG ratio was calculated in HEK 293T cells transiently transfected with a total of 6μg plasmid DNA (1μg pSG-Tax-His, 5μg pcDNA-HBZ-Myc-His). **(E)** T-cell lines were equalized to approximately $1.5x10^5$ cells per mL prior to harvesting whole cell extracts to analyze GSH and GSSG levels. Data is an average of three independent experiments and error bars indicate SEM. Statistical tests (Students' t-test) were carried out between different cell types: *$p \leq 0.05$ compared to CEM, $^{\#}p \leq 0.05$ compared to TL-Om1, $^{\&}p \leq 0.05$ compared to MT-2). **(F)** HEK 293T cells were transfected with a total of 1μg plasmid DNA (100ng HTLV-LTR, 10ng pRLTK-Luc, 250ng pSG-HBZ-Myc). Cells were treated 24hrs post-transfection with 200μM H_2O_2 or PBS for 4hrs prior to quantification of luciferase and Renilla activity. Ratios were calculated by normalizing luciferase activity against Renilla activity. Data is an average of three independent experiments and error bars indicate SEM (Student's t-test, *$p \leq 0.05$).

antioxidant found in all cell types[404]. Glutathione in its reduced form (GSH) is a tripeptide containing one cysteine residue. Exposure to ROS results in thiol oxidation and formation of glutathione disulfide (GSSG) (**Figure 3.13.B**). GSH and GSSG levels can be quantified and the GSH:GSSG ratio can be calculated as a measure of cellular oxidative state - a higher GSH:GSSG ratio indicates a more reduced state while a lower ratio indicates a more oxidized state.

We first confirmed that Tax-induced oxidative stress is observable using this method (**Figure 3.13.C**). In HEK 293T cells transfected with increasing levels of the Tax-expression plasmid (pSG-Tax-His), we found that the GSH:GSSG ratio decreased significantly, even with the lowest level of Tax expression, confirming that Tax strongly induces the production of RNOS. Next, we evaluated how the co-expression of HBZ with Tax alters the cellular oxidative state (**Figure 3.13.D**). HEK 293T cells transfected with HBZ alone did not exhibit a significant change in oxidative state (lane 2), while cells transfected with Tax alone again exhibited a significant decrease in the GSH:GSSG ratio (lane 3). Interestingly, when HBZ was co-expressed with Tax, the GSH:GSSG ratio increased significantly (lane 4), indicating that HBZ functions to relieve Tax-mediated oxidative stress.

We next assessed the oxidative state of HTLV-1-infected T-cell lines (TL-Om1, ATL-2s, MT-2) compared to an uninfected T-cell line (CEM) (**Figure 3.13.E**). We observed a significantly lower GSH:GSSG ratio in all HTLV-1-infected cell lines. Interestingly, cell lines that retain Tax expression (ATL-2s, MT-2) exhibited a significantly lower GSH:GSSG ratio as compared to Tax-devoid TL-Om1 cells. Considering these factors alone, these data are consistent with previous reports which

indicate Tax induces the production of RNOS. To evaluate whether HBZ reduces oxidative stress in HTLV-1-infected cells, we compared the oxidative state of MT-2 cells with that of MT-2 cells stably transfected with the shRNA-HBZ expression vector (MT-2 shRNA HBZ). We found that knocking down HBZ expression significantly lowered the GSH:GSSG ratio, indicating increased levels of oxidation and supporting the role of HBZ in overcoming Tax-mediated RNOS production.

Though Tax expression is silenced in the majority of ATL cells, recent analysis of sense and antisense transcription at the single-cell level suggests sporadic Tax expression may be retained in a small percentage of the population[248,249]. Though the mechanism of 5' LTR transcriptional reactivation remains unclear, evidence suggests that it may be linked to the metabolic and oxidative state of the host cell[249,405]. In support of this hypothesis, H_2O_2 treatment was shown to induce transcriptional activation at Tax-responsive elements in an HTLV-1-infected cell line[249]. An important function of HBZ is to inhibit the transcription from the 5' LTR, likely as a means of immune evasion since Tax is reported to drive a robust cytolytic T-cell (CTL) response[77,81,167,406,407]. We wanted to evaluate whether HBZ plays a role in preventing stress-induced 5' LTR reactivation. Using a 5' LTR luciferase reporter construct (HTLV-Luc), we measured stress induced activation in HEK 293T cells transfected with HBZ or the empty vector (**Figure 3.13.F**). Consistent with previous reports, we observed that exposure to oxidative stress (H_2O_2) significantly activated transcription at the 5'LTR in empty vector-transfected cells (lanes 1-2). However, HBZ expression significantly repressed H_2O_2-induced 5' LTR activation (lanes 3-4). These data suggest that HBZ plays a role in preventing stress-mediated viral reactivation.

Discussion

Here, we report that HBZ upregulates the expression of HMOX-1 at the transcript, protein, and functional levels. HMOX-1 is a major antioxidant enzyme that plays critical roles in maintaining cellular homeostasis and preventing stress-induced senescence and apoptosis. Though it has beneficial tumor suppressor function in healthy tissues, HMOX-1 expression may also promote the survival and proliferation of cancerous cells. Constitutive expression of HMOX-1 is reported in a variety of highly aggressive malignant tissues when compared to expression levels of healthy, non-malignant tissues. Furthermore, many anti-cancer therapies are reported to strongly activate HMOX-1 expression, which is associated with the onset of multi-drug resistance[344,367–371]. PBMCs isolated from patients diagnosed with ATL have been reported to harbor a high degree of drug resistance. Additionally, the onset of multi-drug resistance in these individuals is associated with disease progression and relapse [400,401,403,408–410]. In line with these reports, we found that HMOX-1 was overexpressed in a small group of acute ATL patients. Interestingly, the reduction of HMOX-1 gene expression has been observed to promote apoptosis and restore sensitivity to chemotherapeutic agents in breast cancer and glioma cells[411,412]. Similarly, knockdown of Nrf2 results in a reduction in antioxidant gene expression and has been reported to inhibit cellular proliferation, reduce invasion, and restore susceptibility to anti-cancer treatments[413–418]. We question whether a reduction in HMOX-1 expression or the inhibition of its activity could likewise sensitize ATL cells to chemotherapy drugs.

We also showed that HMOX-1 expression was upregulated in a group of HAM/TSP patients. The symptoms of HAM/TSP are very similar to those of multiple

sclerosis (MS). Interestingly, HMOX-1 overexpression is also reported to occur in inflammatory brain lesions in MS patients, as well as in the brain and spinal cord of experimental autoimmune encephalomyelitis (EAE) mouse models[419–425]. The factors driving the progression of HAM/TSP are not well understood, but these similarities suggest that HMOX-1 may play an important role. For cases of HAM/TSP, as well as ATL, it may be clinically useful to evaluate HMOX-1 expression levels on a much wider scale to determine if overexpression could serve as a marker for disease progression.

HBZ and Tax each contribute to the regulation of viral replication, spread, and maintenance within the host. Though the activities of Tax are important for *de novo* viral replication, the anti-apoptotic, pro-proliferative, and immune evasive functions of HBZ are important for the clonal expansion of HTLV-1-infected cells. Importantly, Tax is a major source of oxidative stress within the host cell through the upregulation of iNOS and hyperactivation of NF-κB signaling[192,193,197,354,355,426,427]. Another important source of free radicals in HTLV-1-infected cells is the viral accessory protein p13. The *p13* gene is located on the sense strand of the provirus and encodes a protein with a putative amphipathic α-helical structure which allows it to be inserted into the inner mitochondrial membrane. There, it is reported to induce an inward flux of K^+ and Ca^{2+} ions, resulting in membrane depolarization and enhancing the activation of electron transport. The upregulation of cellular respiration may be important for *de novo* viral replication, however it is also an important source of free radicals in the host cell[356–360]. The accumulation of RNOS can result in damage to DNA, proteins, and lipids. Importantly, oxidative damage to hemoproteins causes the release of heme prosthetic groups, which can induce iron-mediated toxicity unless they are properly degraded *via* HMOX-1

activity. In addition to preventing iron-mediated toxicity, HMOX-1 metabolic products have been demonstrated to have antioxidant and anti-inflammatory functions of their own [363,364]. Here, we found that HBZ expression significantly reduced Tax-induced oxidative stress, suggesting that HBZ promotes the detoxification of free radicals that result as a consequence of sense proviral gene expression (**Figure 3.14.A**). From these data, it is unclear whether HMOX-1 is directly responsible for this activity, however, because HMOX-1 plays a major role in the reduction of intracellular ROS and free iron levels, it is a likely candidate.

In addition to protecting HTLV-1-infected cells from senescence and apoptosis, HBZ also plays an important role in host cell immune evasion by downregulating sense proviral gene expression at the 5' LTR[77,81,167,406,407]. Although sense transcription is silenced in the majority of ATL cells, sporadic reactivation has been reported in response to host cell metabolic and oxidative states, and further experimental evidence supports the role of oxidative stress in 5' LTR activation (**Figure 3.14.A**)[248,249,293,405,428,429]. We report that HBZ also attenuates stress-mediated activation of sense proviral gene expression, however the exact mechanisms through which inhibition occurs are unknown. One possibility is that HBZ activates the antioxidant response to rapidly detoxify ROS, resulting in decreased 5' LTR activation. However, AP-1 family members have been documented to bind AP-1 sites in the 5' LTR to activate sense transcription. Therefore, stress-induced AP-1 activity may play a role in 5' LTR activation, suggesting that HBZ-mediated inhibition of AP-1 binding may be responsible for transcriptional repression[78–80].

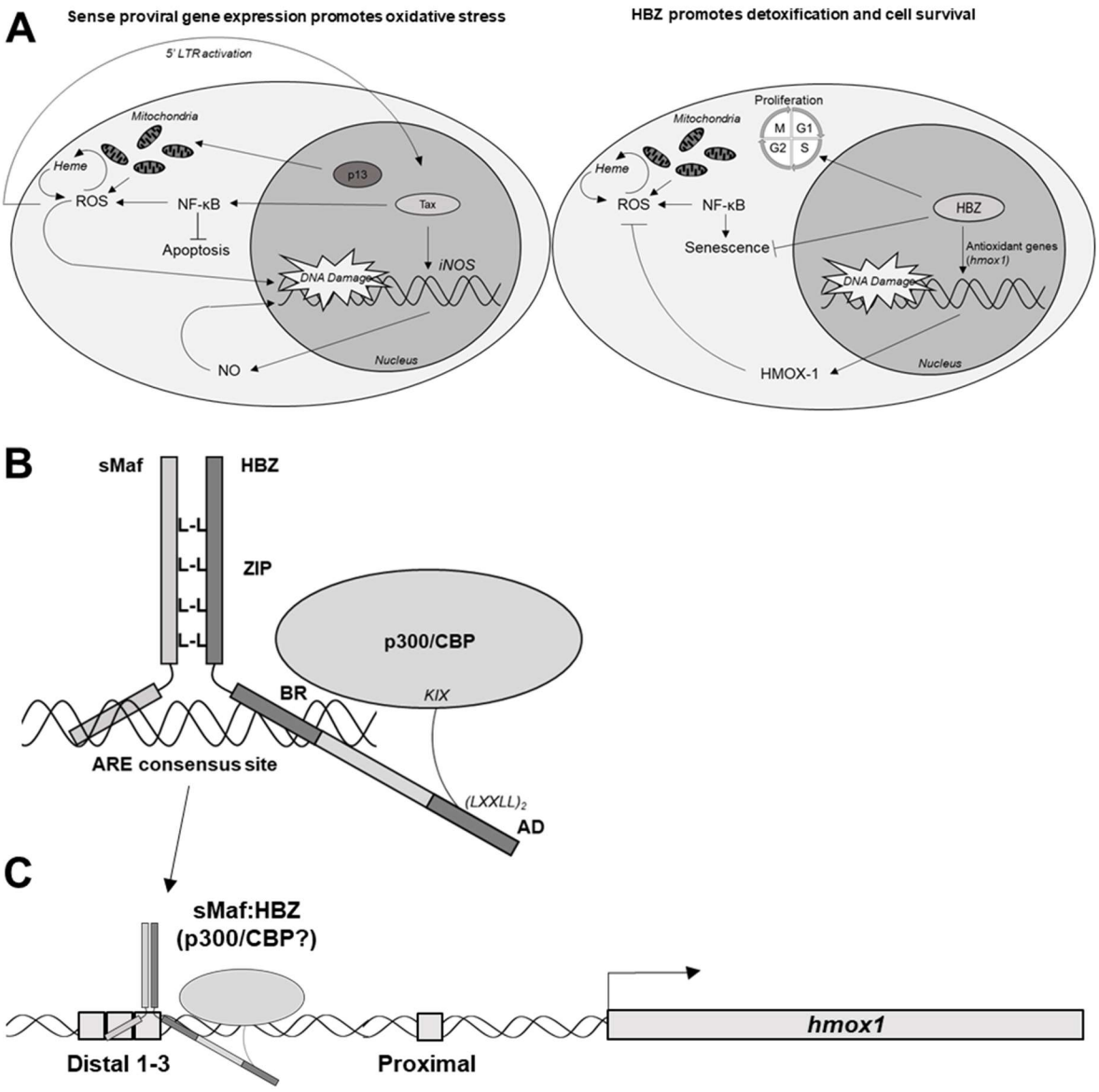

Figure 3.14: A model of HBZ-mediated upregulation of the cellular antioxidant response. (A) During sense proviral gene expression, Tax and p13 are produced, each of which play important roles in promoting *de novo* viral replication. Through these activities, Tax and p13 stimulate the production of free radicals, which can induce damage to DNA and other cellular structures. HBZ is expressed from the antisense strand and is important for maintaining cellular proliferation, preventing NF-κB-induced senescence, and may be important for detoxifying free radicals through its transcriptional upregulation of antioxidant stress response genes, including *hmox1.* **(B)** A proposed model of HBZ:sMaf interactions with cellular coactivators p300/CBP. HBZ and sMafs dimerize *via* hydrophobic leucine interactions in the leucine zipper (ZIP) domain, while the basic regions (BR) are important for DNA binding at antioxidant response elements (AREs). The contribution of the HBZ basic region to DNA binding remains unclear. HBZ recruits cellular coactivators to the complex, likely *via* an interaction between the activation domain (AD) LXXLL motifs and the coactivator KIX domain. **(C)** A proposed model for the recruitment of HBZ:sMaf complexes to the distal ARE site of the *hmox1* gene promoter to activate transcription. Currently, it is unclear whether coactivators are also recruited to the complex.

In this report, we also endeavored to characterize the mechanism through which HMOX-1 overexpression is achieved. We showed that HBZ interacts with the sMafs in a ZIP-dependent manner, and that the AD of HBZ likely facilitates the recruitment of coactivators p300/CBP to the complex (**Figure 3.14.B**). Additionally, we showed that sMafs facilitate the recruitment of HBZ to AREs in the distal *hmox1* promoter *in vivo* and *in vitro* (**Figure 3.14.C**). This finding poses new questions about the DNA-binding activity of HBZ. The DNA-binding domain (DBD) of HBZ does not align well with the consensus DBD sequence of other bZIP transcription factors (bb-bN-AA-b(C/S)R-bb). Furthermore, previous reports indicate that HBZ does not bind directly to DNA unless the DBD sequence is replaced with that of c-Fos, which then allows HBZ:c-Jun heterodimers to bind AP-1 recognition sites[231,430]. Although CNC bZIP transcription factors contain the consensus DBD, they are not demonstrated to stably bind DNA without the tethering activities of sMafs[383]. This led us to question whether there are any similarities between the CNC DBD and the HBZ DBD. Interestingly, an alignment of these sequences showed a conserved glutamine residue which was not observed in AP-1 bZIPs with the exception of B-ATF (**Fig 3.15**). Analysis of the nucleic acid-glutamine interactions has shown that glutamine forms highly specific, bidentate interactions with adenine[431]. To our knowledge, the importance of this glutamine residue in CNC bZIP DNA-binding activity has not yet been addressed. Therefore, it may be useful to evaluate the importance of this residue for ARE recognition and binding in CNC bZIPs as well as in HBZ. Additionally, determining the consensus binding site for HBZ:sMaf complexes will be an important next step in assessing the role of HBZ in the modulation of antioxidant gene expression.

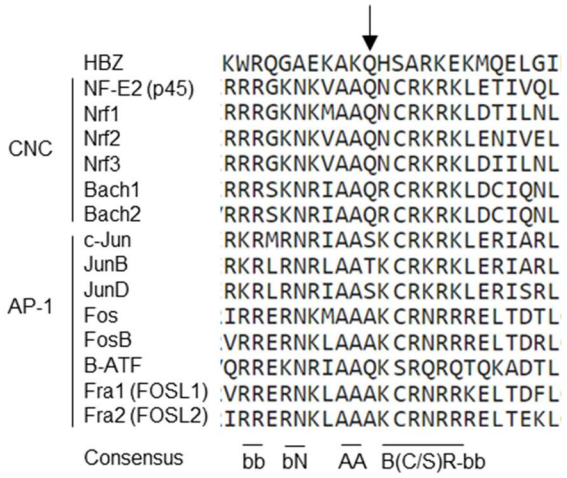

Figure 3.15: Amino acid sequence alignment of DNA-binding motifs in HBZ and CNC bZIPs. The amino acid sequence of the HBZ DNA-binding domain was aligned with the DNA-binding domains of CNC bZIP family proteins. AP-1 family protein DNA-binding domains were aligned for comparison. Arrow indicates glutamine (Q) residue shared by HBZ and CNC bZIP DNA-binding domains. Alignments were performed using UniProt.

Nrf2:sMaf activity at AREs has been implicated in the global regulation of the oxidative stress response[340–343,372–375]. Therefore, HBZ:sMaf transcriptional activity at AREs poses the possibility that HBZ may profoundly affect antioxidant gene expression, potentially leading to large-scale, constitutive activation of the oxidative stress response. Our preliminary work indicates that additional antioxidant response genes (FTH1, SQSTM1, TNFRSF1A, PIM1) are upregulated by HBZ, although they were not evaluated at length. FTH1 encodes the ferritin heavy chain which, along with ferritin light chains, forms a large 24-chain polymer that scavenges and stores intracellular iron, including iron released from HMOX-1-catalyzed heme degradation[432]. Ferritin present in the serum is associated with inflammatory disease[433]. Though little is known about the role of ferritin in HTLV-1 infection, serum ferritin was detected in a group of HAM/TSP patients, indicating a possible link between HBZ and inflammatory disease[434].

SQSTM1 encodes sequestosome 1, also known as p62. This protein is a pro-survival, stress-induced autophagy receptor reported to participate in the degradation of damaged mitochondria and protein aggregates that can result from the activation of NF-κB signaling[435,436]. Interestingly Tax is reported to interact with SQSTM1, which allows constitutive upregulation of NF-κB and may promote viral replication[437,438]. However, when SQSTM1 is overexpressed, it was observed to decrease soluble Tax levels, suggesting sequestration, associated with the downregulation of NF-κB activation[437]. Through this mechanism, HBZ-mediated upregulation of SQSTM1 expression may promote the inactivation of Tax activity and subsequent downregulation of NF-κB[244].

Tumor necrosis factor receptor superfamily 1A (TNFRSF1A) is a receptor for the pro-inflammatory cytokine TNFα, which stimulates an array of cellular signaling

pathways that are important for maintaining cell survival and homeostasis[439,440]. Interestingly, these receptors may also initiate signaling *via* ligand-independent receptor oligomerization[440]. It is possible that increased ligand-dependent or ligand-independent TNF receptor signaling may play a role in HBZ-mediated cell survival.

Recently, STAT3 and its downstream effector kinase PIM1, were shown to be constitutively activated in ATL cells[441]. PIM1 is a stress-induced serine/threonine kinase which has pleiotropic functions, including the regulation of cell cycle progression and apoptosis during oxidative stress[442]. Inhibition of PIM1 activity was shown to trigger pro-apoptotic signaling in ATL cells and reduced tumor growth in an *in vivo* ATL mouse model[441]. Here, we identified PIM1 expression to be upregulated by HBZ, suggesting that PIM1 may be an effective therapeutic target for ATL cells regardless of Tax expression status.

Like HMOX-1, each of these genes (FTH1, SQSTM1, TNFRSF1A, and PIM1) was found to contain at least one ARE site in their promoter, to which Nrf2 and MafK have been previously documented to bind[372–375]. Furthermore, analysis of these transcripts in HeLa cell lines stably expressing HBZ or the HBZ-ΔbZIP truncation mutant revealed a shared dependence upon the bZIP domain for upregulation (**Figure 3.16**). We hypothesize that HBZ upregulates these genes in a similar manner to that of HMOX-1, and that through this mechanism, HBZ can assert widespread control over the host cell oxidative stress response to promote continued survival and clonal proliferation of HTLV-1-infected lymphocytes.

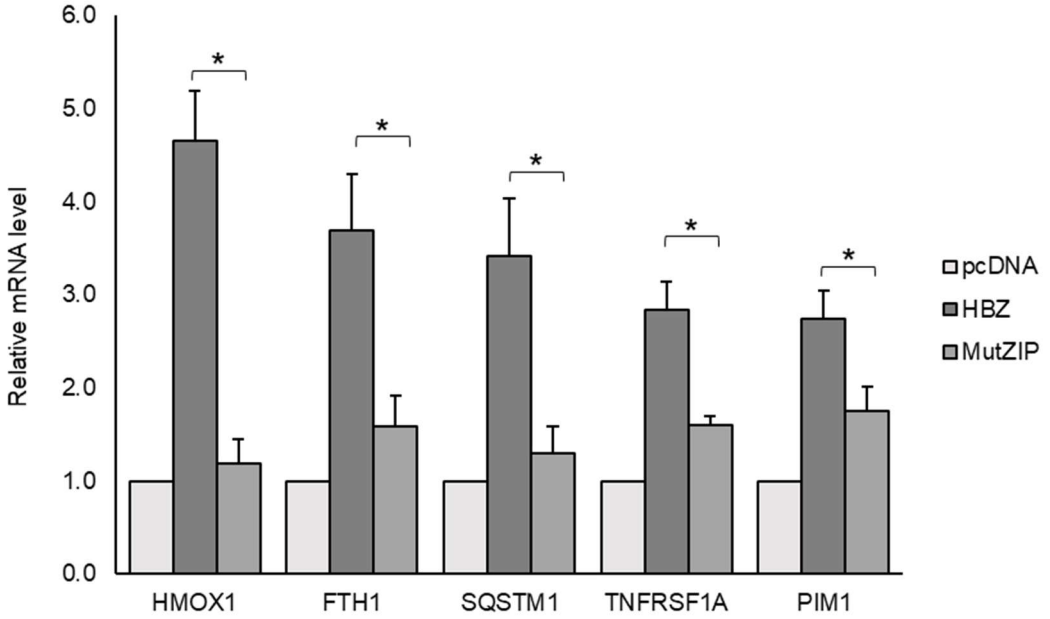

Figure 3.16: Select antioxidant response genes are upregulated in HBZ-expressing cells in a bZIP-dependent manner. qRT-PCR was used to quantify select antioxidant response gene transcripts in HeLa cells stably transfected with pcDNA-HBZ-Myc-His (HBZ), pcDNA-HBZ-MutZIP (MutZIP), or the empty vector (pcDNA). For HMOX-1, data is an average of seven independent experiments. For FTH1, SQSTM1, TNFRSF1A, and PIM1, the data are an average of four independent experiments. For all data, error bars indicate SEM (Student's t-test, * $p \leq 0.05$).

Materials and Methods

Cell lines, plasmids, and antibodies: HEK 293T cells were cultured in Dulbecco's Modified Eagle's Medium (DMEM) supplemented with 10% fetal bovine serum, 2mM L-glutamine, 100U/ml penicillin, and 50µg/mL streptomycin. Clonal HeLa-pCMV and HeLa-pCMV-HBZ-FLAG [240] were cultured in spinner flask suspensions in Minimum Essential Medium supplemented with 5% newborn calf serum, 3% fetal bovine serum, 2mM L-glutamine, 1X MEM non-essential amino acids solution, 1mM sodium pyruvate, 100U/ml penicillin, 50µg/mL streptomycin, and 0.2mg/mL hygromycin B (Invitrogen). Clonal HeLa-pcDNA, HeLa-pcDNA-HBZ-Myc-His, HeLa-pcDNA-HBZ-ΔbZIP-Myc-His, HeLa-pcDNA-HBZ-$(LXXAA)_2$-Myc-His, and HeLa-pcDNA-HBZ-ΔATG cell lines were maintained in supplemented DMEM and were maintained under selection with 0.5mg/mL geneticin (ThermoFisher). T-cell lines were maintained in either supplemented Iscove's Modified Dulbecco's Medium (IMDM) or supplemented Roswell Park Memorial Institute (RPMI) medium. The stable MT-2 shRNA HBZ and empty vector cell lines were maintained in in supplemented IMDM with 1mg/mL geneticin (ThermoFisher)[242].

The following mammalian expression plasmids have been described elsewhere: pcDNA-HBZ Sp1-Myc-His (aa 1-206)[92], pcDNA-HBZ-ΔAD-Myc-His (aa 77-206)[227], pcDNA-HBZ-ΔbZIP-Myc-His (aa 1-130)[81], pcDNA-HBZ-$(LXXAA)_2$-Myc-His, pcDNA-HBZ-MutZIP-Myc-His[377], pcDNA-HBZ-ΔATG[377], pCMV-HBZ-FLAG[240], pSG-HBZ-Myc[377], and pSG-Tax-His[298]. pcDNA3-Myc3-Nrf2 was a gift from Yue Xiong (Addgene plasmid #215555) (Furukawa 2005). Empty vector plasmids pCMV-3Tag-8 and pSG5 were purchased from Agilent Technologies and pcDNA3.1(+)/ Myc-His A was

purchased from Invitrogen. pSG-HBZ-MutZIP-Myc was constructed by digesting the hBZ-MutZIP sequence from pCDNA-HBZ-MutZIP-Myc-His[377] *via* EcoRI digestion and inserting the fragment into the pSG5 vector at an EcoRI site. FLAG-tagged small Maf mammalian expression plasmids were cloned as follows: Sequences encoding MafF, MafG, and MafK were digested (BglII and HindIII) from pDNR-Dual plasmids obtained from the DNASU plasmid repository (HSCD00005183, HSCD00004984, HSCD00002293) and cloned into the pCMV-3Tag-8 backbone vector digested with BamHI and HindIII. The Nrf2 dominant negative expression plasmid was created by amplifying the sequence coordinating to amino acids 401-606 from pcDNA-Myc3-Nrf2 and inserting it into the pcDNA3.1 expression vector via BamHI and XbaI digestion. All plasmids were verified by sequencing and primers are available upon request.

The following antibodies were used for Western blotting and immunoprecipitation experiments: anti-FLAG M2 (Sigma-Aldrich F3165), anti-Myc clone 4A6 (EMD Millipore 05-724), anti-His H-15 (Santa Cruz sc-803), anti-Actin clone C4 (EMD Millipore MAB1501), anti-histone H3 (EMD Millipore #06-755), anti-HMOX1 A-3 (Santa Cruz sc136960), anti-VDAC (Cell Signaling D73D12), anti-MafG (Abcam 154318, 86524), anti-GST (Sigma G7781), anti-p300 N15 (Santa Cruz sc584), anti-CBP A22 (Santa Cruz sc369), anti-MEK1/2 (Cell Signaling L38C12), anti-Nrf2 C20 (Santa Cruz sc722), anti-Bach1(Bethyl A303-057A-T). For Figure 3.5.D, immunoprecipitation was performed using 100μg of anti-MafG antibody obtained from the University of Iowa Developmental Studies Hybridoma Bank (PRCP-MafG-1H7). Anti-HBZ serum was generously provided by Jean-Michel Mesnard[77].

RNA extraction and quantitative real-time PCR: Cells were equalized prior to harvesting RNA using TRIzol Reagent (Invitrogen) according to the manufacturer's instructions. cDNA was synthesized with random hexamers using the RevertAid cDNA synthesis kit (ThermoFisher). Quantitative real-time PCR (qRT-PCR) was performed as previously described[377]. Primer sequences are available upon request. For assays using patient-derived tissues, samples were collected as described previously[443].

HMOX-1 activity assays: These assays for evaluating HMOX-1 activity in cultured cell lines was developed from a previously reported method which analyzed enzymatic activity in mouse tissues[444]. Cell lines indicated in the figure legends were plated (2.0-5.0 x10^6) in the appropriate media. For cells treated with 200μM hydrogen peroxide (H_2O_2), media was switched with low serum media (0.5% FBS) before treatment, which lasted for 4 hours. Cells were collected, pelleted at 350xg for 3 min at 4°C, and washed in 1X phosphate buffered saline (PBS). Cells were resuspended in 200μL detergent-free homogenization buffer (20mM Tris-HCl [pH 7.5], 0.25M sucrose, 1mM EDTA, 2μg/mL leupeptin, 5μg/mL aprotinin, 1mM phenylmethylsulfonyl fluoride [PMSF], and 1mM benzamidine) and each sample was manually homogenized using a dounce tissue grinder. Cell lysates were equalized by quantifying protein content by Bradford protein assay (BioRad) and 200μg of cell lysate was used for each reaction, which contained the following: 20mM Tris-HCl [pH 7.5], 250mM sucrose, 12.5μM hemin (Sigma Aldrich), 1mM NADPH (Sigma Aldrich), and 0.025U bilirubin oxidase (Sigma Aldrich). Reactions were incubated at 37°C for 30 minutes and halted by adding an equal volume of 0.1% formic acid in methanol. Biliverdin d_4 was added to each reaction (0.1ng/μL) to serve as an internal standard, and mixtures were centrifuged at 15,000xg for 20 min at 4°C.

Supernatants were collected and analyzed by LC-MS for biliverdin content. LC-MS analysis was carried out using an Agilent 1200 series high performance liquid chromatograph connected to an Agilent 6220 time-of-flight (TOF) mass spectrometer. Chromatographic separation was performed using an Agilent Zorbax Eclipse Plus C18 column (3.5 µm, 2.1 × 150 mm) held at 35°C. Mobile phase A consisted of water with 1% formic acid whereas mobile phase B consisted of acetonitrile with 1% formic acid. Flow rate was set to 0.25 mL/min. Initial solvent composition was 10% B which was held at 10% B for 1 minute, ramped to 55% B in 1 minute, ramped to 90% B over the next 2 minutes, ramped to 100% B in 2 minutes, and held at 100% B for the next 5 minutes resulting in a total analysis time of 11 minutes. The TOF was operated in positive mode and biliverdin along with biliverdin-d4 were quantified using the [M+H]+ ion. Extracted [M+H]+ ion chromatograms were integrated to give biliverdin peak areas which were then normalized by the peak area of biliverdin-d4. Biliverdin/biliverdin-d4 ratios were compared between groups to determine relative biliverdin concentrations.

Biochemical fractionation of cellular proteins: Membrane-bound protein fractions were collected as previously described[445]. Where indicated, cells were pretreated with 50µM MG132 to stabilize proteins. To collect nuclear and cytoplasmic protein fractions, $1.5x10^6$ cells were washed in 1xPBS and resuspended in lysis buffer [20mM HEPES pH 7.9, 20% [vol/vol] glycerol, 10mM NaCl, 1.5mM $MgCl_2$, 0.2mM EDTA, 1mM DTT, 0.1% NP40, 2µg/mL leupeptin, 5µg/mL aprotinin, 1mM PMSF, and 1mM benzamidine]. Samples were incubated on ice for 10 minutes, and nuclei were pelleted at 2.5krpm for 5 minutes at 4°C. Supernatants (cytoplasmic fraction) were reserved and nuclear pellets were lysed by adding 50µL RIPA buffer [50mM Tris [pH 8.0], 1% Triton X-100, 100mM

NaCl, 1mM $MgCl_2$, 400nM TSA, 2µg/mL leupeptin, 5µg/mL aprotinin, 1mM PMSF, and 1mM benzamidine]. Samples were vortexed and incubated on ice for 15 minutes. Samples were pelleted at 16,000xg for 15 minutes at 4°C and supernatants (nuclear fraction) were reserved. Samples were analyzed by Western blot using the antibodies indicated in the figure legends.

Cellular protein preparation and co-immunoprecipitation: For co-immunoprecipitation assays, HEK 293T ($2.0\text{-}2.5x10^6$) cells were transiently transfected using TurboFect (ThermoFisher) according to the manufacturer's instructions. Cellular protein was harvested 24-48 hours post transfection. Cells were pelleted at 350xg for 3 min at 4°C, washed in 1x PBS, and resuspended in 1mL RIPA buffer [50mM Tris [pH 8.0], 1% Triton X-100, 100mM NaCl, 1mM $MgCl_2$, 400nM TSA, 2µg/mL leupeptin, 5µg/mL aprotinin, 1mM PMSF, and 1mM benzamidine]. Cells were vortexed briefly, and incubated on ice for 20 minutes. Lysates were centrifuged at 16,000xg for 15 minutes at 4°C and soluble protein supernatant was isolated and quantified by Bradford protein assay (Bio-Rad). For co-immunoprecipitations performed with anti-FLAG M2 magnetic resin (Sigma Aldrich M8826), 15µL of resin slurry was washed twice in RIPA buffer and incubated with the indicated amount of protein extract for approximately 16 hours at 4°C. For co-immunoprecipitations performed with anti-Myc antibody, 2µg of the appropriate antibody was pre-bound to 7.5µL packed bead volume of protein G agarose beads (Sigma- Aldrich) for 1 hour at 4°C in 1mL RIPA buffer. Antibody-bound beads were washed once in RIPA before incubating with protein extracts approximately 16 hours at 4°C. Resin was washed four times in RIPA buffer and bound proteins were eluted by SDS dye and resolved by SDS-PAGE and Western blot. Western blots were

probed with the primary antibodies listed in the figure legends, followed by the appropriate HRP-conjugated secondary antibody, and were developed using Pierce ECL Plus chemiluminescence substrate (ThermoFisher), and visualized with a Typhoon 9410 (GE Healthcare).

Bacterial expression vectors, purification of recombinant proteins, and GST pulldown assays: Bacterial expression plasmids were used to express recombinant proteins for purification, including pGEX-GST-HBZ[82], and pGEX-4T-2, which was used to express GST (GE Healthcare), were previously described. The GST-HBZ-AD expression vector was constructed by amplifying the AD-containing sequence (aa 1-57) from the pcDNA-HBZ-Myc-His plasmid[92] and inserting it into the PGEX-4T-2 vector *via* BamHI and EcoRI sites. GST-tagged small Maf bacterial expression vectors (pGEX-MafG) was constructed by PCR amplifying Maf-encoding sequences from pDNR-Dual expression vectors and cloning them into the pGEX-4T-2 digested with BamHI and SmaI. pGEX plasmids were transformed in *Escherichia coli* BL21 codon plus (DE3) (Stratagene), and were purified by glutathione-agarose affinity chromatography. His-tagged small Maf bacterial expression plasmids (pRSETA-MafF, pRSET-MafG) were constructed by cutting Maf-encoding sequences from pDNR-Dual expression vectors (BglII and HindIII), and cloning them into the pRSETA backbone (ThermoFisher) via BamHI and HindIII sites. pRSETA plasmids were transformed in *Escherichia coli* BL21 (DE3)/pLysS (Stratagene) and purified by Ni^{2+} chromatography. The T7-bZIP expression vector was constructed by amplifying the sequence encoding the bZIP domain (aa 120-206) from pcDNA-HBZ-Myc-His[92] and inserting it into the pET3A vector (Novagen) cut with BamHI. T7-bZIP was transformed into *Escherichia coli*

BL21(DE3)/pLysS and purified using the T7-Tag Affinity Purification kit (EMD Millipore). All purified proteins were dialyzed against 0.1M HM (50mM HEPES [pH 7.9], 100mM KCL, 12.5mM $MgCl_2$, 1mM EDTA, 20% [vol/vol] glycerol, 0.025% [vol/vol] Tween 20, 1mM dithiothreitol [DTT]), divided into aliquots, and stored at -80°C. All plasmids were verified by sequencing and primers are available upon request.

GST pull-down assays were performed as previously reported, with minor modifications[81]. Briefly, 20µL of glutathione-agarose beads equilibrated in binding buffer (20mM HEPES [pH 7.9], 2.5mM $MgCL_2$ 5µM $ZnSO_4$, 25mM KCl, 10% [vol/vol] glycerol, 0.05% Nonidet P-40, 1mM DTT, 1mM PMSF). Purified GST-fusion proteins were incubated with equilibrated glutathione-agarose for 1 hr at 4°C in binding buffer, followed by two washes in binding buffer to remove unbound protein. His-tagged MafF was added to the beads and incubated for 16 hours at 4°C. Beads were washed four times in wash buffer (20mM HEPES [pH 7.9], 2.5mM $MgCL_2$ 5µM $ZnSO_4$, 50mM KCl, 10% [vol/vol] glycerol, 0.05% Nonidet P-40, 1mM DTT, 1mM PMSF), and bound protein was eluted using sodium dodecyl sulfate (SDS) loading dye. Proteins were analyzed by SDS-PAGE and Western Blot, using the indicated antibodies.

Electrophoretic mobility shift assays (EMSA): EMSA assays using recombinant purified proteins were performed as described previously[81]. Briefly, the indicated amounts of purified proteins were incubated for 1hr at 20-22°C, then incubated with 2-10fmol of ^{32}P-end-labeled double-stranded DNA probe, 100ng of poly(dA)·poly(dT), 1µg BSA, and 1mM DTT in 0.5x TM 0.1 M for an additional hour, also at 20-22°C. Protein:DNA complexes were resolved on 5% non-denaturing polyacrylamide gels. Gels were dried, and complexes were visualized by PhosphorImager analysis. ARE DNA

probe sequence is as follows: 5'-3': AGCTCGGAATTGCTGACTCAGCATTACTCT. ARE MT DNA probe sequence is as follows: 5'-3': GCTCGGAATCAATGACTCATTGTT ACTCTCG.

Nuclear protein extraction and *in vitro* immobilized DNA-binding assays: Nuclear protein extracts were prepared as follows: $8x10^6$ HEK 293T cells were transfected by calcium phosphate transfection with 50µg of plasmid DNA as indicated in the figure legend (25µg pcDNA-HBZ-Myc-His, 25µg pCMV-MafG-FLAG). Nuclear protein was harvested 48 hours post-transfection using a previously described method (75, 76). Supernatants were collected and dialyzed for approximately 16 hours against 0.1M HM (50mM HEPES [pH7.9], 100mM KCl, 20% [vol/vol] glycerol, 12.5mM MgCl2, 1mM EDTA, 0.025% Tween, 1mM DTT). Nuclear protein concentration was quantified by Bradford protein assay (Bio-Rad).

Immobilized DNA-binding assays were performed using nuclear protein extracts were performed as follows: Per reaction, 7pmol of biotinylated double-stranded DNA oligonucleotide was was bound to 15µL M-280 streptavidin-coupled Dynabeads (Invitrogen) according to the manufacturer's instructions. DNA-bound resin was blocked for one hour in ITB (20mM HEPES [pH 7.9], 0.2mM EDTA, 100mM KCl, 6.25mM MgCl2, 10mM $ZnSO_4$, 20% [vol/vol] glycerol, 0.01% Triton X-100, 5% BSA, 0.2mM PMSF, 1mM benzamidine, 10µg/mL aprotinin, 10µg/mL leupeptin, 1mM DTT) with 5% BSA. The resin was cleared and loaded with 10µg of nuclear protein extracts in a total volume of 500µL of ITB/ 5% BSA and rocked for 2 hours at 4°C. Resin was washed twice in ITB without BSA, three times in ITB without BSA (600mM KCl), and once in 1x PBS. Protein was eluted with SDS dye and resolved by SDS-PAGE and Western blot.

Immobilized DNA-binding assays using purified recombinant protein was performed as follows: Per reaction, 1pmol of biotinylated double-stranded DNA oligonucleotides was bound to 15µL M-280 streptavidin-coupled Dynabeads according to the manufacturer's instructions. DNA-bound resin was incubated with combinations of purified recombinant proteins (4pmol MafG-His, 8pmol GST-HBZ) in protease-inhibitor supplemented EMSA buffer [0.2mM PMSF, 1mM benzamidine, 10µg/mL aprotinin, 10 µg/mL leupeptin, 1mM DTT] for 3 hours at 4°C. Protein-bound resin was washed 3 times in EMSA buffer, and 2 times in EMSA buffer (400mM KCl), and protein was eluted with SDS dye and resolved by SDS-PAGe and Western blot.

Luciferase transcriptional reporter assays: The luciferase reporter plasmid used to evaluate ARE transactivation, pGL-4xARE-Luc, was created by digestion of the pGL4.26 backbone (Promega) with XhoI and HindIII. The 4xARE sequence (GeneArt Gene Synthesis, Invitrogen) was ligated into the digested vector (5'-3':CTCGAGTCGAGCTCGGAATTGCTGACTCAGCATTACTCTCGTCGAGCTCGGAATTGCTGACTCAGCATTACTCTCGTCGAGCTCGGAATTGCTGACTCAGCATTACTCTCGTCGAGCTCGGAATTGCTGACTCAGCATTACTCTCGGATCCAAGCTT). Luciferase reporter assays were performed as follows: On the day prior to transfection, Jurkat T-cells were equalized to $5x10^5$ cells/mL. On the following day, $4x10^6$ were plated and transfected using TurboFect, with a total of 1µg of plasmid DNA (100ng of either pGL4.26 or pGL-4xARE-Luc, 250ng of the appropriate HBZ-expression plasmid). Specific transfection and treatment conditions are described in the figure legends. In assays using Mithramycin A treatment, cells were transfected as described above. At 24hrs post-transfection, cell media was supplemented with 50µM Mithramycin A, or with

the vehicle control (DMSO). Cells were treated for an additional 24 hours before cells were lysed. Luciferase activity in cell lysates was measured using the Luciferase Assay System (Promega) according to the manufacturer's instructions. Background luciferase activity in cells transfected with pGL4.26, containing only a minimal promoter, was subtracted from luciferase activity measured in cells transfected with the pGL-4xTARE-Luc reporter.

For assays using the HLTV-Luc reporter, the internal control plasmid pRLTK-Luc was purchased from Promega and the HTLV-Luc reporter vector (pLTR-Luc) and has been described elsewhere[446]. HEK 293T cells were plated at a density of $4x10^5$ and transfected with a total of 1µg of plasmid DNA (100ng HTLV-Luc, 10ng pRLTK-Luc, 250ng pSG-HBZ-Myc). At 24 hours post-transfection, cells were treated with 200µM H_2O_2, or the vehicle control (PBS), for 4 hours. Luciferase and Renilla activity in cell lysates were measured using the Dual Luciferase Assay System (Promega) according to the manufacturer's instructions. Luciferase activity was normalized against Renilla activity and data are reported as fold change from untreated cells transfected with the empty vector (HBZ^-, $H_2O_2^-$).

Chromatin immunoprecipitation (ChIP): HeLa cell lines stably transfected with pcDNA 3.1, pcDNA-HBZ-Myc-His, or pcDNA-HBZ-ΔATG were plated at $1x10^7$ 24 hours prior to the assay. Chromatin crosslinking was performed by treating the cells with 1% formaldehyde at 37°C for 10 min, followed by the addition of 0.125M glycine to quench the reaction. Cells were collected with a cell scraper, pelleted at 350xg, and washed in 1X PBS. The remainder of the ChIP assay was performed using the Zymo Spin ChIP Kit (Zymo Research) according to the manufacturer's instructions. For each ChIP reaction,

200µg of crosslinked chromatin was diluted to a final volume of 1mL in ChIP chromatin dilution buffer provided in the kit, and was incubated with 5µg of the appropriate antibody for approximately 16 hrs. Antibodies against MafG (ab154318) and the 6x His tag (ab9108) were purchased from Abcam, and the anti-Nrf2 C-20 antibody (sc722) was purchased from Santa Cruz Biotechnology. Preimmune rabbit serum (IgG) was used as a negative control for the immunoprecipitation. ChIP DNA purified according to the kit protocol and was eluted in a total volume of 50µL. ChIP PCR and data analysis were performed as described previously[81]. PCR primers used to amplify proximal and distal HMOX-1 promoter sequences, as well as the HMOX-1 gene control, are listed in Figure 3.8.A. Standard curves were generated for primer sets using five-fold serial dilutions of each input DNA from the ChIP and were included on each experimental plate. PCR efficiencies ranged from 95 to 105%, with correlation coefficients greater than 0.99. Quantitation was performed by comparing threshold cycle values for co-immunoprecipitated DNA to the threshold cycle value for the input DNA in each ChIP[337]. Relative fold enrichment was calculated by dividing the data against the value obtained from the gene-specific primer in pcDNA cell lines, setting the pcDNA "gene" value to 1.

Measuring glutathione ratios to evaluate intracellular oxidative stress: Cells were plated at $2x10^6$ and transfected as indicated in the figure legends. Cells were collected and washed in 1xPBS and lysed in RIPA buffer supplemented with 2µg/mL leupeptin, 5µg/mL aprotinin, 1mM PMSF, 1mM benzamidine, and 20mM iodoacetamide (IAA) and incubated on ice for 30 minutes. Lysates were centrifuged at 16,000xg for 15 minutes at 4°C and the supernatants were reserved. For each analysis, 100µg of cell lysate was resuspended in a total volume of 50µL of RIPA + IAA. Proteins were removed by TCA

precipitation, in which 8µL of 100% trichloroacetic acid was mixed with each sample, incubated on ice for 10 minutes, and centrifuged at 5.6krpm for 5 min at 4°C. Standards of GSH and GSSG were also taken through the same process and used for quantitation. LC-MS was performed using the instrumentation described previously. Separation was achieved using an Agilent Zorbax Eclipse Plus C18 column 3.5 µm, 2.1 × 150 mm) held at 35°C. Mobile phase A consisted of water with 1% formic acid whereas mobile phase B consisted of acetonitrile with 1% formic acid. Flow rate was held at 0.1 mL/min throughout analysis. Initial mobile phase composition began at 5% B which was held for 2 minutes, ramped up to 60% B over the next 11 minutes, ramped to 100% B over the next 2 minutes, and held at 100% B for the next 3 minutes resulting in a total analysis time of 18 minutes. The TOF was operated in positive mode. Reduced and oxidized glutathione were identified and quantified based on the [M+H]+ ion (an IAA modification was taken into account for the reduced form). Concentrations were calculated based on standard calibrations and were used to determine ratios of reduced to oxidized glutathione.

Cell survival assays: Cells were plated at a density of $2.5x10^4$ in 96 well plates and allowed to adhere overnight. The following day, cell media was replaced with low serum media (0.05% serum) supplemented with 40µM hemin or DMSO. Treatments were carried out for approximately 24 hours and cell viability assays were performed using the MTT Cell Growth Assay kit according to the manufacturer's instructions (Sigma-Aldrich).

Acknowledgments

Funding for this study was provided by the National Institute of Health's National Cancer Institute (NIH/NCI CA128800) and by the National Institute of Allergy and Infectious Diseases (NIAID#AI133163) to IL. The funding agencies had no role in the study design, data collection and interpretation, or the decision to submit the work for publication.

Chapter 4

New Insight into the Role of HBZ in the Maintenance of HTLV-1-Infected Cell Populations

The processes through which HTLV-1 drives disease progression are not well defined. The goal of this work was to further evaluate the activities of the HTLV-1-encoded protein HBZ and determine how it contributes to the maintenance of prolonged survival and host cell proliferation, ultimately promoting transformation to a malignant phenotype.

HBZ modulates cellular DNA damage repair mechanisms: A common feature of ATL cells is their unique, polylobulated nuclear morphology, which arises from the accumulation of gross chromosomal abnormalities[153]. Indeed, karyotyping of ATL cells shows abnormalities in both chromosomal numbers and structure, and while disease is not associated with one specific aberration, aggressive ATL subtypes exhibited a greater number of chromosomal defects than less severe ATL subtypes[447]. These findings support that the accumulation of genetic damage is an important component of HTLV-1 disease progression.

The viral protein Tax is well documented to induce genetic instability and it is reported to drive the accumulation DNA damage by increasing the production of reactive oxygen and nitrogen species, inhibiting DNA damage repair pathways, and bypassing DNA-damage cell cycle checkpoints[192–195,197,281–283,285–288,290,448,449]. Even when Tax expression is silenced for the purpose of infected cell immune evasion, Tax-induced genetic damage may remain, increasing the risk of DNA damage-induced cell

cycle arrest, replicative senescence, or apoptosis. HBZ also has pro-oncogenic functions, and unlike Tax, its expression is continuously maintained. The contribution of HBZ to the accumulation of genetic damage is not well characterized, however some reports indicate that HBZ expression delays DNA damage-induced G_2/M arrest, reduces DNA damage-induced p53 activation, and promotes the accumulation of DNA breaks[239–241]. Additionally, HBZ-transgenic mice also develop a malignant lymphoproliferative disease, supporting the role of HBZ in the accumulation of genetic abnormalities[217,221]. Therefore, we investigated the mechanisms through which HBZ promotes deleterious genetic alterations and whether the pro-survival activity of HBZ plays a role in the maintaining cellular integrity in the face of genetic damage, thereby further promoting transformation.

In Aim 1, we evaluated the contribution of HBZ to host cell DNA damage responses, which is discussed in Chapter 2. When assessing the impact of HBZ on the repair of DSBs we found that HBZ attenuates the efficiency of NHEJ, but not HR. We observed that HBZ interacts with two cellular NHEJ-initiating proteins Ku70 and Ku80 *via* its bZIP domain. We also found that NHEJ attenuation was dependent upon the HBZ bZIP domain, suggesting that the suppression of repair is dependent upon HBZ:Ku interactions. The Ku proteins are important for recognizing and stabilizing DNA termini early during NHEJ. Though we expected HBZ to reduce the recruitment of the Ku proteins to DNA termini, this proved to be incorrect. Instead, we found the HBZ expression did not affect Ku-mediated recognition of DSBs, rather, HBZ was recruited to the break site *in vitro*. This led us to hypothesize that HBZ's presence at the break site negatively regulates downstream NHEJ activities. The DNA-dependent protein kinase

DNA-PK is reported to be critical for the completion of NHEJ, as it may play roles in coordinating the recruitment of repair machinery. The DNA-PK complex is formed by the binding the DNA-PK catalytic subunit to Ku70 and Ku80 at the DNA termini, followed by autophosphorylation and activation of kinase activity. We found that HBZ expression resulted in impaired DNA damage-induced DNA-PK autophosphorylation, indicating that its function in regulating repair may be negatively impacted in HBZ-expressing cells (**Figure 2.8**).

Interestingly, DNA-PK has been implicated in promoting p53-dependent apoptosis in response to DNA damage[271–277]. The tumor suppressor p53 regulates many cellular activities, including apoptosis, and its activity is extensively regulated by post-translational phosphorylation and acetylation. Tax has been demonstrated to impair p53-dependent pro-apoptotic signaling by reducing p53 phosphorylation[286]. However, previous work from our group shows that HBZ also impairs p53 activation through the inhibition of cellular acetyltransferases[240,241]. Because DNA-PK has been reported to phosphorylate p53 *in vitro*, our findings suggest that HBZ-mediated attenuation of DNA-PK activity may serve as an anti-apoptotic mechanism to further promote the long-term survival of genetically damaged cells.

Since Tax is reported to inhibit the repair of DSBs though HR, and our findings implicate HBZ in the attenuation of NHEJ, we questioned how DSB repair is regulated in cells which express both Tax and HBZ. Our work demonstrated that Tax activity enhances NHEJ activity in HBZ-expressing cells. These findings suggest that the main mechanism of DNA repair in HTLV-1-infected cells which co-express Tax and HBZ is NHEJ. But in infected cells which have silenced Tax expression, DSBs may be repaired

primarily by HR. Because increased HR frequency has been observed in rapidly-proliferating cells and has been implicated in increasing the risk of chromosomal translocation[261], it is possible that reliance upon HR contributes the accumulation of genetic abnormalities during later phases of infection when Tax expression is largely silenced. Interestingly, HR inhibitors are currently under investigation as novel therapeutics to target rapidly-dividing cancerous cells and confer sensitivity to DNA-damaging agents[450–452]. HR is an important mechanism for repairing stalled and collapsed replication forks, therefore, drugs targeting this activity may be useful for inducing apoptosis. One study performed in ATL cells evaluated the inhibition of WRN helicases, which are highly expressed in leukemic cells and play an important role in HR-dependent maintenance of replication fork fidelity. The authors reported that inhibition of WRN helicases using two different inhibitors resulted in cell cycle arrest and induced apoptosis[453]. This initial study supports the approach of inhibiting HR as a means of depleting ATL cells, however further work will be required to assess its efficacy *in vivo.*

HBZ modulates the cellular antioxidant response: Currently, there are no effective treatment options for people diagnosed with ATL because chemotherapeutic regimens and antiretroviral therapies are highly ineffective. Leukemic cells are reported to develop multi-drug resistance, which is associated with a rapid decline in patient condition[400,401,403,408–410]. The development of drug resistance in malignant cells is also a major concern for a variety of other cancers. In many of these cases, the expression of antioxidant response genes is reported to be upregulated, enhancing drug detoxification and cell survival[344–349]. One of the major physiological consequences of HBZ expression

is the maintenance of long-term host cell survival and proliferation during clonal expansion of HTLV-1-infected lymphocytes. Therefore, we questioned whether HBZ plays a role in the development of drug resistance by manipulating the cellular antioxidant response as a pro-survival mechanism.

In Aim 2, we investigated the role of HBZ in the regulation of the cellular oxidative stress response, which is discussed in Chapter 3. We found that HBZ upregulates the expression of five antioxidant response genes, all of which play various roles in promoting cellular detoxification and survival in response to stress. Of these genes, HMOX-1 is considered to be a prototypical antioxidant protein because its function and transcriptional regulation are extensively characterized. Clinical evidence supports that dysregulation of HMOX-1 gene expression is significantly associated with pathogenesis. Notably, HMOX-1 overexpression is reported in a variety of cancers and is associated with the onset of multi-drug resistance[344,367–371]. Additionally, increased HMOX-1 levels have also been detected in inflammatory brain lesions in multiple sclerosis patients, suggesting that it may also play an important role in neurological inflammatory disease[419–425]. Interestingly, we found that HMOX-1 expression was upregulated in a small group of acute ATL and HAM/TSP patients when compared to asymptomatic carriers, suggesting that constitutive HMOX-1 expression may also play a role in HTLV-1 disease progression. For these reasons, our work focused on understanding the mechanism through which HBZ modulates HMOX-1 gene expression and activity.

A previous study reported that HBZ interacts with the sMaf protein MafG, and that this complex is recruited to consensus AREs *in vitro*. Given that HMOX-1 transcription is extensively regulated by Nrf2:sMaf-mediated transactivation of AREs, we thought it

worthwhile to analyze the recruitment of HBZ and sMafs to the HMOX-1 promoter AREs *in vitro* and *in vivo*. In Chapter 3, we presented evidence which further characterized HBZ:sMaf interactions (**Figure 3.14.B**) and supports that HBZ:sMaf complexes are recruited to these sites to activate transcription, resulting in the upregulation of HMOX-1 gene expression (**Figure 3.14.C**). Because Nrf2:sMaf regulation of AREs has been implicated in the global regulation of the oxidative stress response, HBZ:sMaf transcriptional activity at these sites poses the possibility that HBZ may profoundly affect antioxidant gene expression. In line with this hypothesis, preliminary work confirms that HBZ upregulates four additional antioxidant genes, each of which is reported to contain at least one ARE site in its promoter. Interestingly several of these gene products have been linked to the regulation of apoptotic signaling in ATL cells, supporting that modulation of the antioxidant response may represent another mechanism through which HBZ promotes continued survival of HTLV-1-infected cells.

The induction of antioxidant gene expression is critical for preventing ROS-mediated DNA damage, which can trigger cell cycle arrest, replicative senescence, and the induction of apoptosis[338]. Because cell-free HTLV-1 virions are poorly infectious, a major route of replication is through the clonal proliferation of infected cells[21–23]. In order to maintain the infected cell population in the host, HBZ must ensure that proliferation continues, apoptosis is inhibited, and that infected lymphocytes remain undetectable by Tax-specific CTLs. Evidence presented here supports that HBZ sustains cell survival during oxidative conditions. Furthermore, although HTLV-1-infected cells were observed to be highly stressed, likely due to the expression of pro-oxidative viral proteins Tax and p13, HBZ expression was important for creating a more reduced intracellular

environment. Finally, proviral gene expression has been observed to be activated at the 5' LTR in response to oxidative stress, resulting in increased production of sense strand-encoded proteins Tax and p13. Though HBZ has already been documented to repress Tax-mediated transactivation of the 5' LTR, we observed that it also attenuates oxidative stress-mediated activation. This evidence supports the role of HBZ in preventing the reactivation of sense gene expression in response to oxidative stress as a means of maintaining immune "invisibility" (**Figure 3.14.A**).

Together, these findings support that HBZ promotes the survival of host cells throughout infection and may play a role in enhancing survival in response to ROS-inducing anti-cancer therapies. Therefore, we hypothesize that HMOX-1 may serve as a valuable therapeutic target in drug-resistant ATL cells. Though limited in scope, initial studies have evaluated how the downregulation of HMOX-1 expression affects drug susceptibility in breast and glial cancers. For each case, a decrease in HMOX-1 gene expression results in increased susceptibility to ROS-inducing chemotherapeutic agents[411,412]. As such, a future direction for our work is to evaluate the contribution of HMOX-1 to drug susceptibility in ATL cell lines.

Interestingly, another group reports that treatment with the proteasome inhibitor bortezomib (Table 1.1) is effective at inducing apoptosis in ATL cell lines[454]. Though thought to act primarily by inhibiting the activation of NF-κB signaling, further work has shown that it also promotes oxidative stress. Furthermore, a clinical trial in ATL patients combining bortezomib with EPOCH chemotherapy and the antiviral drug raltegravir showed some efficacy[455]. Paradoxically, bortezomib-mediated ATL cell death was found to be enhanced by the induction of HMOX-1[454]. If these findings are recapitulated *in*

vivo, it may be possible that HMOX-1 overexpression in HTLV-1-infected cells may increase the efficacy of bortezomib treatment. Though further work is needed to understand its implications, HBZ-mediated manipulation of the host cell oxidative stress response may be an important mechanism through which HTLV-1-infected cell populations persist in the host.

Targeting HBZ-mediated viral persistence: Less than 5% of HTLV-1-infected individuals will develop ATL or HAM/TSP, however, for these individuals, there are no effective treatments that significantly extend life expectancy or improve quality of life. In all HTLV-1 carriers, viral infection persists for life, but in the minority of the infected population, disease develops only after years to decades of low viral activity. Ideally, the development and administration of a prophylactic vaccine would be the best approach to avoid initial infection. However, there are currently no preventative vaccines available. A recent study investigated the protective effects of an anti-gp46 antibody, which targets a portion of the viral envelope proteins. When passively administered to mother rats, a large quantity of the antibody was successfully transferred to neonates and resulted in complete protection against HTLV-1 infection[456]. These finding suggest that this may be a valuable approach for preventing mother-to-child transmission of the virus in the future.

Without the availability of a preventative vaccine, many individuals are infected soon after birth through breastfeeding. Furthermore, many individuals are unaware of their infection until they are diagnosed with an HTLV-1-assocaited disease. Therefore, a treatment that depletes the virus from the host will also be required to effectively prevent or reverse HTLV-1-mediated disease progression. Therefore, understanding the

mechanisms through which the virus is maintained in the host is of paramount importance.

Upon transmission of HTLV-1-infected leukocytes, host dendritic cells may play an important role in initial propagation of the virus and transmission of viral particles to host $CD4^+$ T-cells. Though further work is required to establish the role of dendritic cells in maintaining viral persistence within the host, it is possible that they serve as a viral reservoir. Therefore, targeting these cells may be an important approach to depleting the virus from the host.

Current models suggest that early stages of lymphocyte infection involve the strong activation of proviral gene expression to facilitate synthesis of viral gene products and assembly of new viral particles, which are transmitted to new target cells via cell-to-cell contact. The expression of Tax and p13 are important for inhibiting p53-depednent apoptosis, bypassing cell cycle checkpoints, maintaining metabolic activation, and upregulating cellular respiration, all of which contribute to successful *de novo* infection (**Figure 4.1**). Although most antiretroviral therapies target the retroviral replication cycle, these drugs are largely ineffective in limiting HTLV-1 viral spread, likely due to the limited dependence of the virus on *de novo* viral replication. Given that sense proviral gene expression results in increased presentation of highly immunogenic viral antigens, the synthesis of viral particles is limited throughout infection. Additionally, the expression of sense-encoded proteins Tax and p13 promotes the accumulation of toxic RNOS, posing a threat to the fidelity of cellular proteins and DNA (**Figure 4.1**). Therefore, it is unlikely that *de novo* viral replication can be maintained for extended periods of time.

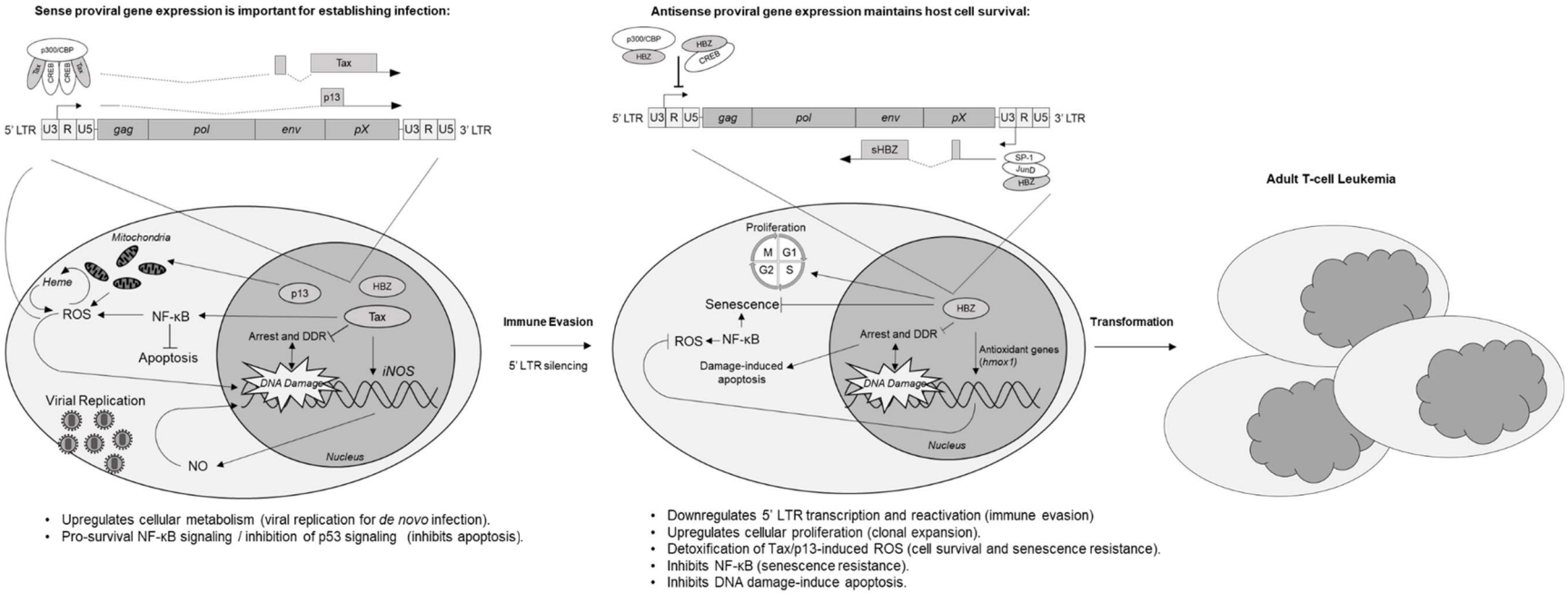

Figure 4.1: A proposed model of HBZ-mediated mechanisms of viral persistence and transformation. HTLV-1 viral spread is reported to occur through two main mechanisms: *de novo* viral replication and clonal expansion. Viral replication is dependent upon the expression of sense-strand encoded proteins, such as Tax. However, there are negative consequences to prolonged sense transcription, including CTL-mediated destruction of the infected cell. HBZ downregulates sense viral transcription to evade detection and promotes viral spread through clonal expansion. Typically, transformation occurs in a single clonal population, which then drives ATL disease progression.

Importantly, HBZ is critical for downregulating sense proviral gene expression at the 5' LTR to reduce viral antigen presentation, allowing infected cells to evade immune detection. Cell clones which are unable to downregulate sense gene expression, likely due to viral integration into highly activated regions of the cellular chromosome, are destroyed through the activity of CTLs (**Figure 4.1**). Therefore, the majority of cells which evade immune detection have entirely silenced sense proviral gene expression, and express only the antisense-encoded HBZ. Interestingly, CTLs do not seem to efficiently target HBZ-expressing cells, perhaps due to low HBZ protein levels and low immunogenicity in comparison to Tax[168,457,458]. Some immunotherapeutic approaches have considered priming a more robust and effective HBZ-specific CTL response. One group demonstrated that a peptide fragment corresponding to a piece of the HBZ bZIP domain (aa157-176) induced a lymphocyte-depleting response *in vivo* that showed some protective effects against disease progression, although multiple boosters were required to achieve this result[459,460]. These results indicate that stimulating an anti-HBZ CTL response may be beneficial for preventing disease progression in ATL patients in the future.

Importantly, although Tax expression is largely inhibited in cells undergoing clonal expansion and progressing to ATL, an anti-Tax immune response remains constantly activated, suggesting that at least a portion of the infected cell population undergoes a degree of viral reactivation. Indeed some reports indicate the sporadic and transient activation of sense transcription[248,249,293]. Though the mechanisms that drive 5' LTR reactivation are unclear, several reports indicate cellular metabolic and oxidative stress contribute (citation). Additionally, we showed evidence supporting that HBZ may

be important for preventing stress-mediated 5'LTR reactivation (**Figure 4.1**). Given that suppression of sense gene expression is critical for avoiding cytolytic destruction of the HTLV-1-infected lymphocyte population, a useful therapeutic approach may be to reactivate 5' LTR transcription.

Evidence supports that the activation of the 5'LTR is dependent upon chromatin remodeling, including histone acetylation, to induce a relaxed chromatin confirmation[70,73]. Therefore, it is proposed that histone hyperacetylation *via* treatment with histone deacetylase inhibitors (HDACi) will promote viral reactivation and result in efficient CTL targeting and depletion of HTLV-1-infected cells. In support of this hypothesis, ATL cells treated with HDACi exhibit increased apoptosis[461,462]. Treatment with an HDACi in an ATL mouse model was also shown to extend survival[462]. Interestingly, HDACi treatment, combined with zidovudine and interferon, has been utilized to some degree in ATL patients, with early results showing some success in depleting ATL cells[463,464].

In conclusion, the work presented here confirms the importance of the viral protein HBZ for maintaining viral persistence within the host. The evidence we discussed offers new insight into what is known about the pro-survival mechanisms employed by HTLV-1 to preserve infected cell populations. Additionally, our findings offer a glimpse into new possible mechanisms of drug resistance in pathogenic cells and pose new questions concerning whether certain shifts in host cell gene expression are commonly associated with disease progression and whether they may be used as predictive markers for patient outcome.

References

1. Rous, P. A sarcoma of the fowl transmissible by an agent separable from the tumor cells. *J. Exp. Med.* **13,** 397–411 (1911).
2. Poiesz, B. J. *et al.* Detection and isolation of type C retrovirus particle from fresh and cultured lymphocytes of a patient with cutaneous T-cell lymphoma. *Proc. Natl. Acad. Sci. USA* **77,** 7415–7419 (1980).
3. Yoshida, M., Miyoshi, I. & Hinuma, Y. Isolation and characterization of retrovirus from cell lines of human adult T-cell leukemia and its implication in the disease. *Proc. Natl. Acad. Sci. USA* **79,** 2031–2035 (1982).
4. Popovic M.S. Reitz Jr, M.G. Sarngadharan, M. Robert-Guroff, V.S. Kalyanaraman, Y. Nakao, I. Miyoshi, J. Minowada, M. Yoshida, Y. Ito, and R.C. Gallo, M. The virus of Japanese adult T-cell leukaemia is a member of the human T-cell leukaemia virus group. *Nature* **300,** 63–66 (1982).
5. Gessain, A. *et al.* Antibodies to human T-lymphotropic virus type I in patients with tropical spastic paraparesis. *Lancet* **ii,** 407–410 (1985).
6. Osame, M. *et al.* HTLV-1 associated myelopathy: a new clinical entity. *Lancet* **1,** 1031–1032 (1986).
7. Goncalves, D. U. *et al.* Epidemiology, treatment, and prevention of human T-cell leukemia virus type 1-associated diseases. *Clin Microbiol Rev* **23,** 577–589
8. Kalyanaraman, V. S. *et al.* A new subtype of human T-cell leukemia virus (HTLV-II) associated with a T-cell variant of hairy cell leukemia. *Science (80-.).* **218,** 571–573 (1982).
9. Araujo, A. & Hall, W. W. Human T-lymphotropic virus type II and neurological disease. *Ann. Neurol.* **56,** 10–19 (2004).
10. Calattini, S. *et al.* Discovery of a new human T-cell lymphotropic virus (HTLV-3) in Central Africa. *Retrovirology* **2,** 30 (2005).
11. Wolfe, N. D. *et al.* Emergence of unique primate T-lymphotropic viruses among central African bushmeat hunters. *Proc. Natl. Acad. Sci. U. S. A.* **102,** 7994–9 (2005).
12. Gessain, A. & Cassar, O. Epidemiological Aspects and World Distribution of HTLV-1 Infection. *Front Microbiol* **3,** 388 (2012).
13. Ehrlich, G. D., Andrews, J., Sherman, M. P., Greenberg, S. J. & Poiesz, B. J. DNA sequence analysis of the gene encoding the HTLV-I p21e transmembrane protein reveals inter- and intraisolate genetic heterogeneity. *Virology* **186,** 619–627 (1992).
14. Bangham, C. R. M. & Ratner, L. How does HTLV-1 cause adult T-cell leukaemia/lymphoma (ATL)? *Curr. Opin. Virol.* **14,** 93–100 (2015).

15. Vrielink, H. & Reesink, H. W. HTLV-I/II prevalence in different geographic locations. *Transfus. Med. Rev.* **18,** 46–57 (2004).

16. Mollenkopf, S. & Murphy, E. L. Measuring incidence of HTLV-1: the other human retrovirus. *Lancet Infect. Dis.* **16,** 1205–1206 (2016).

17. Hino, S. Establishment of the milk-borne transmission as a key factor for the peculiar endemicity of human T-lymphotropic virus type 1 (HTLV-1): the ATL Prevention Program Nagasaki. *Proc. Jpn. Acad. Ser. B. Phys. Biol. Sci.* **87,** 152–66 (2011).

18. Li, H. *et al.* Provirus Load in Breast Milk and Risk of Mother-to-Child Transmission of Human T Lymphotropic Virus Type I. *J. Infect. Dis.* **190,** 1275–1278 (2004).

19. Taylor, G. P. & Matsuoka, M. Natural history of adult T-cell leukemia/lymphoma and approaches to therapy. *Oncogene* **24,** 6047–6057 (2005).

20. Kamihira, S. *et al.* Significance of HTLV-1 proviral load quantification by real-time PCR as a surrogate marker for HTLV-1-infected cell count. *Clin. Lab. Haematol.* **25,** 111–7 (2003).

21. Yamamoto, N., Okada, M., Koyanagi, Y., Kannagi, M. & Hinuma, Y. Transformation of human leukocytes by cocultivation with an adult T cell leukemia virus producer cell line. *Science (80-.).* **217,** 737–739 (1982).

22. Dutartre, H., Clavière, M., Journo, C. & Mahieux, R. Cell-Free versus Cell-to-Cell Infection by Human Immunodeficiency Virus Type 1 and Human T-Lymphotropic Virus Type 1: Exploring the Link among Viral Source, Viral Trafficking, and Viral Replication. *J. Virol.* **90,** 7607–7617 (2016).

23. Pique, C. & Jones, K. S. Pathways of cell-cell transmission of HTLV-1. *Front. Microbiol.* **3,** 378 (2012).

24. Murphy, E. L. *et al.* A case-control study of risk factors for seropositivity to human T-lymphotropic virus type I (HTLV-I) in Jamaica. *Int. J. Epidemiol.* **25,** 1083–9 (1996).

25. Manns, A. *et al.* A prospective study of transmission by transfusion of HTLV-I and risk factors associated with seroconversion. *Int. J. Cancer* **51,** 886–891 (1992).

26. Sullivan, M. T. *et al.* Transmission of human T-lymphotropic virus types I and II by blood transfusion. A retrospective study of recipients of blood components (1983 through 1988). The American Red Cross HTLV-I/II Collaborative Study Group. *Arch. Intern. Med.* **151,** 2043–8 (1991).

27. Armstrong, M. J., Corbett, C., Rowe, I. A., Taylor, G. P. & Neuberger, J. M. HTLV-1 in solid-organ transplantation: current challenges and future management strategies. *Transplantation* **94,** 1075–84 (2012).

28. Kannian, P. & Green, P. L. Human T Lymphotropic Virus Type 1 (HTLV-1): Molecular Biology and Oncogenesis. *Viruses* **2,** 2037–2077 (2010).

29. Cao, S., Maldonado, J. O., Grigsby, I. F., Mansky, L. M. & Zhang, W. Analysis of Human T-Cell Leukemia Virus Type 1 Particles by Using Cryo-Electron Tomography. *J. Virol.* **89,** 2430–2435 (2015).

30. Richardson, J. H., Edwards, A. J., Cruickshank, J. K., Rudge, P. & Dalgleish, A. G. In vivo cellular tropism of human T-cell leukemia virus type 1. *J. Virol.* **64,** 5682–5687 (1990).

31. Jones, K. S., Petrow-Sadowski, C., Huang, Y. K., Bertolette, D. C. & Ruscetti, F. W. Cell-free HTLV-1 infects dendritic cells leading to transmission and transformation of CD4(+) T cells. *Nat. Med.* **14,** 429–36 (2008).

32. Alais, S., Mahieux, R. & Dutartre, H. Viral Source-Independent High Susceptibility of Dendritic Cells to Human T-Cell Leukemia Virus Type 1 Infection Compared to That of T Lymphocytes. *J. Virol.* **89,** 10580–90 (2015).

33. Manel, N. *et al.* The ubiquitous glucose transporter GLUT-1 is a receptor for HTLV. *Cell* **115,** 449–59. (2003).

34. Frauwirth, K. A. *et al.* The CD28 signaling pathway regulates glucose metabolism. *Immunity* **16,** 769–77 (2002).

35. Ghez, D., Lepelletier, Y., Jones, K. S., Pique, C. & Hermine, O. Current concepts regarding the HTLV-1 receptor complex. *Retrovirology* **7,** 99 (2010).

36. Jones, K. S. *et al.* Human T-Cell Leukemia Virus Type 1 (HTLV-1) and HTLV-2 Use Different Receptor Complexes To Enter T Cells. *J. Virol.* **80,** 8291–8302 (2006).

37. Piñon, J. D. *et al.* Human T-cell leukemia virus type 1 envelope glycoprotein gp46 interacts with cell surface heparan sulfate proteoglycans. *J. Virol.* **77,** 9922–30 (2003).

38. Jones, K. S., Petrow-Sadowski, C., Bertolette, D. C., Huang, Y. & Ruscetti, F. W. Heparan Sulfate Proteoglycans Mediate Attachment and Entry of Human T-Cell Leukemia Virus Type 1 Virions into CD4+ T Cells. *J. Virol.* **79,** 12692–12702 (2005).

39. Ghez, D. *et al.* Neuropilin-1 is involved in human T-cell lymphotropic virus type 1 entry. *J. Virol.* **80,** 6844–54 (2006).

40. Jin, Q., Alkhatib, B., Cornetta, K. & Alkhatib, G. Alternate receptor usage of neuropilin-1 and glucose transporter protein 1 by the human T cell leukemia virus type 1. *Virology* **396,** 203–212 (2010).

41. Gross, C. & Thoma-Kress, A. Molecular Mechanisms of HTLV-1 Cell-to-Cell Transmission. *Viruses* **8,** 74 (2016).

42. Nejmeddine, M. & Bangham, C. R. M. The HTLV-1 Virological Synapse. *Viruses* **2,** 1427–1447 (2010).

43. Pais-Correia, A.-M. *et al.* Biofilm-like extracellular viral assemblies mediate HTLV-

1 cell-to-cell transmission at virological synapses. *Nat. Med.* **16,** 83–9 (2010).

44. Thoulouze, M.-I. & Alcover, A. Can viruses form biofilms? *Trends Microbiol.* **19,** 257–62 (2011).

45. Malbec, M., Roesch, F. & Schwartz, O. A new role for the HTLV-1 p8 protein: increasing intercellular conduits and viral cell-to-cell transmission. *Viruses* **3,** 254–9 (2011).

46. Prooyen, N. Van *et al.* Human T-cell leukemia virus type 1 p8 protein increases cellular conduits and virus transmission. (2010). doi:10.1073/pnas.1009635107/-/DCSupplemental.www.pnas.org/cgi/doi/10.1073/pnas.1009635107

47. Ruggero, K. *et al.* Small noncoding RNAs in cells transformed by human T-cell leukemia virus type 1: a role for a tRNA fragment as a primer for reverse transcriptase. *J Virol* **88,** 3612–3622 (2014).

48. Martin, J., Maldonado, J., Mueller, J., Zhang, W. & Mansky, L. Molecular Studies of HTLV-1 Replication: An Update. *Viruses* **8,** 31 (2016).

49. Rho, H. M., Poiesz, B., Ruscetti, F. W. & Gallo, R. C. Characterization of the reverse transcriptase from a new retrovirus (HTLV) produced by a human cutaneous T-cell lymphoma cell line. *Virology* **112,** 355–360 (1981).

50. Mitchell, M. S. *et al.* Synthesis, Processing, and Composition of the Virion-associated HTLV-1 Reverse Transcriptase. *J. Biol. Chem.* **281,** 3964–3971 (2006).

51. Felber, B. K., Paskalis, H., Kleinman-Ewing, C., Wong-Staal, F. & Pavlakis, G. N. The pX protein of HTLV-I is a transcriptional activator of its long terminal repeats. *Science (80-.).* **229,** 675–679. (1985).

52. Brady K.-T. Jeang, J. Duvall and G. Khoury, J. Identification of p40x-responsive regulatory se-quences within the Human T-cell Leukemia Virus Type I long terminal repeat. *J. Virol* **61,** 2175–2181. (1987).

53. Rosen, C. A., Sodroski, J. G. & Haseltine, W. A. Location of cis-acting regulatory sequences in the human T-cell leukemia virus type I long terminal repeat. *Proc. Natl. Acad. Sci. USA* **82,** 6502–6506 (1985).

54. Müller, B. & Kräusslich, H. G. Characterization of human T-cell leukemia virus type I integrase expressed in Escherichia coli. *Eur. J. Biochem.* **259,** 79–87 (1999).

55. Cook, L. B., Rowan, A. G., Melamed, A., Taylor, G. P. & Bangham, C. R. HTLV-1-infected T cells contain a single integrated provirus in natural infection. *Blood* **120,** 3488–3490 (2012).

56. Cook, L. B. *et al.* The role of HTLV-1 clonality, proviral structure, and genomic integration site in adult T-cell leukemia/lymphoma. *Blood* **123,** 3925–31 (2014).

57. Seiki, M., Eddy, R., Shows, T. B. & Yoshida, M. Nonspecific integration of the

HTLV provirus genome into adult T-cell leukaemia cells. *Nature* **309,** 640–642. (1984).

58. Derse, D. *et al.* Human T-Cell Leukemia Virus Type 1 Integration Target Sites in the Human Genome: Comparison with Those of Other Retroviruses. *J. Virol.* **81,** 6731–6741 (2007).

59. Meekings, K. N., Leipzig, J., Bushman, F. D., Taylor, G. P. & Bangham, C. R. M. HTLV-1 integration into transcriptionally active genomic regions is associated with proviral expression and with HAM/TSP. *PLoS Pathog.* **4,** e1000027 (2008).

60. Niederer, H. & Bangham, C. Integration Site and Clonal Expansion in Human Chronic Retroviral Infection and Gene Therapy. *Viruses* **6,** 4140–4164 (2014).

61. Melamed, A. *et al.* Genome-wide Determinants of Proviral Targeting, Clonal Abundance and Expression in Natural HTLV-1 Infection. *PLoS Pathog.* **9,** e1003271 (2013).

62. Albrecht, B. & Lairmore, M. D. Critical role of human T-lymphotropic virus type 1 accessory proteins in viral replication and pathogenesis. *Microbiol Mol Biol Rev* **66,** 396–406, table of contents. (2002).

63. Bindhu, M., Nair, A. & Lairmore, M. D. Role of accessory proteins of HTLV-1 in viral replication, T cell activation, and cellular gene expression. *Front. Biosci.* **9,** 2556–76 (2004).

64. Ahmadi Ghezeldasht, S. *et al.* Human T Lymphotropic Virus Type I (HTLV-I) Oncogenesis: Molecular Aspects of Virus and Host Interactions in Pathogenesis of Adult T cell Leukemia/Lymphoma (ATL). *Iran. J. Basic Med. Sci.* **16,** 179–95 (2013).

65. Johnson, J. M., Harrod, R. & Franchini, G. Molecular biology and pathogenesis of the human T-cell leukaemia/lymphotropic virus Type-1 (HTLV-1). *Int. J. Exp. Pathol.* **82,** 135–47 (2001).

66. Giebler, H. A. *et al.* Anchoring of CREB binding protein to the human T-cell leukemia virus type 1 promoter: a molecular mechanism of Tax transactivation. *Mol. Cell. Biol.* **17,** 5156–64 (1997).

67. Harrod, R. *et al.* p300 and p300/cAMP-responsive element-binding protein associated factor interact with human T-cell lymphotropic virus type-1 Tax in a multi-histone acetyltransferase/activator-enhancer complex. *J. Biol. Chem.* **275,** 11852–11857 (2000).

68. Suzuki, T., Fujisawa, J. I., Toita, M. & Yoshida, M. The trans-activator tax of human T-cell leukemia virus type 1 (HTLV-1) interacts with cAMP-responsive element (CRE) binding and CRE modulator proteins that bind to the 21-base-pair enhancer of HTLV-1. *Proc Natl Acad Sci U S A* **90,** 610–614 (1993).

69. Fujisawa, J. I., Seiki, M., Sato, M. & Yoshida, M. A transcriptional enhancer sequence of HTLV-1 is responsible for transactivation mediated by p40x of HTLV-1. *Embo J* **5,** 713–718 (1986).

70. Lemasson, I., Polakowski, N., Laybourn, P. J. & Nyborg, J. K. Transcription factor binding and histone modifications on the integrated proviral promoter in HTLV-I-infected T-cells. *J Biol Chem* **277,** 49459–49465 (2002).

71. Georges, S. A., Kraus, W. L., Luger, K., Nyborg, J. K. & Laybourn, P. J. p300-Mediated Tax transactivation from recombinant chromatin: Histone tail deletion mimics coactivator function. *Mol. Cell. Biol.* **22,** 127–137. (2002).

72. Lemasson, I., Polakowski, N., Laybourn, P. J. & Nyborg, J. K. Transcription regulatory complexes bind the human T-cell leukemia virus 5' and 3' long terminal repeats to control gene expression. *Mol Cell Biol* **24,** 6117–6126 (2004).

73. Lu, H. *et al.* Acetylation of nucleosomal histones by p300 facilitates transcription from tax-responsive human T-cell leukemia virus type 1 chromatin template. *Mol. Cell. Biol.* **22,** 4450–4462 (2002).

74. Lemasson, I., Polakowski, N. J., Laybourn, P. J. & Nyborg, J. K. Tax-dependent displacement of nucleosomes during transcriptional activation of human T-cell leukemia virus type 1. *J Biol Chem* **281,** 13075–13082 (2006).

75. Kim, Y.-M. M., Geiger, T. R., Egan, D. I., Sharma, N. & Nyborg, J. K. The HTLV-1 tax protein cooperates with phosphorylated CREB, TORC2 and p300 to activate CRE-dependent cyclin D1 transcription. *Oncogene* **29,** 2142–2152 (2010).

76. Kashanchi, F. & Brady, J. N. Transcriptional and post-transcriptional gene regulation of HTLV-1. *Oncogene* **24,** 5938–5951 (2005).

77. Gaudray, G. *et al.* The complementary strand of the human T-cell leukemia virus type 1 RNA genome encodes a bZIP transcription factor that down-regulates viral transcription. *J. Virol.* **76,** 12813–12822 (2002).

78. Basbous, J. *et al.* The HBZ factor of human T-cell leukemia virus type I dimerizes with transcription factors JunB and c-Jun and modulates their transcriptional activity. *J. Biol. Chem.* **278,** 43620–46327 (2003).

79. Matsumoto, J. *et al.* HTLV-1 HBZ suppresses AP-1 activity by impairing both the DNA-binding ability and the stability of c-Jun protein. *Oncogene* **24,** 1001–1010 (2005).

80. Hivin, P. *et al.* The HBZ-SP1 isoform of human T-cell leukemia virus type I represses JunB activity by sequestration into nuclear bodies. *Retrovirology* **4,** 14 (2007).

81. Lemasson, I. *et al.* Human T-cell leukemia virus type 1 (HTLV-1) bZIP protein interacts with the cellular transcription factor CREB to inhibit HTLV-1 transcription. *J. Virol.* **81,** 1543–1553 (2007).

82. Clerc, I. *et al.* An interaction between the human T cell leukemia virus type 1 basic leucine zipper factor (HBZ) and the KIX domain of p300/CBP contributes to the down-regulation of tax-dependent viral transcription by HBZ. *J Biol Chem* **283,** 23903–23913 (2008).

83. Zanella, L., Otsuki, K., Marin, M. A., Bendet, I. & Vicente, A. C. Complete genome sequence of Central Africa human T-cell lymphotropic virus subtype 1b. *J. Virol.* **86,** 12451 (2012).

84. Le Blanc, I. *et al.* HTLV-1 structural proteins. *Virus Res* **78,** 5–16. (2001).

85. Coffin, J. M., Hughes, S. H. & Varmus, H. E. *Retroviruses*. *Retroviruses* (Cold Spring Harbor Laboratory Press, 1997).

86. Nam, S. H., Copeland, T. D., Hatanaka, M. & Oroszlan, S. Characterization of ribosomal frameshifting for expression of pol gene products of human T-cell leukemia virus type I. *J. Virol.* **67,** 196–203 (1993).

87. Seiki, M., Hattori, S., Hirayama, Y. & Yoshida, M. Human adult T-cell leukemia virus: complete nucleotide sequence of the provirus genome integrated in leukemia cell DNA. *Proc. Natl. Acad. Sci. USA* **80,** 3618–3622. (1983).

88. Larocca, D., Chao, L. A., Seto, M. H. & Brunck, T. K. Human T-cell leukemia virus minus strand transcription in infected T-cells. *Biochem Biophys Res Commun* **163,** 1006–1013 (1989).

89. Yoshida, M., Satou, Y., Yasunaga, J., Fujisawa, J. & Matsuoka, M. Transcriptional control of spliced and unspliced human T-cell leukemia virus type 1 bZIP factor (HBZ) gene. *J Virol* **82,** 9359–9368 (2008).

90. Landry, S. *et al.* Upregulation of human T-cell leukemia virus type 1 antisense transcription by the viral tax protein. *J Virol* **83,** 2048–2054 (2009).

91. Cavanagh, M.-H. *et al.* HTLV-I antisense transcripts initiating in the 3'LTR are alternatively spliced and polyadenylated. *Retrovirology* **3,** 15 (2006).

92. Cavanagh, M.-H. *et al.* HTLV-I antisense transcripts initiate in the 3'LTR and are alternatively spliced and polyadenylated. *Retrovirology* **3,** 15 (2006).

93. Satou, Y., Yasunaga, J., Yoshida, M. & Matsuoka, M. HTLV-I basic leucine zipper factor gene mRNA supports proliferation of adult T cell leukemia cells. *Proc Natl Acad Sci U S A* **103,** 720–725 (2006).

94. Murata, K. *et al.* A novel alternative splicing isoform of human T-cell leukemia virus type 1 bZIP factor (HBZ-SI) targets distinct subnuclear localization. *J Virol* **80,** 2495–2505 (2006).

95. Saito, M. *et al.* In vivo expression of the HBZ gene of HTLV-1 correlates with proviral load, inflammatory markers and disease severity in HTLV-1 associated myelopathy/tropical spastic paraparesis (HAM/TSP). *Retrovirology* **6,** 19 (2009).

96. Zhao, T. & Matsuoka, M. HBZ and its roles in HTLV-1 oncogenesis. *Front Microbiol* **3,** 247 (2012).

97. Bogerd, H. P., Tiley, L. S. & Cullen, B. R. Specific binding of the Human T-cell Leukemia Virus Type I Rex protein to a short RNA sequence located within the Rex-response element. *J. Virol.* **66,** 7572–7575 (1992).

98. Nosaka Siomi H, Adachi Y, Isibashi M, Kubota S, Maki M, Hatanaka M, T. Nucleolar tar-geting signal of Human T-cell Leukemia Virus type I rex-encoded protein is essential for cytoplasmic accumulation of unspliced viral mRNA. *Proc Natl Acad Sci USA* **86,** 9798–9802 (1989).

99. Rehberger, S. *et al.* The Activation Domain of a Hormone Inducible HTLV-1 Rex Protein Determines Colocalization with the Nuclear Pore. *Exp. Cell Res.* **233,** 363–371 (1997).

100. Palmeri, D. & Malim, M. H. The human T-cell leukemia virus type 1 posttranscriptional trans-activator Rex contains a nuclear export signal. *J. Virol.* **70,** 6442–5 (1996).

101. Bai, X. T., Sinha-Datta, U., Ko, N. L., Bellon, M. & Nicot, C. Nuclear export and expression of human T-cell leukemia virus type 1 tax/rex mRNA are RxRE/Rex dependent. *J. Virol.* **86,** 4559–65 (2012).

102. Jones, K. S. *et al.* Similar regulation of cell surface human T-cell leukemia virus type 1 (HTLV-1) surface binding proteins in cells highly and poorly transduced by HTLV-1-pseudotyped virions. *J. Virol.* **76,** 12723–34 (2002).

103. Chen, J. *et al.* Cytoplasmic HIV-1 RNA is mainly transported by diffusion in the presence or absence of Gag protein. *Proc. Natl. Acad. Sci.* **111,** E5205–E5213 (2014).

104. Shuker, S. B., Mariani, V. L., Herger, B. E. & Dennison, K. J. Understanding HTLV-I Protease. *Chem. Biol.* **10,** 373–380 (2003).

105. Yamano, Y. *et al.* Correlation of human T-cell lymphotropic virus type 1 (HTLV-1) mRNA with proviral DNA load, virus-specific CD8(+) T cells, and disease severity in HTLV-1-associated myelopathy (HAM/TSP). *Blood* **99,** 88–94 (2002).

106. Kaplan, J. E. *et al.* The risk of development of HTLV-I-Associated Myelopathy/Tropical Spastic Paraparesis among persons infected with HTLV-I. *J Acquir Defic Syndr* **3,** 1096–1101 (1990).

107. Etoh, K. *et al.* Rapid quantification of HTLV-I provirus load: detection of monoclonal proliferation of HTLV-I-infected cells among blood donors. *Int J Cancer* **81,** 859–864 (1999).

108. Nagai, M. *et al.* Analysis of HTLV-I proviral load in 202 HAM/TSP patients and 243 asymptomatic HTLV-I carriers: high proviral load strongly predisposes to HAM/TSP. *J. Neurovirol.* **4,** 586–93 (1998).

109. Matsuzaki, T. *et al.* HTLV-I proviral load correlates with progression of motor disability in HAM/TSP: analysis of 239 HAM/TSP patients including 64 patients followed up for 10 years. *J. Neurovirol.* **7,** 228–34 (2001).

110. Okayama, A. *et al.* Role of HTLV-1 proviral DNA load and clonality in the development of adult T-cell leukemia/lymphoma in asymptomatic carriers. *Int. J. Cancer* **110,** 621–625 (2004).

111. Silva, M. T. T. *et al.* Human T Lymphotropic Virus Type 1 (HTLV-1) Proviral Load in Asymptomatic Carriers, HTLV-1-Associated Myelopathy/Tropical Spastic Paraparesis, and Other Neurological Abnormalities Associated with HTLV-1 Infection. *Clin. Infect. Dis.* **44,** 689–692 (2007).

112. Iwanaga, M. *et al.* Human T-cell leukemia virus type I (HTLV-1) proviral load and disease progression in asymptomatic HTLV-1 carriers: a nationwide prospective study in Japan. *Blood* **116,** 1211–1219 (2010).

113. van Tienen, C. *et al.* Maternal proviral load and vertical transmission of human T cell lymphotropic virus type 1 in Guinea-Bissau. *AIDS Res. Hum. Retroviruses* **28,** 584–90 (2012).

114. Montanheiro, P. A. *et al.* Human T-cell lymphotropic virus type I (HTLV-I) proviral DNA viral load among asymptomatic patients and patients with HTLV-I-associated myelopathy/tropical spastic paraparesis. *Brazilian J. Med. Biol. Res. = Rev. Bras. Pesqui. medicas e Biol.* **38,** 1643–7 (2005).

115. Gabet, A.-S. *et al.* High circulating proviral load with oligoclonal expansion of HTLV-1 bearing T cells in HTLV-1 carriers with strongyloidiasis. *Oncogene* **19,** 4954–4960 (2000).

116. Furtado, M. dos S. B. S. *et al.* Monitoring the HTLV-1 proviral load in the peripheral blood of asymptomatic carriers and patients with HTLV-associated myelopathy/tropical spastic paraparesis from a Brazilian cohort: ROC curve analysis to establish the threshold for risk disease. *J. Med. Virol.* **84,** 664–71 (2012).

117. McKendall, R. R. Neurologic disease due to HTLV-1 infection. *Handb. Clin. Neurol.* **123,** 507–30 (2014).

118. Manns, A., Hisada, M. & La Grenade, L. Human T-lymphotropic virus type I infection. *Lancet* **353,** 1951–1958 (1999).

119. Orland, J. R. *et al.* Prevalence and clinical features of HTLV neurologic disease in the HTLV Outcomes Study. *Neurology* **61,** 1588–94 (2003).

120. Jeffery, K. J. *et al.* HLA alleles determine human T-lymphotropic virus-I (HTLV-I) proviral load and the risk of HTLV-I-associated myelopathy. *Proc. Natl. Acad. Sci. U. S. A.* **96,** 3848–53 (1999).

121. Osame, M. Pathological mechanisms of human T-cell lymphotropic virus type I-associated myelopathy (HAM/TSP). *J. Neurovirol.* **8,** 359–364 (2002).

122. Oh, U. & Jacobson, S. Treatment of HTLV-I-Associated Myelopathy/Tropical Spastic Paraparesis: Toward Rational Targeted Therapy. *Neurol. Clin.* **26,** 781–797 (2008).

123. Fujinami, R. S. & Oldstone, M. B. Amino acid homology between the encephalitogenic site of myelin basic protein and virus: mechanism for autoimmunity. *Science* **230,** 1043–5 (1985).

124. Levin, M. C., Lee, S. M., Morcos, Y., Brady, J. & Stuart, J. Cross-Reactivity between Immunodominant Human T Lymphotropic Virus Type I tax and Neurons: Implications for Molecular Mimicry. *J. Infect. Dis.* **186,** 1514–1517 (2002).

125. Levin, M. C. *et al.* Autoimmunity due to molecular mimicry as a cause of neurological disease. *Nat. Med.* **8,** 509–513. (2002).

126. Tattermusch, S. & Bangham, C. R. M. HTLV-1 infection: what determines the risk of inflammatory disease? *Trends Microbiol.* **20,** 494–500 (2012).

127. Tattermusch, S. *et al.* Systems Biology Approaches Reveal a Specific Interferon-Inducible Signature in HTLV-1 Associated Myelopathy. *PLoS Pathog.* **8,** e1002480 (2012).

128. Osame, M. *et al.* Chronic progressive myelopathy associated with elevated antibodies to human T-lymphotropic virus type I and adult T-cell leukemialike cells. *Ann. Neurol.* **21,** 117–122 (1987).

129. Gessain, A. & Gout, O. Chronic myelopathy associated with human T-lymphotropic virus type I (HTLV-I). *Ann. Intern. Med.* **117,** 933–46 (1992).

130. Matsuo, H. *et al.* Plasmapheresis in treatment of human T-lymphotropic virus type-I associated myelopathy. *Lancet (London, England)* **2,** 1109–13 (1988).

131. Kuroda, Y. *et al.* Treatment of HTLV-I-associated myelopathy with high-dose intravenous gammaglobulin. *J. Neurol.* **238,** 309–14 (1991).

132. Oh, U. & Jacobson, S. Treatment of HTLV-I-associated myelopathy/tropical spastic paraparesis: toward rational targeted therapy. *Neurol Clin* **26,** 781–797 (2008).

133. Junghans, R. P. *et al.* Anti-Tac-H, a humanized antibody to the interleukin 2 receptor with new features for immunotherapy in malignant and immune disorders. *Cancer Res.* **50,** 1495–502 (1990).

134. Lehky, T. J. *et al.* Reduction in HTLV-I proviral load and spontaneous lymphoproliferation in HTLV-I-associated myelopathy/tropical spastic paraparesis patients treated with humanized anti-tac. *Ann. Neurol.* **44,** 942–947 (1998).

135. Izumo, S. *et al.* Interferon-alpha is effective in HTLV-I-associated myelopathy: a multicenter, randomized, double-blind, controlled trial. *Neurology* **46,** 1016–21 (1996).

136. Yamasaki, K. *et al.* Long-term, high dose interferon-alpha treatment in HTLV-I-associated myelopathy/tropical spastic paraparesis: a combined clinical, virological and immunological study. *J. Neurol. Sci.* **147,** 135–44 (1997).

137. Saito, M. *et al.* Decreased Human T Lymphotropic Virus Type I (HTLV-I) Provirus Load and Alteration in T Cell Phenotype after Interferon-α Therapy for HTLV-I–Associated Myelopathy/Tropical Spastic Paraparesis. *J. Infect. Dis.* **189,** 29–40 (2004).

138. Gout, O. *et al.* The effect of zidovudine on chronic myelopathy associated with HTLV-1. *J. Neurol.* **238,** 108–9 (1991).

139. Sheremata, W. A., Benedict, D., Squilacote, D. C., Sazant, A. & DeFreitas, E. High-dose zidovudine induction in HTLV-I-associated myelopathy: safety and possible efficacy. *Neurology* **43,** 2125–9 (1993).

140. Taylor, G. P. *et al.* Effect of lamivudine on human T-cell leukemia virus type 1 (HTLV-1) DNA copy number, T-cell phenotype, and anti-tax cytotoxic T-cell frequency in patients with HTLV-1-associated myelopathy. *J. Virol.* **73,** 10289–95 (1999).

141. Matsuoka, M. Human T-cell leukemia virus type I (HTLV-I) infection and the onset of adult T-cell leukemia (ATL). *Retrovirology* **2,** 27 (2005).

142. Yoshie, O. *et al.* Frequent expression of CCR4 in adult T-cell leukemia and human T-cell leukemia virus type 1-transformed T cells. *Blood* **99,** 1505–1511 (2002).

143. Higashimura, N., Takasawa, N., Tanaka, Y., Nakamura, M. & Sugamura, K. Induction of OX40, a receptor of gp34, on T cells by trans-acting transcriptional activator, Tax, of human T-cell leukemia virus type I. *Jpn. J. Cancer Res.* **87,** 227–31 (1996).

144. Imura, A. *et al.* The human OX40/gp34 system directly mediates adhesion of activated T cells to vascular endothelial cells. *J. Exp. Med.* **183,** 2185–95 (1996).

145. Kiyokawa, T. *et al.* Hypercalcemia and osteoclast proliferation in adult T-cell leukemia. *Cancer* **59,** 1187–1191 (1987).

146. Nosaka, K. *et al.* Mechanism of hypercalcemia in adult T-cell leukemia: overexpression of receptor activator of nuclear factor kappaB ligand on adult T-cell leukemia cells. *Blood* **99,** 634–640 (2002).

147. Ishitsuka, K. & Tamura, K. Human T-cell leukaemia virus type I and adult T-cell leukaemia-lymphoma. *Lancet Oncol* **15,** e517-26 (2014).

148. Fujino, T. & Nagata, Y. HTLV-I transmission from mother to child. *J. Reprod. Immunol.* **47,** 197–206 (2000).

149. Pawson, R. *et al.* Adult T-Cell Leukemia/Lymphoma in London: Clinical Experience of 21 Cases. *Leuk. Lymphoma* **31,** 177–185 (1998).

150. Sugiyama, H. *et al.* Significance of postnatal mother-to-child transmission of human T-lymphotropic virus type-I on the development of adult T-cell leukemia/lymphoma. *J. Med. Virol.* **20,** 253–60 (1986).

151. Miyamoto Yamaguchi K, Nishimura H, Takatsuki K, Motoori TR, Morimatsu M, Yasaka T, Ohya I, Koga T, Y. Familial adult T-cell leukemia. *Cancer* **55,** 181–185 (1985).

152. Kawano, F., Yamaguchi, K., Nishimura, H., Tsuda, H. & Takatsuki, K. Variation in

the clinical courses of adult T-cell leukemia. *Cancer* **55,** 851–856 (1985).

153. Tsukasaki, K. *et al.* Definition, prognostic factors, treatment, and response criteria of adult T-cell leukemia-lymphoma: a proposal from an international consensus meeting. *J Clin Oncol* **27,** 453–459 (2009).

154. Shimoyama, M. Diagnostic criteria and classification of clinical subtypes of adult T-cell leukaemia-lymphoma. A report from the Lymphoma Study Group (1984-87). *Br. J. Haematol.* **79,** 428–437 (1991).

155. Hermine, O., Ramos, J. C. & Tobinai, K. A Review of New Findings in Adult T-cell Leukemia-Lymphoma: A Focus on Current and Emerging Treatment Strategies. *Adv. Ther.* **35,** 135–152 (2018).

156. Takasaki, Y. *et al.* Long-term study of indolent adult T-cell leukemia-lymphoma. *Blood* **115,** 4337–4343 (2010).

157. Tsukasaki, K. & Tobinai, K. Human T-cell lymphotropic virus type I-associated adult T-cell leukemia-lymphoma: new directions in clinical research. *Clin. Cancer Res.* **20,** 5217–25 (2014).

158. Marcais, A. *et al.* Therapeutic options for adult T-cell leukemia/lymphoma. *Curr Oncol Rep* **15,** 457–464 (2013).

159. Okamura, J., Uike, N., Utsunomiya, A. & Tanosaki, R. Allogeneic stem cell transplantation for adult T-cell leukemia/lymphoma. *Int. J. Hematol.* **86,** 118–25 (2007).

160. Hishizawa, M. *et al.* Transplantation of allogeneic hematopoietic stem cells for adult T-cell leukemia: a nationwide retrospective study. *Blood* **116,** 1369–1376 (2010).

161. Ishida, T. *et al.* Impact of Graft-versus-Host Disease on Allogeneic Hematopoietic Cell Transplantation for Adult T Cell Leukemia-Lymphoma Focusing on Preconditioning Regimens: Nationwide Retrospective Study. *Biol. Blood Marrow Transplant.* **19,** 1731–1739 (2013).

162. Ando, S. *et al.* HTLV-1 Tax-Specific CTL Epitope–Pulsed Dendritic Cell Therapy Reduces Proviral Load in Infected Rats with Immune Tolerance against Tax. *J. Immunol.* **198,** 1210–1219 (2017).

163. Revaud, D. *et al.* Development of an Anti-HTLV-1 Vaccine for the Treatment of Adult T-Cell Leukemia/Lymphoma. in *Blood 57th ASH Annual Meeting* **126,** 4010 (2015).

164. Gillet, N. A. *et al.* The host genomic environment of the provirus determines the abundance of HTLV-1-infected T-cell clones. *Blood* **117,** 3113–3122 (2011).

165. Bushman, F. *et al.* Genome-wide analysis of retroviral DNA integration. *Nat. Rev. Microbiol.* **3,** 848–858 (2005).

166. Bangham, C. R. M., Cook, L. B. & Melamed, A. HTLV-1 clonality in adult T-cell

leukaemia and non-malignant HTLV-1 infection. *Semin. Cancer Biol.* **26,** 89–98 (2014).

167. M, K., I, M. & Inoko H, Igarashi H. Kumashima G, Sato S, Morita M, Kidokoro M, Sugimoto M, Funahashi S, Osame M, Shida H., H. S. Predominant recognition of human T cell leukemia virus type I (HTLV-I) pX gene products by human CD8+ cytotoxic T cells directed against HTLV-I-infected cells. *Int. Immunol.* **3,** 761–767 (1991).

168. Suemori, K. *et al.* HBZ is an immunogenic protein but not a target antigen for HTLV-1-specific cytotoxic T lymphocytes. *J Gen Virol* (2009).

169. Furukawa, Y., Kubota, R., Tara, M., Izumo, S. & Osame, M. Existence of escape mutant in HTLV-I tax during the development of adult T-cell leukemia. *Blood* **97,** 987–993 (2001).

170. Takeda, S. *et al.* Genetic and epigenetic inactivation of tax gene in adult T-cell leukemia cells. *Int J Cancer* **109,** 559–567 (2004).

171. Tamiya, S. *et al.* Two types of defective human T-lymphotropic virus type I provirus in adult T-cell leukemia. *Blood* **88,** 3065–3073 (1996).

172. Koiwa, T. *et al.* 5'-long terminal repeat-selective CpG methylation of latent human T-cell leukemia virus type 1 provirus in vitro and in vivo. *J Virol* **76,** 9389–9397 (2002).

173. Nomura, M. *et al.* Repression of tax expression is associated both with resistance of human T-cell leukemia virus type 1-infected T cells to killing by tax-specific cytotoxic T lymphocytes and with impaired tumorigenicity in a rat model. *J Virol* **78,** 3827–3836 (2004).

174. Hanon, E. *et al.* Abundant tax protein expression in CD4+ T cells infected with human T-cell lymphotropic virus type I (HTLV-I) is prevented by cytotoxic T lymphocytes. *Blood* **95,** 1386–92 (2000).

175. Etoh, K. *et al.* Persistent clonal proliferation of human T-lymphotropic virus type I-infected cells in vivo. *Cancer Res* **57,** 4862–4867 (1997).

176. Wattel, E., Cavrois, M., Gessain, A. & Wain-Hobson, S. Clonal expansion of infected cells: a way of life for HTLV-I. *J Acquir Immune Defic Syndr Hum Retrovirol* **13,** S92–99. (1996).

177. Yasunaga, J. & Matsuoka, M. Leukemogenesis of adult T-cell leukemia. *Int. J. Hematol.* **78,** 312–20 (2003).

178. Tanaka, G. *et al.* The Clonal Expansion of Human T Lymphotropic Virus Type 1–Infected T Cells: A Comparison between Seroconverters and Long-Term Carriers. *J. Infect. Dis.* **191,** 1140–1147 (2005).

179. Tsukasaki, K. *et al.* Integration patterns of HTLV-I provirus in relation to the clinical course of ATL: frequent clonal change at crisis from indolent disease. *Blood* **89,** 948–56 (1997).

180. Mesri, E. A., Feitelson, M. A. & Munger, K. Human viral oncogenesis: a cancer hallmarks analysis. *Cell Host Microbe* **15,** 266–82 (2014).

181. Okamoto, T. *et al.* Multi-step carcinogenesis model for adult T-cell leukemia. *Jpn J Cancer Res* **80,** 191–195 (1989).

182. Armitage, P. & Doll, R. The age distribution of cancer and a multi-stage theory of carcinogenesis. *Br. J. Cancer* **8,** 1–12 (1954).

183. Matsuoka, M. & Yasunaga, J. Human T-cell leukemia virus type 1: replication, proliferation and propagation by Tax and HTLV-1 bZIP factor. *Curr Opin Virol* **3,** 684–691 (2013).

184. Currer, R. *et al.* HTLV tax: a fascinating multifunctional co-regulator of viral and cellular pathways. *Front. Microbiol.* **3,** 406 (2012).

185. Sun, S. C. & Ballard, D. W. Persistent activation of NF-kappaB by the tax transforming protein of HTLV-1: hijacking cellular IkappaB kinases. *Oncogene* **18,** 6948–6958 (1999).

186. Ballard E. Böhnlein, J.W. Lowenthal, Y. Wano, B.R. Franza and W.C. Greene, D. W. HTLV-I Tax induces cellular proteins that activate the kB element in the IL-2 receptor a gene. *Science (80-.).* **241,** 1652–1655 (1988).

187. Grassmann, R., Aboud, M. & Jeang, K. T. Molecular mechanisms of cellular transformation by HTLV-1 Tax. *Oncogene* **24,** 5976–5985 (2005).

188. Arima, N. *et al.* Human T-cell leukemia virus type I Tax induces expression of the Rel-related family of kappa B enhancer-binding proteins: evidence for a pretranslational component of regulation. *J. Virol.* **65,** 6892–9 (1991).

189. Leung, K. & Nabel, G. J. HTLV-I transactivator induces interleukin-2 receptor expression through an NF-kB-like factor. *Nature* **333,** 776–778 (1988).

190. Ruben H. Poteat, T.-H. Tan, K. Kawakami, R. Roeder, W. Haseltine and C.R. Rosen, S. Cellular transcription factors and regulation of IL-2 receptor gene expression by HTLV-I Tax gene product. *Science (80-.).* **241,** 89–92 (1988).

191. Morgan, M. J. & Liu, Z. Crosstalk of reactive oxygen species and NF-κB signaling. *Cell Res.* **21,** 103–115 (2011).

192. Kinjo, T., Ham-Terhune, J., Peloponese Jr., J. M. & Jeang, K. T. Induction of reactive oxygen species by human T-cell leukemia virus type 1 tax correlates with DNA damage and expression of cellular senescence marker. *J Virol* **84,** 5431–5437 (2010).

193. Baydoun, H. H., Cherian, M. A., Green, P. & Ratner, L. Inducible nitric oxide synthase mediates DNA double strand breaks in Human T-Cell Leukemia Virus Type 1-induced leukemia/lymphoma. *Retrovirology* **12,** 71 (2015).

194. Lemoine, F. J. & Marriott, S. J. Genomic instability driven by the human T-cell leukemia virus type I (HTLV-I) oncoprotein, Tax. *Oncogene* **21,** 7230–4. (2002).

195. Nicot, C. HTLV-I Tax-Mediated Inactivation of Cell Cycle Checkpoints and DNA Repair Pathways Contribute to Cellular Transformation: 'A Random Mutagenesis Model'. *J. Cancer Sci.* **2,** (2015).

196. Philpott, S. M. & Buehring, G. C. Defective DNA repair in cells with human T-cell leukemia/bovine leukemia viruses: role of tax gene. *J Natl Cancer Inst* **91,** 933–942 (1999).

197. Baydoun, H. H., Bai, X. T., Shelton, S. & Nicot, C. HTLV-I tax increases genetic instability by inducing DNA double strand breaks during DNA replication and switching repair to NHEJ. *PLoS One* **7,** e42226 (2012).

198. Kao, S. Y. & Marriott, S. J. Disruption of nucleotide excision repair by the human T-cell leukemia virus type 1 Tax protein. *J Virol* **73,** 4299–4304 (1999).

199. Morimoto, H., Tsukada, J., Kominato, Y. & Tanaka, Y. Reduced expression of human mismatch repair genes in adult T-cell leukemia. *Am. J. Hematol.* **78,** 100–107 (2005).

200. Azran, I., Schavinsky-Khrapunsky, Y. & Aboud, M. Role of Tax protein in human T-cell leukemia virus type-I leukemogenicity. *Retrovirology* **1,** 20 (2004).

201. Bellon, M., Baydoun, H. H., Yao, Y. & Nicot, C. HTLV-I Tax-dependent and -independent events associated with immortalization of human primary T lymphocytes. *Blood* **115,** 2441–2448 (2010).

202. Tanaka, A. *et al.* Oncogenic transformation by the tax gene of human T-cell leukemia virus type I in vitro. *Proc Natl Acad Sci U S A* **87,** 1071–1075 (1990).

203. Pozzatti, R., Vogel, J. & Jay, G. The human T-lymphotropic virus type I tax gene can cooperate with the ras oncogene to induce neoplastic transformation of cells. *Mol Cell Biol* **10,** 413–417 (1990).

204. Fujita, M. & Shiku, H. Differences in sensitivity to induction of apoptosis among rat fibroblast cells transformed by HTLV-I tax gene or cellular nuclear oncogenes. *Oncogene* **11,** 15–20 (1995).

205. Gao, L. *et al.* HTLV-1 Tax transgenic mice develop spontaneous osteolytic bone metastases prevented by osteoclast inhibition. *Blood* **106,** 4294–4302 (2005).

206. Hasegawa, H. *et al.* Thymus-derived leukemia-lymphoma in mice transgenic for the Tax gene of human T-lymphotropic virus type I. *Nat Med* **12,** 466–472 (2006).

207. Ohsugi, T. A transgenic mouse model of human T cell leukemia virus type 1-associated diseases. *Front Microbiol* **4,** 49 (2013).

208. Grassmann, R. *et al.* Transformation to continuous growth of primary human T lymphocytes by human T cell leukemia virus type I X-region genes transduced by a herpesvirus saimiri vector. *Proc Natl Acad Sci USA* **86,** 3355–3551 (1989).

209. Grassmann, R. *et al.* Role of human T-cell leukemia virus type 1 X region proteins in immortalization of primary human lymphocytes in culture. *J. Virol.* **66,** 4570–

4575 (1992).

210. Akagi, T. & Shimotohno, K. Proliferative response of Tax1-transduced primary human T cells to anti-CD3 antibody stimulation by an interleukin-2-independent pathway. *J Virol* **67,** 1211–7. (1993).

211. Schmitt, I., Rosin, O., Rohwer, P., Gossen, M. & Grassmann, R. Stimulation of cyclin-dependent kinase activity and G1- to S-phase transition in human lymphocytes by the human T-cell leukemia/lymphotropic virus type 1 Tax protein. *J Virol* **72,** 633–640 (1998).

212. Akagi, T., Ono, H. & Shimotohno, K. Characterization of T cells immortalized by Tax1 of human T-cell leukemia virus type 1. *Blood* **86,** 4243–9 (1995).

213. Matsuoka, M. & Jeang, K.-T. Human T-cell leukaemia virus type 1 (HTLV-1) infectivity and cellular transformation. *Nat. Rev. Cancer* **7,** 270–80 (2007).

214. Satou, Y. & Matsuoka, M. Implication of the HTLV-I bZIP factor gene in the leukemogenesis of adult T-cell leukemia. *Int J Hematol* **86,** 107–112 (2007).

215. Li, Z. *et al.* High-affinity neurotrophin receptors and ligands promote leukemogenesis. *Blood* **113,** 2028–2037 (2009).

216. Zhao, T. *et al.* HTLV-1 bZIP factor enhances TGF-β signaling through p300 coactivator. *Blood* **118,** 1865–76 (2011).

217. Satou, Y. *et al.* HTLV-1 bZIP factor induces T-cell lymphoma and systemic inflammation in vivo. *PLoS Pathog* **7,** e1001274 (2011).

218. Sugata, K. *et al.* HTLV-1 bZIP factor impairs cell-mediated immunity by suppressing production of Th1 cytokines. *Blood* **119,** 434–44 (2012).

219. Yamamoto-Taguchi, N. *et al.* HTLV-1 bZIP Factor Induces Inflammation through Labile Foxp3 Expression. *PLoS Pathog.* **9,** e1003630 (2013).

220. Polakowski, N., Gregory, H., Mesnard, J.-M. M. & Lemasson, I. Expression of a protein involved in bone resorption, Dkk1, is activated by HTLV-1 bZIP factor through its activation domain. *Retrovirology.* **7,** 61 (2010).

221. Esser, A. K. *et al.* HTLV-1 viral oncogene HBZ induces osteolytic bone disease in transgenic mice. *Oncotarget* **8,** 69250–69263 (2017).

222. Arnold, J. *et al.* Enhancement of infectivity and persistence in vivo by HBZ, a natural antisense coded protein of HTLV-1. *Blood* **107,** 3976–82 (2006).

223. Ma, G., Yasunaga, J. & Matsuoka, M. Multifaceted functions and roles of HBZ in HTLV-1 pathogenesis. *Retrovirology* **13,** 16 (2016).

224. Cook, P. R., Polakowski, N. & Lemasson, I. HTLV-1 HBZ protein deregulates interactions between cellular factors and the KIX domain of p300/CBP. *J. Mol. Biol.* **409,** 384–398 (2012).

225. Hivin, P. *et al.* Nuclear localization of HTLV-I bZIP factor (HBZ) is mediated by

three distinct motifs. *J Cell Sci* **118,** 1355–1362 (2005).

226. Angel, P. and M. K. The role of Jun, Fos and the AP-1 complex in cell-proliferation and transformation. *Biochim Biophys Acta* **1072,** 129–157 (1991).

227. Thebault, S., Basbous, J., Hivin, P., Devaux, C. & Mesnard, J. M. HBZ interacts with JunD and stimulates its transcriptional activity. *FEBS Lett* **562,** 165–170 (2004).

228. Kuhlmann, A.-S. S. *et al.* HTLV-1 HBZ cooperates with JunD to enhance transcription of the human telomerase reverse transcriptase gene (hTERT). *Retrovirology* **4,** 92 (2007).

229. Zhao, T. *et al.* HTLV-1 bZIP factor supports proliferation of adult T cell leukemia cells through suppression of C/EBPα signaling. *Retrovirology* **10,** 159 (2013).

230. Reinke, A. W., Grigoryan, G. & Keating, A. E. Identification of bZIP interaction partners of viral proteins HBZ, MEQ, BZLF1, and K-bZIP using coiled-coil arrays. *Biochemistry* **49,** 1985–97 (2010).

231. Clerc, I. *et al.* Propensity for HBZ-SP1 isoform of HTLV-I to inhibit c-Jun activity correlates with sequestration of c-Jun into nuclear bodies rather than inhibition of its DNA-binding activity. *Virology* **391,** 195–202 (2009).

232. Gazon, H., Barbeau, B., Mesnard, J.-M. & Peloponese, J.-M. Hijacking of the AP-1 Signaling Pathway during Development of ATL. *Front. Microbiol.* **8,** 2686 (2018).

233. Gazon, H. *et al.* Human T-cell leukemia virus type 1 (HTLV-1) bZIP factor requires cellular transcription factor JunD to upregulate HTLV-1 antisense transcription from the 3' long terminal repeat. *J. Virol.* **86,** 9070–9078 (2012).

234. Kawatsuki, A., Yasunaga, J.-I., Mitobe, Y., Green, P. L. & Matsuoka, M. HTLV-1 bZIP factor protein targets the Rb/E2F-1 pathway to promote proliferation and apoptosis of primary CD4(+) T cells. *Oncogene* **35,** 4509–17 (2016).

235. Hagiya, K., Yasunaga, J., Satou, Y., Ohshima, K. & Matsuoka, M. ATF3, an HTLV-1 bZip factor binding protein, promotes proliferation of adult T-cell leukemia cells. *Retrovirology* **8,** 19 (2011).

236. Mitobe, Y., Yasunaga, J. -i., Furuta, R. & Matsuoka, M. HTLV-1 bZIP Factor RNA and Protein Impart Distinct Functions on T-cell Proliferation and Survival. *Cancer Res.* **75,** 4143–4152 (2015).

237. Kinosada, H. *et al.* HTLV-1 bZIP Factor Enhances T-Cell Proliferation by Impeding the Suppressive Signaling of Co-inhibitory Receptors. *PLOS Pathog.* **13,** e1006120 (2017).

238. Sugata, K. *et al.* HTLV-1 Viral Factor HBZ Induces CCR4 to Promote T-cell Migration and Proliferation. *Cancer Res.* **76,** 5068–5079 (2016).

239. Vernin, C. *et al.* HTLV-1 bZIP Factor HBZ Promotes Cell Proliferation and Genetic Instability by Activating OncomiRs. *Cancer Res.* **74,** (2014).

240. Wright, D. G. *et al.* Human T-cell leukemia virus type-1-encoded protein HBZ represses p53 function by inhibiting the acetyltransferase activity of p300/CBP and HBO1. *Oncotarget* **7,** 1687–706 (2015).

241. Wurm, T., Wright, D. G., Polakowski, N., Mesnard, J.-M. M. & Lemasson, I. The HTLV-1-encoded protein HBZ directly inhibits the acetyl transferase activity of p300/CBP. *Nucleic Acids Res* **40,** 5910–25 (2012).

242. Polakowski, N. *et al.* HBZ stimulates brain-derived neurotrophic factor/TrkB autocrine/paracrine signaling to promote survival of human T-cell leukemia virus type 1-Infected T cells. *J Virol* **88,** 13482–13494 (2014).

243. Tanaka-Nakanishi, A., Yasunaga, J. -i., Takai, K. & Matsuoka, M. HTLV-1 bZIP factor suppresses apoptosis by attenuating the function of FoxO3a and altering its localization. *Cancer Res* **74,** 188–200 (2014).

244. Zhi, H. *et al.* NF-κB hyper-activation by HTLV-1 tax induces cellular senescence, but can be alleviated by the viral anti-sense protein HBZ. *PLoS Pathog* **7,** e1002025 (2011).

245. Zhao, T. *et al.* Human T-cell leukemia virus type 1 bZIP factor selectively suppresses the classical pathway of NF-kappaB. *Blood* **113,** 2755–2764 (2009).

246. Halin, M. *et al.* Human T-cell leukemia virus type 2 produces a spliced antisense transcript encoding a protein that lacks a classic bZIP domain but still inhibits Tax2-mediated transcription. *Blood* **114,** 2427–2438 (2009).

247. Rende, F. *et al.* Kinetics and intracellular compartmentalization of HTLV-1 gene expression: nuclear retention of HBZ mRNAs. *Blood* **117,** 4855–4859 (2011).

248. Billman, M. R., Rueda, D. & Bangham, C. R. M. Single-cell heterogeneity and cell-cycle-related viral gene bursts in the human leukaemia virus HTLV-1. *Wellcome open Res.* **2,** 87 (2017).

249. Mahgoub, M. *et al.* Sporadic on/off switching of HTLV-1 Tax expression is crucial to maintain the whole population of virus-induced leukemic cells. *Proc. Natl. Acad. Sci. U. S. A.* **115,** E1269–E1278 (2018).

250. Miyazato, P., Matsuo, M., Katsuya, H. & Satou, Y. Transcriptional and Epigenetic Regulatory Mechanisms Affecting HTLV-1 Provirus. *Viruses* **8,** 171 (2016).

251. Shen, Z. Genomic instability and cancer: An introduction. *J. Mol. Cell Biol.* **3,** 1–3 (2011).

252. Helleday, T., Eshtad, S. & Nik-Zainal, S. Mechanisms underlying mutational signatures in human cancers. *Nat. Rev. Genet.* **15,** 585–598 (2014).

253. Khanna, K. K. & Jackson, S. P. DNA double-strand breaks: signaling, repair and the cancer connection. *Nat. Genet.* **27,** 247–254 (2001).

254. De Bont, R. & van Larebeke, N. Endogenous DNA damage in humans: a review of quantitative data. *Mutagenesis* **19,** 169–185 (2004).

255. Costanzo, V., Chaudhuri, J., Fung, J. C. & Moran, J. V. Dealing with dangerous accidents: DNA double-strand breaks take centre stage. Symposium on Genome Instability and DNA Repair. *EMBO Rep.* **10,** 837–42 (2009).

256. Hoeijmakers, J. H. J. Genome maintenance mechanisms for preventing cancer. *Nature* **411,** 366–374 (2001).

257. Sieber, O. M., Heinimann, K. & Tomlinson, I. P. M. Genomic instability — the engine of tumorigenesis? *Nat. Rev. Cancer* **3,** 701–708 (2003).

258. Jasin, M. & Rothstein, R. Repair of strand breaks by homologous recombination. *Cold Spring Harb. Perspect. Biol.* **5,** a012740 (2013).

259. Li, X. & Heyer, W.-D. Homologous recombination in DNA repair and DNA damage tolerance. *Cell Res.* **18,** 99–113 (2008).

260. Branzei, D. & Foiani, M. Regulation of DNA repair throughout the cell cycle. *Nat. Rev. Mol. Cell Biol.* **9,** 297–308 (2008).

261. Bishop, A. J. & Schiestl, R. H. Homologous recombination as a mechanism for genome rearrangements: environmental and genetic effects. *Hum. Mol. Genet.* **9,** 2427–334 (2000).

262. Mao, Z., Jiang, Y., Liu, X., Seluanov, A. & Gorbunova, V. DNA repair by homologous recombination, but not by nonhomologous end joining, is elevated in breast cancer cells. *Neoplasia* **11,** 683–91 (2009).

263. Chang, H. H. Y., Pannunzio, N. R., Adachi, N. & Lieber, M. R. Non-homologous DNA end joining and alternative pathways to double-strand break repair. *Nat. Rev. Mol. Cell Biol.* **18,** 495–506 (2017).

264. Neal, J. A. & Meek, K. Choosing the right path: does DNA-PK help make the decision? *Mutat. Res.* **711,** 73–86 (2011).

265. Chen, B. P. C. *et al.* Cell Cycle Dependence of DNA-dependent Protein Kinase Phosphorylation in Response to DNA Double Strand Breaks. *J. Biol. Chem.* **280,** 14709–14715 (2005).

266. Lieber, M. R. The mechanism of double-strand DNA break repair by the nonhomologous DNA end-joining pathway. *Annu. Rev. Biochem.* **79,** 181–211 (2010).

267. Chiruvella, K. K., Liang, Z. & Wilson, T. E. Repair of Double-Strand Breaks by End Joining. *Cold Spring Harb. Perspect. Biol.* **5,** a012757–a012757 (2013).

268. Davis, A. J. & Chen, D. J. DNA double strand break repair via non-homologous end-joining. *Transl. Cancer Res.* **2,** 130–143 (2013).

269. Uematsu, N. *et al.* Autophosphorylation of DNA-PKCS regulates its dynamics at DNA double-strand breaks. *J. Cell Biol.* **177,** 219–29 (2007).

270. Weterings, E. & Chen, D. J. DNA-dependent protein kinase in nonhomologous end joining: a lock with multiple keys? *J. Cell Biol.* **179,** 183–6 (2007).

271. Wang, S. *et al.* The catalytic subunit of DNA-dependent protein kinase selectively regulates p53-dependent apoptosis but not cell-cycle arrest. *Proc. Natl. Acad. Sci. U. S. A.* **97,** 1584–8 (2000).

272. Woo, R. A. *et al.* DNA damage-induced apoptosis requires the DNA-dependent protein kinase, and is mediated by the latent population of p53. *EMBO J.* **21,** 3000–8 (2002).

273. Mukherjee, B. *et al.* DNA-PK phosphorylates histone H2AX during apoptotic DNA fragmentation in mammalian cells. *DNA Repair (Amst).* **5,** 575–590 (2006).

274. Achanta, G., Pelicano, H., Feng, L., Plunkett, W. & Huang, P. Interaction of p53 and DNA-PK in response to nucleoside analogues: potential role as a sensor complex for DNA damage. *Cancer Res.* **61,** 8723–9 (2001).

275. Burma, S. & Chen, D. J. Role of DNA–PK in the cellular response to DNA double-strand breaks. *DNA Repair (Amst).* **3,** 909–918 (2004).

276. Dhanalakshmi, S., Agarwal, C., Singh, R. P. & Agarwal, R. Silibinin Up-regulates DNA-Protein Kinase-dependent p53 Activation to Enhance UVB-induced Apoptosis in Mouse Epithelial JB6 Cells. *J. Biol. Chem.* **280,** 20375–20383 (2005).

277. Wang, Y. *et al.* DNA-PK-mediated phosphorylation of EZH2 regulates the DNA damage-induced apoptosis to maintain T-cell genomic integrity. *Cell Death Dis.* **7,** e2316 (2016).

278. Uchiyama, T., Yodoi, J., Sagawa, K., Takatsuki, K. & Uchino, H. Adult T-cell leukemia: clinical and hematologic features of 16 cases. *Blood* **50,** 481–492 (1977).

279. Takatsuki, K. Discovery of adult T-cell leukemia. *Retrovirology* **2,** 16 (2005).

280. Itoyama, T. *et al.* Cytogenetic analysis and clinical significance in adult T-cell leukemia/lymphoma: a study of 50 cases from the human T-cell leukemia virus type-1 endemic area, Nagasaki. *Blood* **97,** (2001).

281. Liang, M.-H., Geisbert, T., Yao, Y., Hinrichs, S. H. & Giam, C.-Z. Human T-lymphotropic virus type 1 oncoprotein tax promotes S-phase entry but blocks mitosis. *J. Virol.* **76,** 4022–33 (2002).

282. de la Fuente, C. *et al.* Involvement of HTLV-I Tax and CREB in aneuploidy: a bioinformatics approach. *Retrovirology* **3,** 43 (2006).

283. Bellon, M. *et al.* Increased expression of telomere length regulating factors TRF1, TRF2 and TIN2 in patients with adult T-cell leukemia. *Int. J. Cancer* **119,** 2090–2097 (2006).

284. Semmes, O. J., Barret, J. F., Dang, C. V & Jeang, K. T. Human T-cell leukemia virus type I Tax masks c-Myc function through a cAMP-dependent pathway. *J. Biol. Chem.* **271,** 9730–9738 (1996).

285. Majone, F., Semmes, O. J. & Jeang, K.-T. Induction of Micronuclei by HTLV-I Tax: A Cellular Assay for Function. *Virology* **193,** 456–459 (1993).

286. Dayaram, T., Lemoine, F. J., Donehower, L. A. & Marriott, S. J. Activation of WIP1 phosphatase by HTLV-1 Tax mitigates the cellular response to DNA damage. *PLoS One* **8,** e55989 (2013).

287. Durkin, S. S. *et al.* HTLV-1 Tax oncoprotein subverts the cellular DNA damage response via binding to DNA-dependent protein kinase. *J. Biol. Chem.* **283,** 36311–20 (2008).

288. Chandhasin, C., Ducu, R. I., Berkovich, E., Kastan, M. B. & Marriott, S. J. Human T-cell leukemia virus type 1 tax attenuates the ATM-mediated cellular DNA damage response. *J. Virol.* **82,** 6952–61 (2008).

289. Haoudi, A. & Semmes, O. J. The HTLV-1 Tax Oncoprotein Attenuates DNA Damage Induced G1 Arrest and Enhances Apoptosis in p53 Null Cells. *Virology* **305,** 229–239 (2003).

290. Kao, S. Y., Lemoine, F. J. & Marriott, S. J. Suppression of DNA repair by human T cell leukemia virus type 1 Tax is rescued by a functional p53 signaling pathway. *J Biol Chem* **275,** 35926–31. (2000).

291. Lemoine, F. J. & Marriott, S. J. Accelerated G(1) phase progression induced by the human T cell leukemia virus type I (HTLV-I) Tax oncoprotein. *J Biol Chem* **276,** 31851–7. (2001).

292. Marriott, S. J. & Semmes, O. J. Impact of HTLV-I Tax on cell cycle progression and the cellular DNA damage repair response. *Oncogene* **24,** 5986–5995 (2005).

293. Rauch, D. A. & Ratner, L. Targeting HTLV-1 activation of NFκB in mouse models and ATLL patients. *Viruses* **3,** 886–900 (2011).

294. Miyazaki, M. *et al.* Preferential selection of human T-cell leukemia virus type 1 provirus lacking the 5' long terminal repeat during oncogenesis. *J Virol* **81,** 5714–5723 (2007).

295. Fan, J. *et al.* APOBEC3G Generates Nonsense Mutations in Human T-Cell Leukemia Virus Type 1 Proviral Genomes In Vivo. *J. Virol.* **84,** 7278–7287 (2010).

296. Barbeau, B. & Mesnard, J. M. Making sense out of antisense transcription in human T-cell lymphotropic viruses (HTLVs). *Viruses* **3,** 456–468 (2011).

297. Kataoka, K. *et al.* Integrated molecular analysis of adult T cell leukemia/lymphoma. *Nat. Genet.* **47,** 1304–1315 (2015).

298. Laverdure, S., Polakowski, N., Hoang, K. & Lemasson, I. Permissive sense and antisense transcription from the 5' and 3' long terminal repeats of Human T-cell Leukemia Virus type 1 Running Title: Permissive transcription from the HTLV-1 LTRs. *J. Virol.* **90,** 3600–3610 (2017).

299. Lemasson, I., Thebault, S., Sardet, S., Devaux, C. & Mesnard, J. M. Activation of

E2F-mediated Transcription by Human T-cell Leukemia Virus Type I Tax Protein in a p16(INK4A)-negative T-cell Line. *J. Biol. Chem.* **273,** 23598–23604 (1998).

300. Wurm, T. & Lemasson, I. Potential interference of HTLV-1 HBZ protein with the DNA damage response pathway. *Retrovirology* **8,** A203 (2011).

301. Ducu, R. I., Dayaram, T. & Marriott, S. J. The HTLV-1 Tax oncoprotein represses Ku80 gene expression. *Virology* **416,** 1–8 (2011).

302. Seluanov, A., Mao, Z. & Gorbunova, V. Analysis of DNA double-strand break (DSB) repair in mammalian cells. *J. Vis. Exp.* (2010). doi:10.3791/2002

303. Pierce, A. J., Johnson, R. D., Thompson, L. H. & Jasin, M. XRCC3 promotes homology-directed repair of DNA damage in mammalian cells. *Genes Dev.* **13,** 2633–8 (1999).

304. Leahy, J. J. J. *et al.* Identification of a highly potent and selective DNA-dependent protein kinase (DNA-PK) inhibitor (NU7441) by screening of chromenone libraries. *Bioorg. Med. Chem. Lett.* **14,** 6083–6087 (2004).

305. Huang, F. *et al.* Identification of specific inhibitors of human RAD51 recombinase using high-throughput screening. *ACS Chem. Biol.* **6,** 628–35 (2011).

306. Labhart, P. Ku-dependent nonhomologous DNA end joining in Xenopus egg extracts. *Mol. Cell. Biol.* **19,** 2585–93 (1999).

307. Di Virgilio, M. & Gautier, J. Repair of double-strand breaks by nonhomologous end joining in the absence of Mre11. *J. Cell Biol.* **171,** 765–71 (2005).

308. Goodarzi, A. A. *et al.* DNA-PK autophosphorylation facilitates Artemis endonuclease activity. *EMBO J.* **25,** 3880–9 (2006).

309. Hammel, M. *et al.* Ku and DNA-dependent protein kinase dynamic conformations and assembly regulate DNA binding and the initial non-homologous end joining complex. *J. Biol. Chem.* **285,** 1414–23 (2010).

310. Polo, S. E. & Jackson, S. P. Dynamics of DNA damage response proteins at DNA breaks: a focus on protein modifications. *Genes Dev.* **25,** 409–33 (2011).

311. Lee, K.-J. *et al.* Phosphorylation of Ku dictates DNA double-strand break (DSB) repair pathway choice in S phase. *Nucleic Acids Res.* **44,** 1732–1745 (2016).

312. Davis, A. J., Chen, B. P. C. & Chen, D. J. DNA-PK: a dynamic enzyme in a versatile DSB repair pathway. *DNA Repair (Amst).* **17,** 21–9 (2014).

313. Chan, D. W. *et al.* Autophosphorylation of the DNA-dependent protein kinase catalytic subunit is required for rejoining of DNA double-strand breaks. *Genes Dev.* **16,** 2333–8 (2002).

314. Jiang, W. *et al.* Differential Phosphorylation of DNA-PKcs Regulates the Interplay between End-Processing and End- Ligation during Nonhomologous End-Joining. *Mol. Cell* **58,** 172–185 (2015).

315. Cui, X. *et al.* Autophosphorylation of DNA-dependent protein kinase regulates DNA end processing and may also alter double-strand break repair pathway choice. *Mol. Cell. Biol.* **25,** 10842–52 (2005).

316. Ding, Q. *et al.* Autophosphorylation of the catalytic subunit of the DNA-dependent protein kinase is required for efficient end processing during DNA double-strand break repair. *Mol. Cell. Biol.* **23,** 5836–48 (2003).

317. Dobbs, T. A., Tainer, J. A. & Lees-Miller, S. P. A structural model for regulation of NHEJ by DNA-PKcs autophosphorylation. *DNA Repair (Amst).* **9,** 1307–14 (2010).

318. Muslimović, A., Nyström, S., Gao, Y. & Hammarsten, O. Numerical Analysis of Etoposide Induced DNA Breaks. *PLoS One* **4,** e5859 (2009).

319. Ivashkevich, A. N. *et al.* γH2AX foci as a measure of DNA damage: A computational approach to automatic analysis. *Mutat. Res. Mol. Mech. Mutagen.* **711,** 49–60 (2011).

320. Ma, Y. *et al.* The DNA-dependent protein kinase catalytic subunit phosphorylation sites in human artemis. *J. Biol. Chem.* **280,** 33839–33846 (2005).

321. Stronach, E. A. *et al.* DNA-PK mediates AKT activation and apoptosis inhibition in clinically acquired platinum resistance. *Neoplasia* **13,** 1069–80 (2011).

322. Doug W. Chan, Ruiqiong Ye, Christian J. Veillette, and & Lees-Miller*, S. P. DNA-Dependent Protein Kinase Phosphorylation Sites in Ku 70/80 Heterodimer. *Biochemistry* **38,** 1819–1828 (1999).

323. Lee, K.-J., Jovanovic, M., Udayakumar, D., Bladen, C. L. & Dynan, W. S. Identification of DNA-PKcs phosphorylation sites in XRCC4 and effects of mutations at these sites on DNA end joining in a cell-free system. *DNA Repair (Amst).* **3,** 267–276 (2004).

324. Yu, Y. *et al.* DNA-PK and ATM phosphorylation sites in XLF/Cernunnos are not required for repair of DNA double strand breaks. *DNA Repair (Amst).* **7,** 1680–1692 (2008).

325. Wang, Y.-G., Nnakwe, C., Lane, W. S., Modesti, M. & Frank, K. M. Phosphorylation and regulation of DNA ligase IV stability by DNA-dependent protein kinase. *J. Biol. Chem.* **279,** 37282–90 (2004).

326. Zhao, Y. *et al.* Preclinical Evaluation of a Potent Novel DNA-Dependent Protein Kinase Inhibitor NU7441. *Cancer Res.* **66,** 5354–5362 (2006).

327. Gao, Y. *et al.* A targeted DNA-PKcs-null mutation reveals DNA-PK-independent functions for KU in V(D)J recombination. *Immunity* **9,** 367–76 (1998).

328. Hosoi, Y. *et al.* A phosphatidylinositol 3-kinase inhibitor wortmannin induces radioresistant DNA synthesis and sensitizes cells to bleomycin and ionizing radiation. *Int. J. Cancer* **78,** 642–647 (1998).

329. Kurimasa, A. *et al.* Requirement for the kinase activity of human DNA-dependent protein kinase catalytic subunit in DNA strand break rejoining. *Mol. Cell. Biol.* **19,** 3877–84 (1999).

330. Neal, J. A. *et al.* Unraveling the complexities of DNA-dependent protein kinase autophosphorylation. *Mol. Cell. Biol.* **34,** 2162–75 (2014).

331. Britton, S., Coates, J. & Jackson, S. P. A new method for high-resolution imaging of Ku foci to decipher mechanisms of DNA double-strand break repair. *J. Cell Biol.* **202,** 579–595 (2013).

332. Mao, Z., Bozzella, M., Seluanov, A. & Gorbunova, V. DNA repair by nonhomologous end joining and homologous recombination during cell cycle in human cells. *Cell Cycle* **7,** 2902–6 (2008).

333. Richardson, C., Moynahan, M. E. & Jasin, M. Double-strand break repair by interchromosomal recombination: suppression of chromosomal translocations. *Genes Dev.* **12,** 3831–42 (1998).

334. Kingston, R. E. *et al.* Calcium Phosphate Transfection. in *Current Protocols in Molecular Biology* 9.1.1-9.1.11 (John Wiley & Sons, Inc., 2003). doi:10.1002/0471142727.mb0901s63

335. Abmayr, S. M., Yao, T., Parmely, T. & Workman, J. L. Preparation of nuclear and cytoplasmic extracts from mammalian cells. *Curr. Protoc. Mol. Biol.* **Chapter 12,** Unit 12.1 (2006).

336. Polakowski, N., Han, H. & Lemasson, I. Direct inhibition of RNAse T2 expression by the HTLV-1 viral protein Tax. *Viruses* **3,** 1485–1500 (2011).

337. Frank, S. R., Schroeder, M., Fernandez, P., Taubert, S. & Amati, B. Binding of c-Myc to chromatin mediates mitogen-induced acetylation of histone H4 and gene activation. *Genes Dev* **15,** 2069–2082. (2001).

338. Sies, H., Berndt, C. & Jones, D. P. Oxidative Stress. *Annu. Rev. Biochem.* **86,** 715–748 (2017).

339. Chen, J.-H., Ozanne, S. E. & Hales, C. N. Methods of Cellular Senescence Induction Using Oxidative Stress. in *Methods in molecular biology (Clifton, N.J.)* **371,** 179–189 (2007).

340. Nguyen, T., Nioi, P. & Pickett, C. B. The Nrf2-Antioxidant Response Element Signaling Pathway and Its Activation by Oxidative Stress. *J. Biol. Chem.* **284,** 13291–13295 (2009).

341. Nguyen, T., Huang, H. C. & Pickett, C. B. Transcriptional regulation of the antioxidant response element. Activation by Nrf2 and repression by MafK. *J Biol Chem* **275,** 15466–15473 (2000).

342. Katsuoka, F. & Yamamoto, M. Small Maf proteins (MafF, MafG, MafK): History, structure and function. *Gene* **586,** 197–205 (2016).

343. Baird, L. & Dinkova-Kostova, A. T. The cytoprotective role of the Keap1–Nrf2 pathway. *Arch. Toxicol.* **85,** 241–272 (2011).

344. Leone, A., Roca, M. S., Ciardiello, C., Costantini, S. & Budillon, A. Oxidative Stress Gene Expression Profile Correlates with Cancer Patient Poor Prognosis: Identification of Crucial Pathways Might Select Novel Therapeutic Approaches. *Oxid. Med. Cell. Longev.* **2017,** 1–18 (2017).

345. Peiris-Pagès, M., Martinez-Outschoorn, U. E., Sotgia, F. & Lisanti, M. P. Metastasis and Oxidative Stress: Are Antioxidants a Metabolic Driver of Progression? *Cell Metab.* **22,** 956–958 (2015).

346. Sporn, M. B. & Liby, K. T. NRF2 and cancer: the good, the bad and the importance of context. *Nat. Rev. Cancer* **12,** 564–571 (2012).

347. Kansanen, E., Kuosmanen, S. M., Leinonen, H. & Levonen, A.-L. The Keap1-Nrf2 pathway: Mechanisms of activation and dysregulation in cancer. *Redox Biol.* **1,** 45–49 (2013).

348. Moon, E. J. & Giaccia, A. Dual roles of NRF2 in tumor prevention and progression: possible implications in cancer treatment. *Free Radic. Biol. Med.* **79,** 292–9 (2015).

349. Hawk, M. A., McCallister, C. & Schafer, Z. T. Antioxidant Activity during Tumor Progression: A Necessity for the Survival of Cancer Cells? *Cancers (Basel).* **8,** (2016).

350. Kubota, R. Pathogenesis of human T-lymphotropic virus type 1-associated myelopathy/tropical spastic paraparesis. *Clin. Exp. Neuroimmunol.* **8,** 117–128 (2017).

351. Matsuoka, M. & Green, P. L. The HBZ gene, a key player in HTLV-1 pathogenesis. *Retrovirology* **6,** 71 (2009).

352. Bangham, C. R. M. & Matsuoka, M. Human T-cell leukaemia virus type 1: parasitism and pathogenesis. *Philos. Trans. R. Soc. B Biol. Sci.* **372,** 20160272 (2017).

353. Taylor, J. M. & Nicot, C. HTLV-1 and apoptosis: role in cellular transformation and recent advances in therapeutic approaches. *Apoptosis* **13,** 733–747 (2008).

354. Kimura, R. *et al.* Human T cell leukemia virus type I tax-induced IκB-ζ modulates tax-dependent and tax-independent gene expression in T cells. *Neoplasia* **15,** 1110–24 (2013).

355. Takahashi, M. *et al.* HTLV-1 Tax oncoprotein stimulates ROS production and apoptosis in T cells by interacting with USP10. *Blood* **122,** 715–725 (2013).

356. Silic-Benussi, M. *et al.* Modulation of mitochondrial K+ permeability and reactive oxygen species production by the p13 protein of human T-cell leukemia virus type 1. *Biochim. Biophys. Acta - Bioenerg.* **1787,** 947–954 (2009).

357. Silic-Benussi, M. *et al.* HTLV-1 p13, a small protein with a busy agenda. *Mol. Aspects Med.* **31,** 350–358 (2010).

358. Biasiotto, R. *et al.* The p13 protein of human T cell leukemia virus type 1 (HTLV-1) modulates mitochondrial membrane potential and calcium uptake. *Biochim. Biophys. Acta - Bioenerg.* **1797,** 945–951 (2010).

359. D'Agostino, D. M., Silic-Benussi, M., Hiraragi, H., Lairmore, M. D. & Ciminale, V. The human T-cell leukemia virus type 1 p13II protein: effects on mitochondrial function and cell growth. *Cell Death Differ.* **12,** 905–915 (2005).

360. D'Agostino, D. M. *et al.* The p13II protein of HTLV type 1: comparison with mitochondrial proteins coded by other human viruses. *AIDS Res. Hum. Retroviruses* **16,** 1765–70 (2000).

361. Kannagi, M., Matsushita, S. & Harada, S. Expression of the target antigen for cytotoxic T lymphocytes on adult T-cell-leukemia cells. *Int J Cancer* **54,** 582–588 (1993).

362. Li, M., Kesic, M., Yin, H., Yu, L. & Green, P. L. Kinetic analysis of human T-cell leukemia virus type 1 gene expression in cell culture and infected animals. *J Virol* **83,** 3788–3797 (2009).

363. Ryter, S. W., Alam, J. & Choi, A. M. K. Heme Oxygenase-1/Carbon Monoxide: From Basic Science to Therapeutic Applications. *Physiol. Rev.* **86,** 583–650 (2006).

364. Morse, D. & Choi, A. M. K. Heme Oxygenase-1. *Am. J. Respir. Cell Mol. Biol.* **27,** 8–16 (2002).

365. Dunn, L. L. *et al.* New insights into intracellular locations and functions of heme oxygenase-1. *Antioxid. Redox Signal.* **20,** 1723–42 (2014).

366. Gozzelino, R., Jeney, V. & Soares, M. P. Mechanisms of Cell Protection by Heme Oxygenase-1. *Annu. Rev. Pharmacol. Toxicol.* **50,** 323–354 (2010).

367. Chang, L. C. *et al.* The Ratio of Hmox1/Nrf2 mRNA Level in the Tumor Tissue Is a Predictor of Distant Metastasis in Colorectal Cancer. *Dis. Markers* **2016,** (2016).

368. Furfaro, A. L. *et al.* The Nrf2/HO-1 Axis in Cancer Cell Growth and Chemoresistance. *Oxid. Med. Cell. Longev.* **2016,** 1–14 (2016).

369. Sunamura, M. *et al.* Heme oxygenase-1 accelerates tumor angiogenesis of human pancreatic cancer. *Angiogenesis* **6,** 15–24 (2003).

370. Was, H. *et al.* Overexpression of heme oxygenase-1 in murine melanoma: Increased proliferation and viability of tumor cells, decreased survival of mice. *Am. J. Pathol.* **169,** 2181–2198 (2006).

371. Bahmani, P. *et al.* The expression of Heme oxygenase-1 in human-derived cancer cell lines. *Iran. J. Med. Sci.* **36,** 260–265 (2011).

372. Chorley, B. N. *et al.* Identification of novel NRF2-regulated genes by ChIP-Seq:

influence on retinoid X receptor alpha. *Nucleic Acids Res* **40,** 7416–7429 (2012).

373. Hirotsu, Y. *et al.* Nrf2-MafG heterodimers contribute globally to antioxidant and metabolic networks. *Nucleic Acids Res* **40,** 10228–10239 (2012).

374. Gerstein, M. B. *et al.* Architecture of the human regulatory network derived from ENCODE data. *Nature* **489,** 91–100 (2012).

375. Malhotra, D. *et al.* Global mapping of binding sites for Nrf2 identifies novel targets in cell survival response through ChIP-Seq profiling and network analysis. *Nucleic Acids Res.* **38,** 5718–5734 (2010).

376. Pae, H. O., Oh, G. S., Choi, B. M., Chae, S. C. & Chung, H. T. Differential expressions of heme oxygenase-1 gene in CD25- and CD25+ subsets of human CD4+ T cells. *Biochem Biophys Res Commun* **306,** 701–705 (2003).

377. Polakowski, N. & Lemasson, I. Regulation of HTLV-1 Transcription by Viral and Cellular Proteins. in *Recent Advances in Human Retroviruses: Principles of Replication and Pathogenesis. Advances in Retroviral Research* (eds. Lever, A. M. L. & Jeang, K. T.) 129–169 (World Scientific Publishing Co., 2010).

378. Arnold, J., Zimmerman, B., Li, M., Lairmore, M. D. & Green, P. L. Human T-cell leukemia virus type-1 antisense-encoded gene, Hbz, promotes T-lymphocyte proliferation. *Blood* **112,** 3788–3797 (2008).

379. Kuhlmann, A. S. *et al.* HTLV-1 HBZ cooperates with JunD to enhance transcription of the human telomerase reverse transcriptase gene (hTERT). *Retrovirology* **4,** 92 (2007).

380. Fujita, R. *et al.* NF-E2 p45 is important for establishing normal function of platelets. *Mol. Cell. Biol.* **33,** 2659–70 (2013).

381. Warnatz, H.-J. *et al.* The BTB and CNC Homology 1 (BACH1) Target Genes Are Involved in the Oxidative Stress Response and in Control of the Cell Cycle. *J. Biol. Chem.* **286,** 23521–23532 (2011).

382. Motohashi, H., Katsuoka, F., Shavit, J. A., Engel, J. D. & Yamamoto, M. Positive or negative MARE-dependent transcriptional regulation is determined by the abundance of small Maf proteins. *Cell* **103,** 865–875 (2000).

383. Itoh, K. *et al.* An Nrf2/small Maf heterodimer mediates the induction of phase II detoxifying enzyme genes through antioxidant response elements. *Biochem Biophys Res Commun* **236,** 313–322 (1997).

384. Ogawa, K. *et al.* Heme mediates derepression of Maf recognition element through direct binding to transcription repressor Bach1. *EMBO J.* **20,** 2835–43 (2001).

385. Igarashi, K. *et al.* Regulation of transcription by dimerization of erythroid factor NF-E2 p45 with small Maf proteins. *Nature* **367,** 568–572 (1994).

386. Oyake, T. *et al.* Bach proteins belong to a novel family of BTB-basic leucine zipper transcription factors that interact with MafK and regulate transcription

through the NF-E2 site. *Mol Cell Biol* **16,** 6083–6095 (1996).

387. Toki, T. *et al.* Human small Maf proteins form heterodimers with CNC family transcription factors and recognize the NF-E2 motif. *Oncogene* **14,** 1901–1910 (1997).

388. Rushmore, T. H., Morton, M. R. & Pickett, C. B. The antioxidant responsive element. Activation by oxidative stress and identification of the DNA consensus sequence required for functional activity. *J. Biol. Chem.* **266,** 11632–9 (1991).

389. Kataoka, K. *et al.* Small Maf proteins heterodimerize with Fos and may act as competitive repressors of the NF-E2 transcription factor. *Mol Cell Biol* **15,** 2180–2190 (1995).

390. Yamamoto, T. *et al.* Predictive base substitution rules that determine the binding and transcriptional specificity of Maf recognition elements. *Genes to Cells* **11,** 575–591 (2006).

391. Reichard, J. F., Motz, G. T. & Puga, A. Heme oxygenase-1 induction by NRF2 requires inactivation of the transcriptional repressor BACH1. *Nucleic Acids Res.* **35,** 7074–86 (2007).

392. Igarashi, K. & Sun, J. The Heme-Bach1 Pathway in the Regulation of Oxidative Stress Response and Erythroid Differentiation. *Antioxid. Redox Signal.* **8,** 107–118 (2006).

393. Sun, Z., Chin, Y. E. & Zhang, D. D. Acetylation of Nrf2 by p300/CBP augments promoter-specific DNA binding of Nrf2 during the antioxidant response. *Mol Cell Biol* **29,** 2658–2672 (2009).

394. Alam, J. *et al.* Nrf2, a Cap'n'Collar transcription factor, regulates induction of the heme oxygenase-1 gene. *J. Biol. Chem.* **274,** 26071–8 (1999).

395. Kitamuro, T. *et al.* Bach1 functions as a hypoxia-inducible repressor for the heme oxygenase-1 gene in human cells. *J. Biol. Chem.* **278,** 9125–33 (2003).

396. Sun, J. *et al.* Hemoprotein Bach1 regulates enhancer availability of heme oxygenase-1 gene. *EMBO J.* **21,** 5216–24 (2002).

397. Bryan, H. K., Olayanju, A., Goldring, C. E. & Park, B. K. The Nrf2 cell defence pathway: Keap1-dependent and -independent mechanisms of regulation. *Biochem. Pharmacol.* **85,** 705–17 (2013).

398. Kwak, M.-K., Itoh, K., Yamamoto, M. & Kensler, T. W. Enhanced expression of the transcription factor Nrf2 by cancer chemopreventive agents: role of antioxidant response element-like sequences in the nrf2 promoter. *Mol. Cell. Biol.* **22,** 2883–92 (2002).

399. Lee, O.-H., Jain, A. K., Papusha, V. & Jaiswal, A. K. An Auto-regulatory Loop between Stress Sensors INrf2 and Nrf2 Controls Their Cellular Abundance. *J. Biol. Chem.* **282,** 36412–36420 (2007).

400. Wang, J. *et al.* Possible roles of an adult T-cell leukemia (ATL)-derived factor/thioredoxin in the drug resistance of ATL to adriamycin. *Blood* **89,** 2480–2487 (1997).

401. Mühleisen, A. *et al.* Tax contributes apoptosis resistance to HTLV-1-infected T cells via suppression of Bid and Bim expression. *Cell Death Dis* **5,** e1575 (2014).

402. Sakaki, Y. *et al.* Human T-cell lymphotropic virus type I Tax activates lung resistance-related protein expression in leukemic clones established from an adult T-cell leukemia patient. *Exp. Hematol.* **30,** 340–5 (2002).

403. Lau, A., Nightingale, S., GP, G. P. T., Gant, T. W. & Cann, A. J. Enhanced MDR1 gene expression in human T-cell leukemia virus-I-infected patients offers new prospects for therapy. *Blood* **91,** 2467–2474 (1998).

404. Mirończuk-Chodakowska, I., Witkowska, A. M. & Zujko, M. E. Endogenous non-enzymatic antioxidants in the human body. *Adv. Med. Sci.* **63,** 68–78 (2018).

405. Kulkarni, A. *et al.* Glucose Metabolism and Oxygen Availability Govern Reactivation of the Latent Human Retrovirus HTLV-1. *Cell Chem. Biol.* **24,** 1377–1387.e3 (2017).

406. Ichikawa, A. *et al.* Detection of Tax-specific CTLs in lymph nodes of adult T-cell leukemia/lymphoma patients and its association with Foxp3 positivity of regulatory T-cell function. *Oncol. Lett.* **13,** 4611–4618 (2017).

407. Rowan, A. G. & Bangham, C. R. M. Is There a Role for HTLV-1-Specific CTL in Adult T-Cell Leukemia/Lymphoma? *Leuk. Res. Treatment* **2012,** 1–7 (2012).

408. Ohno, N. *et al.* Prognostic significance of multidrug resistance protein in adult T-cell leukemia. *Clin. Cancer Res.* **7,** 3120–6 (2001).

409. Ikeda, K. *et al.* Adult T-cell leukemia cells over-express the multidrug-resistance-protein (MRP) and lung-resistance-protein (LRP) genes. *Int. J. Cancer* **82,** 599–604 (1999).

410. Su, I. J., Chang, I. C. & Cheng, A. L. Expression of growth-related genes and drug-resistance genes in HTLV-I-positive and HTLV-I-negative post-thymic T-cell malignancies. *Ann. Oncol. Off. J. Eur. Soc. Med. Oncol.* **2 Suppl 2,** 151–5 (1991).

411. Zhu, X.-F. *et al.* Knockdown of heme oxygenase-1 promotes apoptosis and autophagy and enhances the cytotoxicity of doxorubicin in breast cancer cells. *Oncol. Lett.* **10,** 2974–2980 (2015).

412. Liu, Y. *et al.* Inhibition of heme oxygenase-1 enhances anti-cancer effects of arsenic trioxide on glioma cells. *J. Neurooncol.* **104,** 449–458 (2011).

413. Homma, S. *et al.* Nrf2 enhances cell proliferation and resistance to anticancer drugs in human lung cancer. *Clin. Cancer Res.* **15,** 3423–32 (2009).

414. Wang, X.-J. *et al.* Nrf2 enhances resistance of cancer cells to chemotherapeutic

drugs, the dark side of Nrf2. *Carcinogenesis* **29,** 1235–1243 (2008).

415. Jiang, T. *et al.* High levels of Nrf2 determine chemoresistance in type II endometrial cancer. *Cancer Res.* **70,** 5486–96 (2010).

416. Zhang, C. *et al.* NRF2 promotes breast cancer cell proliferation and metastasis by increasing RhoA/ROCK pathway signal transduction. *Oncotarget* **7,** 73593–73606 (2016).

417. Ma, X. *et al.* Nrf2 knockdown by shRNA inhibits tumor growth and increases efficacy of chemotherapy in cervical cancer. *Cancer Chemother. Pharmacol.* **69,** 485–494 (2012).

418. Chau, L.-Y. Heme oxygenase-1: emerging target of cancer therapy. *J. Biomed. Sci.* **22,** 22 (2015).

419. Schipper, H. M. Heme oxygenase-1: transducer of pathological brain iron sequestration under oxidative stress. *Ann. N. Y. Acad. Sci.* **1012,** 84–93 (2004).

420. Poon, H. F., Calabrese, V., Scapagnini, G. & Butterfield, D. A. Free radicals: key to brain aging and heme oxygenase as a cellular response to oxidative stress. *J. Gerontol. A. Biol. Sci. Med. Sci.* **59,** 478–93 (2004).

421. van Horssen, J. *et al.* Severe oxidative damage in multiple sclerosis lesions coincides with enhanced antioxidant enzyme expression. *Free Radic. Biol. Med.* **45,** 1729–37 (2008).

422. Stahnke, T., Stadelmann, C., Netzler, A., Brück, W. & Richter-Landsberg, C. Differential upregulation of heme oxygenase-1 (HSP32) in glial cells after oxidative stress and in demyelinating disorders. *J. Mol. Neurosci.* **32,** 25–37 (2007).

423. Liu, Y. *et al.* Heme oxygenase-1 plays an important protective role in experimental autoimmune encephalomyelitis. *Neuroreport* **12,** 1841–5 (2001).

424. Emerson, M. R. & LeVine, S. M. Heme oxygenase-1 and NADPH cytochrome P450 reductase expression in experimental allergic encephalomyelitis: an expanded view of the stress response. *J. Neurochem.* **75,** 2555–62 (2000).

425. Chakrabarty, A., Emerson, M. R. & LeVine, S. M. Hemeoxygenase-1 in SJL mice with experimental allergic encephalomyelitis. *Mult. Scler. J.* **9,** 372–381 (2003).

426. Los, M. *et al.* Human T cell leukemia virus-I (HTLV-I) Tax-mediated apoptosis in activated T cells requires an enhanced intracellular prooxidant state. *J Immunol* **161,** 3050–3055 (1998).

427. Shankar, D. B. *et al.* The role of CREB as a proto-oncogene in hematopoiesis and in acute myeloid leukemia. *Cancer Cell* **7,** 351–362 (2005).

428. Abou-Kandil, A., Chamias, R., Huleihel, M., Godbey, W. T. & Aboud, M. Role of caspase 9 in activation of HTLV-1 LTR expression by DNA damaging agents. *Cell Cycle* **10,** 3337–45 (2011).

429. Chamias, R., Huleihel, M. & Aboud, M. The mechanism of HTLV-1 LTR activation by TPA varies in different human T-cell lines: role of specific PKC isoforms. *Leuk. Res.* **34,** 93–9 (2010).

430. Hivin, P. *et al.* A modified version of a Fos-associated cluster in HBZ affects Jun transcriptional potency. *Nucleic Acids Res* **34,** 2761–72 (2006).

431. Luscombe, N. M., Laskowski, R. A. & Thornton, J. M. Amino acid-base interactions: a three-dimensional analysis of protein-DNA interactions at an atomic level. *Nucleic Acids Res.* **29,** 2860–74 (2001).

432. Wang, J. & Pantopoulos, K. Regulation of cellular iron metabolism. *Biochem. J.* **434,** 365–81 (2011).

433. Orino, K. & Watanabe, K. Molecular, physiological and clinical aspects of the iron storage protein ferritin. *Vet. J.* **178,** 191–201 (2008).

434. Regner, A., Bianchini, O., Jardim, C. & Menna-Barreto, M. HTLV-I-associated myelopathy: are ferritin, S100beta protein, or guanine nucleotides CSF markers of disease? *J. Neurovirol.* **8,** 64–7 (2002).

435. Glick, D., Barth, S. & Macleod, K. F. Autophagy: cellular and molecular mechanisms. *J. Pathol.* **221,** 3–12 (2010).

436. Katsuragi, Y., Ichimura, Y. & Komatsu, M. p62/SQSTM1 functions as a signaling hub and an autophagy adaptor. *FEBS J.* **282,** 4672–4678 (2015).

437. Schwob, A., Palgen, J.-L., Mahieux, R. & Journo, C. SQSTM1/p62 regulates HTLV-1 tax mediated NF-κB activation. *Retrovirology* **12,** O38 (2015).

438. Tang, S.-W., Chen, C.-Y., Klase, Z., Zane, L. & Jeang, K.-T. The cellular autophagy pathway modulates human T-cell leukemia virus type 1 replication. *J. Virol.* **87,** 1699–707 (2013).

439. Blaser, H., Dostert, C., Mak, T. W. & Brenner, D. TNF and ROS Crosstalk in Inflammation. *Trends Cell Biol.* **26,** 249–261 (2016).

440. Sedger, L. M. & McDermott, M. F. TNF and TNF-receptors: From mediators of cell death and inflammation to therapeutic giants – past, present and future. *Cytokine Growth Factor Rev.* **25,** 453–472 (2014).

441. Bellon, M., Lu, L. & Nicot, C. Constitutive activation of Pim1 kinase is a therapeutic target for adult T-cell leukemia. *Blood* **127,** 2439 (2016).

442. Bachmann, M. & Möröy, T. The serine/threonine kinase Pim-1. *Int. J. Biochem. Cell Biol.* **37,** 726–730 (2005).

443. Gazon, H. *et al.* Impaired expression of DICER and some microRNAs in HBZ expressing cells from acute adult T-cell leukemia patients. *Oncotarget* **7,** 30258–75 (2016).

444. Iwamori, S. *et al.* A novel and sensitive assay for heme oxygenase activity. *Am. J. Physiol. Physiol.* **309,** F667–F671 (2015).

445. Baghirova, S., Hughes, B. G., Hendzel, M. J. & Schulz, R. Sequential fractionation and isolation of subcellular proteins from tissue or cultured cells. *MethodsX* **2,** 440–5 (2015).

446. Colgin, M. A. & Nyborg, J. K. The human T-cell leukemia virus type 1 oncoprotein Tax inhibits the transcriptional activity of c-Myb through competition for the CREB binding protein. *J Virol* **72,** 9396–9399 (1998).

447. Kamada N Miyamoto K, Sanada I, Sadamori N, Fukahara S, Abe S, Shiraishi Y, Abe T, Kaneko Y, Shimoyama M., S. M. Chromosome abnormalities in adult T cell leukemia/lymphoma: a karyotype review committee report. *Cancer Res* **52,** 1481–1493 (1992).

448. Semmes, O. J. & Jeang, K. T. Mutational analysis of human T-cell leukemia virus type I Tax: regions necessary for function determined with 47 mutant proteins. *J. Virol.* **66,** 7183–7192 (1992).

449. Grassmann, R., Aboud, M. & Jeang, K.-T. Molecular mechanisms of cellular transformation by HTLV-1 Tax. *Oncogene* **24,** 5976–5985 (2005).

450. Chernikova, S. B., Game, J. C. & Brown, J. M. Inhibiting homologous recombination for cancer therapy. *Cancer Biol. Ther.* **13,** 61–8 (2012).

451. Puigvert, J. C., Sanjiv, K. & Helleday, T. Targeting DNA repair, DNA metabolism and replication stress as anti-cancer strategies. *FEBS J.* **283,** 232–245 (2016).

452. Hosoya, N. & Miyagawa, K. Targeting DNA damage response in cancer therapy. *Cancer Sci.* **105,** 370–88 (2014).

453. Moles, R., Bai, X. T., Chaib-Mezrag, H. & Nicot, C. WRN-targeted therapy using inhibitors NSC 19630 and NSC 617145 induce apoptosis in HTLV-1-transformed adult T-cell leukemia cells. *J. Hematol. Oncol.* **9,** 121 (2016).

454. Hamamura, R. *et al.* Induction of heme oxygenase-1 by cobalt protoporphyrin enhances the antitumour effect of bortezomib in adult T-cell leukaemia cells. *Br. J. Cancer* **97,** 1099–1105 (2007).

455. Ratner, L. *et al.* Dose-adjusted EPOCH chemotherapy with bortezomib and raltegravir for human T-cell leukemia virus-associated adult T-cell leukemia lymphoma. *Blood Cancer J.* **6,** e408 (2016).

456. Fujii, H. *et al.* A Potential of an Anti-HTLV-I gp46 Neutralizing Monoclonal Antibody (LAT-27) for Passive Immunization against Both Horizontal and Mother-to-Child Vertical Infection with Human T Cell Leukemia Virus Type-I. *Viruses* **8,** 41 (2016).

457. Hilburn, S. *et al.* In vivo Expression of Human T-lymphotropic Virus Type 1 Basic Leucine-Zipper Protein Generates Specific CD8+ and CD4+ T-Lymphocyte Responses that Correlate with Clinical Outcome. *J. Infect. Dis.* **203,** 529–536 (2011).

458. Rowan, A. G. *et al.* Cytotoxic T lymphocyte lysis of HTLV-1 infected cells is limited

by weak HBZ protein expression, but non-specifically enhanced on induction of Tax expression. *Retrovirology* **11,** 116 (2014).

459. Sugata, K. *et al.* Protective effect of cytotoxic T lymphocytes targeting HTLV-1 bZIP factor. *Blood* **126,** 1095–1105 (2015).

460. Mahieux, R. A vaccine against HTLV-1 HBZ makes sense. *Blood* **126,** 1052–3 (2015).

461. Nishioka, C. *et al.* Histone deacetylase inhibitors induce growth arrest and apoptosis of HTLV-1-infected T-cells via blockade of signaling by nuclear factor κB. *Leuk. Res.* **32,** 287–296 (2008).

462. Zimmerman, B. *et al.* Efficacy of novel histone deacetylase inhibitor, AR42, in a mouse model of, human T-lymphotropic virus type 1 adult T cell lymphoma. *Leuk. Res.* **35,** 1491–7 (2011).

463. Ramos, J. C. *et al.* Targeting HTLV-I latency in Adult T-cell Leukemia/Lymphoma. *Retrovirology* **8,** A48 (2011).

464. Marçais, A., Suarez, F., Sibon, D., Bazarbachi, A. & Hermine, O. Clinical trials of adult T-cell leukaemia/lymphoma treatment. *Leuk. Res. Treatment* **2012,** 932175 (2012).